# Decellularisation and characterisation of porcine bone-medial meniscus-bone

Jahid Hasan

Submitted in accordance with the requirements for the degree of Doctor of Philosophy

The University of Leeds

Faculty of Biological Sciences

June 2014

The candidate confirms that the work submitted is his/her own
and that appropriate credit has been given where reference has
been made to the work of others

# Acknowledgements

# Summary

The meniscus in the knee functions to absorb shock and transmit load within the joint. Problems arise when the meniscus is injured or damaged as the meniscus' healing potential is limited by the limited vascular supply extending only ~20% of the way through the mature meniscus. Current treatment options are only effective at abating further degeneration and osteoarthritis due to altered joint mechanics. Replacement of the meniscus has the potential to prevent the onset of osteoarthritis by restoring native joint mechanics.

Here we aim to develop a decellularisation protocol for porcine medial meniscus with added bone blocks for easy fixation for use as a meniscal replacement. Menisci were decellularised using a low sodium dodecyl sulphate (SDS) method including freeze-thaw cycles, hypertonic, hypotonic and nuclease wash steps, as well as mechanical removal of cellular material. Decellularised menisci were then characterised histologically, immunohistochemically, biochemically and biomechanically for successful decellularisation and compared to native meniscus.

Histology revealed the absence of whole cells and nuclei from meniscus and bone, while quantification of DNA revealed ~96% and ~91% removal of DNA from meniscus and bone, respectively. Immunohistochemical analysis showed retention of major structural collagens I, II and II; however there was complete removal of collagen IV and some loss of collagen VI. Hydroxyproline assay showed retention of collagen and the collagen content of native meniscus was 802.90 ($\pm$ 52.95, 95% CL) mg.g$^{-1}$ dry weight and for decellularised meniscus was 935.35 ($\pm$ 18.03, 95% CL) mg.g$^{-1}$ dry weight, however there was a complete loss of GAGs from the decellularised matrices as revealed by Safranin O staining and quantified using dimethyl methylene blue assay (23.49 $\pm$ 8.63 µg.mg$^{-1}$ vs. 0.30 $\pm$ 0.47 µg.mg$^{-1}$, 95% C.I.). There was also a 51% reduction in calcium content of the decellularised bone blocks when compared to native bone blocks.

Material properties of meniscus were obtained using uniaxial tensile and indentation testing with no significant differences observed between native and decellularised groups under tension although greater deformation was seen for decellularised samples under compression. Unconfined compression of bone

however revealed a significant decrease in the compressive modulus and strength of decellularised bone blocks. Differential scanning calorimetry revealed no significant differences in thermal stability between native and decellularised meniscus except for in the attachment region where collagen was mechanically manipulated prior to decellularisation. Magnetic resonance imaging (MRI) also revealed no gross differences between native and decellularised bone and meniscus.

Extract and contact cytotoxicity assays were used to determine biocompatibility of decellularised bone-meniscus-bone and residual SDS content determined using radio-labelled $^{14}$C SDS. There was 0.289 $\mu$g.mg$^{-1}$ of residual SDS in decellularised bone-meniscus-bone and assays showed no cytotoxicity to 3T3 and BHK cells. The immunogenic galactose-$\alpha$-1,3-galactose epitope could not be detected in decellularised meniscus by immunohistochemistry.

In conclusion, a protocol for the successful decellularisation of porcine bone-medial meniscus-bone has been developed which retains the structure and tensile properties of native meniscus and is non-cytotoxic. Further investigation is required to determine whether loss of mechanical strength in the bone will prevent effective fixation *in vivo*.

# Table of Contents

# List of figures

# List of tables

# List of Abbreviations

| | |
|---|---|
| **ACL** | Anterior cruciate ligament |
| **AAS** | Atomic absorption spectroscopy |
| **AH** | Anterior horn |
| **AM** | Anterior middle |
| **ANOVA** | Analysis of variance |
| **APCs** | Antigen-presenting cells |
| **ATP** | Adenosine triphosphate |
| **bFGF** | Basic fibroblast growth factor |
| **BHK** | Baby hamster kidney |
| **BM** | Bone marrow |
| **BNB** | Bone-meniscus-bone |
| **BSA** | Bovine serum albumin |
| **CHAPS** | 3-[(3-cholamidopropyl) dimethylammonio]-1-propanesulfonate |
| **CI** | Confidence intervals |
| **CMI** | Collagen meniscal implant |
| **DAB** | 3,3'-diaminobenzidine |
| **DABCO** | 1,4-diazabicyclo [2.2.2]octane |
| **DAPI** | 4',6-diamidino-2-phenylindole |
| **DMEM** | Dulbecco's modified Eagle`s medium |
| **DMMB** | Dimethylmethylene blue |
| **DMSO** | Dimethyl sulfoxide |
| **DNA** | Deoxyribonucleic acid |
| **DPBSa** | Dulbecco's phosphate buffered saline |
| **DSC** | Differential scanning calorimetry |
| **ECM** | Extracellular matrix |
| **EDTA** | Ethylene diaminetetraacetic acid |
| **FA** | Flip angle |
| **FBS** | Fetal bovine serum |
| **GAGs** | Glycosaminoglycans |

| | |
|---|---|
| **GAPDH** | Glyceraldehyde 3-phosphate dehydrogenase |
| **GMEM** | Glasgow's minimal essential medium |
| **H&E** | Haematoxylin and Eosin |
| **HLA** | Human leukocyte antigen |
| **HRP** | Horse radish peroxidase |
| **ICP-MS** | Inductively coupled plasma mass spectrometry |
| **IGF** | Insulin-like growth factor |
| **IL-1β** | Interleukin-1-beta |
| **LCL** | Lateral collateral ligament |
| **LVDT** | Linear variable differential transducer |
| **M** | Middle |
| **MCL** | Medial collateral ligament |
| **MHC** | Major histocompatibility complex |
| **MMP2** | Matrix Metalloproteinase 2 |
| **MMP3** | Matrix metalloproteinase 3 |
| **MRI** | Magnetic resonance imaging |
| **mRNA** | Messenger ribonucleic acid |
| **MSC** | Mesenchymal stem cells |
| **MSD** | Minimum significant difference |
| **NBF** | Neutral buffered formailin |
| **NMR** | Nuclear Magnetic resonance |
| **NOS2** | Nitric oxide synthase |
| **p(DTD DD)** | Poly(desaminotyrosyl-tyrosine dodecyl dodecanedioate) |
| **PAA** | Peracetic acid |
| **PBS** | Phosphate buffered Saline |
| **PCL** | Posterior cruciate ligament |
| **PCR** | Polymerase chain reaction |
| **PERV** | Porcine endogenous retrovirus |
| **PGA** | Poly glycolic acid |
| **PH** | Posterior horn |
| **PLLA** | Poly L-lactic acid |
| **PM** | Posterior middle |
| **PMCP** | Perimeniscal capillary plexus |

| | |
|---|---|
| **PMSF** | Phenylmethylsulfonyl fluoride |
| **PPD** | Poly p-dioxanone |
| **RNA** | Ribonucleic acid |
| **SDS** | Sodium dodecyl sulphate |
| **SIS** | Small intestinal submucosa |
| **TBS** | Tris buffered saline |
| **TE** | Echo time |
| **TGF-β** | Transforming growth factor beta |
| **TR** | Repetition time |
| **UV** | Ultra violet |
| **VEGF** | Vascular endothelial growth factor |
| **α-gal** | Galactosyl-α(1,3)galactose |
| **α-SMA** | Alpha smooth muscle actin |
| **3D-FLASH** | 3D Fast Low Angle Shot |

# Chapter 1.    Introduction

The menisci play a key role in the knee including load transmission, joint stabilization and shock absorption. They are a pair of semi-lunar fibrocartilaginous structures found between the femoral condyles and tibial plateau in the knee joint (Arnoczky *et al.*, 1996; Fithian *et al.*, 1990; Rath & Richmond, 2000).  Meniscal injury is common and can occur from both athletic events and activities of daily living. Treatment of meniscal injury will usually require surgery. Currently the most frequent orthopaedic procedure is arthroscopy which can represent up to 20% of all procedures in the United States (Renstrom & Johnson, 1990).  Until recently total meniscectomy was used to treat meniscal injury.  However, it is now known that this results in supra-physiological stress on the articular cartilage, which can eventually lead to knee damage and osteoarthritis. This has led to efforts in devising alternative treatments that avoid meniscectomy (McDermott & Amis, 2006; Lohmander *et al.*, 2007).  The meniscus does have some ability to repair itself and is limited to the vascularised periphery (Arnoczky & Warren, 1982). This means that any damage suffered to the internal avascular regions is not repaired intrinsically, leading to further deterioration with time.  Therefore, alternative methods are necessary to facilitate meniscal healing.  Tissue engineering techniques aimed at regenerating menisci offer a promising solution, however there is very limited understanding in this field in comparison to other tissues (Hasan *et al.,* 2013).

## 1.1   The Knee Joint

The knee joint is one of several synovial joints in the human body, characterised by the joint capsule surrounding the articulating surfaces of the joint and the presence of lubricating synovial fluid.
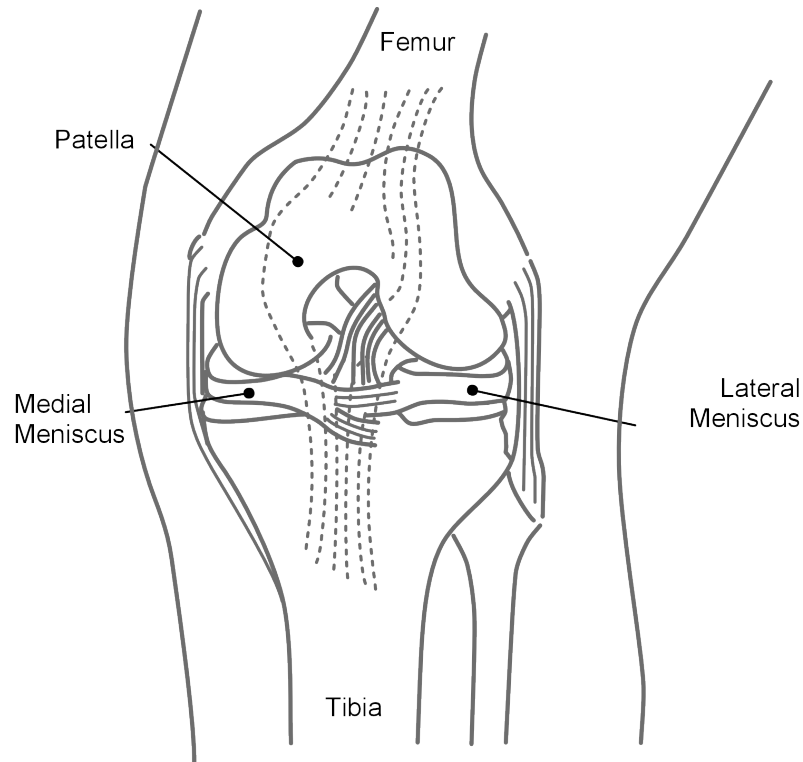
**Figure 1.1: Anterior view of the left knee joint.** Adapted from Hasan *et al.* (2013).

The knee joint consists of four bones, which provide rigidity and structural support. The femur, or thighbone, is attached to the tibia by ligaments and the knee capsule, running parallel to which is the fibula (Figure 1.1). The patella, or knee cap, is located on the anterior face of the knee joint and articulates with the femur along the femoropatellar groove. It is attached to both the quadriceps tendon, connecting it to the quadriceps femoris muscle, as well as the patellar tendon, which connects it to the tibia. The articulating surfaces, the femoral condyles and tibial plateau, are covered in cartilage between which rest the menisci.

### 1.1.1 Ligaments

The knee joint is stabilised by four main ligaments (Figure 1.1): the anterior cruciate ligament (ACL), the posterior cruciate ligament (PCL), the lateral collateral ligament (LCL) and the medial collateral ligament (MCL) (Tham *et al.*, 2008). The ACL is attached to the lateral femoral condyle from where it

inserts itself into the midline of the tibia. The main function of the ACL is to prevent anterior translation of the tibia with respect to the femur. Other functions include prevention of excessive rotation of the tibia as well as limiting varus-valgus angulation and hyperextension of the knee (Tham *et al.*, 2008). During full extension of the knee the ACL is taut and extends parallel to the intercondylar roof notch.

The PCL arises from the posterior intercondylar fossa of the tibia from where it crosses paths with the ACL, giving them a cruciform configuration and hence their names, to attach itself to the lateral aspect of the medial femoral condyle. During full extension of the knee the PCL is lax and has a curved orientation (Tham *et al.*, 2008).

The LCL is attached to the lateral femoral condyle and runs to the lateral side of the fibular head. The LCL has no attachments to the lateral meniscus and is the primary restraint to varus forces in the knee. The MCL runs from the medial condyle of the femur, immediately below the adductor tubercle, to the medial surface of the tibia. Unlike the LCL, it intimately adheres to the medial meniscus.

The meniscofemoral ligaments run from the posterior horn of the lateral meniscus to the lateral aspect of the medial femoral condyle. They are named based on their location in relation to the PCL. The ligament of Humphrey runs anteriorly to the PCL, while the ligament of Wrisberg runs posteriorly. Gupte and colleagues (2002) found a 93% incidence of these ligaments in a cadaveric study, with 50% revealing presence of both. It is important to note this in order not to confuse the presence of these ligaments with pathology as they are not always present.

### 1.1.2  Cartilage

The articulating surfaces in the knee joint are covered in a smooth, white tissue known as articular cartilage, or hyaline cartilage. As its name implies articular cartilage is imperative in the movement of one bone against

another. Articular cartilage is composed of a large proportion of water, with the solid phase consisting of mainly type II collagen and aggrecan (Kempson, 1980). This combination of collagen and aggrecan, through regulation of osmotic pressure, creates a swollen, hydrated tissue that resists compression.

### 1.1.3 The Menisci

The menisci are a pair of semi-lunar, fibrocartilage structures located between the femoral condyles and tibial plateau where they assist in load transmission and shock absorption (Figure 1.1). The proximal surfaces of the menisci are in contact with the femoral condyles and are slightly concave in shape, as opposed to the distal surfaces which are slightly convex and in contact with the tibial plateau (McDevitt & Webber, 1990). The meniscal surfaces are smooth, even when viewed by scanning electron microscopy (Ghadially, 1978). The shape and smoothness of the menisci help accommodate the two articular surfaces with which they are in contact, ensuring smooth movement of the knee joint.

The menisci are not identical in shape or in terms of their respective attachments. The medial meniscus is C-shaped as opposed to the more O-shaped lateral meniscus (Figure 1.2). The medial meniscus is also smaller and less mobile than its counterpart, resulting in an increase in the possibility of injury. The lateral meniscus is uniform in width from anterior to posterior, whereas the medial meniscus is wider near the posterior horn than the anterior horn. In humans, the anterior and posterior horns of both menisci insert into the intercondylar fossa whereas in pigs the posterior horn of the lateral meniscus is attached to the femur. The medial meniscus is more firmly anchored in place than the lateral meniscus due to a continuous attachment to the joint capsule via the MCL.
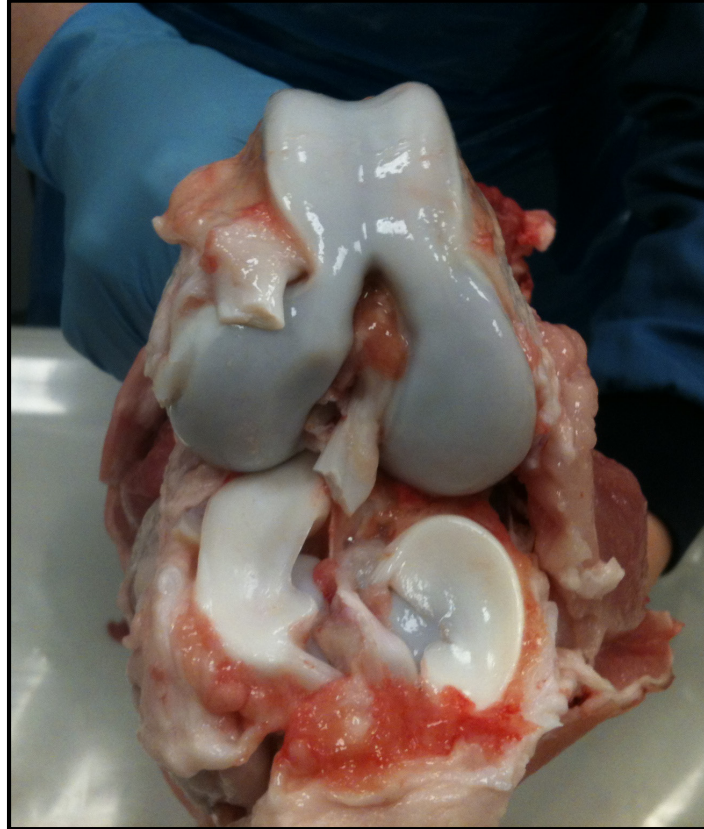
**Figure 1.2**:   **Superior view of porcine tibial plateau showing meniscal attachments**

## 1.1.4  General Structure and Morphology of Menisci

When first formed in the body both the medial and lateral menisci are completely vascular.  This initial vascularity diminishes rapidly with maturity to adulthood when ~10-30% of the meniscus is vascularised (Greis, 2002).  This change in vascularity has been shown to be due to changes in the endostatin/cartilage XVIII level, which acts as an inhibitor to vascular in-growth (Pufe *et al.*, 2004).   Endostatin is present in homogenous concentrations throughout the meniscus in early development, but the levels in the inner two-thirds decrease with age, restricting vascularisation to the periphery of the meniscus.  The vascular supply to the menisci originates from the lateral medial genicular arteries, branches from which form the perimeniscal capillary plexus (PMCP).
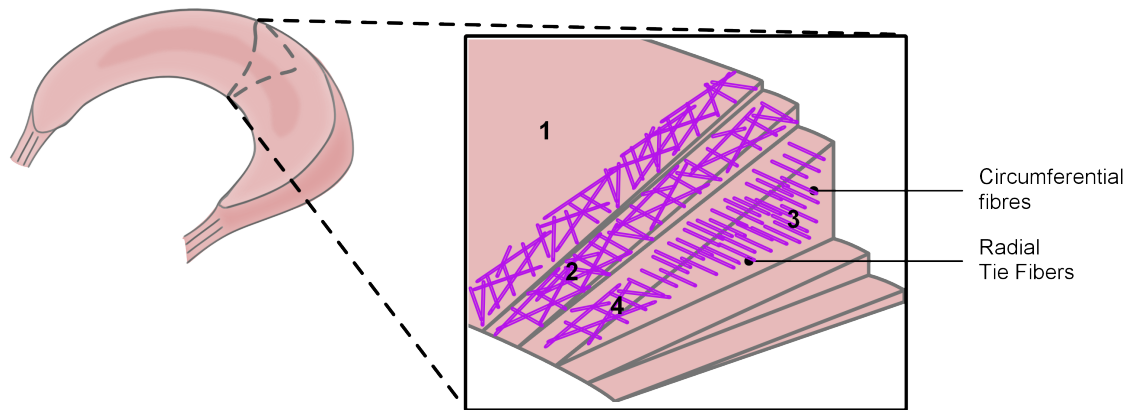
**Figure 1.3**: Meniscus collagen organization (Hasan *et al.,* 2013). Fibres are oriented randomly in the superficial (1) and lamellar (2) layers. Circumferential fibres are present in the red zone (3) and white zone (4) deep portions with radial tie-fibres interspersed.

Three distinct layers of the meniscus have been revealed using scanning electron microscopy:

- A superficial fibril network covering the femoral and tibial surfaces
- A lamellar layer
- A central main layer

As shown in Figure 1.3 the superficial fibril network is composed of a network of fibrils 10 µm wide with no specific orientation, that form a mesh contacting the femoral and tibial surfaces (1). Beneath the superficial network is the lamellar layer (2). The collagen fibrils located in the external circumference of the anterior and posterior segments are arranged in a radial direction. In all other parts the collagen fibril bundles intersect at various angles. The central main region is the main portion of the meniscus and is composed of collagen fibres in a circumferential orientation (3).

The meniscus is more commonly divided into the following regions: The meniscal horn towards the front of the knee known as the anterior region, the meniscal horn towards the back of the knee known as the posterior region, and between the anterior and posterior regions known as the middle region (Figure 1.4).
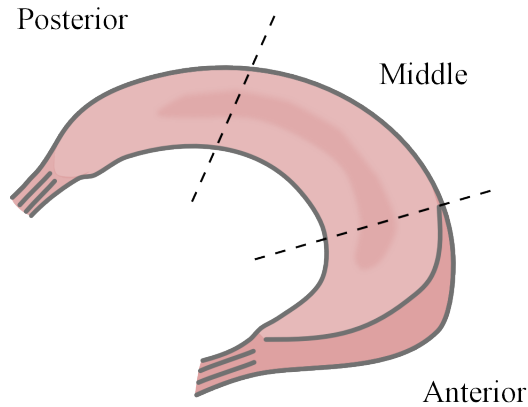
**Figure 1.4: Right medial meniscus showing meniscal regions.**

Further sub-divisions can be made when the meniscus is viewed in cross-section. The vascularised region attached to the capsule is known as the red zone, the avascular region known as the white zone, and the zone in between these two known as the red-white zone.

## 1.2 Meniscal Cell Types

Four morphologically different cell types have been identified in the menisci (Figure 1.5). In the red vascularised margin, consisting mainly of fibrocartilage, cells have been shown to have a stellate appearance and numerous long thin cytoplasmic projections (Figure 1.5; (1)) (Hellio le Graverand *et al.*, 2001). Cells present in the deeper fibrocartilaginous region, which is less extensively vascularised, have been shown to have fewer projections, at most one or two (Figure 1.5; (2)), and the projections join cells from both these regions into sheets (Hellio le Graverand *et al.*, 2001). In the avascular hyaline-like region of the menisci, cells have a more rounded morphology (Figure 1.5; (3)) and are said to be chondrocyte-like, with no projections (Hellio le Graverand *et al.*, 2001). The cells that line the aforementioned regions have been found to be fibroblast-like with fusiform morphology (Figure 1.5; (4)) (Hellio le Graverand *et al.*, 2001). It is this variation that has made it difficult to classify the cells in the menisci, and hence various terms have been used to describe them. For example, fibroblast, chondrocyte, fibrocyte and fibrochondrocyte have all been used to

describe cells found within the menisci (Ghadially *et al.*, 1978; Webber *et al.*, 1985; Hellio le Graverand *et al.*, 2000; Pangborn & Athanasiou, 2005a).  In this review the cells will be termed meniscal fibrochondrocytes in order to avoid confusion.
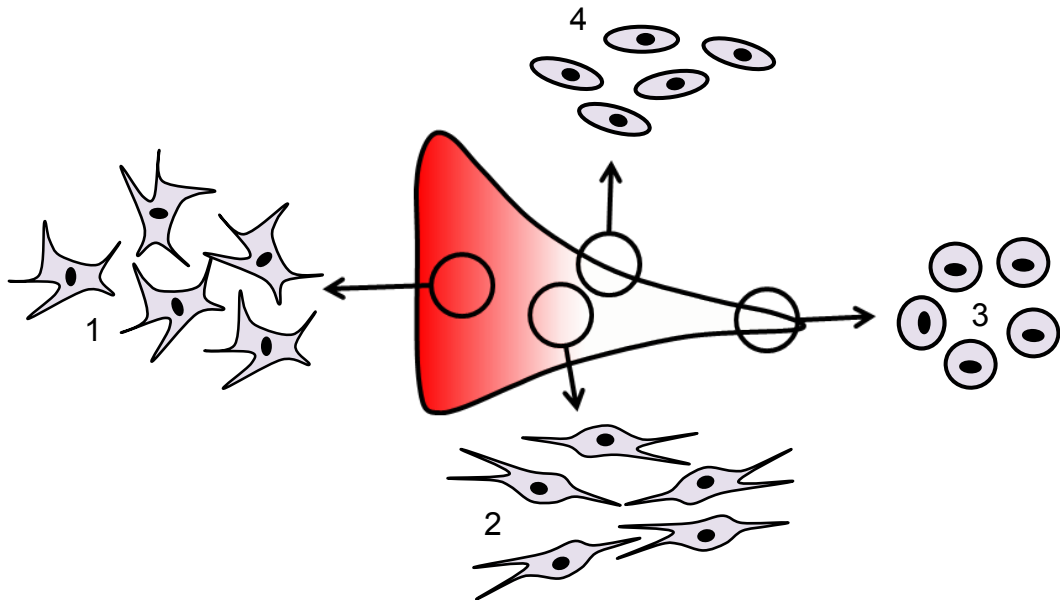


**Figure 1.5:  The morphology and distribution of cell types in the menisci.**  1) Cells in the red zone have many projections and include vascular cells, 2) cells in the red-white zone have fewer projections and have been termed fibrochondrocytes, 3) cells in the white zone are round with no projections and resemble chondrocytes, and 4) cells in the superficial layer are flattened and resemble fibroblasts.

## 1.2.1  Biochemical Constituents

Water has been shown to be the most abundant component of the menisci, constituting 70% of the total wet weight (Brindle *et al.*, 2001), with the remaining 30% composed of organic matter (Figure 1.6).  Of this 30%, collagen accounts for 75% with proteoglycans, cells and adhesion glycoproteins forming the other 25% (Arnoczky *et al.*, 1988; Fithian *et al.*, 1990; McDevitt & Webber, 1990).

Collagen is the most abundant protein in the human body (Gloria *et al.*, 2002) and it has been shown that type I collagen is the predominant meniscal

collagen, accounting for approximately 90% of all collagen present in the menisci (Sweigart *et al.*, 2001). A major type II collagen network is also present; however this network is not as extensive as the hybrid network found in articular cartilage that incorporates the proteoglycan aggrecan (Tanaka *et al.*, 1999; Melrose *et al.*, 2005). Types III, IV, V and VI collagen have also been shown to be present in the menisci but at far lower concentrations (Tanaka *et al.*, 1999; Melrose *et al.*, 2005). Cheung (1987) found the inner one-third of the bovine meniscus resembles hyaline cartilage, both in gross appearance and histology, whereas the outer two-thirds appear fibrocartilaginous. The inner one-third comprises 10% of the wet weight of the whole meniscus with collagen accounting for 70% of the dry weight, compared to the outer two-thirds in which 80% of the dry weight is collagen (Cheung, 1987). Collagen is not the only fibrillar component present in the meniscus. Elastin, accounting for only 0.6% of the dry weight, plays an important role in the recovery of the meniscus from mechanical stresses (Hopker *et al.*, 1986; Sweigart *et al.*, 2001). It is distributed throughout the meniscus, oriented in the direction of the collagen fibres, and the highest levels are found on the peripheral surfaces (Stapleton *et al.*, 2008).
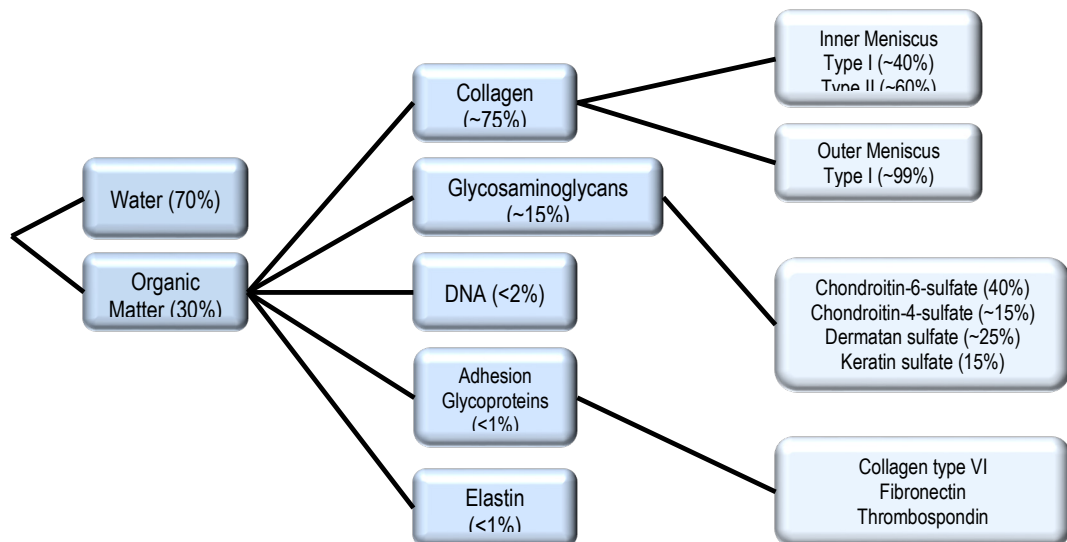


**Figure 1.6: Composition of the meniscus**

Proteoglycans are large, negatively charged hydrophilic molecules composed of a protein core to which one or more glycosaminoglycans

(GAGs) are covalently bound (McDevitt & Webber, 1990). Proteoglycans are commonly separated by size into large and small groups. Large proteoglycan molecules, such as aggrecan and perlecan, assist in the hydration of the meniscus and can entrain 50 times their weight in water (Sweigart *et al.*, 2001). Perlecan plays an important role in the organisation, stabilisation, and cellular attachment and migration within the meniscal extracellular matrix (Melrose *et al.*, 2005). Aggrecan, on the other hand, confers important load-bearing properties to the meniscus, and both perlecan and aggrecan have been shown to be immunolocalised to the tip of the white zone of the meniscus as well as around groups of rounded chondrocyte-like cells in the middle and white zone meniscus (Melrose *et al.*, 2005). Smaller proteoglycans, such as biglycan and decorin, play important roles in load bearing as well as fibril organisation within the meniscus (Sweigart *et al.*, 2001). Work carried out by Scott *et al.* (1997) has shown biglycan as the most abundant small proteoglycan in the menisci, followed by decorin and finally fibromodulin. Biglycan constitutes 53% of the proteoglycan content of the white zone of the porcine meniscus, 52% (w/w) of the red-white zone, and 38% of the red zone (Scott *et al.*, 1997). Decorin constitutes 23%, 28% and 32% of the white, red-white and red zones, respectively (Scott *et al.*, 1997). It has been suggested that the distribution and characteristics of small proteoglycans reflect regional adaptation due to functional demands within the meniscus (Scott *et al.*, 1997). GAGs only constitute a small fraction of total meniscal mass at 0.6-0.8% (Herwig *et al.*, 1984) of which 40% is chondroitin 6-sulphate, 20% is chondroitin 4-sulphate, 20% is dermatan sulphate, 15% is keratan sulphate, and 3% hyaluronan (Herwig *et al.*, 1984). Dermatan sulphate was the predominant GAG chain identified on the small proteoglycans biglycan and decorin (Scott *et al.*, 1997). Meniscal degeneration is shown to decrease GAG content as well as increase water content (Herwig *et al.*, 1984).

## 1.2.2 **Expression Profiles of Meniscal Cells**

Fibrochondrocytes from all regions of the meniscus work in cohort to produce the extracellular matrix molecules required for the meniscus to remain healthy and function properly. The main types of collagen present in the meniscus are types I and II; however collagen III, IV, V and VI are also produced in lower concentrations (Melrose *et al.*, 2005; Stapleton, 2008). The cells of the inner two thirds of the meniscus, which have a more rounded morphology, have been shown to synthesize greater levels of proteoglycans (Tanaka *et al.*, 1999). Proteoglycan synthesis has been shown to be sensitive to transforming growth factor beta (TGF-β) in a dose-dependent manner (Tanaka *et al.*, 1999), suggesting these cells have a chondrocytic phenotype. Perlecan, a large proteoglycan expressed by cells with an oval or rounded morphology, has been shown to be localized in the white zones of the meniscus and strongly cell-associated (Melrose *et al.*, 2005). Levels of perlecan fall with age and degeneration of the meniscus (Melrose *et al.*, 2005). Chondroitin sulphate is the most abundant GAG produced by meniscal cells followed by keratan sulphate (Gruber *et al.*, 2008).

Meniscal cells from different regions of the meniscus have different synthetic profiles and gene expression patterns. Although type I collagen can be found throughout the bovine, canine and porcine meniscus (Kambic & McDevitt, 2005; Melrose *et al.*, 2005; Upton *et al.*, 2006a; Stapleton, 2008), type II collagen is more abundant in the white zone of the meniscus where it forms an organized network (Kambic & McDevitt, 2005; Melrose et al., 2005; Stapleton, 2008). The cells in the white zone also stain positively for alpha smooth muscle actin (α-SMA) giving the cells a contractile phenotype, and hence they have been described as myofibroblasts (Mueller *et al.*, 1999a). Mueller *et al.* (1999a) showed that α-SMA was present in ~10% of cells in normal meniscal tissue; however, during monolayer culturing of these cells α-SMA was present in all cells. White zone cells can generally be characterised by their higher production of type II collagen and the proteoglycan aggrecan (Kambic & McDevitt, 2005; Verdonk *et al.*, 2005a; Valiyaveettil *et al.*, 2005). Messenger ribonucleic acid (mRNA) levels of nitric

oxide synthase (NOS2), a pro-inflammatory enzyme implicated in protein biosynthesis in cartilage and the meniscus (Cao *et al.*, 1998), has also been reported to be higher in the white zone of the porcine meniscus with levels similar to those for hyaline cartilage (Upton *et al.*, 2006a). Gene expression in the red zone more resembles that for fibrous tissues with increased mRNA levels for type I collagen and the proteases MMP2 and MMP3 (Upton *et al.*, 2006a).

### 1.2.3 Effect of Biomechanical Stimulation on Protein Expression

The production of the wide range of proteins in the meniscus is known to vary with age, injury and location in the tissue. However, it is also true that mechanical stimulation can lead to variation. Upton *et al.* (2006c) have shown using finite element modelling that different mechanical stresses are present for different regions of the meniscus. Supplying a biaxial strain to the meniscus leads to cells in the white zone experiencing a 7% tensile strain in the direction of the collagen fibres and the elongated cells experiencing between 2 and 4% (Upton *et al.*, 2006b). Cells from all regions of the porcine meniscus have been shown to increase protein synthesis and nitric oxide production upon experiencing a biaxial strain (Upton *et al.*, 2006c), however white zone cells produced more proteoglycans (Upton *et al.*, 2006c).

Static and dynamic loading conditions produced distinct gene expression patterns in cultures containing isolated porcine meniscal cells and have been found to differentially regulate mRNA levels for different proteins (Upton *et al.*, 2003). Dynamic compression led to a 2.1 fold decrease in the mRNA levels of decorin, a 4.0 fold decrease in type II collagen mRNA and an increase in nitric oxide production (Fink *et al.*, 2001; Upton *et al.*, 2006c). Static compression led to a 4.5-, 3.3- and 4.0-fold decrease in mRNA levels for decorin, type I collagen and type II collagen, respectively (Upton *et al.*, 2006c). There was also an increase in the collagenase mRNA levels suggesting mechanical stimuli can regulate collagen levels (Upton *et al.*, 2006c). Djurasovic *et al.* (1998) attempted to remove mechanical stimuli

from the meniscus to assess changes in aggrecan levels by immobilizing a limb at 90° flexion. This led to a 5.5-fold decrease in the gene expression for aggrecan in the lower portion and a 2.0-fold decrease in the anterior section of the lateral meniscus.

## 1.3    Biomechanical Properties and Functions of the Menisci

Previous studies have shown that the menisci play important roles in joint stabilisation and load transmission (Shoemaker & Markolf, 1985; Fithian *et al.*, 1990; Arnoczky *et al.*, 1996; Rath & Richmond, 2000; Peña *et al.*; 2006). In order to successfully carry out these functions the menisci must withstand the different forces acting on them. The conforming geometry of the menisci gives the first indication of their ability to deal with these forces. The wedge shape increases the congruency between the femoral component and tibial plateau, allowing stable articulation between these surfaces. Beaupré *et al.* (1986) suggested there was direct translation of compressive forces from the white zone wedge shape to tensile forces in the red zone through the meniscal fibres. Both Shaffer *et al.* (2000) and McDermott *et al.* (2004) have measured human menisci with the lateral meniscus measuring ~32-36 mm anteroposteriorly and approximately 27-29 mm mediolaterally. The medial meniscus measures in at ~40-46 mm and ~27 mm in the respective directions (Shaffer *et al.*, 2000; McDermott *et al.*, 2004). In the circumferential direction the lateral meniscus is a little shorter than the medial at ~92 mm and ~99 mm, respectively (McDermott *et al.*, 2004).

### 1.3.1  Collagen Organization

As previously mentioned (Section 1.2.3.1) the menisci are composed of three distinct layers: superficial, lamellar and central (Figure 1.3). The collagen matrix in these layers is highly organized and imparts the necessary

characteristics required to aid the menisci in withstanding the forces acting on them. Fibres in the superficial layer show no specific orientation and this is also true for fibres in the lamellar layer, noting the exception of radially oriented fibres in the anterior and posterior sections (Bullough *et al.*, 1970; Skaggs *et al.*, 1994; Peterson & Tillman, 1998). The fibres in the bulk of the meniscus in the central portion mainly exhibit a circumferential orientation (Bullough *et al.*, 1970; Aspden *et al.*, 1985) along with a few radial fibres which begin at the periphery of the meniscus and travel into the central portion (Ghadially *et al.*, 1983; Fithian *et al.*, 1990; Skaggs *et al.*, 1994). The circumferentially oriented collagen fibres convert axial load into hoop stresses, dissipating it through the meniscus (Krause *et al.*, 1976).

## 1.3.2 **Biphasic Behaviour**

As ~70% of a meniscus is composed of water, with cells and extracellular matrix constituting the remaining 30%, the menisci are considered as biphasic tissues (Favenesi *et al.*, 1983; McDermott *et al.*, 2008a). Zhu *et al.* (1994) demonstrated that it is the interactions between the collagen fibres, negatively charged proteoglycans and water that imparts the biphasic (manifested through time-dependent viscoelastic) properties to the menisci. As load is applied to the meniscus, frictional drag forces help limit water flow as water is forced from the extracellular matrix absorbing some of the initial shock (McDermott *et al.*, 2008a). Once the load is released the negatively charged sulphate and carboxyl groups on the GAGs attract water back in to rehydrate the tissue (Fithian *et al.*, 1990). Finite element analysis has also revealed that the fluid phase initially appears to support a significant portion of the load (Spilker *et al.*, 1992) due to the hydrostatic pressure developed, before further loading leads to transfer of the load from the fluid to the solid phase (McDermott *et al.*, 2008a). Using a non-invasive accelerometry method to detect bone vibrations resulting from gait it has been shown that the shock absorbing capacity of a normal knee is 20% higher than that of a pathological one (Voloshin & Wosk, 1983).

### 1.3.3 **Material Properties**

The material properties of the meniscus govern its ability to function properly within the knee joint. The meniscus has been described as an anisotropic tissue due to the directional variation in its material properties (Fithian *et al.*, 1990; Gabrion *et al.*, 2005). Previous studies have shown that samples of meniscal tissue taken from the central layer in the circumferential direction had much higher moduli than samples taken in the radial direction, whereas tissue samples taken from the randomly oriented superficial layer displayed no such differences (Bullough *et al.*, 1970; Whipple *et al.*, 1985; Proctor *et al.*, 1989; McDermott *et al.*, 2008a).

### 1.3.4 **Compressive Properties**

The compressive modulus, a measure of stiffness, and the permeability, a measure of the ease at which fluid flows through a material, are the two most discussed compressive properties in the literature. DeHoll *et al.* (1999) assessed these two properties in bovine medial menisci using an automated creep indentation method and, although there were no differences in permeability, the aggregate modulus was found to be 50% and 91% higher in the anterior portion than the posterior and central portions, respectively. Confined compression creep testing and direct permeability testing found the mean water content of the meniscus to be 73.8%, with the mean aggregate modulus and permeability 0.41 MPa and 0.81 x $10^{-15}$ $m^4N^{-1}s^{-1}$ (Proctor *et al.*, 1989), respectively. The mean values for the aggregate modulus and permeability are displayed in Table 1.1. Disparity in these results may have arisen from differences in curve-fitting and testing methods, from the biphasic theory applied by Proctor *et al.* (1989)*,* an alternatively developed local optimization technique applied to the biphasic theory by Joshi *et al.* (1995), and the finite element analysis used by Sweigart *et al.* (2004).

**Table 1.1: Compressive biphasic properties of the meniscus**

| Reference | Source | Meniscus | Aggregate Modulus (MPa) | | | Permeability $(10^{-15}\ m^4\ N^{-1}\ s^{-1})$ |
|---|---|---|---|---|---|---|
| | | | Anterior | Central | Posterior | |
| Proctor *et al.* (1989) | Bovine | Medial | 0.38 | 0.40 | 0.49 | 0.81 |
| Joshi *et al.* (1995) | Bovine | Medial | - | - | 0.11 | 3.6 |
| | Human | Medial | - | - | 0.22 | 2.0 |
| DeHoll *et al.* (1999) | Bovine | Medial | 0.19 | 0.13 | 0.12 | 5.6 |
| Sweigart *et al.* (2004) | Bovine | Medial | 0.19 | 0.13 | 0.12 | 5.6 |
| | Human | Medial | 0.16 | 0.11 | 0.10 | 1.8 |

When bearing load the knee joint is subjected to compression and hence contact stresses. The larger the contact area the smaller the contact stresses, and vice-versa. Walker and Erkman (1975) showed using casting methods that under a 150 kg load the contact areas covered by the menisci were between 59 and 71%. Another study showed that there was an increase in joint contact pressure of up to 235% after removal of menisci, due to concentration of load onto a much smaller joint contact area (Baratz *et al.*, 1986). The menisci, through optimisation of congruency between the femoral condyles and tibial plateau, increase the joint contact area and hence reduce joint contact stresses (Figure 1.7). Fukubayashi and Kurosawa (1980) showed that meniscectomy reduces the contact area from 115 mm$^2$ to 52 mm$^2$ while increasing peak contact pressure from 3 MPa to 6 MPa. In another study it was shown that a healthy knee can absorb up to 52% of load exerted on it whereas a degenerate joint could only absorb around 24% (Hoshino & Wallace, 1987). It has also been suggested that meniscectomy accelerates cartilage deformation by slowing recovery of cartilage due to the increased contact pressures (Song *et al.*, 2008).

Meniscus

A

B

Femoral

Condyle

Tibial

Plateau

Intact knee

After meniscectomy
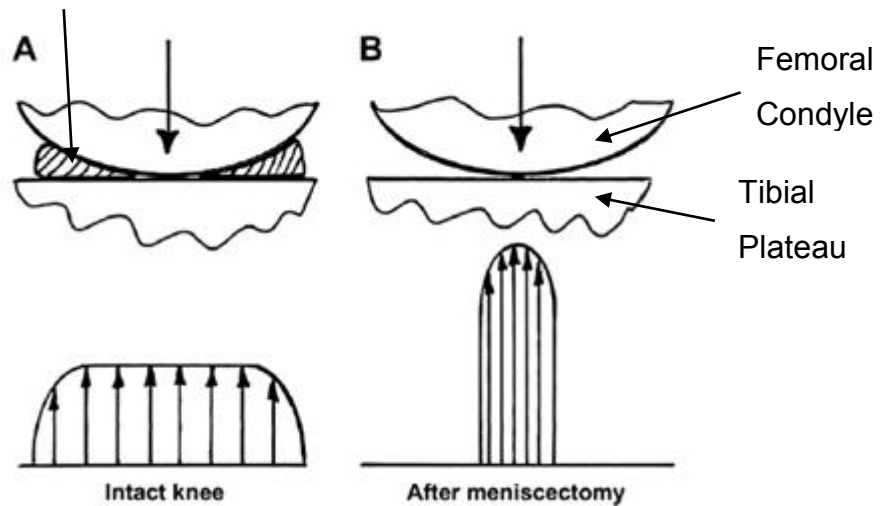
**Figure 1.7: Joint contact areas with and without menisci (McDermott and Amis, 2006).** A) The menisci improve congruency between the femoral condyles and the tibial plateau, increasing joint contact area and hence reducing contact pressure. B) Removal of the meniscus reduces the joint contact area thereby increasing contact pressure.

### 1.3.5 Tensile Properties

It is clear from the literature that a standard method for testing the tensile strength of meniscal tissue is not available. Sample geometry varies from the typical dumbbell shape specimens to the uniform width rectangular specimens. However, the use of dumbbell shaped samples has no rationale in meniscal tensile testing due to the presence of non-continuous fibres present in the wider sections where splitting can occur (McDermott *et al.*, 2008a). It is also evident that tissue specimen dimensions play a critical role in the tensile properties as described by Lechner *et al.* (2000). Standard testing assumes that the material being tested is homogeneous, whereas meniscal tissue is composed of collagen fibres of varying diameters as well as weak matrix tissue (Petersen & Tillmann, 1998). It was found that 27% of thinner samples failed prematurely during testing as opposed to only 17% of thicker samples (Lechner *et al.*, 2000). This suggests the thinner samples that were successfully tested had a higher proportion of collagen fibres,

increasing the tensile modulus (Masouros *et al*, 2008). A summary of tensile properties of meniscal samples of varying dimensions is shown in Table 1.2.

**Table 1.2**: **Tensile properties of the meniscus (Adapted from Masouros et al., 2008)**

| Reference | Source | Meniscus | Geometry | Sample Dimensions (mm) | Tensile Modulus (MPa) |
|---|---|---|---|---|---|
| Proctor *et al.* (1989) | Bovine | Medial | Dumbbell | 0.4 x 1.0 | 129 |
| Fithian *et al.* (1990) | Human | Medial | | - | 118 |
| Tissakht & Ahmed (1995) | Human | Medial | Rectangular | 1.5-2.0 x 1.75-3.0 | 83 |
| Goertzen *et al.* (1997) | Bovine | Medial | Dumbbell | 0.75 x 2.6 | 316 |
| Lechner *et al.* (2000) | Human | Medial | Dumbbell | 0.5 x 1.0<br>1.5 x 1.0<br>3.0 x 1.0 | 121<br>85<br>60 |

Regional variations in the tensile properties of the meniscus have also been demonstrated. The general trend in the medial meniscus appears to show that the stiffness for the anterior region is higher than that for the central and posterior regions (Fithian *et al.*, 1990; Tissakht & Ahmed, 1995; Lechner *et al.*, 2000; Chia & Hull, 2008; Bursac *et al.*, 2009). Lechner *et al.* suggested this was due to a greater density of collagen fibres in the radially thinner anterior horn of the medial meniscus imparting higher stiffness to the tissue. It has been shown that the lateral meniscus exhibits higher tensile moduli than the medial (Tissakht & Ahmed, 1995). It has also been shown that there is a higher GAG content in the anterior medial meniscus than in the posterior or central regions, which results in a greater ability to resist compressive forces through hydrostatic pressure (Chia & Hull, 2008; Bursac *et al.*, 2009).

## 1.3.6 **Load Bearing and Transmission**

It has been well established that the menisci perform load bearing functions within the knee joint. Forces acting on the knee during normal activities such as walking or climbing stairs can reach between 2.7 to 4.9 times bodyweight (Paul, 1976). It has been suggested that the menisci bear anywhere between 45% and 75% of the load transmitted through the knee (Shrive, 1974; Krause *et al.*, 1976; Peña *et al.*, 2006) and this is dependent on health of tissue as well as level of flexion. As the knee flexes the contact area between the condyles diminishes by 4% for every 30° of flexion under a 150 kg load (Walker & Hajek, 1972). Without the menisci the contact areas decrease to between a third and a half, and subsequently stresses increase 2 to 3 fold (Kurosawa *et al.*, 1980). When investigating load absorbing mechanisms in the knee, Hoshino and Wallace (1987) showed that the transmitted force increased by 180% in a replacement knee. It was also found that the peak force transmitted increased as degeneration of menisci, cartilage and subchondral bone progressed.

Even though the menisci are attached to the tibial plateau at the posterior and anterior horns a small amount of displacement occurs during flexion (Figure 1.8). This displacement allows the menisci to maintain congruency between the surfaces and optimise load bearing. Using an MRI system these displacements have been measured revealing anterior horn displacement of 7.1 mm and 9.1 mm for medial and lateral menisci, respectively (Vedi *et al.*, 1999). The lateral meniscus is more mobile than the medial meniscus as it is not as tightly attached to the joint capsule. Due to this immobilisation the medial meniscus is subjected to higher contact stresses which may contribute to an increased frequency of injury, particularly to the posterior horn.
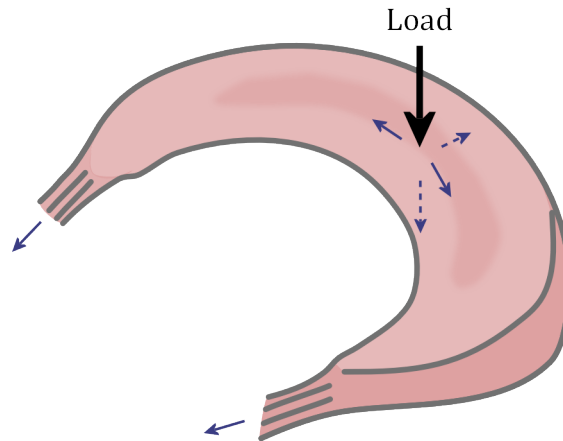
**Figure 1.8: Transmission of load through the meniscus (Hasan *et al.*, 2013).**

### 1.3.7 **Stabilisation**

As well as playing a major role in load bearing, the menisci have been shown to assist in joint stabilisation. Although the ACL plays the most important role in stabilising the knee joint (Levy *et al.* 1982), it has been shown that the menisci act as secondary stabilisers. Levy *et al.* (1982) showed that although meniscectomy has no significant impact on stabilisation of normal knee joints, in ACL deficient knees the medial meniscus restricts displacement of the tibia, stabilising the knee joint. They went on to suggest that when the ACL is disrupted, displacement of the tibia wedges the medial meniscal horn between the bones and prevents further displacement. Further work on meniscal stabilisation after ACL resection has shown that there is an increase of 197% in the forces within the medial meniscus (Allen *et al.*, 2000). It has also been shown that meniscectomy of the ACL deficient knee resulted in further anterior translation of the tibia.

### 1.3.8 **Lubrication and Tribology**

As the menisci are located between two articulating surfaces, it has been suggested that they play a role in joint lubrication. Using a tribological simulation, McCann *et al.* (2009) studied the friction and wear of bovine knee

articular cartilage. They found that meniscectomy increased peak contract stress under a 1000N load from 4.9 MPa to 17.1 MPa leading to an increase in frictional shear stress and biomechanical wear of the underlying cartilage. Lubricin (PRG4), a protein found in synovial fluid implicated in lubrication and anti-adhesion, has been detected on the meniscal surface, ligaments, synovium and cartilage using immunostaining techniques (Sun *et al.*, 2006; Lee *et al.*, 2008). Lubricin was also detected within and near meniscal cells along the radial tie fibres and circumferential meniscal cells by Schumacher *et al.* (2005) who suggested that lubricin was synthesized and secreted by meniscal cells and may play a role in boundary lubrication. It has been shown that synovial fluid lacking lubricin failed to reduce friction and increased wear in the knee joint (Jay *et al.*, 2007). These results were supported by Schmidt *et al.* (2007) who found that lubricin and hyaluronic acid contribute to low friction in a dose dependent manner, both individually and also in synergy. Lubricin levels have also been shown to be affected by the onset of disease and degeneration (Teeple *et al.*, 2008). Lubricin levels were found to be lower in ACL-deficient knees leading to further degeneration of the joint (Teeple *et al.*, 2008), and have been shown to be regulated by transforming growth factor beta 1 (TGF-$\beta$1), which enhances lubricin expression, and interleukin-1-beta (IL-1$\beta$), which reduces lubricin expression and is highly expressed in arthritic joints (Lee *et al.*, 2008).

## 1.4 Meniscal Injury and Degeneration

Normal menisci are semi-lunar, fibrocartilage structures. Deviations from this can occur in several ways including disease, degeneration, traumatic injury or abnormal development. Abnormal development usually results in a discoid meniscus, where the white zone extends over the cartilage surfaces to either completely or partially cover them, forming a disc-like structure (Vandermeer & Cunningham, 1989). The incidence of discoid menisci has been reported to be between 0.8 and 5% and can cause pain, clicking and limitation of joint motion (Vandermeer & Cunningham, 1989; Washington *et*

*al.*, 1995). The menisci are also affected by metabolic diseases such as calcium pyrophosphate crystal deposition, hemochromatosis and ochronosis which can cause calcification as well as discoloration of meniscal tissue (Bjelle, 1981). These afflictions leave the menisci unable to function normally and, as they are due to systemic changes within the body, cannot be treated locally. Other conditions such as degeneration and trauma can be treated as they directly affect the meniscus.

## 1.4.1 Degeneration

It is known that degeneration renders the menisci more prone to injury (Hough & Webber, 1990). Osteoarthritis leads to degenerative changes in the menisci as well as the surrounding cartilage, and has been implicated in ~75% of all meniscal tears and extrusions (Berthiaume *et al.*, 2005; Lange *et al.*, 2007). Osteoarthritis affects the geometry of menisci, causing thickening of the medial posterior and lateral anterior horns. This in turn can affect the biomechanics of the tissue leading to injury (Bamac *et al.*, 2006). Adams *et al.* (1983) assessed the GAG content of menisci in beagles induced with osteoarthritis. It was found one week after induction that the water content increased as the GAG content decreased, however after 15 months the water content had returned to normal and the GAG content had reached elevated levels, suggesting stiffening of the tissue. In another study it was shown that osteoarthritis leads to joint space narrowing (Sugita *et al.*, 2001). This is due to radial displacement of the medial meniscus, which preserves this part of the tissue but compromises all other functionality, potentially leading to injury.

## 1.4.2 Injury and Epidemiology

The most common form of meniscal injury is mechanical failure of the tissue due to degeneration or trauma resulting in a tear. Meniscal tears (Figure 1.9) can be categorised into the following types: Longitudinal, horizontal,

radial, oblique and complex (Smillie, 1968; Greis *et al.*, 2002; Boyd & Myers, 2003; Schlossberg *et al.*, 2007). Longitudinal tears occur in a vertical direction and can vary in length from ~1mm to the length of the meniscus (Greis *et al.*, 2002). A variation of a longitudinal tear is known as the bucket handle tear and these occur when the tear spans the entire thickness of the meniscus, splitting a section mediolaterally (Greis *et al.*, 2002; Schlossberg *et al.*, 2007). Oblique tears also occur in a vertical direction however these tears start from the white zone of the meniscus and slant inwards, and along with longitudinal tears have been shown to make up 81% of all tears (Greis *et al.*, 2002). Horizontal tears develop due to shear stresses generated by inferior and superior sections of the meniscus and are more common in elderly patients (Greis *et al.*, 2002). Radial tears are similar to oblique tears in that they begin at the edge of the white zone however radial tears extend radially towards the periphery and disrupt the meniscus' ability to contain hoop stresses (Greis *et al.*, 2002; Boyd & Myers, 2003). Complex tears are composed of several different tears, associated with degeneration and incidence has been shown to increase with age (Greis *et al.*, 2002; Boyd & Myers, 2003).

The causes of meniscal injury can be divided into 3 types: sports injuries, non-sporting injuries, and unidentifiable injury. Sporting injury is injury incurred through sporting activities and accounts for 32.4% of all meniscal injury with a mean age of ~33 years at time of injury (Drosos & Pozo, 2003). Non-sporting injuries account for 38.8% of all tears, the majority (71.9%) of which occur through daily activities, with a common cause cited as ascent from a squatting position (Drosos & Pozo, 2003). The remaining 28.8% arise through unidentifiable injury (Drosos & Pozo, 2003). Degenerative changes may be responsible for the occurrence of the non-sporting and unidentifiable injuries as these tend to occur with increasing age (~42 years of age) and require far less force than injuries occurring through sport (Drosos & Pozo, 2003).
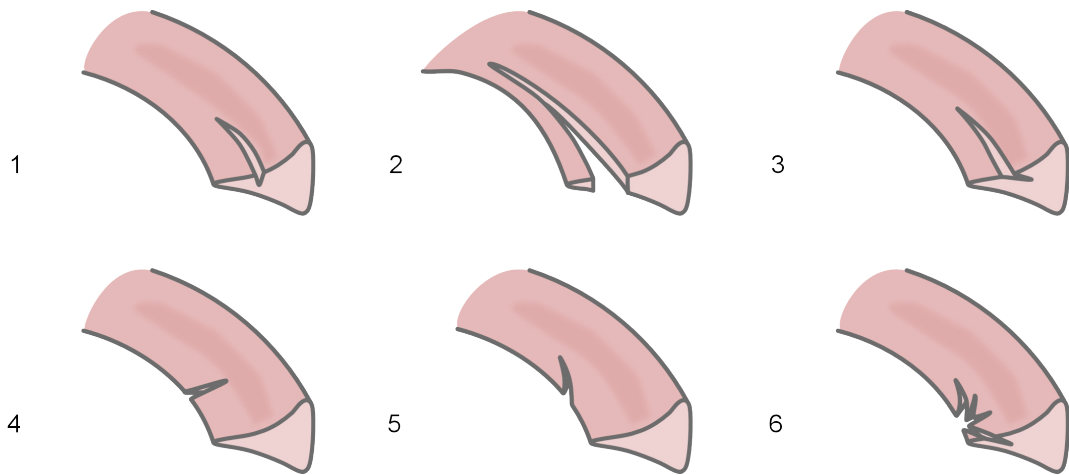
**Figure 1.9: Meniscal tears.** 1) Longitudinal, 2) Bucket-handle, 3) Horizontal, 4) Radial, 5) Oblique, 6) Complex.

Meniscal tears can reveal themselves through various symptoms. Common symptoms include pain, a catching sensation, "giving way" and effusion (Choi & Victoroff, 2006). Incidence of meniscal tears has been shown to be approximately 60-70 per 100,000 with 70-80% of tears occurring in males (Dandy, 1990; Greis *et al.*, 2002). Dandy (1990) showed that tears appear to be more common in the right knee with 56.5% of tears occurring in this location. The majority of medial meniscal tears have been found to be longitudinal (75%) with horizontal tears (23%) second most common (Dandy, 1990), whereas longitudinal tears constituted a smaller proportion of tears in the lateral meniscus (54%) and, oblique (15%) and complex (15%) tears represented similarly large proportions (Dandy, 1990). It has also been suggested that the meniscus is reliant on the ligaments of the knee as there is an increase in meniscal injury with ACL deficiency (Noyes *et al.*, 1980; Allen *et al.*, 2000; Greis *et al.*, 2002). Moglo and Shirazi-Adl (2002) showed that through to 30° of flexion the medial meniscus is subjected to higher loads and stresses in an ACL-deficient knee. This suggests that the meniscus is heavily reliant on the ligaments of the knee to function properly and remain healthy.

### 1.4.3 **Meniscectomy**

Total meniscectomy was used widely to treat meniscal injuries and defects however once meniscectomy had been described as "not totally innocuous" (Fairbank, 1948) repair of the meniscus was popularised. Total meniscectomy has been shown to produce clinically good results 10 years after surgery (Perey *et al.*, 1962) however it has since come to light that meniscectomy causes joint space narrowing, lowers the rate of regeneration, leads to an increase in the degenerative changes in the surrounding cartilage, and hence a higher incidence of osteoarthritis (Fairbank, 1948; Jackson, 1968; Cox et al., 1975; McGinity et al., 1977; Allen et al., 1984; Moon & Chung, 1988; Messner & Gao, 1998; Shelbourne & Dickens, 2007). These discoveries facilitated a switch to partial meniscectomy as the chosen form of treatment as well as surgical repair and implantation (Fairbank, 1948; Messner & Gao, 1998; Brindle et al., 2001) and partial meniscectomy is currently one of the most commonly performed arthroscopic procedures. It preserves the load distribution characteristics of the meniscus (Burks et al., 1997; Messner & Gao, 1998) with studies showing the amount of degeneration that takes place after partial meniscectomy is proportional to the amount of tissue resected during the procedure (Cox et al., 1975; Berjon et al., 1991; Burks et al., 1997; Andersson-Molina et al., 2002). Although results are favourable when compared to total meniscectomy (Burks et al., 1997; Shelbourne & Dickens, 2007), degeneration still occurs. Restoration of meniscal tissue to its native state is most desirable and this can be achieved by promoting a healing response.

### 1.4.4 **Repair and Regeneration**

Surgery related to the meniscus accounts for around one million procedures a year in the United States of America alone (Rodkey *et al.,* 1999; Cook *et al.,* 2006) burdening health services in terms of time, expenditure and resources. Many meniscal surgeries are secondary surgeries and so a reduction in the number of these surgeries would prove highly beneficial to

the health services providing them, allowing reallocation of resources to more urgent departments.

The meniscus is not a homogeneous tissue hence its capacity for healing is limited. As only the red zone is vascularised (Figure 1.10), general prognosis for healing is excellent in this area (Brindle *et al.*, 2001). Healing is poorest in the avascular white zone as there is no access to a blood supply or source of reparative cells (Arnoczky & Warren, 1983; Brindle *et al.*, 2001). Current repair techniques are only effective in the vascularised zone of the meniscus but fail to encourage healing in the avascular zone (Adams *et al.*, 2005). Several methods have been devised to aid the healing of the meniscus, ranging from the creation of channels to introduce blood and reparative cells to tears; to suturing and resorbable scaffolds (Ghadially *et al.*, 1986; Zhang *et al.*, 1988; Gershuni *et al.*, 1989; Fox *et al.*, 1993; Zhang *et al.*, 1995; Zhang & Arnold, 1996). Trephination involves the creation of a channel from the vascularised zone to the tear (Zhang & Arnold, 1996) with use of this method resulting in very good results with Fox *et al.* (1993) reporting good results in 90% of cases and Zhang *et al.* (1988) showing that trephination led to healing of all tears, either partially or fully. Trephination provides an improved healing rate in the white zone compared to suturing alone (Zhang & Arnold, 1996). Suturing may stabilise a tear, however it does not encourage healing due to the lack of a blood supply (Zhang *et al.*, 1995). Other ways of introducing a blood supply and/or reparative cells to the site of injury are using a vascularised synovial flap or a fibrin clot (Ghadially *et al.*, 1986; Arnoczky *et al.*, 1988; Gershuni *et al.*, 1989; Shirakura *et al.*, 1997). Ghadially *et al.* (1986) created bucket-handle tears in the avascular zone of ovine menisci and repaired them using sutures alone or by introducing a flap of synovium to the tear. Menisci that were sutured did not display any indication of healing; whereas the menisci repaired using synovium showed some healing. These results are supported by another study in which 11 of 35 menisci repaired using a free synovium flap were healed as opposed to none in the control groups (Shirakura *et al.*, 1997). Use of a fibrin clot in meniscal lesion repair has shown that it is possible to repair tears in the avascular zone using this method (Arnoczky *et al.*, 1988). Surgical

techniques range from arthroscopic to open repair (DeHaven *et al.*, 1999). There are various alternatives to suturing available that work on the same premise. The Meniscus Arrow (Bionx, Blue Bell, Pennsylvania), The Meniscal Dart (Arthrex, Naples, Florida), The T-Fix Suture Bar (Smith & Nephew, Endoscopy Division, Andover, Massachusetts), and The Clearfix Meniscal Screw (Johnson & Johnson) (DeHaven *et al.*, 1999; Farng & Sherman, 2004).

The nature of the repaired tissue must also be considered when critiquing a technique. Ideal repair tissue should be as similar to native meniscal tissue histologically, morphologically and biomechanically as possible. It has been shown that calcification increases with meniscal injury and may be a secondary symptom of degeneration (Noble & Hamblen, 1975). Apoptosis also increases with meniscal degeneration or trauma and is seen in chondral tissues of patients with osteoarthritis (Uysal *et al.*, 2008). Repair tissue similar to normal meniscal repair tissue has been produced using a fibrin clot however it was dissimilar to normal meniscal tissue (Arnoczky *et al.*, 1988). The biomechanical strength of meniscal repair tissue must also be considered. Meniscus repaired using sutures or a fibrin clot had regained 26% and 42.5% of its original strength for the suture and fibrin glue techniques, respectively. A secondary area of weakness was also discovered in the peri-scar tissue in the line of the scar and this reduced in size after 12 weeks of healing (Roeddecker *et al.*, 1994).
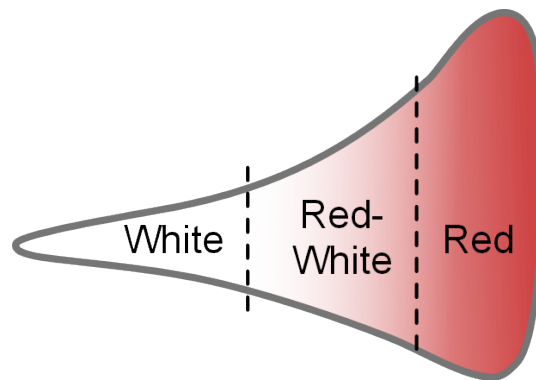
**Figure 1.10: Vascularisation of the meniscus.** The level of healing that takes place is proportional to the level of vascularisation in the meniscus. Red represents vascularised tissue, with white representing avascular tissue.

### 1.4.5 **Replacement**

Replacement of the meniscus is more favourable than repair as it has a greater potential to protect the joint surfaces. Transplantation also becomes an option when patients have suffered degenerative changes to the joint due to previous meniscectomy or when an irreparable tear is encountered. There are two main types of meniscal transplantation: autogenous and allogeneic.

#### 1.4.5.1    Autogenous transplantation

Autogenous transplantation refers to transplantation of tissue originating within the individual to whom it is to be applied. The advantages of autogenous transplants are that they are not rejected by the immune system and there are no issues regarding transmission of infection. Disadvantages include size limitations, longer time in surgery and cosmetic issues due to harvesting of tissue, and donor site morbidity. Tissue has been sourced from a variety of locations including the patellar tendon (Kohn *et al.*, 1992; Johnson & Feagin, 2000) and quadriceps (Kohn, 1993). In order to assess the viability of autogenous transplantation, as well as provide a premise for allogeneic transplantation, Stone *et al.* (1995) carried out autogenous

transplantation of meniscal cartilage in dogs. In this study the meniscus was excised and replanted and gross healing occurred in 50% of cases. Collagen abnormalities at the healing interface and within the tissue were noted and limping was seen in 79% of dogs. Degenerative joint disease in the form of joint space narrowing and osteophyte formation was also seen in 50% of dogs. The method of fixation could have affected the results and fixation using bone plugs may improve outcomes as even though the replacement tissue was fresh and ideally sized it has been shown that fixation using bone plugs yields improved results compared to soft-tissue fixation (Paletta *et al.*, 1997, Kim *et al.*, 2012). The authors went on to conclude that since a seemingly perfect model of meniscal replacement, where menisci were autogenous, fresh and perfectly matched in size, had failed to produce successful results, it was doubtful that studies using autografts and allografts would produce favourable results. The same approach was repeated in an ovine model and showed autogenous transplants to have a protective effect on articular cartilage (Szomor *et al.*, 2000). Studies on the potential of autografts for meniscal replacement are summarised in Table 1.3.

Although the basis for autogenous transplantation is good, evidence indicates that this does not translate clinically. Problems arise with the biomechanics of the grafted tissue as it is less able to withstand the forces encountered in the knee. This may be due to insufficient remodelling and vascularisation, and in some cases shrinkage of the graft leading to exposure of cartilage surfaces resulting in continued degeneration. Hence, meniscal autografts are not seen as a suitable replacement for menisci.

### 1.4.5.2    Allogeneic transplantation

Allogeneic transplants are grafts taken from genetically non-identical members of the same species. Advantages of allogeneic transplants are that there is no donor site morbidity, they are cosmetically better and less time is spent in surgery as there is no need to harvest from the recipient. There are also no size limitations therefore revisions can be made depending on requirements during surgery (Prokopis & Schepsis, 1999). As the

donated tissue is not genetically identical, there may be problems with immune rejection, and disease transmission is a possibility (Nemzek *et al.*, 1994; Tomford, 1995; Prokopis & Schepsis, 1999; Golshayan *et al.*, 2007). It is also a more costly process than autogenous transplantation (Prokopis & Schepsis, 1999).  Historically disease transmission was a real concern in transplants especially as it is not always possible to detect viruses in transplanted material (Tomford, 1995).  Human immunodeficiency virus (HIV), syphilis, and hepatitis B and C are all transferable via transplantation. In a study carried out by Nemzek *et al.* (1994) of retroviral transmission in transplanted menisci and patellar ligaments, although there was no rejection of grafts, transmission of retrovirus occurred in all cases.  In order to address this issue sterilisation of tissue using gamma irradiation has been undertaken, however the dose required has been shown to produce detrimental changes in the viscous and elastic properties of the graft (Yahia *et al.*, 1993; Vangsness *et al.*, 2003).  Tissue banking services in the UK perform mandatory screening on all donated tissue for HIV, hepatitis C virus (HCV), hepatitis B virus (HBV) and syphilis.  Additional testing may be required for malaria, West Nile virus and Chaga's disease (Section 20 - Tissue banking: selection of donors, Guidelines for the Blood Transfusion Services).

Allografts described in the literature are fresh, fresh-frozen, cryopreserved and freeze-dried.  Various studies have been carried out using the different types in human and animal models, and these are summarised in Table 1.4 and Table 1.5, respectively.  Rejection of grafts does not seem to be an issue with a low level immunological reaction reported at most (Rodeo *et al.*, 2000). Fresh grafts have been reported to be superior due to the fact that viable cells are present and able to produce extracellular matrix once transplanted (Rodeo *et al.*, 2000).  However it had already been shown that all donor cells are replaced by host cells after implantation (Jackson *et al.*, 1993). Disadvantages of fresh grafts include difficulty in sizing, sterility and availability (Shelton, 2007).  They also produce the most pronounced immunologic reaction (Peters & Wirth, 2003).  Cryopreserved grafts maintain a viable cell population and so have been used as an alternative to fresh

grafts. However, frozen grafts have been considered more favourable than cryopreserved grafts as freezing is less costly and there is less chance of transmission of infection due to loss of cell viability (Fabbriciani *et al.*, 1997). The number of times a graft is frozen and thawed has been shown to have an effect on a meniscus' ability to withstand compression (Lewis *et al.*, 2008). Menisci subjected to a single freeze-thaw cycle have been shown to have a higher Young's modulus than menisci that underwent four cycles of freezing and thawing (Lewis *et al.*, 2008). Freeze-drying leads to shrinkage and has an adverse effect on the biomechanical properties of grafts and is no longer recommended (Sekiya & Ellingson, 2006). Since it has been shown that any remaining donor cells are gradually replaced by host cells (Arnoczky *et al.*, 1992; Jackson *et al.*, 1993; Rodeo *et al.*, 2000), it may be more important to maintain the extracellular matrix for a functioning transplant (Beaver *et al.*, 1992).

It should also be noted that fixation methods, sizing, alignment of the joint, and patient selection are all critical in the success of a transplant. Suture-only fixation techniques, as opposed to bone-blocks in addition to sutures, can lead to increases in peak contact pressure and tears where sufficient healing has failed to take place (McDermott *et al.*, 2008b). Fixation plays an important role in the level of congruity achieved in the joint and is essential for function through development of hoop stresses upon loading, the mechanism by which the meniscus protects the articular cartilage (McDermott *et al.*, 2004). Bone-blocks may produce better clinical results (Rodeo *et al.*, 2000), however accurate placement of these bony attachments is crucial to success, and inaccurate placement has been shown to produce unfavourable results (Szomor *et al.*, 2000). The size of the graft is also critical to achieving congruity, and this can be predicted accurately (5% mean error) from tibial plateau measurements (McDermott *et al.*, 2004).

**Table 1.3: Meniscal autograft studies**

| Reference | Model | Meniscus | Autograft used | Findings |
|---|---|---|---|---|
| Jackson *et al.* (1992) | Caprine | Medial | Meniscus | Normal peripheral revascularisation and healing. Water content increased by 6% and proteoglycan content increased. |
| Kohn *et al.* (1992) | Ovine | Medial | Patellar tendon | Remodelling and revascularisation of tissue. Lower failure stress and tensile modulus compared to normal meniscus. Shrinkage of meniscus. Some degenerative changes |
| Kohn (1993) | Ovine | Medial | Infrapatellar fat pad Patellar tendon | Lower tensile properties than in normal. Higher for tendon than fat pad graft. |
| | Human | | Quadriceps tendon | No complications or further cartilage degeneration. |
| Stone *et al.* (1995) | Canine | Medial | Autogenous meniscus | Gross healing in 50%. Significant collagen organisation abnormalities. |
| Bruns *et al.* (1998) | Ovine | Medial | Perichondral tissue | Remodelling of graft to resemble meniscus. Lower failure stress and tensile modulus compared to normal. Less intense revascularisation than in normal meniscus. Calcification in central meniscal regions. Menisci retained normal size |
| Johnson & Feagin (2000) | Human | Lateral | Semitendinosus tendon (4) Patellar tendon (1) | Slight clinical improvement in one patient. Joint surface was not preserved. |
| Szomor *et al.* (2000) | Ovine | Medial | Autogenous meniscus (8) Allogeneic meniscus (8) | Gross healing to periphery for all transplants. Transplants reduced damage to articular cartilage when compared to meniscectomy. Mild surface fibrillation and Fibrinoid degeneration. |

There is much discussion as to what level of error is acceptable and further studies on the sensitivity of the knee joint to sizing errors is needed. Various studies have shown that correction of joint alignment in addition to transplantation can aid the success of the procedure (Beaver *et al.*, 1992; Garrett, 1993; van Arkel & de Boer, 1995; Cameron & Saha, 1997; Goble *et al.*, 1999; Verdonk *et al.*, 2005b), and it has been recommended that malalignment is corrected before any transplantation can take place (van Arkel & de Boer, 1995).

## 1.4.6 **Immunology**

To prevent rejection of allogeneic transplants, such as organ transplants, immunosuppressive drugs target the immune response non-specifically. Using this strategy lifelong administration may be required and can lead to susceptibility to infection, tumours and cardiovascular disease, among other side effects. Therefore specific strategies allowing for the tolerance of allogeneic transplants without the need for immunosuppressant therapy need to be developed. The major histocompatibility complex (MHC) is a large set of genes that is unique in each individual (except monozygotic twins) and plays an important role in the immune system. Proteins encoded by the MHC genes are displayed on the surface of cells and the MHC molecules present foreign peptide antigens to be recognised by T cells which mediate the immune response. The MHC in humans is known as the human leukocyte antigen (HLA) system. HLA antigens are divided into three groups, class I, II and III. Class I consists of A, B and C antigens which present peptides from within the cell; and class II consists of D (Dp, Dq and Dr) antigens which present peptides from outside the cell. Recognition of mismatched-MHC antigens by T cells in allogeneic transplants leads to graft rejection. T cells can initiate rejection of allogeneic transplants in three ways (Golshayan *et al.*, 2007): directly, indirectly and semi-directly (Figure 1.11).

It has been postulated that the meniscus is immunopriveliged. Several studies have shown that there has been no rejection following allogeneic

meniscal transplantation (Milachowski *et al.*, 1989; Garrett & Stevenson, 1991; Ochi *et al.*, 1993; de Boer & Koudstaal, 1994; Nemzek *et al.*, 1994; van Arkel & de Boer, 1995; Fabbriciani *et al.*, 1997). There have also been cases where a low level immunological reaction has been encountered (Langer *et al.*, 1978; Rodeo *et al.*, 2000); however this has not affected the clinical outcome. This may be due to the dense extracellular matrix which may act to protect the meniscal cellular antigens (Fabbriciani *et al.*, 1997) or due to the lack of a blood supply which would be necessary for lymphocyte access. Hence the likelihood of triggering an immune response is reduced.

### 1.4.7 **Xenotransplantation**

Xenogeneic meniscal transplantation is gaining popularity due to a potentially unlimited source of tissue. Since the meniscus appears to be immunopriveliged, this will no doubt fuel this fire. However, there are a number of issues that may prevent xenotransplantation translating to the clinic. These include ethical, legal and religious reasons. It has also been shown that using a cellular meniscus as a replacement can potentially lead to xenozoonoses. In a study by Martin *et al.* (1998) it was shown that porcine endogenous retrovirus (PERV) mRNA was present after co-culture of human kidney cells with pig primary aortic endothelial cells, implying infection of human cells by PERV. This may be overcome by the fact that it is possible to raise PERV-free pigs (Hammer, 2003) and also through removal of all cellular and nuclear material through decellularisation. Pig menisci are the closest match to human menisci in terms of size, which is why there is more in the literature regarding pig immunogenicity than other animals. Hyperacute rejection has been shown to be a major problem for pig to primate organ transplantation (Galili *et al.*, 1997; McPherson *et al.*, 2000) and is due to presence of the Galactosyl-α(1,3)galactose (α-gal) epitope on cell membrane glycolipids and glycoproteins of lower mammals. The α-gal epitope is not present in humans or Old World monkeys due to mutations of α1,3-galctosyltransferase, the enzyme responsible for producing α-gal.

Hyperacute rejection occurs due to the fact that humans naturally produce large titres of antibodies to α-gal, possibly due to constant exposure to intestinal bacteria which express epitopes which cross-react with the α-gal epitope.

These antibodies bind to endothelial cells present in the donor graft resulting in complement-mediated hyperacute rejection. Subsequent thrombosis in the graft vasculature then leads to graft hypoxia and death. Anti-α-gal antibodies bound to xenograft cells can also mediate the destruction of xenograft cells by interacting with macrophages and natural killer cells via their Fc receptors leading to subsequent lysis of the graft cells. This is known as the antibody dependent cellular cytotoxicity mechanism (Galili *et al.*, 1997). Kasimir *et al.* (2005) showed that incomplete decellularisation which fails to remove the α-gal epitopes can lead to xenograft rejection. This was supported in another study using mice negative for α-gal antibodies, in which Raeder *et al.* (2002) also showed that the α-gal epitope did not interfere with the ability of xenogeneic ECM to serve as a scaffold when there is a lack of an immune response.

**Table 1.4: Meniscal allograft studies in Humans**

| Reference | Meniscus (Number) | Allograft type (Number) | Findings |
|---|---|---|---|
| Milachowski *et al.* (1989) | Medial (11) | Freeze-dried and irradiated (8) Fresh-frozen (3) | No adverse immunological reactions. Shrinkage seen in all cases with one meniscus completely destroyed at 2 years. Synovitis present in 4 patients with freeze-dried grafts. Complete healing in frozen menisci. Failures = 5 up to 14 years |
| | Lateral (11) | Freeze-dried and irradiated (8) Fresh-frozen (3) | |
| Garrett & Stevenson (1991) | Medial (4) Lateral (2) | Fresh | Secure healing with horns anchored firmly. No sign of rejection or progression of degeneration. Pain and clicking noted in 3 cases. |
| Garrett (1993) | Medial (34) Lateral (8) | Fresh (27) Cryopreserved (16) | Healing of rim and lack of shrinkage present in 20 of 28 cases arthroscopically assessed. Degeneration of articular cartilage present. Failures = 8 up to 7 years |
| De Boer & Koudstaal (1994) | Medial (18) Lateral (7) | Cryopreserved | Revascularisation, recellularisation and healing present. Fewer cells in central areas. No rejection of grafts. Failures = 3 |
| Van Arkel & De Boer (1995) | Medial (10) Lateral (15) | Cryopreserved | Healing and revascularisation present. Improved stability and function of joint. No inflammation or rejection. Failures = 3 due to malalignment up to 24 months |
| Cameron & Saha (1997) | Medial (37) Lateral (30) | Fresh-frozen | Peripheral healing and no shrinkage of graft. Improvements in function and pain. 87% good to excellent results. Gross nonhealing evident in 3 patients. Failures = 7 up to 5 years |

| | | | |
|---|---|---|---|
| Verdonk (1997) | Medial (23) Lateral (17) | Fresh | Slow in-growth of host cells up to 2 years with some donor cells surviving. Transient synovitis present in 4 cases but did not affect clinical outcome. Failures = 5 up to 6 years |
| Carter (1999) | Medial (39) Lateral (7) | Cryopreserved | Normal appearance. Good healing and repopulation with cells. Improvements in pain and function. Failures = 5 up to 5 years |
| Goble *et al.* (1999) | ? (47) | Cryopreserved | Good healing and function in 71%. Pain reduced in 70% of cases. 80% viable meniscal tissue present in 57% of subjects. Shrinkage and accelerated graft wear evident. Failures = 11 up to 2 years |
| Rodeo *et al.* (2000) | Medial (17) Lateral (16) | Fresh-frozen | Allografts showed incomplete repopulation with cells derived from synovium. Low level immunological rejection but did not affect clinical outcome. Failures = 12 up to 47 months |
| Stollsteimer *et al.* (2000) | Medial (11) Lateral (12) | Cryopreserved | Improvement in pain and function. Shrinkage of graft to ~63% of normal meniscal size. Failures = 2 up to 69 months |
| Rath *et al.* (2001) | Medial (15) Lateral (7) | Cryopreserved | Complete healing to bed and revascularisation. Decrease in pain and improvement in function. Reduced cellularity in all grafts and reduced biochemical function. Failures = 8 up to 8 years |
| Verdonk *et al.* (2005b) | Medial (39) Lateral (61) | Fresh | Pain and function greatly improved. Effects remained in 70% of patients after 10 years. Failures = 21 up to 14 years |
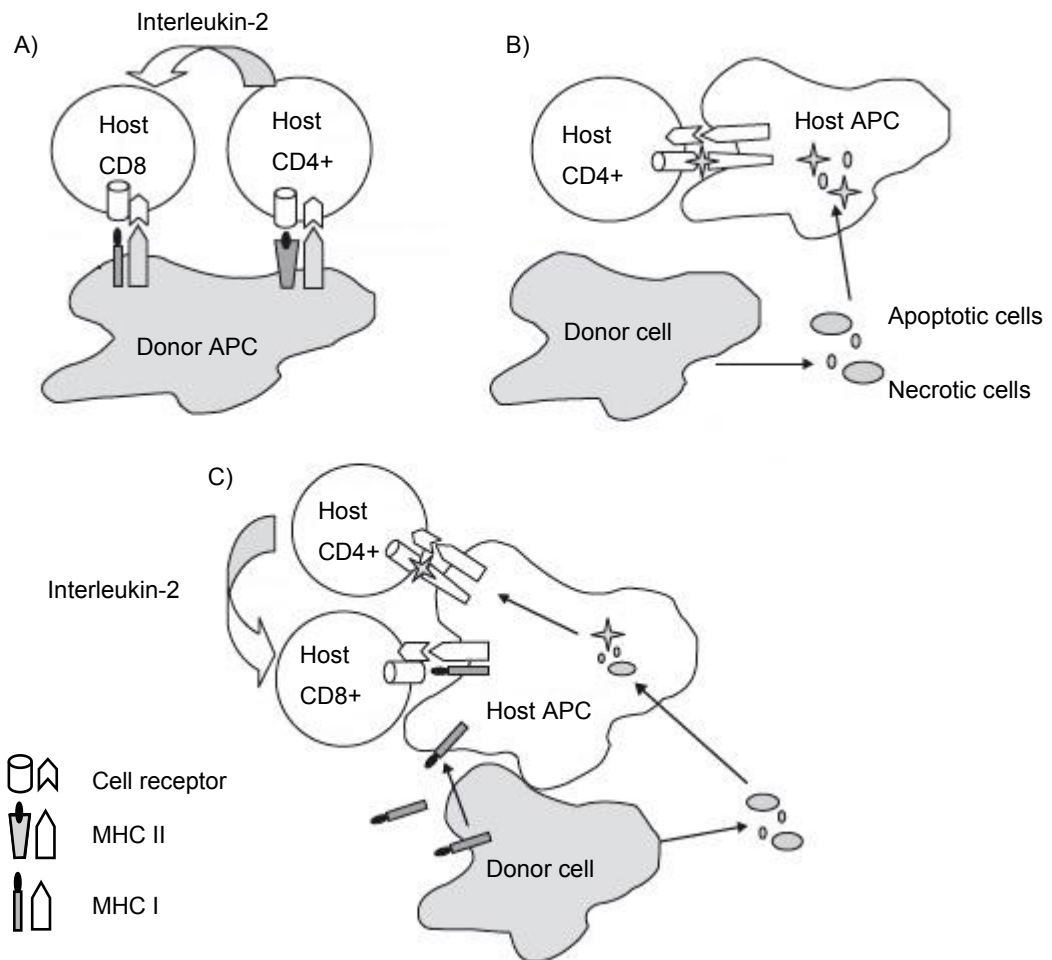
**Figure 1.11: Allorecognition pathways.** A) Direct pathway. B) Indirect pathway. C) Semi-direct pathway (Adapted from Golshayan et al., 2007). In the direct pathway allogeneic class II MHC on donor antigen-presenting cells (APCs) is recognised by CD4+ T helper cells. Cytotoxic CD8+ T cells activated by the same APCs are then enlisted by these primed, allospecific helper T cells to impart an immune response. The indirect pathway differs from the direct in that donor MHC molecules shed from the graft are picked up and processed by host APCs to be presented as peptides recognisable by helper T cells. The semi-direct pathway involves aspects of both the direct and indirect pathways. Donor MHC I molecules are acquired and presented to cytotoxic T cells as in the direct pathway by host APCs, which also present donor MHC class II molecules to helper T cells as in the indirect pathway. In this way linked-help can occur as T cells are primed by the same APC.

## 1.5    Tissue Engineering of the Knee Meniscus

A tissue engineered meniscal replacement conforming to the biological and biomechanical characteristics of native menisci prevent degeneration of the joint eradicating the need for further surgery or treatment thereby reducing the burden on health services and improve patients' lives.  Many attempts have been made to tissue engineer a meniscus with limited success so far (Table 1.6 and Table 1.7).  It is very challenging to recapitulate the meniscus owing to its highly organized nature and heterogeneous cell population.  An ideal meniscal replacement has to be biocompatible, integrate with the surrounding tissue, allow neovascularisation, prevent degeneration of cartilage surfaces by remodelling in a timely manner whilst maintaining biomechanical and lubrication properties until regeneration has occurred and neo-tissue is able to withstand the biomechanical forces acting through the meniscus.  Ultimately, there are two strategies for engineering a meniscal replacement: a cell-based method in which scaffolds are seeded with cells before implantation or a cell-free method in which acellular scaffolds are designed to promote and support regeneration once implanted through the infiltration of endogenous cells from the surrounding tissue.  A variation of the cell-based method that is currently gaining momentum is the scaffold-free approach in which stem cells or native meniscal cell types are cultured under specific conditions to produce meniscus-like ECM.  This aim with this approach is to eradicate the issues associated with the use of certain scaffolds such as adverse host responses, interference with cell-cell interactions and ECM alignment.  Biomechanically anisotropic tissue has been developed with collagen I, II and GAG deposition using articular chondrocytes and fibrochondrocytes in a  co-culture system utilising a meniscus-shaped mould (Aufderheide & Athanasiou, 2007).  The ideal approach for meniscal replacement has, however yet to be determined, with each method showing merit and impetus for further investigation.

**Table 1.5: Animal meniscal allograft studies**

| Reference | Source | Meniscus (Number) | Allograft type (Number) | Findings |
|---|---|---|---|---|
| Milachowski *et al.* (1989) | Ovine | Medial (30) | Freeze-dried (15) Irradiated (15) | Complete healing, revascularisation and remodelling. No rejection. Less revascularisation in irradiated menisci. Grafts had lower tensile moduli when compared to normal menisci after 48 weeks. |
| Arnoczky *et al.* (1992) | Canine | Medial (16) | Fresh-frozen | Repopulation with cells derived from synovium. Central core remained acellular at 6 months. Remodelling of collagen network. No evidence of gross degeneration. Failures = None at 6 months |
| Jackson *et al.*( 1992) | Caprine | Medial | Fresh Cryopreserved | Normal peripheral revascularisation and healing. Water content increased by 6% and proteoglycan content increased. Failures = None at 6 months |
| Yahia *et al.* (1993) | Lapine | ? | Fresh-frozen Irradiated | Smaller effect on elastic stiffness than in irradiated grafts. No change in failure strength when compared to normal tissue. Adverse effect on viscous and elastic properties when irradiated. Lower Failure strength. |
| Fabbriciani *et al.* (1997) | Caprine | Medial (30) | Fresh-frozen (15) Cryopreserved (15) | Healing at horns and periphery. No rejection. Grafts remodelled and revascularised at 1 year. Increase in water content and progressive decrease in GAG content. No differences noted between fresh-frozen and cryopreserved grafts. |
| Szomor *et al.* (2000) | Ovine | Medial (28) | Fresh | Transplanted menisci less shiny than normal. Fibrinoid degeneration and areas of hypocellularity present. Failures = None at 4 months |

The mechanical environment within the knee also needs to be considered when developing a tissue engineering strategy. Whether the implanted material is a combination of cells and scaffold or scaffold alone it must be able to function under load without deforming or failing and provide the correct environment for cells to adhere and interact. Certain cell types exhibit material-specific interactions dependent on material modulus with Engler *et al.* (2006) showing that mesenchymal stem cells, a cell source widely investigated in meniscal tissue engineering, commit to specific lineages dependent on matrix stiffness.

### 1.5.1 Scaffold Based Meniscal Tissue Engineering

Scaffold based approaches include the use of synthetic materials, naturally derived materials and acellular biological tissues (Table 1.6 and Table 1.7). Synthetic materials are easily processed, offer minimal batch to batch variability compared to naturally derived materials, and can have their mechanical and chemical properties tailored making them attractive options in generating a scaffold. On the other hand, they lack the signalling cues present in naturally derived materials and can cause a mild immune response. Interest in the use of synthetic materials for meniscal tissue engineering has declined following a period of intense investigation. This may be due to evidence of adverse host responses (Veth *et al.*, 1986; Klompmaker *et al.*, 1996; Tienen *et al.*, 2006) and failure to provide suitable environments for cellular ingrowth and matrix synthesis (Veth *et al.*, 1986; Wood *et al.*, 1990). More recent studies, however, have shown some promise, possibly due to advances in biomaterials science and there are now approaches based on the use of advanced polymers such as poly L-lactic acid (PLLA), poly p-dioxanone (PPD), and polyurethane that are more biocompatible than polymers previously used. Studies investigating acellular PLLA-PPD and PLLA scaffolds have shown regeneration of surgically created meniscal defects in animal models with integration to the native tissue (Testa Pezzin *et al.*, 2003) and protection of cartilage surfaces

from damage (Cook & Fox, 2007). Even so, synthetic materials will always induce a foreign body reaction and, if unchecked, the infiltration of cells and regeneration can be prevented by the formation of fibrotic scar tissue which can isolate the implant from the surrounding milieu. Hence, produced from synthetic polymers have been coated in natural ECM components such as hyaluronan (Chiari et al., 2006). The degradation rate can also be controlled to reduce the concentrations of inflammatory degradation products released by the scaffold.

Various natural scaffolds have been investigated for tissue engineering the meniscus. Collagen, decellularised menisci and small intestinal submucosa (SIS) have all been evaluated in an attempt to address meniscal regeneration (Cook et al., 2001; Reguzzoni et al., 2005; Bradley et al., 2007; Stapleton et al., 2008; Yamasaki et al., 2008). Porcine small intestinal submucosa has been used in animal models of Achilles tendon repair to promote a regenerative response rather than a healing response where scar-tissue is formed (Badylak et al., 1995). After implantation SIS behaves as a temporary scaffold which degrades in 8 weeks having initiated a remodelling response (Badylak et al., 1995; Record et al., 2001; Gilbert et al., 2007). It has been shown to improve limb function and reduce cartilage damage when used in repair of meniscal defects in dogs (Cook et al., 2006). SIS has been used to treat avascular meniscal defects where it was shown to integrate well, produce an organized collagen matrix, and improve clinical function (Cook et al., 2001), however the repair tissue that was formed did not have significantly different Poisson's ratio, permeability or shear modulus to the tissue formed when no treatment was applied (Welch et al., 2002). SIS has also been shown to produce an unorganized matrix which resulted in increased degeneration of the cartilage surfaces when used to fill meniscal defects in rabbits (Bradley et al., 2007). Currently SIS has been licensed as a clinical treatment for several applications other than meniscal repair.

**Table 1.6: In vitro meniscal tissue engineering**

| Ref | Material | Model | Cells, Growth Factors | Study length | Results |
|-----|----------|-------|-----------------------|--------------|---------|
| *Scaffold-based* | | | | | |
| Balint et al. (2012) | Collagen reinforced with p(DTD DD) | Bovine | - | - | Stiffness similar to ovine medial meniscus. Correlation between applied axial load and resultant circumferential tensile load. |
| Ionescu et al. (2012) | Poly-caprolactone | Bovine | bFGF or TGF-β3 | 1 wk | Addition of TGF increased integration strength 10-fold, increased GAG production with no change in collagen deposition. Reduction seen when both added together. |
| **Decellularised Meniscus** | | | | | |
| Maier *et al.* (2007) | Decellularised meniscus | Ovine | $10^5$ fibrochondrocytes per mL | 4 wks | Non-toxic. Higher stiffness and compressive modulus to native meniscus. |
| Stapleton et al. (2008) | Decellularised porcine meniscus | Porcine | - | - | Complete cell removal. No expression of xenogeneic epitope. Retention of histoarchitecture. 59.4% loss of GAGs. Retention of biomechanical properties. Collagen I, II and III, and chondroitin sulphate present. |
| Sandmann et al. (2009) | Decellularised human meniscus | Human | - | - | Complete cell removal. No significant differences in stiffness, residual force and collagen I, II and III histoarchitecture from native. |
| Stabile et al. (2010) | Decellularised ovine meniscus | Ovine | - | - | Complete removal of cellular material, ~55% reduction in DNA, maintenance of material properties, biocompatible, increased porosity. |
| *Cell-based* | | | | | |
| Aufderheide & Athanasiou (2005) | Agarose | Leporine | $2.5 \times 10^7$ fibrochondrocytes per cm$^3$, TGF-β1 | 3 wks | Cell death; individual cells of rounded morphology. Aggregate modulus = ~10 kPa. |

| Puetzer et al. (2012) | Alginate | Bovine | $50 \times 10^6$ meniscal cells per mL | 4-6 wks | Increase of collagen bundle size with loading. Increase in GAG content with loading however this plateau`d except for in samples loaded then left static for 4 weeks where GAG plateau`d after 2 weeks and sharply rose after 6 weeks. Equilibrium modulus of samples increased with extended loading. |
|---|---|---|---|---|---|
| **Collagen** | | | | | |
| Gruber *et al.* (2008) | Collagen | Human | $10^5$ fibrochondrocytes per scaffold, TGF-β1 | 2 wks | Attachment of cells. Presence of collagen I and II, and chondroitin sulphate. Significant increase in proteoglycan production when exposed to TGF-β. |
| Mueller *et al.* (1999b) | Collagen I-GAG | Bovine or Canine | $1.8 \times 10^7$ fibrochondrocytes per cm$^3$ | 3 wks | Shrinkage to 54% of original size. Fibroblast-like and chondrocyte-like cells present which formed cellular capsule. GAG and collagen production. |
| | Collagen II-GAG | Bovine or Canine | $1.8 \times 10^7$ fibrochondrocytes per cm$^3$ | 3 wks | 12% shrinkage. Cells distributed throughout scaffold. Presence of collagen I and II, and GAGs. |
| **Hyaluronan** | | | | | |
| Marsano *et al.* (2006) | Hyaluronan | Human | $3.9 \times 10^7$ fibrochondrocytes per cm$^3$ in mixed flasks | 4 wks | Bi-zonal tissue formation. White zone rich in GAG and stiffer in compression. Red zone rich in collagen and stiffer in tension. Meniscus-like collagen organization. |
| Tan *et al.* (2010) | Hyaluronan-Chitosan | Murine | $2 \times 10^4$ meniscal cells per well | 2 wks | Collagen I/II + chondroitin sulfate surface triggered redifferentiation of dedifferentiated meniscal cells. |
| **Polymers** | | | | | |
| Aufderheide & Athanasiou (2005) | PGA | Leporine | $5 \times 10^7$ fibrochondrocytes per cm$^3$ | 7 wks | Cellularity increased; presence of collagen and GAGs. Aggregate modulus = 2.6 ± 0.6 kPa. |

| | | | | | |
|---|---|---|---|---|---|
| Pangborn & Athanasiou (2005b) | PGA | Leporine | $2.5 \times 10^7$ fibrochondrocytes per $cm^3$, TGF-β1 | 3 wks | Supports cell growth and ECM production. TGF-β1 stimulated collagen and GAG synthesis. |
| Aufderheide & Athanasiou (2007) | PGA | Bovine | 50:50 articular chondrocytes and fibrochondrocytes, $2.3 \times 10^7$ | 8 wks | Cell death; presence of randomly oriented collagen and GAGs. Tensile modulus = 16 ± 5 kPa in circumferential direction. |
| Freymann et al. (2012) | PGA-hyaluronan | Human | $8.8 \times 10^6$ meniscus derived cells per scaffold | 3 wks | Increase in matrix protein expression compared to control. Decrease in collagen X expression for all groups. Suggested redifferentiation of meniscus cells by scaffold. |
| Fox *et al.* (2010) | PGA-PLLA | Equine | $4 \times 10^5$ fibroblast-like synoviocytes per $cm^3$, bFGF, TGF-β1, IGF | 6 wks | No integration of cell-scaffold construct to meniscal tissue. No measurable collagen or GAGs. |
| Baker et al. (2009) | Polycaprolactone | Human | $2.5 \times 10^5$ meniscus derived cells per scaffold | 10 wks | Higher stiffness compared to unseeded scaffold. Reduced collagen and increased sGAG compared to native tissue. |
| Mandal et al. (2011) | Silk fibroin | Human | $0.8 \times 10^6$ BM-MSCs per layer of scaffold, bFGF, TGF-β1 | 4 wks | Increase in collagen and GAG content. Evidence for differentiation of MSCs to chondrogenic phenotype. Doubling of compressive modulus in cultured scaffolds compared to scaffold alone. |

The collagen meniscal implant, or CMI® (ReGen Biologics, Hackensack, NJ, USA), is a replacement composed of type I collagen and has been used to stimulate meniscal tissue ingrowth. There are no storage or handling issues associated with collagen (Setton *et al*., 1999), and as collagen has maintained a highly preserved structure through evolution there is no antigenicity (van der Rest and Garrone, 1991). Matrix characteristics such as porosity, pore size, permeability, shape and mechanical properties can also be adjusted *in vitro* (Setton *et al*., 1999). *In vivo* studies in animals have shown that the CMI® promoted the in-growth of fibrochondrocytes and preserved the cartilage surfaces (Reguzzoni *et al*., 2005; Steadman & Rodkey, 2005). However, it has also been shown that an unorganized and biomechanically unstable matrix is produced in patients using CMI® and it is therefore a poor substitute (Buma *et al*., 2007). Collagen implants have had more success *in vivo* (Steadman & Rodkey, 2005) than decellularised menisci and SIS (Welch *et al*., 2002; Peretti *et al*., 2004). Collagen and collagen-GAG composites, hyaluronan, and decellularised or devitalized meniscus are all currently under investigation as possible meniscal replacement or repair materials. Varying degrees of success has been achieved with these with evidence of stem cell differentiation and ECM deposition *in vitro*, and integration and regeneration of defects *in vivo*. Decellularisation of porcine or human menisci to produce a natural scaffold has been gaining momentum in recent years (Maier *et al*., 2007; Stapleton *et al*., 2008; Sandmann *et al*., 2009). Decellularisation aims to remove all immunogenic constituents of the tissue and provide an ideal structural framework for recellularisation either *in vitro* or *in vivo*. Further work is required in this area to demonstrate practical feasibility.

## 1.5.2 **Cell Based Meniscal Tissue Engineering**

*In vitro* investigations into meniscal tissue engineering utilise natural, synthetic and combination biomaterials coupled with cells from various sources (Table 1.6 and Table 1.7). In some cases cells are used to gauge

the biocompatibility of the chosen scaffold material as well as its ability to influence cell interaction and expression, although scaffold integration has been shown to be enhanced in preclinical studies which include a cell population with improved ECM deposition and organization (Angele *et al*., 2008; Gu *et al*., 2012). This may be because the remodelling response is accelerated as cells are already present and do not need to migrate into the scaffold (Gu *et al*., 2012). Polyglycolic acid (PGA) has been investigated extensively as a synthetic scaffold for meniscal tissue engineering and has been reported to be biocompatible with a non-toxic degradation profile. Cell proliferation, collagen synthesis and GAG production have all been shown to be improved when PGA scaffolds are compared to agarose scaffolds (Aufderheide & Athanasiou, 2005). A study by Kang *et al.* (2006) using a meniscus-shaped PGA scaffold seeded with fibrochondrocytes before implantation demonstrated significant regeneration of fibrocartilage as well as zonal production of collagen I and II as seen in native menisci (Kang *et al*., 2006).

Collagen based scaffolds have been shown to allow recellularisation and matrix production, with the addition of growth factors enhancing these properties (Gruber *et al*., 2008). Cell behaviour has also been shown to be sensitive to collagen-GAG composites, with a collagen II-GAG composite promoting increased production of matrix components and reduced shrinkage as opposed to a collagen I-GAG composite (Mueller *et al*., 1999b). Hyaluronan has also shown promise as it can be used to produce bi-zonal tissue similar to meniscal tissue (Marsano *et al*., 2006).

Fibrochondrocytes have been heavily investigated as a cell source for meniscal tissue engineering (Hidaka *et al*., 2002; Aufderheide & Athanasiou, 2005; Pangborn & Athanasiou, 2005; Maier *et al*., 2007; Baker *et al*., 2009; Freymann *et al*., 2012). Chondrocytes have also been well characterised and have been induced to produce meniscus-like ECM through manipulation of the culture conditions. Other more readily available and easily procured cells have also been assessed for suitability in meniscal tissue engineering. These include various sources of stem cells (Horie *et al*., 2009; Zhang *et al*.,

2009; Zellner *et al*., 2010; Mandal *et al*., 2011) which are yet to be understood in this application, as well as meniscal fibrochondrocytes or chondrocytes. However, stem cells have shown promise in producing a meniscus-like ECM. Bone marrow derived mesenchymal stem cells have been shown to produce dense ECM containing type II collagen when seeded onto hyaluronan-gelatin composite scaffolds (Angele *et al*., 2008). Synovium-derived stem cells have been utilised in an injectable system for meniscal repair and have been shown to develop a gene expression profile which was more similar to meniscal cells than when bone marrow derived mesenchymal stem cells were used (Horie *et al*., 2009). Investigations which have focussed upon the use of cells in combination with scaffolds or in self-assembly approaches (Table 1.7) have, however, failed to articulate how the approach can be readily translated to routine clinical use.

Practical and regulatory considerations will determine the successful translation to the clinic of scaffold-only or scaffold seeded with cells approach. An ideal scaffold should have the appropriate mechanical properties to fulfil the load bearing and biotribological function of the meniscus immediately upon implantation whilst also encouraging the infiltration of a cell population to instigate regeneration. Scaffold-only approaches could provide an off-the-shelf class III medical device at a relatively low cost making it accessible to a large number of patients. Approaches which include a living cell population may promote faster healing and regeneration compared to scaffold-only approaches however their use adds a level of complexity to the procedure. Cells have to be harvested, most likely from an autologous source for immune-compatibility resulting in potential donor site morbidity, and cultured to obtain sufficient numbers for implantation. This approach would be subject to additional regulatory requirements as it would be classed as an Advanced Therapy Medicinal Product (ATMP) and so a longer development life-cycle resulting

**Table 1.7: In vivo meniscal tissue engineering**

| Ref | Material | Model | Cells, Growth Factors | Follow-up | Results |
|---|---|---|---|---|---|
| *Scaffold-based* | | | | | |
| **Carbon Fibre** | | | | | |
| Veth et al. (1983) | Carbon fibre | Leporine | - | 17 wks | None to partial repair in 43% with fibrosis in 57%. Fibrocartilage formation along carbon fibres. |
| Veth et al. (1986) | Carbon fibre-PLLA-poly-urethane | Canine | - | 19 wks | Infiltration of vessels and neo-tissue. Inflammation of synovium due to carbon fibre. |
| Wood et al. (1990) | Carbon fibre-polyester | Leporine | - | 26 wks | Inflammation around polyester fibres. Osteophyte formation and no cellular infiltration visible. |
| **CMI** | | | | | |
| Stone et al. (1997) | CMI | Human | - | 3 yrs | Repopulation by fibrochondrocytes. Presence of unorganized and immature collagen fibres. |
| Reguzzoni et al. (2005) | CMI | Human | - | 26 wks | Implant healed to the meniscal capsule and stumps and displayed revascularisation and ECM production. |
| Steadman & Rodkey (2005) | CMI | Human | - | 6 yrs | Chondral surfaces protected with uniform ECM production and improvement in symptoms. |
| Rodkey et al. (2008) | CMI | Human | - | 7 yrs | Formation of repair tissue which appeared meniscus-like. Improvement in activity. |
| Bulgheroni et al. (2010) | CMI | Human | | 2, 5 yrs | Shrinkage of CMI but protection of chondral surfaces. Bone oedema was present in 13 patients. Two types of tissue formed after 5 years with increased cellularity and vascularity. |
| Zaffagnini et al. (2011) | CMI | Human | - | 10 yrs | Protection of cartilage surfaces with improvements from preoperative state |
| **Repair Materials** | | | | | |

| Tienen et al. (2006) | Estane | Canine | - | 26 wks | Degenrative lesions formed on inner rim. Integration seen at periphery with collagen I production and neovascularisation. Neotissue had inferior mechanical properties compared to native meniscus. |
|---|---|---|---|---|---|
| Kopf et al. (2010) | Poly (ethylene, terephthalate) (Ethibond®) | Ovine | VEGF | 8 wks | No improvement compared to controls |
| Reckers et al. (2009) | Fibrin glue | Leporine | | 4 wks | Loosening of meniscus with cell infiltration impaired. |
| Ishida et al. (2007) | Gelatin hydrogel | Leporine | Platelet-rich Plasma | 4, 8, 12 wks, | Protection of cartilage surfaces with Safranin O staining present after 12 weeks. |
| Kobayashi et al. (2010) | Meniscal fragments | Leporine | - | 3, 6, 12 wks | Rough, meniscus-like tissue formed but thinner radially than native meniscus. Thick synovium also formed. |
| Reckers et al. (2009) | Octyl cyanoacrylate suture | Leporine | - | 4 wks | Necrosis of transplanted menisci. Suturing alone displayed best outcome. |
| **Polymers** | | | | | |
| Testa Pezzin et al. (2003) | PLLA-PPD | Leporine | | 14 wks | Some correctly aligned collagenous tissue formation with fibrochondrocyte infiltration. |
| Chiari et al. (2006) | Polycaprolactone-Hyaluronan | Ovine | - | 6 wks | Soft tissue swelling in 4 cases (2 each) and both meniscectomies. Tissue ingrowth and vascularisation at periphery. Synovium regenerated. Graft extrusion and wrinkling. |
| Tienen et al. (2006b) | Polycaprolactone-polyurethane | Canine | - | 26 wks | Fibrocartilage ingrowth. Collagen I in peripheral fibrous zones and collagen II in central cartilaginous zones. Small synovial reaction to polymer. Giant cells and macrophages present. |
| Welsing et al. (2008) | Polycaprolactone-polyurethane | Canine | - | 24 mths | Zonal tissue formation with thin fibrovascular rim and larger avascular cartilage-like inner zone. Collagen I, II and proteoglycans present. Fragmentation of scaffold. Cartilage degeneration similar to meniscectomy group. |

| Hannink et al. (2011) | Polycaprolactone-polyurethane | Canine | - | 6, 24 mths | Cartilage degeneration seen at 6 months with further degeneration into calcified zone seen after 24 months. |
|---|---|---|---|---|---|
| Cook and Fox (2007) | poly-L-lactic acid | Canine | - | 24 wks | No articular cartilage damage. Complete healing (n = 2) and partial healing (n = 3) in avascular region of dogs receiving scaffold. No healing in controls. Load to failure was 52% for scaffold-treated menisci compared to intact menisci. Trephined menisci had zero strength. |
| De Groot et al. (1997) | poly-L-lactic acid and ε-caprolactone | Canine | - | 26 wks | Fibrocartilage ingrowth. Formation of fibrocartilage linked to compressive modulus of scaffold. |
| Klompmaker et al. (1992) | Polyurethane | Canine | - | 52 wks | Formation of collagen I and II. Giant cells, macrophages and lymphocytes present on polymer surface. |
| Klompmaker et al. (1996) | Polyurethane | Canine | - | 28 wks | Formation of collagen I and II. Giant cells, macrophages and lymphocytes present. Degeneration of cartilage. |
| Brophy et al. (2009) | Polyurethane | Ovine | - | | Compressive modulus of 4.5 ± 1.3 MPa and 0.3 ± 0.1 MPa at 70% and 25% strain, respectively. Decreased mean contact area compared to intact knee. |
| Galley et al. (2011) | Polyurethane | Ovine | - | 3, 6 and 12 mths | Tissue ingrowth into scaffold. Lower equilibrium modulus than intact meniscus after 12 months. |
| Verdonk et al. (2011) | Polyurethane (Actifit®) | Human | - | 24 mths | Ingrowth of vascularised neomatrix. Protection of cartilage surfaces. Zonal tissue formation. |
| **SIS** | | | | | |
| Cook et al. (2006) | Small intestinal submucosa (SIS) | Canine | | 3, 6, 12 mths | Mature repair tissue visible for SIS group. Significantly lower articular cartilage damage than meniscectomy. Compressive moduli comparable to untreated group after 12 months. |
| *Cell-based* | | | | | |

**Injectable**

| | | | | | |
|---|---|---|---|---|---|
| Mizuno et al. (2008) | - | Murine | $10^7$ Synovium-derived MSCs | 12 wks | Formation of fibrocartilage time-dependent increase in collagen II expression. Stem cells appeared morphologically similar to meniscal cells. |
| Horie et al. (2009) | - | Murine | $5 \times 10^6$ Synovium-derived MSCs | 2, 4, 8, 12 wks | Formation of fibrocartilage time-dependent increase in collagen II expression. Stem cells appeared morphologically similar to meniscal cells. Similar results with BM MSCs, however synovium derived stem cell genetic profile similar to meniscal cells |
| Zhang et al. (2009) | Calcium alginate gel | Caprine | BM MSCs transfected with IGF-1 | 4, 8, 16 wks | Integration and formation of cartilage-like tissue. Chondrocyte-like cells present. Collagen I present. |

**Self-assembled**

| | | | | | |
|---|---|---|---|---|---|
| Aufderheide & Athanasiou (2007) | Agarose wells | Bovine | 50:50 articular chondrocytes and fibrochondrocytes, $2.3 \times 10^7$ cells | 8 wks | Collagen fibre alignment with presence of collagen I and II, and GAGs. Biomechanically anisotropic neotissue. |
| Hoben et al. (2007) | Agarose wells | Bovine | 50:50 co-culture of fibrochondrocytes and chondrocytes, $2.75 \times 10^7$ cells each | 4 wks | Presence of collagen I and II, and GAGs. |
| | | | $5.5 \times 10^7$ fibrochondrocytes | | Presence of collagen I and GAGs. Significant contracture of construct. |

**Meniscus**

| | | | | | |
|---|---|---|---|---|---|
| Peretti et al. (2004) | Decellularised meniscus | Porcine | Autologous chondrocytes | 9 wks | Repair not homogeneous. GAG production. |
| Yamasaki et al. (2008) | Devitalized meniscus | Murine | $2 \times 10^5$ BM MSCs per scaffold | 8 wks | Expression of ECM. Degeneration comparable to meniscectomised knees. |

| Weinand et al. (2009) | Devitalized meniscus and woven PLGA mesh | Murine | Porcine chondrocytes at 1, 2 and 5 million cells per mL | 12 wks | Most homogeneous cell attachment found using dynamic oscillation. Integration of devitalized meniscus scaffold to surrounding tissue. |
|---|---|---|---|---|---|
| Isoda & Saito (1998) | Fibrin | Leporine | Fibrochondrocytes | 8 wks | Matrix production and cell proliferation |
| Zellner et al. (2010) | Hyaluronan-gelatin 70:30 | Leporine | $1.5 \times 10^6$ MSCs per scaffold | 12 wks | Defects filled with dense ECM. Collagen II present. Integration to native meniscal tissue. |
| **Polymers** | | | | | |
| Ibarra et al. (1997) | PGA | Murine | $2.5 \times 10^7$ bovine fibrochondrocytes per mL | 16 wks | Production of collagen and proteoglycan. Matrix architecture similar to meniscal repair tissue. |
| Hidaka et al. (2002) | PGA | Murine | $2 \times 10^7$ bovine fibrochondrocytes per $cm^3$ | 8 wks | Production of collagen and proteoglycan. Less extensive collagen network than normal meniscus. |
| Kang et al. (2006) | PGA-PLGA | Leporine | $2 \times 10^6$ meniscal cells per scaffold | 6, 10 wks | Fibrocartilage produced. Time-dependent increase in collagen and proteoglycan content. Degeneration of tibial cartilage. |
| Gu et al. (2012) | PLGA | Canine | $1.5 \times 10^7$ canine myoblasts per scaffold, CDMP-2, TGF-β1 | 12 wks | Formation of cartilage-like regions with collagen I, II and aggrecan production. |
| Kon et al. (2012) | Polycaprolactone-Hyaluronan | Ovine | $4 \times 10^7$ autologous chondrocytes per scaffold | 12 mths | Osteoarthritis present in all groups. Less severe in scaffold groups, both cell seeded and unseeded. Foreign body reactions present. Hyaline-like matrix production in cell seeded constructs, with fibrous, GAG-rich matrix production in unseeded constructs. |

in increased cost to the patient and/or health service provider thereby reducing availability to patients.

An alternative avenue may be to harvest a population of cells during surgery which could be subjected to minimal manipulation and used in conjunction with the scaffold to enhance the regenerative properties of the implanted scaffold. As no *ex vivo* manipulation is involved the device would still be regulated as a class III medical device, thereby remaining cost-effective and accessible to a larger number of patients.

### 1.5.3 Conclusion

Tissue engineering aims to create functional tissue with the potential for regeneration and growth. The choice of scaffold for this purpose is crucial. The ideal scaffold should be biocompatible, biomechanically and geometrically suited to resist forces within the knee as healing progresses, non-immunogenic, and, if acellular, allow for endogenous cell population and vascularisation. Although different materials have been investigated, an ideal conduit is yet to be developed. Promising results have been obtained using both natural and synthetic materials. Approaches which use a combination of cells and scaffold materials to recapitulate the meniscus prior to implantation are at a much earlier stage of development and there is little consideration of how these approaches might be translated to the clinic in the literature.

## 1.6    Aims and Objectives

An acellular porcine medial meniscus has been developed which has great potential for clinical translation in the repair/ replacement of meniscal tissue. The biomimetic acellular scaffold may be implanted directly and regenerated by the recipients own endogenous stem cells or alternatively, it may be seeded with cells and used as a cellularised replacement. In order to produce a replacement that can be surgically implanted, the acellular meniscus should ideally retain bone plugs at either end (bone-meniscus-bone graft).

Proposed Methodology:

a) Development of a method for effective decellularisation of the fresh porcine medial meniscus without compromising bony attachments.

b) Comparison of fresh and decellularised porcine medial menisci by histological, immunohistochemical and biochemical methods.

c) Biomechanical characterisation of the fresh and decellularised porcine medial meniscal tissue and bony attachments using simple compression and indentation tests.

# Chapter 2.     Materials and Methods

## 2.1    Materials

### 2.1.1 **Equipment**

Details of the equipment and suppliers of the equipment used throughout this study are presented in Table 2.1.

**Table 2.1: Equipment used during the course of studies**

| Equipment | Model | Supplier |
| --- | --- | --- |
| Aspirator | Vacusafe | Integra Biosciences |
| Autoclave | - | - |
| Balance | GR200/GX2000 | Jencons plc |
| Bone Saw | 310 | EXAKT Technologies Inc |
| Centrifuge | Harrier 15/80 | |
| Class II safety cabinet | Heraeus 85 | Kendro |
| Cryomill | Spex Sampleprep 6770 | Fisher Scientific |
| Dehydration and infiltration system | 510 | EXAKT Technologies Inc |
| Digital camera | Evolution MP Colour | Media Cybernetics |
| Differential Scanning Calorimeter | | |
| Filter paper | Various | Scientific Laboratory Systems Ltd |
| Freezer (-25 °C) | Electrolux 3000 | Jencons plc |

| | | |
|---|---|---|
| Freeze dryer | LSBC50 | Modulyo |
| Fridge | Electrolux ER8817 C | Jencons plc |
| Fume hood | - | Whiteley |
| Gel Imaging System | LOGIC 1500 | Kodak |
| Grinder | 400 CS | EXAKT Technologies Inc |
| Haemocytometer | Neubauer MNK-420-010N | Fischer scientifiv |
| Heating block | - | - |
| Heated forceps | Speci-leps | Bios Europe |
| Histology Cassettes | CMB-160-030R | Thermo Fisher Scientific Ltd |
| Histology water bath | 3L Histology | Leica Microsystems |
| Hot plate | E18.1 | Raymond A Lamb |
| Hot wax dispenser | E66 wax dispenser | Raymond A Lamb |
| Incubator | MCO-17A | Sanyo |
| Inverted microscope | IX71 | Olympus UK Ltd |
| Light polymerization unit | 520 | EXAKT Technologies Inc |
| Linear variable differential transformer (LVDT) | RDP DS-200H | Electrosence |
| Luminescence counter and liquid scintillation counter | Packard TopCount NX | Perkin Elmer |
| Magnifying lamp | D20251 | Fisher Scientific |
| Microscope | Olympus BX51 | Microscopes, Medical |

| | | Diagnostic Systems and Olympus Patient Systems Ltd (Olympus UK Ltd) |
|---|---|---|
| Microtome | RM2125RTR | Leica Microsystems |
| Magnetic Resonance Imager | Bruker AVANCE II 400 mHz 9.4T NMR | Bruker |
| Orbital shaker | IKA KS 130 Basic | Scientific Laboratory Systems Ltd |
| PCR machine | PCR Sprint Thermal Cycler | Thermo Electron Corporation |
| pH meter | Jenway 3510 | VWR International |
| Piezo-electric force transformer | 060-1896-02 | Electrosence |
| Pipette | Gilson Pipetman P2, P20, P200, P1000 | Anachem Ltd |
| Pipette boy | Acu classic | Scientific Laboratory Systems Ltd |
| Plate reader | Multiskan Spectrum 1500 | Thermo Fisher Scientific Ltd |
| Precision adhesive press | 402 | EXAKT Technologies Inc |
| Shaking table | IKA KS 130 Basic | Jencons plc |
| Slide holder | E102 | Raymond A lamb |
| Spectrophotometer | Nanodrop ND-1000 | Labtech Int |
| Tensile testing machine | 3365 | Instron |

| | | |
|---|---|---|
| Tissue processor | Leica TP 1020 | Leica Microsystems |
| Vacuum adhesive press | 401 | EXAKT Technologies Inc |
| Vortexer | MS2 minishaker | IKA |
| Water bath | Grant | Jencons plc |
| Water Pik Ultra Water Flosser | WP100 | WaterPik |
| Water purifier | Option 7 | ELGA |

## 2.1.2 **Chemicals**

Details of the chemicals and the suppliers of the chemicals used throughout this study are shown in Table 2.2.

**Table 2.2: Chemicals used during the course of studies**

| Chemical/Reagent | Supplier |
|---|---|
| Acetone | European Bios |
| Acetic Acid | Thermo Fisher  Scientific Ltd |
| Alcian Blue | Bios Europe Ltd |
| Ammonium oxalate | Thermo Fisher Scientific Inc |
| Anhydrous sodium hydrogen phosphate | BDH Laboratory Supplies |
| Aprotinin | Mayfair  house  Leeds  Teaching  Hospital Pharmacy |
| ATPLite-M assay | PerkinElmer Ltd |
| Bovine serum albumin | Sigma-Aldrich Ltd |

| | |
|---|---|
| Calcium Chloride | VWR International |
| Calf thymus DNA | Sigma-Aldrich Ltd |
| Chloramine T | Sigma-Aldrich Ltd |
| Chondroitin sulfate | Sigma-Aldrich Ltd |
| Citric acid monohydrate | Sigma-Aldrich Ltd |
| DABCO | Sigma-Aldrich Ltd |
| DAPI | Sigma-Aldrich Ltd |
| Di-sodium hydrogen orthophosphate | VWR International |
| DPBSa | Oxoid Ltd |
| DPX mountant | Bios Europe Ltd |
| Eosin | Thermo Fisher Scientific Inc |
| Ethanol | Thermo Fisher Scientific Inc |
| Ethylenediaminetetraacetic acid (disodium salt) | VWR International |
| Fast green | Sigma-Aldrich Ltd |
| Foetal bovine serum | Lonza |
| Formic Acid | Sigma- Aldrich Ltd |
| Glacial acetic acid | VWR International |
| Giemsa stain | BDH Laboratory Supplies |
| Glycerol | Sigma-Aldrich Ltd |
| Haematoxylin | Bios Europe Ltd |
| Hydrochloric acid | Sigma-Aldrich Ltd |

| | |
|---|---|
| Hydrogen Peroxide | Sigma- Aldrich Ltd |
| ImmEdge Hydrophibic Barrier Pen | Vector Laboratories |
| Isopropanol | Thermo Fisher Scientific |
| L-Cystine hydrochloride | Sigma- Aldrich Ltd |
| Magnesium chloride | VWR International |
| Methanol | Vichers Laboratories |
| Miller's staining kit | Bios Europe Ltd |
| Neutral buffered formalin | Bios Europe Ltd |
| Oxalic acid | Thermo Fisher Scientific Inc |
| p-dimethylbenzaldehyde | Sigma-Aldrich Ltd |
| Paraffin wax pellets | Bios Europe Ltd |
| PBS tablets | Thermo Fisher Scientific Inc |
| Peracetic acid | Sigma-Aldrich Ltd |
| Perchloric acid | BDH Laboratory Supplies |
| pH buffers | Thermo Fisher Scientific Inc |
| Potassium permanganate | BDH Laboratory Supplies |
| RNAase A | Sigma-Aldrich Ltd |
| Sirius red | Raymond A Lamb Ltd |
| Sodium acetate | Thermo Fisher Scientific Ltd |
| Sodium azide | G Biosciences |
| Sodium chloride | VWR International |
| Sodium di-hydrogen orthophosphate | VWR International |

| | |
|---|---|
| Sodium hydroxide | VWR International |
| Trigene | Scientific Laboratory Supplies Ltd |
| Tris base | Sigma-Aldrich Ltd |
| Trypan Blue | Sigma-Aldrich Ltd |
| Tween 20 | Sigma-Aldrich Ltd |
| Virkon | Scientific Laboratory Supplies Ltd |
| Xylene | Bios Europe Ltd |

### 2.1.3 **Cells**

The cell culture reagents used throughout this study are listed in Table 2.3 and cell types and suppliers are listed in Table 2.4**.**

**Table 2.3: Cell culture reagents used during the course of the studies**

| Reagent | Supplier |
|---|---|
| Dulbecco's modified Eagle`s medium (DMEM) | Lonza |
| Fetal bovine serum (FBS) | Lonza |
| Glasgow's minimal essential medium (GMEM) | Sigma-Aldrich |
| L-Glutamine (200 mM) | Lonza |
| Penicillin-streptomycin (5000 $U.mL^{-1}$, 5000 $U.mL^{-1}$) | Lonza |
| Trypsin-EDTA | Sigma-Aldrich |
| Tryptose phosphate broth | Sigma-Aldrich |

**Table 2.4: Cells used during the course of the studies**

| Name | Type | Source | Supplier |
|---|---|---|---|
| 3T3 | Fibroblasts | Murine | European Collection of Animal Cell Cultures |
| Baby Hamster Kidney (BHK) | Fibroblasts | Cricetine | Health Protection Agency |

### 2.1.4 **Antibodies**

Details of the antibodies used for investigations are presented in Table 2.5 and Table 2.6. The LabVision UltraVIsion ONE Detection System (Thermo Fisher Scientific) was used to visualise antibodies.

**Table 2.5: Primary antibodies**

| Antigen | Clone | Antigen retrieval | Isotype | Working dilution | Supplier |
|---|---|---|---|---|---|
| α-gal | M86 | Proteinase K | IgM | 1:4 | Enzo Life Sciences |
| Collagen I | - | Proteinase K | IgG | 1:50 | Millipore |
| Collagen II | COLL-II | Proteinase K | IgG | 1:50 | Millipore |
| Collagen III | - | Proteinase K | IgG | 1:100 | Abcam |
| Collagen IV | CIV22 | Proteinase K | IgG | 1:4 | Dako |
| Collagen VI | - | Proteinase K | IgG | 1:50 | AbD Serotec |
| Osteocalcin | 8H12F9H10 | Proteinase K | $IgG_{2a}$ | 1:50 | AbD Serotec |

**Table 2.6: Isotype control antibodies**

| Isotype | Source | Supplier |
|---------|--------|----------|
| IgG$_1$ | Mouse | Dako (X0931) |
| IgG$_{2a}$ | Mouse | Dako (X0932) |
| IgM | Mouse | Dako (X0942) |

## 2.1.5 **Kits**

Kits used throughout the studies are listed in Table 2.7.

**Table 2.7: Kits used throughout the studies**

| Kit | Use | Supplier |
|-----|-----|----------|
| LabVision UltraVIsion ONE Detection System | Antibody visualisation | Thermo Fisher Scientific |
| DNeasy Blood & Tissue | DNA extraction | Qiagen |

## 2.1.6 **Consumables**

### 2.1.6.1 Dissection instruments

A size 22 scalpel handle, scissors and forceps were obtained from Seward Thackray. Single-use size 22 scalpel blades were purchased from Thermo Fisher Scientific Ltd.

### 2.1.6.2 Glassware

Glassware (bottles, beakers and measuring cylinders) were cleaned by soaking overnight in Neutracon® detergent followed by washes in tap water and a final wash in distilled water.

### 2.1.6.3    Sterile plasticware

Specimen containers (60 ml, 150 ml and 250 ml) were purchased from Scientific Laboratory Supplies Ltd.   Stripette® disposable pipettes were supplied by Sigma Aldrich Ltd.

### 2.1.7  **Stock solutions**

#### 2.1.7.1    Phosphate buffered saline (PBS)

One PBS tablet was dissolved in 100 mL of distilled water and kept at room temperature.

#### 2.1.7.2    Tris buffered saline (TBS)

Tris solution (pH 7.6), 2M 25 ml was mixed with 50 ml 3M NaCl solution. The volume was made up to 1 L using distilled water. The pH of the solution was adjusted to pH 7.6.  The solution was sterilised by autoclaving and stored at room temperature.

#### 2.1.7.3    3T3 culture medium

3T3 cells were cultured using Dulbecco's modified Eagle's medium (DMEM) supplemented with 10% (v/v) foetal bovine serum (FBS), 2mM L-glutamine and 100 U.mL$^{-1}$ each of penicillin and streptomycin.

#### 2.1.7.4    BHK culture medium

BHK cells were cultured using Glasgow's minimal essential medium (GMEM) supplemented with 5% (v/v) FBS, 2.5% (v/v) tryptone phosphate broth (TPB), 1 mM L-glutamine, and 100 U.mL$^{-1}$ each of penicillin and streptomycin.

## 2.1.8  Decellularisation solutions

2.1.8.1   Hypotonic buffer (10 mM tris, 2.7 mM EDTA, 10 KIU.mL$^{-1}$ aprotinin)

Trizma base (1.21 g) and EDTA (1 g) were dissolved in 900 mL distilled water using a magnetic stirrer and stirrer bar.  The pH was then adjusted to 8.0 – 8.2 by adding 6M hydrochloric acid or 6M sodium hydroxide drop wise, after which the volume was made up to 1 L using distilled water.

2.1.8.2   SDS hypotonic buffer (0.1% (w/v) SDS, 10 mM tris, 2.7 mM EDTA, 10 KIU.mL$^{-1}$ aprotinin)

SDS (0.5 g) was added to hypotonic buffer (500 mL) using a magnetic stirrer and stirrer bar.

2.1.8.3   Wash buffer (10 KIU.mL$^{-1}$ aprotinin)

One PBS tablet per 100 mL was added to distilled water to the volume required, to which aprotinin (10 KIU.mL$^{-1}$) was added.

2.1.8.4   Wash buffer with EDTA (2.7 mM EDTA, 10 KIU.mL$^{-1}$ aprotinin)

EDTA (0.1% w/v) was added to wash buffer.

2.1.8.5   Nuclease solution (50 mM tris, 21 mM MgCl$_2$, 50 µg.mL$^{-1}$ BSA, 50 U.mL$^{-1}$ DNase, 1 U.mL$^{-1}$ RNase)

Trizma base (6.1 g) and magnesium chloride (2.0 g) were added to 80 mL of distilled water using a magnetic stirrer and stirrer bar and the pH adjusted to 7.5 – 7.7 using 6M hydrochloric acid or 6M sodium hydroxide. The volume was then made up to 990 mL with distilled water.  Immediately prior to use BSA (50 µg.mL$^{-1}$), RNase (1 U.mL$^{-1}$) and DNase (50 U.mL$^{-1}$) were added and the solution used within 10 minutes.

2.1.8.6   Hypertonic buffer (50 mM tris, 1.5 M sodium chloride)

Sodium chloride (87.66 g) and tris (6.06 g) were added into 900 mL distilled water.  The pH was adjusted to 7.5 – 7.7 using 6M hydrochloric acid or 6M

sodium hydroxide. The volume was then made up to 1000 mL using distilled water.

2.1.8.7    Peracetic acid (PAA) solution (0.1% v/v)

Peracetic acid solution (1.57 mL) was added to 500 mL of PBS solution and the pH adjusted to 7.2 – 7.5 using 6M hydrochloric acid or 6M sodium hydroxide. The solution was made fresh and used within 10 minutes.

## 2.2 Methods

### 2.2.1 Basic techniques

#### 2.2.1.1 Measurement of pH

The pH of solutions was measured using a Jenway 3020 pH meter. Calibration was carried out using standard solutions at pH 4, 7 and 10. The pH was altered using 6M hydrochloric acid or 6M sodium hydroxide and the pH was measured using temperature compensation.

#### 2.2.1.2 Microscopy

Bright-field microscopy was carried out using an Olympus BX51 upright microscope. Inverted microscopy was performed using an Olympus IX71 inverted microscope. Images were captured using an attached Evolution MP Colour digital camera controlled using cell^B® imaging software with correct Kohler illumination. Fluorescence microscopy was carried out by illuminating fluorescently stained slides using a BX51-RFA fluorescent vertical illuminator and the same Olympus BX51 upright microscope. Images were captured using an attached Evolution MP Colour digital camera controlled using cell^B® imaging software.

#### 2.2.1.3 Moist heat sterilisation

Solutions suitable for autoclaving were sterilised by autoclaving at 121 °C and 15 psi for 20 minutes with caps loosened slightly.

#### 2.2.1.4 Dry heat sterilisation

Items were wrapped in foil and placed in an oven and held at a temperature of 180 °C for 4 hours.

## 2.2.2 **Dissection**

### 2.2.2.1 Equipment

Equipment used to dissect menisci and bone-meniscus-bone are listed in Table 2.8.

**Table 2.8: Dissection equipment**

| Equipment | Size | Supplier |
|---|---|---|
| Bench top clamp | - | Irwin |
| Hand saw | - | - |
| Scalpel handle | Size 4 | Scientific Laboratory Supplies Ltd |
| Rat tooth forceps | - | Seward Thackray |
| Curved scissors | - | Seward Thackray |

### 2.2.2.2 Dissection method

Porcine right hind legs from female white pigs (~6 months old, 75kg) were obtained from the abattoir (J. Penny, Rawdon, Leeds) within 24 hours of slaughter. Menisci and bone-meniscus-bone were obtained as shown in Figure 2.1. Incisions were made in the porcine knee to isolate the knee joint capsule (A). The patella was then removed by cutting through the patella tendon and down into the intercondylar fossa (B). Incisions were made in order to separate the femur from the tibia and this exposed the tibial plateau and menisci (C). If retrieving only meniscus, then the medial meniscus was obtained at this stage by cutting through the meniscal horns. If dissecting bone-meniscus-bone the lateral meniscus was cut at the horns (D) leaving the top of the tibial plateau and medial meniscus intact. The top of the tibial plateau was sawn off (E) with ~2 cm of bone remaining to the surface (F). Rat tooth forceps were used to remove connective tissue and separate the meniscus from the PMCP (G). The tibial plateau was then clamped and the lateral region of the tibial plateau removed (H). This flat edge enabled improved clamping of the remaining sample and so

further portions of bone were removed using a saw to leave a single segment of bone to which the meniscus was attached (I, J). At this point, rat tooth forceps were again employed to remove tissue from around the attachment sites of the medial meniscus, including remaining portions of the ACL and PCL (K). The bone was then sawn through the middle and separated into individual bone blocks (L). These were cut to ~10 mm x 10 mm x 15 mm (M, N) and excess blood removed by washing in PBS (O). Menisci were then stored at -20 °C in sterile plastic pots containing PBS soaked filter paper.



**Figure 2.1: Dissection of bone-meniscus-bone.**

## 2.2.3 **Tissue preparation**

### 2.2.3.1    Fixation

Meniscus was cut into pieces no more than 4 mm in thickness along the radial axis and bone was cut into pieces measuring 3 mm x 11 mm x 15 mm and placed in labelled histocassettes.   These were then either immersed in 10% (v/v) neutral buffered formalin for 48 hours if destined for histology or immersed in zinc fixative for 16 hours if destined for immunohistochemistry.  Zinc fixative solution (pH 7.4) was comprised of 5 $g.L^{-1}$ zinc acetate, 5 $g.L^{-1}$ calcium acetate, and 0.5 $g.L^{-1}$ zinc chloride.

### 2.2.3.2    Decalcification

Samples of previously fixed bone were decalcified in 125 $g.L^{-1}$ EDTA under agitation at 37 °C.  EDTA was changed every other day and decalcification assessed using the calcium oxalate test.

### 2.2.3.3    Calcium oxalate test

Reagents:

- Citric-Phosphate buffer
  - 7.5 $g.L^{-1}$ citric acid
  - 4.0 $g.L^{-1}$ anhydrous sodium hydrogen phosphate
- Saturated ammonium oxalate solution

Samples (0.5 mL) were taken of solutions being used to decalcify bone and placed into bijouxs.   Citrate-phosphate buffer (1 mL) and saturated ammonium oxalate solution (2.5 mL) were added to each sample and mixed by inverting.  Samples were left undisturbed for 20 minutes after which they were checked for precipitate formation.   Presence of a precipitate indicated the presence of calcium ions in the sample and incomplete decalcification.

### 2.2.3.4    Lyophilisation

Tissue was cut into ~1 mm$^3$ pieces using a scalpel and weighed into bijouxs.  Lids were left slightly loose and bijouxs containing samples were placed in a freeze-drier (Thermo, ModulyoD) at -50 °C, 0.15 – 0.2 bar, and freeze dried to constant weight.

### 2.2.3.5    Homogenisation

Freeze-dried tissue was placed in a Spex Sampleprep cryomill and comminuted to a fine powder by mechanical disruption for five minutes.

### 2.2.3.6    Acid hydrolysis

Tissue samples were hydrolysed to break down proteins to their constituent amino acids for subsequent determination of hydroxyproline.  Samples (100 mg) were added to SureSeal polypropylene tubes and 5 mL of 6M hydrochloric acid added.  Tubes were then sealed and wrapped in parafilm to avoid evaporation, and incubated in a heating block at 120 °C for 6 hours.  Samples were then neutralised using 6M sodium hydroxide.

### 2.2.3.7    Papain digestion

Reagents:

- Digestion solution
    - 1250 U papain
    - 0.788 g.L$^{-1}$ L-cysteine hydrochloride
    - 1.8612 g.L$^{-1}$ EDTA
    - PBS

Lyophilised samples were digested using papain for subsequent quantification of sulphated glycosaminoglycans.  Samples (50 mg) were incubated in papain digestion solution (5 mL) at 60 °C in a water bath for 72 hours until fully digested.

## 2.2.4 **Histological techniques**

### 2.2.4.1 Paraffin embedding

Menisci were cut radially into 10 slices approximately 4 mm in width. Each slice was then placed into 50 mL 10% (v/v) NBF for 48 hours prior to being placed into cassettes for dehydration using an automated tissue processor. The programme used immersed the slices sequentially into the following reagents: 10% (v/v) NBF for 1 hour (this step was omitted when zinc fixative was used), 70% (v/v) ethanol for 1 hour, 90% (v/v) ethanol for 1 hour, 100% (v/v) ethanol for 2 hours 20 minutes, 100% (v/v) ethanol for 3 hours 20 minutes, 100% (v/v) ethanol for 4 hours 20 minutes, xylene for 1 hour, xylene for 1 hour 30 minutes, xylene for 2 hours, molten wax for 1 hour 30 minutes, molten wax for 2 hours, and molten wax for 2 hours. Once this had finished the slices were taken and placed into wax moulds and covered in molten wax then left to solidify. The wax moulds were then removed and any excess wax trimmed using a forceps handle.

### 2.2.4.2 Sectioning of wax-embedded tissue blocks and slide preparation

Blocks were sectioned using a microtome set to cut at a width of 6 µm and a cutting angle of 4°. Sections were transferred to a water bath (45 °C) using forceps and a soft brush and then transferred onto SuperFrost Plus slides. These were then placed onto a hot plate (55 °C) to facilitate adhesion to the slide and dry the sections.

### 2.2.4.3 Dewaxing and rehydration of paraffin embedded sections

Slides were placed in two pots of xylene for ten minutes each before being transferred to three pots of absolute ethanol for three, two and two minutes, respectively. Slides were then immersed in 70% (v/v) ethanol for two minutes and then transferred to running tap water for three minutes.

### 2.2.4.4 Dehydration and mounting of stained slides

Slides were placed in 70% (v/v) ethanol for five seconds before being transferred to three pots of absolute ethanol for one, two and three minutes

respectively. They were then transferred to two pots of fresh xylene for ten minutes each after which sections were mounted using a single drop of DPX mountant and covered using a cover slip. Slides were then left to dry inside the fume hood for a minimum of three hours.

### 2.2.4.5   Resin embedding

Fixed bone was dehydrated in a graded ethanol series (0%, 20%, 40%, 60%, 80%, 100%) before infiltration of Technovit resin in a graded resin-ethanol series (20:80, 40:60, 60:40, 80:20, 100:0). Once infiltration reached 100:0 stage samples were placed under vacuum in 100% resin for seven days. Samples were then removed from vacuum and placed in moulds and immersed in resin to be photo-cured under UV light over 24 hours. Once cured resin blocks were removed from moulds and attached to slides using cement.

### 2.2.4.6   Sectioning of resin-embedded tissue blocks and slide preparation

Slides with resin blocks were ground down to the sample using an automatic grinder. An additional slide was glued to the exposed face to sandwich the resin block between two slides. The cemented side was attached to the slide holder of the bone saw (EXACT) by vacuum and set 400 µm from the secondary slide. A slice was then cut and ground down in increments to 20 µm and section thickness was confirmed using a digital micrometer.

## 2.2.5  Histological staining

### 2.2.5.1   Alcian Blue – Glycosaminoglycans

Reagents:

- 10 g.L$^{-1}$ Alcian blue – pH 2.5
- 525 mM Acetic acid

- Eosin

Slides containing paraffin embedded sections were dewaxed and rehydrated before a brief initial wash in 3% (v/v) acetic acid. Slides were then immersed in 1% (w/v) alcian blue for 15 minutes after which each slide was blotted dry using tissue paper. The slides were subsequently immersed in eosin for one minute before dehydration and mounted for viewing.

2.2.5.2    Haematoxylin and eosin – Cell morphology and histoarchitecture

Reagents:

- Haematoxylin
- Eosin

Slides were dewaxed and rehydrated before immersion into pre-made haematoxylin solution for one minute. Slides were then transferred to running tap water until the water ran clear after which they were immersed in eosin for three minutes. Slides were then dehydrated and mounted.

2.2.5.3    Safranin O – Proteoglycans

Reagents:

- 1 g.L$^{-1}$ Safranin O
- 0.2 g.L$^{-1}$ Fast green
- 1.21 M Acid alcohol
- 175 mM Acetic acid
- Haematoxylin (Weigart's)

Sections were dewaxed and rehydrated before immersion in Weigart's haematoxylin for three minutes. This was followed by a wash in running tap water for 10 minutes before differentiation in acid alcohol for one minute. A 5 minute rinse in running tap water followed after which sections were immersed in fast green for five minutes. This was rinsed off using a

10-15 second rinse in acetic acid before immersion in safranin O solution for 4 minutes and finally dehydration and mounting.

## 2.2.5.4 Sirius red/Miller's elastin – Collagen and Elastin

Reagents:

- 50 g.L$^{-1}$ Potassium permanganate
- 10 g.L$^{-1}$ Oxalic acid
- 1 g.L$^{-1}$ Sirius red

Slides were dewaxed and rehydrated then immersed into 5% (w/v) potassium permanganate for five minutes. Each slide was then rinsed using distilled water before immersion into 1% (w/v) oxalic acid for two minutes. Slides were then rinsed using distilled water, first for one minute then for four minutes. They were then transferred to 70% (v/v) ethanol for one minute followed by immersion in 95% (v/v) ethanol for one minute. Slides were then stained using Miller's stain for one hour after which they were transferred to 70% (v/v) ethanol until they ran clear. Slides were then transferred to 95% (v/v) ethanol for one minute, rinsed in tap water for two minutes, then stained using Weigart`s haematoxylin for ten minutes. They were then rinsed again, firstly using tap water for one minute followed by distilled water for 30 seconds. Slides were then stained using picro Sirius red for one hour, rinsed using distilled water and blotted dry using tissue paper, before being dehydrated and mounted.

## 2.2.5.5 4',6-diamidino-2-phenylindole (DAPI) – DNA

Reagents:

- DAPI dye solution
  - 1.211 g.L$^{-1}$ Tris base
  - 0.3724 g.L$^{-1}$ Disodium ethylenediaminetetraacetic acid
  - 5.8 mg.L$^{-1}$ Sodium chloride
  - 1 mg.L$^{-1}$ DAPI dye
  - pH adjusted to 7.4 before use

Dewaxed and rehydrated slides were placed into a slide holder and stained using DAPI dye solution in the dark and at room temperature for 10 minutes followed by three washes using PBS for ten minutes each. Sections were then mounted using a glass cover slip and 1,4-diazabicyclo[2.2.2]octane (DABCO):glycerol (1:9) mountant. Sections were then viewed using ultra violet microscopy under a DAPI filter.

### 2.2.5.6 McNeal's Tetrachrome – Bone

Reagents:

- 0.25 M Formic Acid
- McNeal's Tetrachrome
- 6.87 M Glycerol
- 12.04 M Methanol
- 0.05 $g.L^{-1}$ Toluidine Blue
- 0.1 $g.L^{-1}$ Methylene Blue
- 0.16 $g.L^{-1}$ Azure A Eosinate
- 0.02 $g.L^{-1}$ Methyl violet
- 1 $g.L^{-1}$ Basic Fuchsin

Slides were etched by immersion in ethanol followed by formic acid for 10 minutes each. Distilled water was then used to rinse the slides before immersion into 10% McNeals Tetrachrome for five minutes. Excess stain was then removed by washing in running tap water. This was followed by a dip in 70% (w/w) ethanol and immersion in basic fuchsin for 30 seconds. Slides were finally washed in tap water and allowed to air dry for two hours.

### 2.2.5.7 Safranin O – Proteoglycans

Reagents:

- 1 $g.L^{-1}$ Safranin O
- 0.2 $g.L^{-1}$ Fast green
- 1.21 M Acid alcohol
- 175 mM Acetic acid

- Haematoxylin (Weigart's)

Sections of native and decellularised meniscus were dewaxed and rehydrated before immersion in Weigart's haematoxylin for three minutes. This was followed by a wash in running tap water for 10 minutes before differentiation in acid alcohol for one minute. A 5 minute rinse in running tap water followed after which sections were immersed in fast green for five minutes. This was rinsed off using a 10-15 second rinse in acetic acid before immersion in safranin O solution for 4 minutes and finally dehydration and mounting. Stained sections were viewed using an upright microscope under bright-field illumination.

## 2.2.6 **Biochemical Assays**

### 2.2.6.1    Collagen

Reagents:

- Assay buffer
  - 33.25 $g.L^{-1}$ Citric acid
  - 140 mM Acetic acid
  - 80 $g.L^{-1}$ Sodium acetate-3-hydrate
  - 20% (v/v) Propan-1-ol
  - Distilled water
- Ehrlichs reagent
  - Propan-1-ol
  - 150 $g.L^{-1}$ p-dimethylbenzaldehyde
  - 60% (v/v) Propan-1-ol
  - 2.77 M Perchloric acid
  - Distilled water
- 14.1 $g.L^{-1}$ Chloramine T solution

Collagen content was determined using the hydroxyproline assay. Homogenised and lyophilised meniscus tissue samples of known weight

were added to SureSeal polypropylene tubes and hydrolysed using 5 mL of 6M hydrochloric acid at 120 °C for 6 hours in a heating block (Section 2.2.3.6). Hydrolysed samples were neutralised using 6M sodium hydroxide and the volume recorded. Standard and test solutions (50 μL) were added to wells of a 96-well flat-bottomed plate. Chloramine T solution (50 μL) was added to each well and placed on a shaker for two minutes at 60 rpm followed by addition of 100 μL of Ehrlich's reagent to each well and incubation at 56 °C in a water bath for 45 minutes. Plates were then read at 570 nm in a plate reader and absorbance values converted to hydroxyproline concentration by linear regression from the standard curve. The hydroxproline content of the tissue samples was calculated and then multiplied by 7.14 to obtain collagen content

## 2.2.6.2    Glycosaminoglycans (GAGs)

Reagents:

- Dimethylmethylene blue dye
  - 16 mg.L$^{-1}$ Dimethyl methylene blue
  - 2 g.L$^{-1}$ sodium formate
  - 0.2% (v/v) formic acid
  - 0.5% (v/v) ethanol
- Assay buffer
  - 68.5 mM sodium di-hydrogen orthophosphate
  - 31.5 mM di-sodium hydrogen orthophosphate

Quantification of GAGs was performed colorimetrically using the dimethylmethylene blue (DMB) assay. Lyophilised samples of known weight were digested using 5 mL of papain (Section 2.2.3.7) and then diluted in assay buffer (1:10, 1:50, 1:100). Concurrently, assay standards were made up from chondroitin sulphate and assay buffer (0, 3.125, 6.25, 12.5, 25, 50, and 100 μg.mL$^{-1}$). Each sample and standard (40 μL) were added to three wells each of a flat-bottomed 96-well plate along with 250 μL of DMB dye and gently shaken for 2 minutes on a plate shaker. Plates were then placed in a plate reader and optical density read at 525 nm. A

standard curve was plotted from the chondroitin sulphate standards and linear regression performed to interpolate the sample GAG concentrations. The GAG content of the tissue was then calculated in $\mu$g.mg$^{-1}$.

2.2.6.3    Quantification of meniscus DNA content

Reagents:

- DNeasy kit

Menisci were cut into ~1 mm$^3$ pieces and weighed into 2 mL micro-centrifuge tubes (25 mg for fresh and 150 mg for decellularised).  For fresh menisci, 180 µL buffer ATL and 20 µL proteinase K (>600 mAU.mL$^{-1}$) from a DNeasy kit (Qiagen) were added and samples were incubated at 56 °C in a water bath overnight.  The volumes of buffer ATL and proteinase K were doubled for decellularised menisci.  Samples were retrieved and DNA purified using the mini-spin columns provided in the DNeasy kit to a final volume of 400 µL.  Purified samples were then assayed at 260 nm using a NanoDrop 1000 spectrophotometer (Thermo Scientific).

2.2.6.4    Quantification of bone DNA content

Reagents:

- DNeasy kit
- Digestion buffer:
  - 10 g.L$^{-1}$ SDS
  - 125 g.L$^{-1}$ (w/v) EDTA
  - 10% (v/v) Proteinase K (>600 mAU.mL$^{-1}$)

Bone blocks were cut into ~2 mm$^3$ pieces and freeze-dried to constant weight prior to comminution using a cryomill.  Samples were then weighed into 2 mL micro-centrifuge tubes (25 mg for fresh and 100 mg for decellularised).  For all samples, 1520 µL of digestion buffer was added and samples were incubated at 56 °C in a shaking incubator overnight to

agitate samples. A further 80 µL of proteinase K was then added and samples were once again incubated at 56 °C in a water bath for 3 hours. Samples were retrieved and DNA from 400 µL of each digest was purified using a single mini-spin column to a final volume of 400 µL resulting in four columns per sample. Final eluants were pooled together and assayed at 260 nm using a NanoDrop 1000 spectrophotometer (Thermo Scientific).

## 2.2.7  Immunohistochemistry

### 2.2.7.1    Antigen retrieval

Antigen retrieval was performed using proteinase K (Dako, 20 mg.mL$^{-1}$) digestion of zinc-fixed paraffin wax embedded sections. Drops of proteinase K solution were used to cover the entire section and left at room temperature for 20 minutes before rinsing with TBS to terminate the reaction.

### 2.2.7.2    Immunohistochemical staining

Reagents:

- TBS pH 7.6
- TBS containing 0.05 % (v/v) Tween 20, pH 7.6
- Antibody diluent:
  - TBS (pH 7.6)
  - 0.1 g.L$^{-1}$ Sodium azide
  - 0.1 g.L$^{-1}$ Bovine serum albumin (BSA).
  - The pH was adjusted to pH 7.6
- 3% (v/v) hydrogen peroxide ($H_2O_2$):
  - 30 % (v/v) $H_2O_2$
  - PBS pH 7.6
- Lab Vision Ultravision Detection System

Paraffin wax embedded sections were dewaxed and rehydrated (Section 2.2.4.3) prior to antigen retrieval. Peroxidase blocking was then performed

by immersion in 3% (v/v) $H_2O_2$ for 20 minutes at room temperature and washed in distilled water. A hydrophobic pen was used to ring the sections, which were then washed once by immersion in TBS and drops of V block solution (Ultravision Detection kit) were placed on each section for 10 minutes. Sections were then washed twice using TBS for 10 minutes on a plate rocker before incubation with the primary antibody (50 µL) which was diluted in PBS to the working concentration (Table 2.5) for one hour in a moist environment. Isotype control antibodies were diluted to the same protein concentration as primary antibodies, while a negative control was also employed where antibody diluent (50 µL) was used instead of an antibody. Subsequent washing in TBS containing Tween, and TBS (twice for 10 minutes each) preceded incubation with HRP polymer solution (Ultravision Detection kit) for 30 minutes at room temperature in the dark. Slides were again washed using TBS containing Tween and TBS (twice for 10 minutes each) after which 3,3'-diaminobenzidine (DAB) plus chromagen (50 µL) was added to each section and left to allow the colour to develop for 10 minutes. The reaction was terminated by washing the slides in slow running tap water following which sections were counterstained using haematoxylin and dehydrated and mounted as already described.

## 2.2.8  Cell culture

Cell culture was performed in a class II microbiological safety cabinet

### 2.2.8.1  Cell counting

Cell suspensions were diluted to the desired level using PBS and 10 µL of trypan blue was added to 90 µL of diluted cell suspension. Samples were transferred to a haemocytometer and visualised under an inverted-microscope for counting. Four grids were counted and the total divided by four to obtain an average count. Live cells appeared clear while dead cells appeared blue due to infiltration of trypan blue through cell membranes. The following formula was used to calculate cell density:

$$Cell\ density = \frac{Total\ count}{Grids} \times 10^4 \times Dilution\ factor$$

### 2.2.8.2 Cell resurrection from frozen

Cryovials were retrieved from liquid nitrogen storage and thawed for 2 minutes in a water bath at 37 °C, or until all ice crystals had melted. The vial contents were then transferred to a falcon tube and 10 mL of pre-warmed cell culture medium was added over the course of a minute. The cell suspension was then centrifuged at 150 g for 10 minutes and resuspended in 15 mL of pre-warmed medium and added to a T75 flask. The flask was incubated at 37 °C and in an atmosphere of 5% (v/v) $CO_2$ in air with the first medium change occurring the following day and subsequent medium changes every 2-3 days until passage at approximately 80% confluence.

### 2.2.8.3 Passage

Flasks were removed from the incubator and the cell monolayer washed using 10 mL of PBS without calcium and magnesium. Trypsin-EDTA (2 mL) was added and the flask incubated at 37 °C for 5 minutes or until all cells had detached from the culture surface. Cell culture medium was added in a 3:1 ratio to the Trypsin-EDTA to terminate the reaction. The suspension was then transferred to a centrifuge tube and centrifuged at 150 g for 10 minutes. The supernatant was aspirated from the tube without dislodging the cell pellet and 10 mL of culture medium was added. The cell pellet was resuspended by gentle trituration using a 5 mL pipette and a sample taken for counting (Section 2.2.8.1). Cells were then seeded into T75 flasks at 2 x $10^4$ cells.$cm^{-2}$ and incubated at 37 °C and in an atmosphere of 5% (v/v) $CO_2$ in air.

### 2.2.9 Numerical analysis

All numerical analysis within this study was performed using Microsoft Office Excel 2007.

## 2.2.9.1 Confidence limits

In order to present data as the mean ± 95% confidence intervals (C.I.), data was analysed using the 'Descriptive Statistics' function of the 'Data Analysis' add-on within Microsoft Office Excel 2007 using α=0.05.

$$mean = \frac{\Sigma x}{n}$$

$$\sigma = \sqrt{\frac{\Sigma x^2}{n-1}}$$

$$SE = \frac{\sigma}{\sqrt{n}}$$

$$95\% \ C.I. = SE \ x \ t \ value$$

where,

$x$      value

$n$      sample size

$\sigma$      standard deviation

$SE$      standard error

## 2.2.9.2 Statistical analysis

To compare the means of two groups the student's t-test was used, with an analysis of variance (ANOVA) used when more than two groups were compared. The minimum significant difference (MSD), calculated using the T-method was used to differentiate between individual group means (Sokal & Rohlf, 1981) with p values smaller than 0.05 considered significant.

$$Standard \ error = \sqrt{\frac{\sigma_1^2}{n_1} + \frac{\sigma_2^2}{n_2}}$$

$$Critical \ value = Q\alpha[k, v]$$

$$MSD = SE \times Critical\ value$$

where,

α      p = 0.05

k      number of groups

v      degrees of freedom = $n$ - 1

### 2.2.9.3    Arcsin transformation

As many biological variables do not meet the assumptions of parametric statistical tests, it is sometimes necessary to transform the data so that it fits these assumptions better.   In order to accurately compute 95% confidence intervals and perform statistical analysis values presented as proportions or percentages, values were first transformed to arcsin.  Back transformation was performed for presentation.

### 2.2.9.4    Linear regression

To interpolate sample concentrations from standard curves linear regression was applied.  The gradient of the linear portion of a standard curve was determined and used to calculate concentrations from optical density values obtained for samples (Figure 2.2).
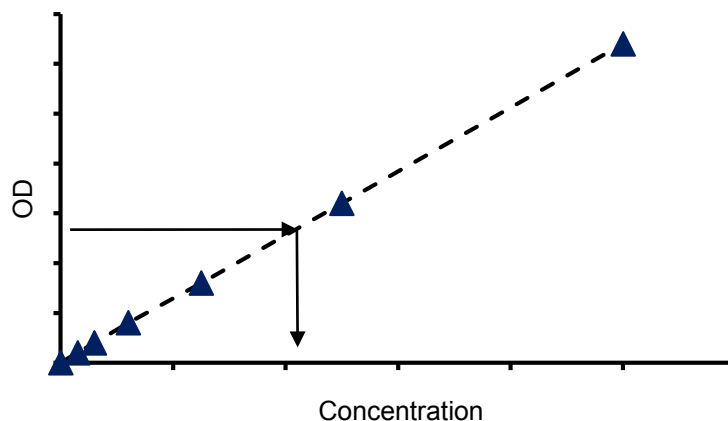


**Figure 2.2: Linear regression of standard curve.**

# Chapter 3.    Decellularisation of bone-meniscus-bone

## 3.1    Introduction

Decellularised natural tissue matrices retain the natural organization and cell signalling cues present in extracellular matrix, and if taken from a xenogeneic source are readily available making them ideal candidates for meniscal replacement.  Investigations of synthetic materials for meniscal replacement has so far yielded limited success with integration and promotion of matrix formation however cartilage degeneration has also been noted (Kang *et al.*, 2006; Galley *et al.*, 2011).  The use of natural materials for meniscal replacement has also shown some success with improvements shown from the pre-operative state using the CMI (Zaffagnini *et al.*, 2011).  The majority of studies, however, focus on the repair of meniscal defects over total replacement thereby circumventing the challenges associated with anatomical fixation of the meniscus.  Repair tissue formed from the treatment of defects has been shown to be mechanically inferior to native meniscal tissue (Tienen *et al.*, 2006).

It is hypothesised that the decellurisation of a readily available xenogeneic meniscus incorporating bone blocks for ease of fixation will produce a meniscal replacement with the natural cell signalling cues and biomechanical properties of the native meniscus.  Porcine tissue is readily available through abattoirs and the porcine meniscus is anatomically similar to human meniscus.

Several methods exist for the removal of cells from tissues however the level of decellularisation varies between groups.  Ideally, for total decellularisation to be achieved 100% of cellular material should be removed since cellular remnants have been implicated in the tissue remodelling outcome through modulation of macrophage phenotype (Brown *et al.*, 2009; Nagata *et al.*, 2010).

Methods for decellularisation usually comprise a combination of physical, chemical and biological methods. Physical methods are included to allow reagents in the subsequent steps to penetrate the tissue effectively. Chemical reagents are used to solubilise and wash out cellular material with enzymes used to target specific matrix-protein interactions and clear nuclear material. Final wash steps are usually incorporated to remove process reagents to avert host cytotoxicity.

### 3.1.1 Chemical agents

#### 3.1.1.1 Acids and bases

Acids and bases work through the hydrolytic degradation of biomolecules, solubilising cellular components. Peracetic acid is included as a disinfection step towards the end of decellularisation protocols and has been shown to remove residual nucleic acids without damaging the extracellular matrix (Hodde *et al.*, 2007). Bases are also used to remove hair from porcine dermis but can remove growth factors and adversely impact the mechanical properties (Reing *et al.*, 2010) by cleavage of collagen fibrils (Gorschewsky *et al.*, 2005).

#### 3.1.1.2 Solvents

Solvents act to lyse cells by dehydration and can solubilise lipids. They have been reported to effectively remove cells from dense tissue whilst also having a disinfectant action, however solvents may also precipitate proteins and crosslink collagen (Reing *et al.*, 2010; Lumpkins *et al.*, 2008; Dong *et al.*, 2009). Deeken *et al.* utilised tributyl phosphate, which forms stable complexes with metals, to decellularise porcine diaphragm tendon showing retention of collagen architecture and mechanical properties.

#### 3.1.1.3 Detergents

Detergents have been widely used in the decellularisation of tissues. They can be split into ionic, non-ionic, and zwitterionic detergents. Anionic

detergents, such as sodium dodecyl sulfate (SDS), solubilise cell and nuclear membranes and can also denature proteins. SDS has been shown to effectively remove cell and nuclear material but can also remove GAGs and growth factors, and damage collagen fibres (Reing *et al.*, 2010; Lumpkins *et al.*, 2008; Stapleton *et al.*, 2008; Deeken *et al.*, 2011). This is especially true at high SDS concentrations with studies decellularising with 1% (w/v) SDS reporting fragmentation and swelling of collagen fibres (Bodnar *et al.*, 1986; Courtman *et al.*, 1994) while 0.1% (w/v) SDS has been shown to effectively decellularise porcine heart valves without negatively impacting the ECM (Booth *et al.*, 2002). Other anionic detergents of note are sodium deoxycholate and Triton X-200. Sodium deoxycholate has been used to decellularise porcine bladder (Brown *et al.*, 2009), porcine adipose tissue (Brown *et al.*, 2011) and porcine pulmonary valves (Cebatori *et al.*, 2010), showing mixed results with effective removal of lipids (Brown *et al.*, 2011) but unsuccessful removal of all cells and DNA (Partington *et al.*, 2013) whilst also proving difficult to wash out resulting in cytotoxicity (Cebatori *et al.*, 2010). Hudson *et al.* (2004) showed Triton X-200 to be more efficacious in decellularising thin tissues but when compared to other detergents tissue treated with Triton X-200 showed greater damage.

Non-ionic detergents disrupt DNA-protein and lipid-protein interactions (Seddon *et al.*, 2004). Triton X-100 has been extensively studied for its ability to solubilise proteins and is gentler than SDS. This allows for protein-protein interactions to be sustained, however it is only efficient in decellularising thin tissues (Reing *et al.*, 2010; Yang *et al.*, 2009; Guo *et al.*, 2010). Zwitterionic detergents have also been reported to decellularise thin tissues with only mild disruption of the extracellular matrix (Hudson *et al.*, 2004). They are generally more damaging to proteins than ionic and non-ionic detergents as they incorporate aspects of both other types of detergent (Seddon *et al.*, 2004).

### 3.1.1.4 Hypertonic and hypotonic agents

Osmotic shock has also been used to lyse cells by employing hypotonic reagents (Cox and Emili *et al.*, 2006; Stapleton *et al.*, 2008), while hypertonic solutions dissociate DNA from proteins (Xu *et al.*, 2007). These agents are not effective at removing cellular remnants from tissue and are usually used in combination protocols to enhance the action of detergent and enzymatic steps (Stapleton *et al.*, 2008; Yang *et al.*, 2009).

### 3.1.2 **Biological agents**

### 3.1.2.1 Enzymes

Enzymes are employed in a decellularisation protocol for the highly specific removal of cellular or matrix components. Nucleases are used to aid in the removal of nuclear material from tissues by cleaving DNA and RNA. Cells need to be lysed to allow access of the enzymes to the nuclear material therefore nuclease steps are incorporated towards the end of a protocol. For more effectual fragmentation and hence more efficient removal of DNA, non-restriction endonucleases such as Benzonase may be used (Petersen *et al.*, 2010). Utilisation of other enzymes is dependent on the requirement to retain extracellular matrix components. Trypsin treatment may show improved GAG retention compared to detergents (Grauss *et al.*, 2005) however prolonged exposure leads to disruption of collagen and hence compromises the mechanical properties of natural matrices (Yang *et al.*, 2009). Decellularisation of ovine meniscus using trypsin and collagenase has been shown to result in partial digestion and loss of GAGs from the matrix which resulted in a mechanically stiffer tissue (Maier *et al.*, 2007). Contrary to this, using a 0.05% trypsin solution in a combination protocol to decellularise rabbit meniscus Stabile *et al.* (2010) found no statistically significant differences in the tensile and compressive properties between untreated and decellularised meniscus.

### 3.1.2.2    Non-enzymatic agents

Chelating agents such as ethylenediaminetetraacetic acid (EDTA) and ethylene    glycol tetraacetic acid (EGTA) work by chelating Ca and Mg ions and are therefore useful in disrupting cell-matrix interactions (Klebe, 1974) and inhibition of metalloproteinases (Booth *et al.*, 2002).  They are used to protect the ECM from damage by endogenous proteases released by the disruption of cells due to other decellularising agents (Booth *et al.*, 2002; Deeken *et al.*, 2010; Reing *et al.*, 2010), along with serine protease inhibitors such as aprotinin (Booth *et al.*, 2002; Stapleton *et al.*, 2008) and phenylmethylsulfonyl fluoride (PMSF), which is only suitable for research purposes due to its highly toxic nature and limited half life (Woods & Gratzer, 2005).

### 3.1.3  **Physical methods**

Aside from applying chemical and biological agents, tissues can be subjected to physical treatments to aid decellularisation.  Freeze/thaw cycles lyse cells by the generation of intercellular ice crystals and can also increase the penetration of reagents by creating space within the matrix (Gulati *et al.*, 1988; Stapleton *et al.*, 2008; Brown *et al.*, 2009).  Ice crystals can also have a deleterious effect on tissues by disrupting or fracturing the ECM.  Direct removal of cells or tissues through hydrostatic force or mechanical abrasion can also be used to enhance decellularisation however application of force can directly damage the ECM (Freytes *et al.*, 2008).  Other physical methods that have been used in decellularisation include changes in pressure, which can be used to burst cells and facilitate the removal of cellular material (Funamoto *et al.*, 2010), and electroporation whereby cell membranes are disrupted by a pulsed electrical field (Phillips *et al.*, 2010).  Again, both of these methods have the potential to damage the ECM.

### 3.1.4 **Work leading to the current study**

Initial work within the group on decellularisation aimed to develop a method for decellularisation of heart valves. Booth *et al.* (2002) investigated various detergents including 3-[(3-cholamidopropyl)dimethylammonio]-1-propanesulfonate (CHAPS), SDS, sodium deoxycholate, Triton-X, and Tween 20 and found that only SDS and sodium deoxycholate provided effective decellularisation of porcine aortic valves and patella tendon (US Patent 7354749, 2008). SDS at 0.03-0.1% (w/v) was utilised in these studies to minimise damage to the matrix and prevent cytotoxicity from potential retention, whilst protease inhibitors, EDTA and aprotinin, were also included to negate damage from endogenous proteases released during the process and preserve the ECM. This method was then adapted for the decellularisation of porcine meniscus (Stapleton *et al.*, 2008) where there is a real clinical need for a meniscal replacement as the meniscus lacks the ability to repair itself owing to its avascular nature and current repair and replacement techniques only delay the onset of osteoarthritis. Again, this incorporated a low SDS concentration solution as well as protease inhibitors, however additional steps were required due to the dense nature of the meniscus. Freeze-thaw cycles and an optional ultrasonication step were included to allow more effective diffusion of reagents into the tissue. A successful protocol was developed (US Patent 20100152852) however surgical attachment of the meniscal implant to the patient knee was still an issue as soft tissue fixation leads to the formation of mechanically inferior repair tissue. Therefore, it was hypothesised that the incorporation of bone blocks would allow easier fixation while maintaining anatomical positioning and maintenance of mechanical integrity.

## 3.2 Aims and objectives

### 3.2.1 Aims

The aim of the work presented within this chapter was to develop a protocol for the effective decellularisation of porcine bone-medial meniscus-bone.

### 3.2.2 Objectives

- To develop a decellularisation protocol for the removal of cellular and nuclear content from porcine medial meniscus and bone attachments while retaining native histoarchitecture
- To characterise the native and decellularised porcine bone-medial meniscus-bone using:
- Histology for cellular and nuclear content and visualisation of the histoarchitecture
- Extraction and quantification of DNA content

## 3.3 Methods

### 3.3.1 Decellularisation

#### 3.3.1.1 Meniscus – Original method from Stapleton *et al.*

The decellularisation treatment initially applied to the porcine medial meniscus (Figure 3.3.1) was based on the method described in Stapleton *et al.* (2008).  Menisci (n = 3) were dissected from porcine knees less than 24 hours after slaughter and subjected to decellularisation.  Treated menisci were then retrieved and prepared as described in Sections 2.2.3 and 2.2.4 for H&E (Section 2.2.5.2) and DAPI (Section 2.2.5.5) staining to observe changes to meniscal histoarchitecture and detect residual nuclear material.  The solutions used were prepared as described in Section 2.1.7. For all steps sterile 150 mL containers were used and 100 mL of each solution was used per meniscus.  Shaking tables were set at 320 rpm except for the nuclease step, which was at 80 rpm, and the final wash buffer steps which were carried out at 160 rpm.  Menisci underwent three freeze/thaw cycles during which they were frozen at -20 °C for 3 hours, or until fully frozen, and defrosted at room temperature for 4 hours, or until fully defrosted.  Specimens were then processed through three freeze/thaw cycles while immersed in hypotonic buffer (10 mM tris, 10 KIU.mL$^{-1}$ aprotinin).  Menisci were then washed using hypotonic buffer at 4 °C for 24 hours, hypotonic buffer at 37 °C for 24 hours, SDS hypotonic buffer (0.1% (w/v) SDS , 10 mM tris, 10 KIU.mL$^{-1}$ aprotinin) at 45 °C for 24 hours twice. These steps were repeated twice in the order stated.  This was followed by three washes in wash buffer (PBS, 10 KIU.mL$^{-1}$ aprotinin) at room temperature for 24 hours each, and three further washes in nuclease solution (50 mM tris, 21 mM MgCl, 50 µg.mL$^{-1}$ BSA  50 U.mL$^{-1}$ DNAase , 1 U.mL$^{-1}$ RNAase) at 37 °C for three hours each.  The menisci were then washed using wash buffer with EDTA (2.7 mM EDTA, 10 KIU.mL$^{-1}$ aprotinin) at room temperature for 12-16 hours, hypertonic solution for 24 hours at 37 °C, wash buffer with EDTA at room temperature for 12-16 hours before disinfection using PAA solution for three hours at 27 °C.  The following steps were carried out aseptically inside a class II cabinet.  The

disinfected menisci were then washed using wash buffer with EDTA at 45 °C for 24 hours, wash buffer with EDTA at 37 °C for 24 hours, and five washes in wash buffer with EDTA at 4 °C for 24 hours.

| | Step | | |
|---|---|---|---|
| 1 | • Freeze/thaw for 3 hours | x3 | |
| 2 | • Freeze/thaw in Hypotonic Buffer for 3 hours | x3 | |
| 3 | • Hypotonic Buffer @ 4 °C for 24 hours | | |
| 4 | • Hypotonic Buffer @ 37 °C for 24 hours | | x3 |
| 5 | • SDS Hypotonic Buffer @ 45 °C for 24 hours | x2 | |
| 6 | • Wash Buffer @ RT for 24 hours | x3 | |
| 7 | • Nuclease treatment @ 37 °C for 3 hours | x3 | |
| 8 | • Wash Buffer with EDTA @ RT for 12-16 hours | | |
| 9 | • Hypertonic solution @ 37 °C for 24 hours | | |
| 10 | • Wash Buffer with EDTA @ RT for 12-16 hours | | |
| 11 | • PAA @ 27 °C for 3 hours | | |
| 12 | • Wash Buffer with EDTA @ 45 °C for 24 hours | | |
| 13 | • Wash Buffer with EDTA @ 37 °C for 24 hours | | |
| 14 | • Wash Buffer with EDTA @ 4 °C for 24 hours | x5 | |

**Figure 3.3.1: Original decellularisation method**

3.3.1.2    Meniscus – Method 1

Decellularisation was identical to the original method (Section 3.3.1.1) except all reagents were prepared without EDTA.    Steps that were changed from the original method are highlighted in red in Figure 3.3.2. Menisci (n = 3) were dissected from porcine knees less than 24 hours after slaughter and subjected to decellularisation.    Treated menisci were then

retrieved and prepared as described in Sections 2.2.3 and 2.2.4 for H&E (Section 2.2.5.2) and DAPI (Section 2.2.5.5) staining.

| | | |
|---|---|---|
| 1 | • Freeze/thaw for 3 hours | x3 |
| 2 | • Freeze/thaw in Hypotonic Buffer for 3 hours | x3 |
| 3 | • Hypotonic Buffer @ 4 °C for 24 hours | |
| 4 | • Hypotonic Buffer @ 37 °C for 24 hours | x3 |
| 5 | • SDS Hypotonic Buffer @ 45 °C for 24 hours | x2 |
| 6 | • Wash Buffer @ RT °C for 12 hours | x3 |
| 7 | • Nuclease treatment @ 37 °C for 3 hours | x3 |
| 8 | • Wash Buffer @ RT for 12-16 hours | |
| 9 | • Hypertonic solution @ 37 °C for 24 hours | |
| 10 | • Wash Buffer @ RT for 12-16 hours | |
| 11 | • PAA @ 27 °C for 3 hours | |
| 12 | • Wash Buffer @ 45 °C for 24 hours | |
| 13 | • Wash Buffer @ 37 °C for 24 hours | |
| 14 | • Wash Buffer @ 4 °C for 24 hours | x5 |

**Figure 3.3.2: Decellularisation method 1**

### 3.3.1.3    Meniscus – Method 2

Menisci (n = 6) were dissected from porcine knees less than 24 hours after slaughter and subjected to decellularisation.  Treated menisci were then retrieved and three were prepared as described in Sections 2.2.3 and 2.2.4 for histology.  The remaining three menisci were assayed for residual DNA as described in Section 2.2.6.3.  Decellularisation was identical to Method 1 (Section 3.3.1.2) with the addition of an extra cycle of hypotonic buffer at 4 °C for 24 hours, hypotonic buffer at 37 °C for 24 hours, SDS hypotonic

buffer at 45 °C for 24 hours and hypotonic buffer at 45 °C for 24 hours prior to the three washes in wash buffer preceding nuclease treatment. Steps changed from method 1 are highlighted in red in Figure 3.3.3.

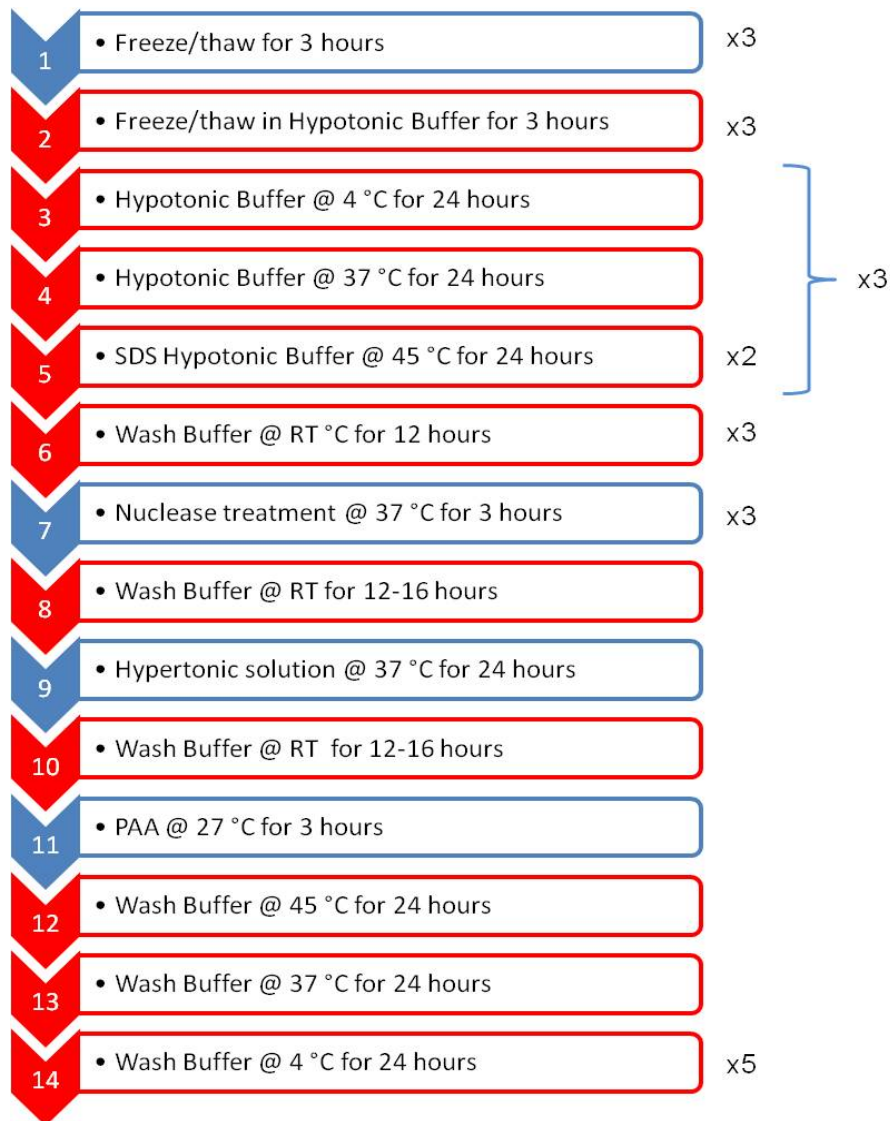| Step | Process | Repeat |
|---|---|---|
| 1 | • Freeze/thaw for 3 hours | x3 |
| 2 | • Freeze/thaw in Hypotonic Buffer for 3 hours | x3 |
| 3 | • Hypotonic Buffer @ 4 °C for 24 hours | |
| 4 | • Hypotonic Buffer @ 37 °C for 24 hours | x4 |
| 5 | • SDS Hypotonic Buffer @ 45 °C for 24 hours | x2 |
| 6 | • Wash Buffer @ RT for 24 hours | x3 |
| 7 | • Nuclease treatment @ 37 °C for 3 hours | x3 |
| 8 | • Wash Buffer @ RT for 12-16 hours | |
| 9 | • Hypertonic solution @ 37 °C for 24 hours | |
| 10 | • Wash Buffer @ RT for 12-16 hours | |
| 11 | • PAA @ 27 °C for 3 hours | |
| 12 | • Wash Buffer @ 45 °C for 24 hours | |
| 13 | • Wash Buffer @ 37 °C for 24 hours | |
| 14 | • Wash Buffer @ 4 °C for 24 hours | x5 |

**Figure 3.3.3: Decellularisation method 2**

### 3.3.1.4    Meniscus – Method 3

Menisci (n = 6) were dissected from porcine knees less than 24 hours after slaughter and subjected to decellularisation. Treated menisci were then retrieved and three were prepared as described in Sections 2.2.3 and 2.2.4 for histology. The remaining three menisci were assayed for residual DNA as described in Section 2.2.6.3. Decellularisation was identical to Method 1 (Section 3.3.1.2) except that the three 24 hour washes in wash buffer

preceding the nuclease treatment were split into six 12 hour washes in wash buffer to aid removal of SDS from the tissue prior to the nuclease step. Steps changed from method 2 are highlighted in red in Figure 3.3.4.

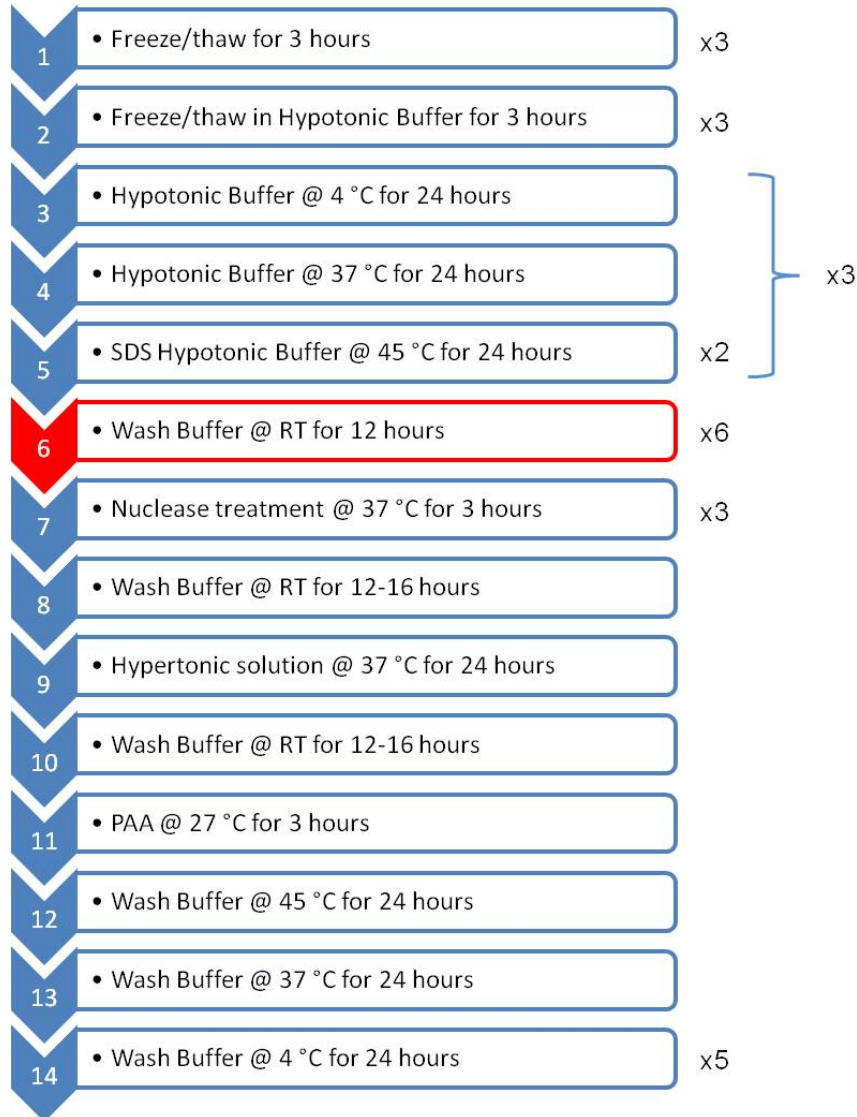| Step | Process | Repeat |
|---|---|---|
| 1 | • Freeze/thaw for 3 hours | x3 |
| 2 | • Freeze/thaw in Hypotonic Buffer for 3 hours | x3 |
| 3 | • Hypotonic Buffer @ 4 °C for 24 hours | |
| 4 | • Hypotonic Buffer @ 37 °C for 24 hours | x3 |
| 5 | • SDS Hypotonic Buffer @ 45 °C for 24 hours | x2 |
| 6 | • Wash Buffer @ RT for 12 hours | x6 |
| 7 | • Nuclease treatment @ 37 °C for 3 hours | x3 |
| 8 | • Wash Buffer @ RT for 12-16 hours | |
| 9 | • Hypertonic solution @ 37 °C for 24 hours | |
| 10 | • Wash Buffer @ RT for 12-16 hours | |
| 11 | • PAA @ 27 °C for 3 hours | |
| 12 | • Wash Buffer @ 45 °C for 24 hours | |
| 13 | • Wash Buffer @ 37 °C for 24 hours | |
| 14 | • Wash Buffer @ 4 °C for 24 hours | x5 |

**Figure 3.3.4: Decellularisation method 3**

### 3.3.1.5   Bone-meniscus-bone

Bone-meniscus-bone (BMB; n = 6) was dissected from porcine knees less than 24 hours after slaughter and subjected to decellularisation. Treated BMB's were then retrieved and menisci removed from the bone by sharp dissection. Three were prepared as described in Sections 2.2.3 and 2.2.4

for histology with the remaining three assayed for residual DNA as described in Section 2.2.6.3. Bone (n = 3) was fixed (Section 2.2.3.1) and embedded in resin (Section 2.2.4.5) for histology (Section 2.2.5.6). The remaining bone (n = 3) was assayed for residual DNA (Section 2.2.6.4). The solutions used were prepared as described in Section 2.1.7. For all steps menisci with bone (BMB) were placed in individual 250 mL containers and 150 mL of each solution was used per BMB. Shaking tables were set at 320 rpm except for the nuclease step, which was at 80 rpm, and the final wash buffer steps which were carried out at 160 rpm. Collagen fibres were teased apart at the attachment site using a scalpel, rat-tooth forceps and a magnifying lamp in order to allow diffusion of solutions into the enthesis (Figure 3.3.5) after which the bone was treated using a water flosser (Figure 3.3.6) and PBS to remove bone marrow from the bone attachments.
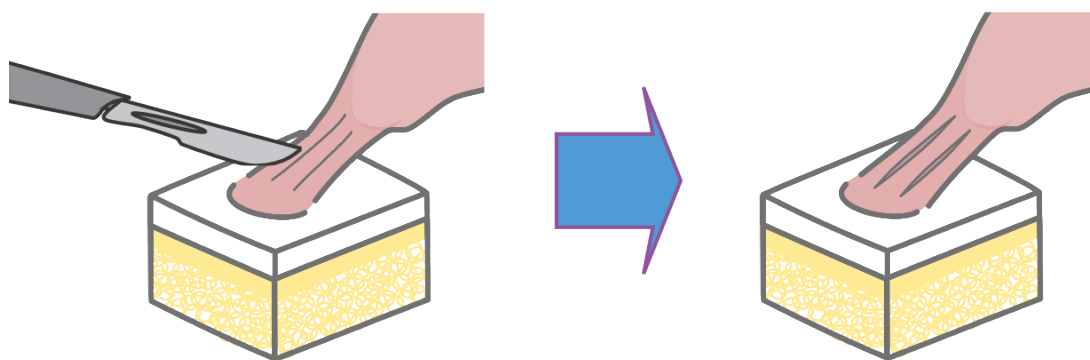


**Figure 3.3.5: Introduction of incisions to the attachment site to aid diffusion of decellularisation reagents.**

Tip

Reservoir

Release
valve

Power
switch

Dial

**Figure 3.3.6: Waterpik.** PBS stored in the reservoir was pumped through the nozzle at high velocity to clear trabecular bone of bone marrow.

BMB were then subject to three freeze/thaw cycles during which they were frozen at -20 °C for three hours, or until fully frozen, and defrosted at room temperature for 4 hours, or until fully defrosted. Specimens were then put through three freeze/thaw cycles while immersed in hypotonic buffer (10 mM tris, 10 KIU.mL$^{-1}$ aprotinin). Menisci were then washed using hypotonic buffer at 4 °C for 24 hours, hypotonic buffer at 42 °C for 24 hours, SDS hypotonic buffer (0.1% (w/v) SDS , 10 mM tris, 10 KIU.mL$^{-1}$ aprotinin) at 42 °C for 24 hours and hypotonic buffer at 42 °C for 24 hours. These steps were repeated twice in the order stated. This was followed by three washes in wash buffer (PBS, 10 KIU.mL$^{-1}$ aprotinin) at 4 °C for 24 hours each, and three further washes in nuclease solution (50 mM tris, 21 mM MgCl$_2$, 50 µg.mL$^{-1}$ BSA  50 U.mL$^{-1}$ DNAase , 1 U.mL$^{-1}$ RNAase)  at 37 °C for three hours each. The menisci were then washed using wash buffer at 4 °C for 12-16 hours, hypertonic solution (50 mM tris, 1.5 M sodium chloride) for 24 hours at 42 °C, wash buffer at 4 °C for 12-16 hours before

disinfection using 0.1% (v/v) peracetic acid solution for three hours at 27 °C. The following steps were carried out aseptically inside a class II cabinet. The disinfected menisci were washed using wash buffer at 42 °C for 24 hours twice, followed by wash buffer at 4 °C for 24 hours, and this cycle was repeated a further four times. Steps changed from method 3 are highlighted in red in Figure 3.3.7.
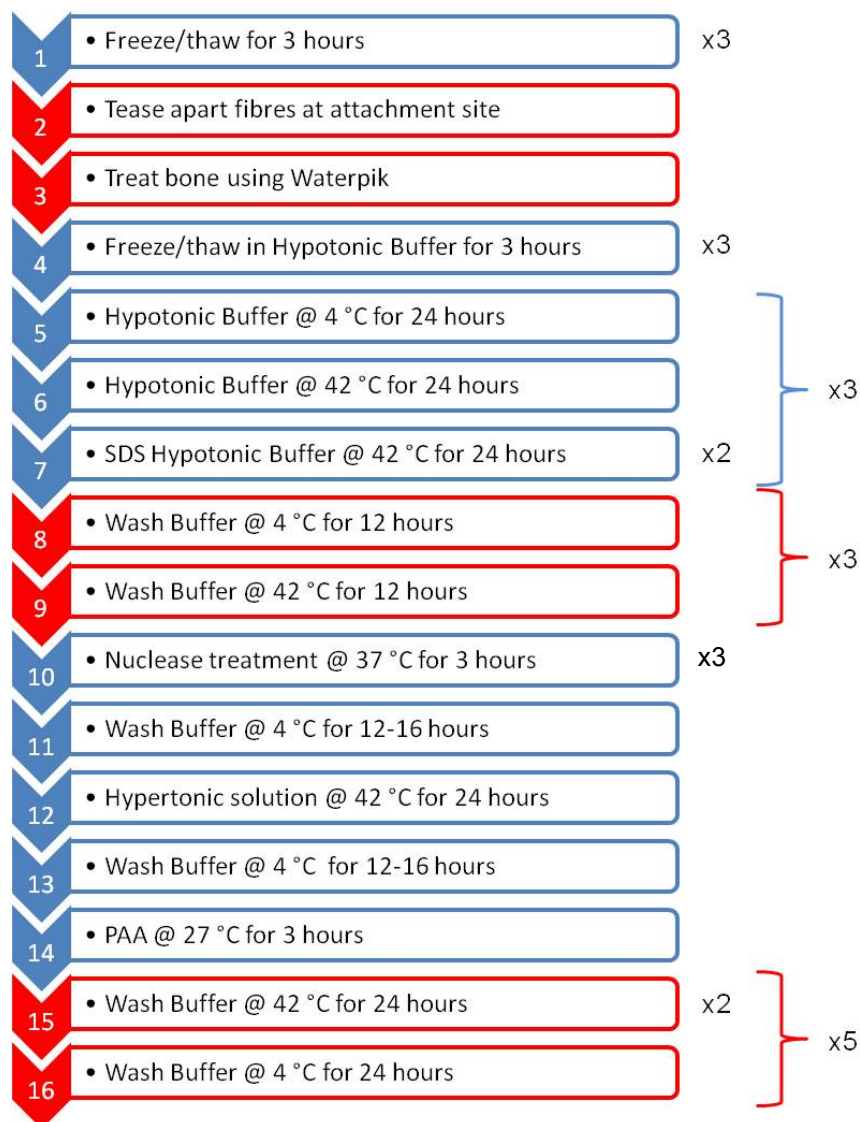


| | | |
|---|---|---|
| 1 | • Freeze/thaw for 3 hours | x3 |
| 2 | • Tease apart fibres at attachment site | |
| 3 | • Treat bone using Waterpik | |
| 4 | • Freeze/thaw in Hypotonic Buffer for 3 hours | x3 |
| 5 | • Hypotonic Buffer @ 4 °C for 24 hours | |
| 6 | • Hypotonic Buffer @ 42 °C for 24 hours | x3 |
| 7 | • SDS Hypotonic Buffer @ 42 °C for 24 hours | x2 |
| 8 | • Wash Buffer @ 4 °C for 12 hours | x3 |
| 9 | • Wash Buffer @ 42 °C for 12 hours | |
| 10 | • Nuclease treatment @ 37 °C for 3 hours | x3 |
| 11 | • Wash Buffer @ 4 °C for 12-16 hours | |
| 12 | • Hypertonic solution @ 42 °C for 24 hours | |
| 13 | • Wash Buffer @ 4 °C for 12-16 hours | |
| 14 | • PAA @ 27 °C for 3 hours | |
| 15 | • Wash Buffer @ 42 °C for 24 hours | x2 |
| 16 | • Wash Buffer @ 4 °C for 24 hours | x5 |

**Figure 3.3.7: Bone-meniscus-bone decellularisation protocol**

### 3.3.2 **Tissue sampling for histology**

Native and decellularised menisci (n = 3) were cut radially into ten Sections and prepared for Sectioning as described in Section 2.2.4.1. Each slice was then sectioned with one in every ten sections selected for staining. Both bone attachments from three native and decellularised bone-meniscus-bone were cut into three pieces measuring 3 mm x 11 mm x 15 mm and prepared for cutting and grinding as described in Sections 2.2.3.1 and 2.2.4.5. Two slices measuring ~400 µm thick were taken from each resin block and ground down to ~20 µm as described in Section 2.2.4.6 prior to staining.

### 3.3.3 **DNA extraction and quantitative analysis**

Native and decellularised menisci (n = 3) were cut into five slices along the radial axis: anterior horn (AH), anterior middle (AM), middle (M), posterior middle (PM), and posterior horn (PH). Each slice was then cut into ~1 mm$^3$ pieces with four samples taken from each slice and processed as described in Section 2.2.6.3. Both bone blocks from each native and decellularised bone-meniscus-bone were separated into bone and enthesis pieces and then cut into ~2 mm$^3$ pieces. The entire bone block was processed as described in Section 2.2.6.4 with four samples taken from each bone block and enthesis.

#### 3.3.3.1 Validation of DNA assay

Sections of bone stained with H&E were used to validate the bone DNA assay. Three squares (10 µm) were placed randomly onto the image and any cells falling within or touching the squares were counted. Sections were taken from resin embedded samples and so a section thickness of 20 µm was assumed. Cell counts were averaged to obtain the cell density within bone samples and this used in conjunction with an average DNA content of 6 pg per cell to obtain the average DNA content in bone. A bone density of 0.2 – 2 g.cm$^{-3}$, depending on location within the bone, was then

assumed and multiplied with the section volume to obtain the section mass. The average DNA content in bone was then divided by the section mass to obtain the DNA concentration of bone. This was calculated as ~1000 ng of DNA per mg of bone.

### 3.3.4  Qualitative analysis of DNA

#### 3.3.4.1  Polymerase chain reaction (PCR)

DNA extracted from native and decellularised bone-meniscus-bone (Sections 2.2.6.3 and 2.2.6.4) was used to amplify collagen I, glyceraldehyde 3-phosphate dehydrogenase (GAPDH) and β-actin genes using PCR. Upstream and downstream primers were designed using Primer3 (Untergrasser *et al.*, 2012) from sequences available on the Nucleotide database (NCBI). Primers (1 µL) for each gene were mixed with 2x PCR Master Mix (25 µL; Promega, UK), nuclease-free water (22 µL) and sample DNA (1 µL) in a PCR tube. Tubes were then spun down in a microcentrifuge to ensure all reagents were mixed. Tubes were then placed in a thermal cycler and the following program run:

**Initial Denaturation**     95 °C        3 minutes
**Denaturation**             95 °C        30 seconds  ⎫
**Annealing**                56 °C        30 seconds  ⎬    35 cycles
**Extension**                72 °C        30 seconds  ⎭
**Final Extension**          72 °C        10 minutes
**End**

#### 3.3.4.2  Primers

Primers for porcine GAPDH, Collagen I and β-actin were obtained from X and are described below.

*Porcine GAPDH:*

- Upstream primer      GGGCATGAACCATGAGAAGT
- Downstream primer      AAGCAGGGATGATGTTCTGG
- Product size      230 base pairs

Predicted Sequence

GGGCATGAACCATGAGAAGTATGACAACAGCCTCAAGATCATCAGCA
ATGCCTCCTGTACCACCAACTGCTTGGCACCCCTGGCCAAGGTCATC
CATGACAACTTCGGCATCGTGGAAGGACTCATGACCACAGTCCATGC
CATCACTGCCACCCAGAAGACTGTGGATGGCCCCTCTGGGAAACTGT
GGCGTGATGGCCGAGGGGCTCTCCAGAACATCATCCCTGCTT

*Collagen I:*

- Upstream primer      TAGCCCTGTCTGCTTCCTGT
- Downstream primer      TGCAGTTTTGGTTTTTGGTC
- Product size      243 base pairs

Predicted Sequence

TAGCCCTGTCTGCTTCCTGTAAACTCCCTCCGCCCCAATCTGGCTCCC
TCCCACCCAACCCAATTGCCCCTGACCCTGGAAACAAACAAACACCC
CAAACGGAAACCCCCCCAAAAGCCAAAAAATGGGAGACAATTTCACAT
GGACTTTGGAAAATATTTTTTTCCTTTGCATTCATCTCTCAAACTTAGTT
TTTAAATCTTTGACCAACTGAACTGAACATGACCAAAAACCAAAACTGC
A

*ẞ-actin:*

- Upstream primer      ACGTGGACATCAGGAAGGAC
- Downstream primer      ACATCTGCTGGAAGGTGGAC
- Product size      210 base pairs

Predicted Sequence:

ACGTGGACATCAGGAAGGACCTCTACGCCAACACGGTGCTGTCTGGC
GGGACCACCATGTACCCCGGCATCGCCGACAGGATGCAGAAGGAGA
TCACGGCCCTGGCGCCCAGCACCATGAAGATCAAGATCATCGCCCCT
CCCGAGCGCAAGTACTCCGTGTGGATCGGGGGGCTCCATCCTGGCCT
CGCTGTCCACCTTCCAGCAGATGT

## 3.3.4.3 Agarose gels

Reagents

- 40 g.L$^{-1}$ Agarose in tris/acetate/EDTA (TAE) buffer
- 0.00005% (v/v) SYBR SAFE DNA gel stain

Agarose gels were made by adding agarose in TAE buffer to a final concentration of 40 g.L$^{-1}$. The mixture was placed in an Erlenmeyer flask and heated in a microwave for one minute or until all the agarose had dissolved. The mixture was then cooled to ~60 °C before the gel was cast by pouring the agarose solution into a gel casting tray and allowing it to set.

## 3.3.4.4 Gel electrophoresis

PCR products were run through 4% (w/v) agarose gels at 12 V over 30 minutes to separate and identify DNA fragments. Quick-Load PCR marker (Bolabs) was run concurrently as a size reference (Table 3.1).

**Table 3.1: Quickload PCR marker (2 kb)**

| Fragment | Size (base pairs) | Mass (ng) |
|----------|-------------------|-----------|
| 1 | 2000 | 100 |
| 2 | 800 | 40 |
| 3 | 400 | 20 |
| 4 | 200 | 10 |
| 5 | 100 | 5 |

## 3.4    Results

### 3.4.1  Evaluation of decellularisation

The degree of decellularisation for each method was determined initially using histological methods and later by extraction and quantification of residual DNA (Figure 3.4.6) with comparisons to native meniscus and bone.  Haematoxylin and eosin staining displayed cell nuclei, cytoplasm and extracellular matrix and DAPI staining revealed DNA.  Serial sections of decellularised menisci were taken with representative images shown in Figure 3.4.3 to Figure 3.4.8.

#### 3.4.1.1    Original method

On gross inspection meniscus decellularised using the original method developed by Stapleton *et al.* (2008) appeared white in colour with a glossy appearance.  No obvious changes to the structure or size of the menisci were observed.



**Figure 3.4.1:  Native porcine meniscus (left) and decellularised porcine meniscus (right).**

H&E staining of native meniscus (Figure 3.4.2) revealed cells located throughout the tissue with varying densities depending on region.  Cells in the white zone existed in small groups within lacunae and had a round morphology (Figure 3.4.2 A) while cells located in the superficial zone appeared to have a more elongated appearance (Figure 3.4.2 B).  A synovium could also be seen measuring ~5 µm in thickness on the

outermost surface with a thicker layer of collagen fibres (~100 μm) running parallel to the surface just underneath. The red-white zone displayed the lowest cell density with cells showing a less rounded morphology than those in the white zone but with one or two projections (Figure 3.4.2 C). Large collagen fibre bundles with orientation and structure synonymous with radial tie fibres could also be seen distributed through the red-white zone. Areas densely populated with cells characteristic of vasculature were evident in the red zone, containing cells with many projections (Figure 3.4.2 D). Decellularisation using the original method resulted in complete removal of cellular material from all zones except the white zone as shown by H&E staining (Figure 3.4.3). Staining revealed the introduction of spaces within the ECM of decellularised meniscus however general histoarchitecture was retained. The synovium was lost however the superficial layer remained intact (Figure 3.4.3 C). Use of the original method to decellularise menisci (n = 3) resulted in incomplete decellularisation of the tissue. The white zone displayed some staining present in lacunae suggesting the presence of cell debris. Upon further investigation using DAPI staining it was revealed that the staining was apparently due to presence of dsDNA and was present in all decellularised menisci. Therefore, the original method was unsuccessful in decellularising porcine medial menisci.

### 3.4.1.2    Method 1

Menisci were subjected to the original decellularisation protocol with EDTA removed from all wash solutions to determine what effect this have since it was not desirable to include EDTA in a process for the subsequent decellularisation of bone-meniscus-bone. Whole porcine menisci (n = 3) were subject to the decellularisation process and the extent of decellularisation evaluated by histology and DAPI staining of tissue Sections (Figure 3.4.4). H&E staining revealed the retention of matrix histoarchitecture throughout the meniscus with radial tie fibers present in the red-white and red zone regions (Figure 3.4.4 A and E). There was also an absence of nuclear material in the red, superficial and red-white zones

however there was some haematoxylin staining in the white zone (Figure 3.4.4 G). DAPI staining suggested that this was dsDNA whilst also verifying the absence of dsDNA from all other regions (Figure 3.4.4 H). Therefore Method 1 did not successfully decellularise porcine medial meniscus.
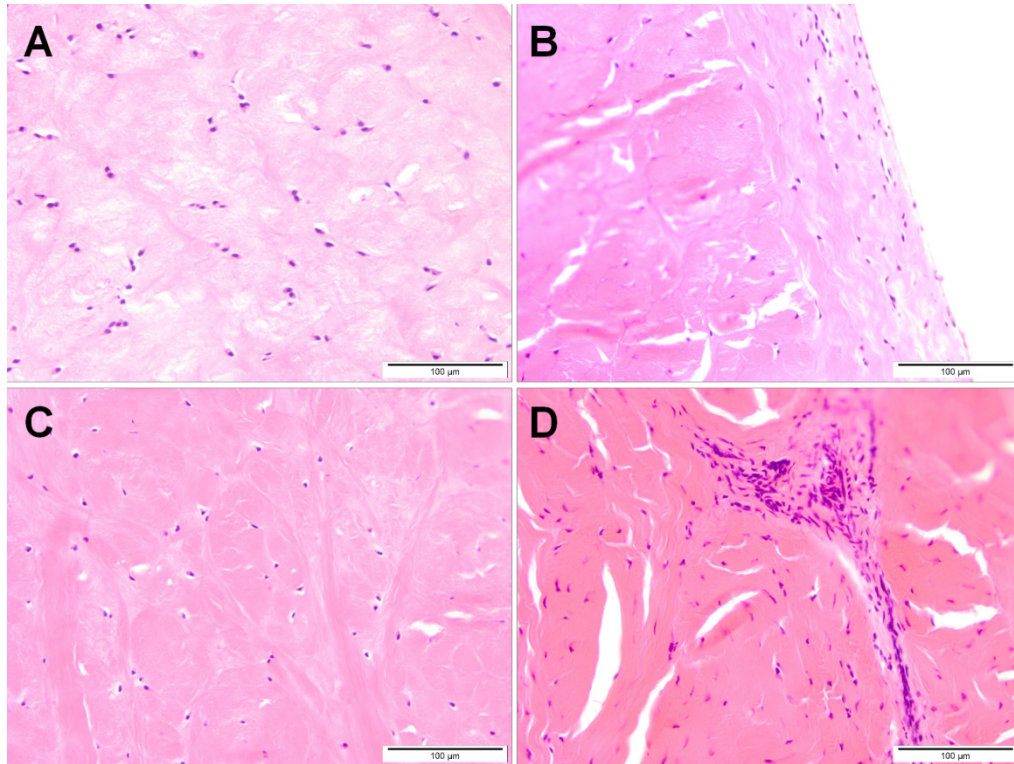


**Figure 3.4.2: H&E staining of native porcine meniscus showing the white (A), superficial (B), red-white (C), and red (D) zones.** Magnification 200x unless stated, Images are representative of the results obtained from n = 3 menisci.

3.4.1.3    Methods 2 and 3

A further six medial menisci were subject to decellularisation using methods 2 and 3. Introduction of the extra detergent cycle in method 2 as described in Section 3.3.1.3 resulted in similar results to Method 1 (Figure 3.4.4). The red zone was clear of cellular staining with spaces visible between the matrix where vascular cells existed previously (Figure 3.4.5 A). Again, the synovium was not present however the superficial layer was intact (Figure 3.4.5 C). The red-white zone did not display any staining for cellular remnants but radial tie fibres were visible suggesting retention of

ECM structure (Figure 3.4.5 E). The white zone was stained weakly by eosin and several round spaces were visible. Some eosin staining was present in these spaces previously occupied by cells in the white zone (Figure 3.4.5 G), suggesting the presence of cellular debris from the collapse of lacunae (Kheir *et al.*, 2011). As no haematoxylin staining was present it was deduced that there was no dsDNA present. Decellularisation using method 3 yielded almost identical results to method 2. Collagen structures were preserved, but as with the previous methods the synovium was lost (Figure 3.4.5 D). A similar level of eosin staining was seen in the white zone (Figure 3.4.5 H) compared to method 2 however the matrix appeared to retain its structure better. Both methods were successful in removing all nuclear material from porcine menisci with no nuclear staining present upon histological assessment. Staining also revealed retention of histoarchitecture however there was removal of the synovial membrane and the introduction of spaces between collagen fibres. DNA was quantified for method 3 menisci as this appeared to be an effective decellularisation protocol. Samples were taken from throughout the tissue to ensure removal of DNA from the entire meniscus. This revealed regional variations in DNA content (Figure 3.4.6) however none of these were statistically significant (p>0.05). The mean DNA content of native porcine meniscus was $960.19 \pm 61.32$ ng.mg$^{-1}$ dry weight of tissue and $41.83 \pm 11.88$ ng.mg$^{-1}$ dry weight of tissue for decellularised porcine meniscus, equating to a 95.64% reduction in total DNA.
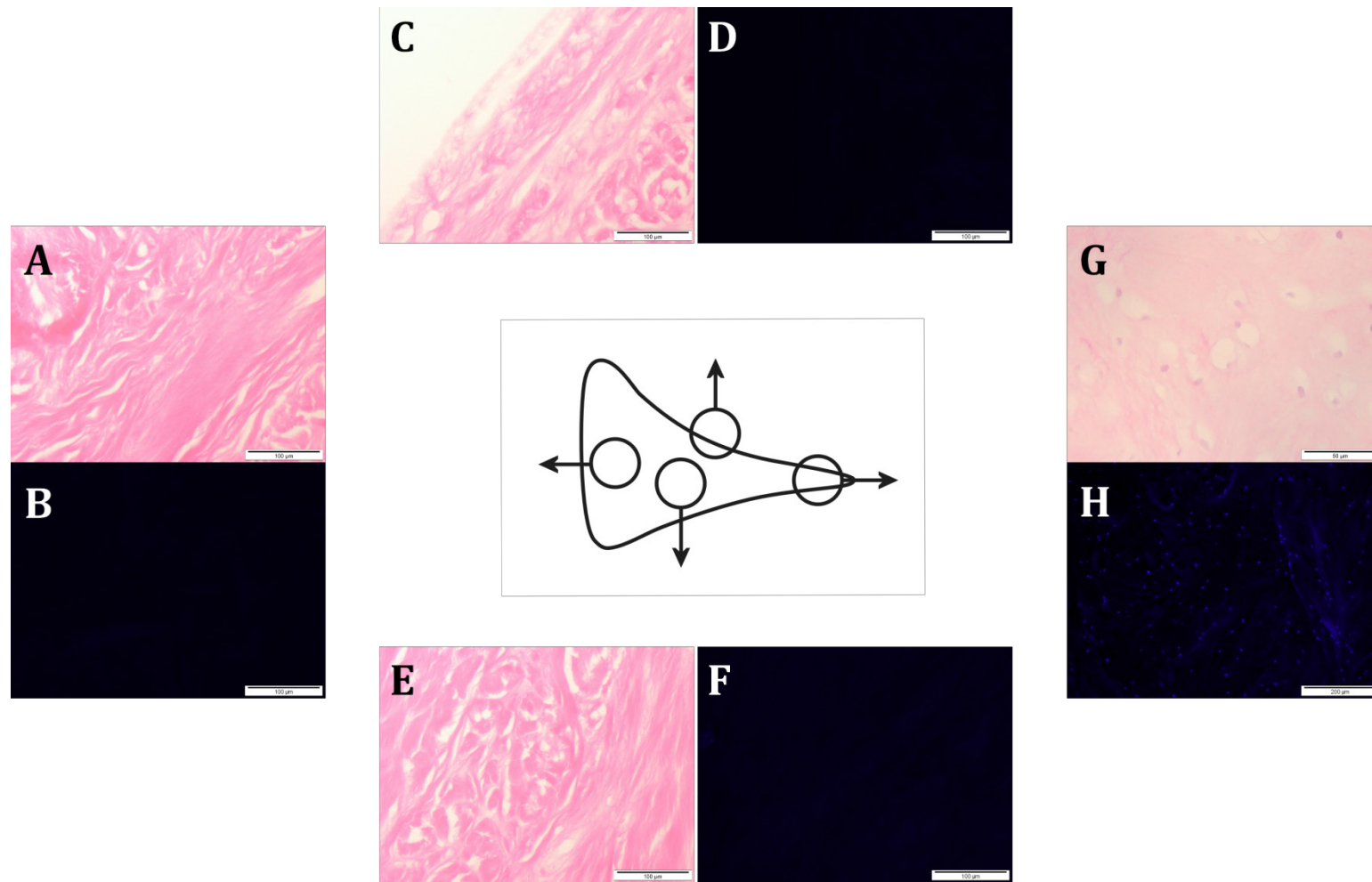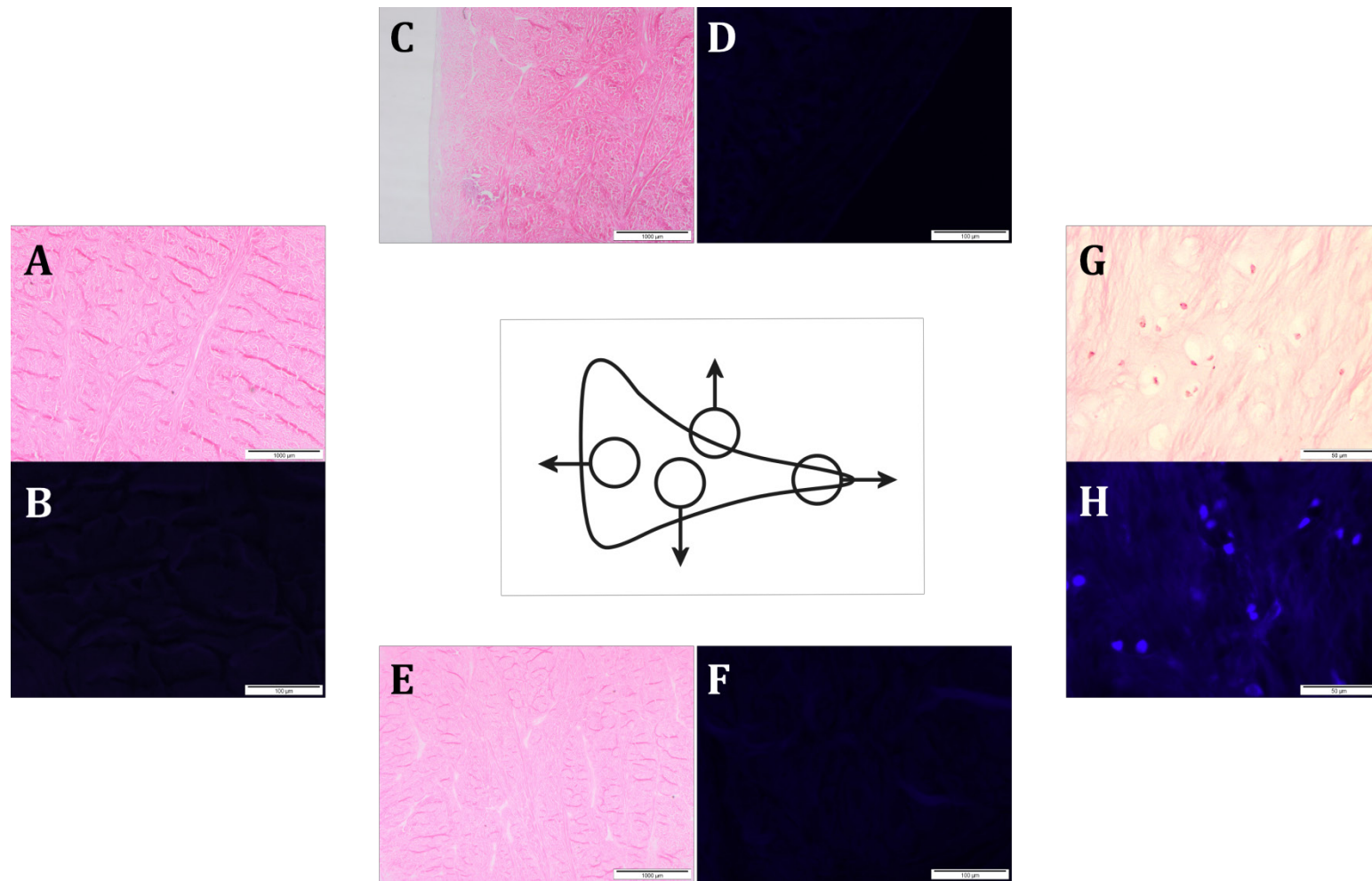
**Figure 3.4.3: Radial Sections of decellularised meniscus (original method) stained with H&E and DAPI.** A) H&E staining of decellularised meniscus red zone B) DAPI staining of decellularised meniscus red zone C) H&E staining of decellularised meniscus superior surface D) DAPI staining of decellularised meniscus superior surface E) H&E staining of decellularised meniscus red-white zone F) DAPI staining of decellularised meniscus red-white zone G) H&E staining of decellularised meniscus white zone (400x) H) DAPI staining of decellularised meniscus white zone (100x). Magnification 200x unless stated, Images are representative of the results obtained from n = 3 menisci.
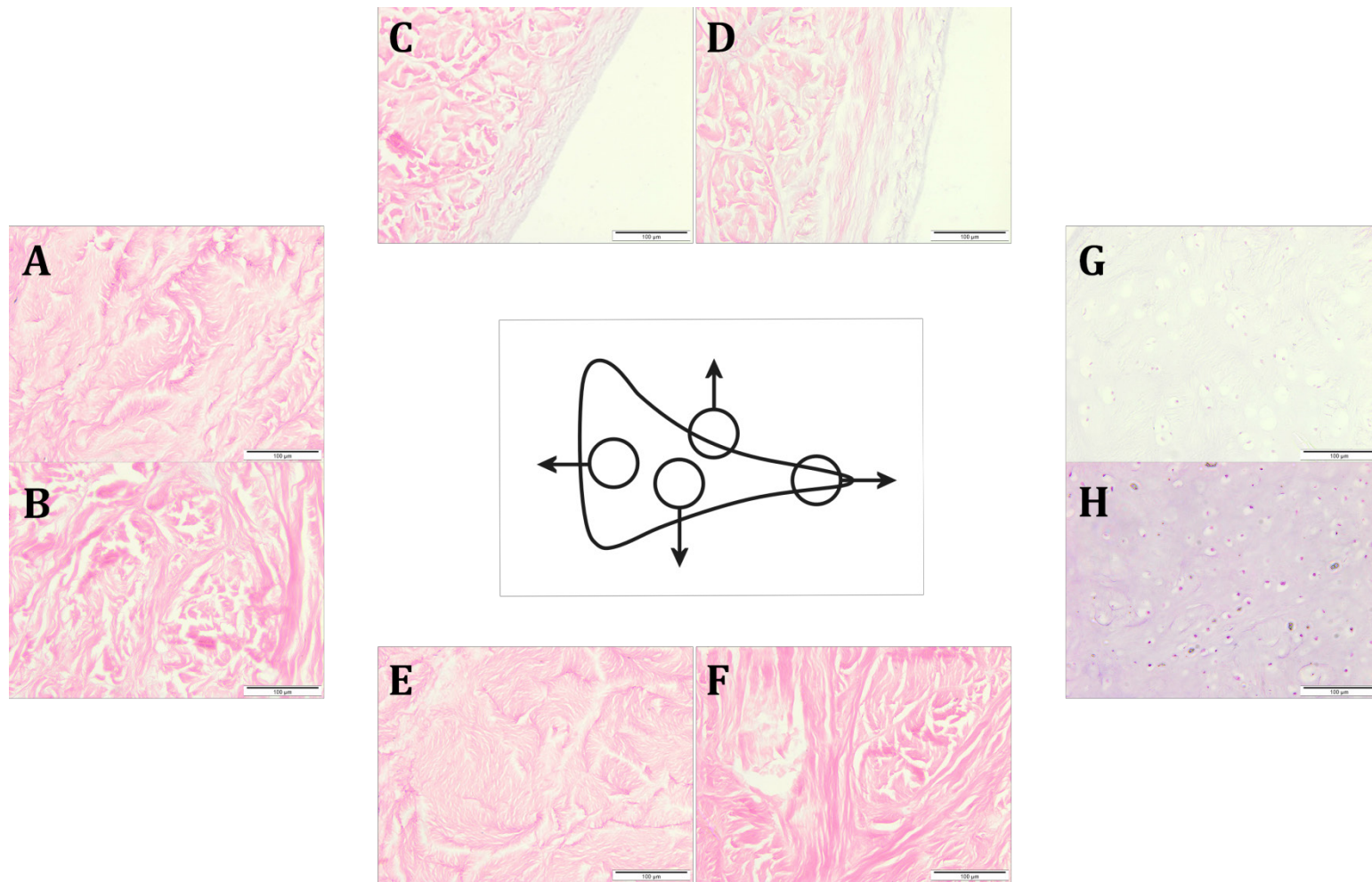
**Figure 3.4.4: Radial Sections of decellularised meniscus (method 1) stained with H&E and DAPI.** A) H&E staining of decellularised meniscus red zone (20x) B) DAPI staining of decellularised meniscus red zone C) H&E staining of decellularised meniscus superior surface (20x) D) DAPI staining of decellularised meniscus superior surface E) H&E staining of decellularised meniscus red-white zone (20x) F) DAPI staining of decellularised meniscus red-white zone G) H&E staining of decellularised meniscus white zone (400x) H) DAPI staining of decellularised meniscus white zone (400x). Magnification 200x unless stated, Images are representative of the results obtained from n = 3 menisci.

**Figure 3.4.5: Radial Sections of decellularised meniscus (method 2 and 3) stained with H&E.** A) Method 2 meniscus red zone B) Method 3 meniscus red zone C) Method 2 meniscus superior surface D) Method 3 meniscus superior surface E) Method 2 meniscus red-white zone F) Method 3 meniscus red-white zone G) Method 2 meniscus white zone H) Method 3 meniscus white zone. Magnification 200x unless stated, Images are representative of the results obtained from n = 3 menisci.
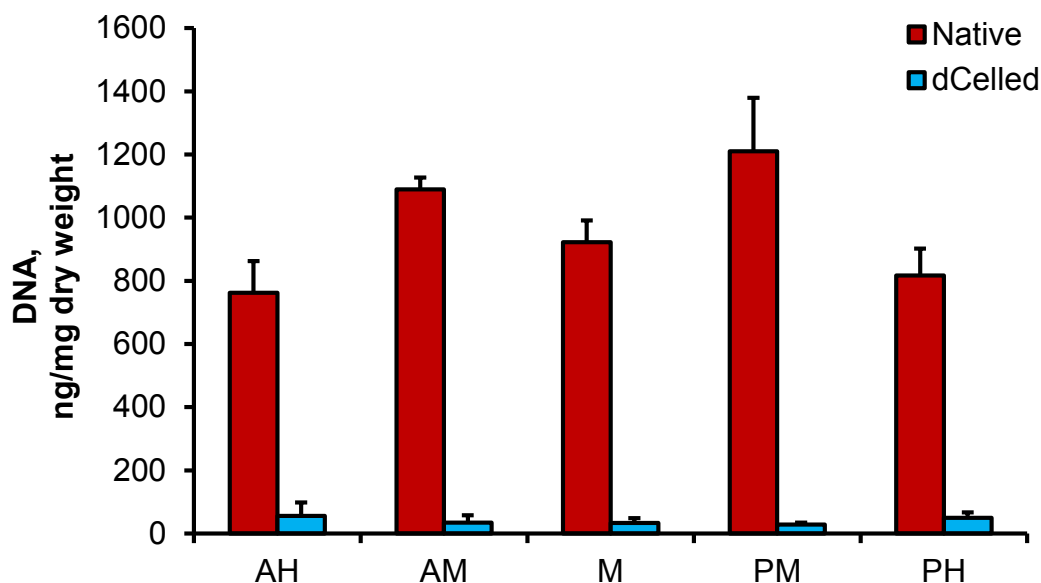
**Figure 3.4.6: DNA content of native and decellularised meniscus by spectrophotometric analysis of extracted DNA at 260 nm.** Data presented as mean (n = 3) $\pm$ 95% C.I. AH – anterior horn, AM – anterior-middle, M – middle, PM – posterior-middle, PH – posterior horn. The data was analysed using two one-way ANOVA`s for native and decellularised menisci and this revealed no significant variation in the data.

### 3.4.1.4 Decellularisation of bone-meniscus-bone

The protocol for decellularising bone-meniscus-bone was adapted from method 3 with additional steps incorporated to aid decellularisation of bone attachments. The initial freeze-thaw cycles were followed by mechanical manipulation of the attachment site to introduce space between the collagen fibre bundles which would improve process reagent access to the enthesis region. Bone attachments were also treated using a waterpik at this stage to remove bone marrow, again to improve access for process reagents. The volume of solution in each pot was also increased from 100 mL to 150 mL given the increased size and weight of tissue equating to 8-9 mL per gram of tissue, with all steps carried out at either 4 °C or 42 °C, except for the nuclease and sterilisation steps, to limit microbial growth. The change from 45 °C to 42 °C incubations was enforced when temperature monitoring of incubators revealed temperature fluctuations up to 48 °C when set at 45 °C, which could potentially cause denaturation of

meniscal ECM. Setting the temperature at 42 °C meant the temperature could only reach a maximum of 45 °C.

Decellularisation did not appear to alter the size and geometry of porcine bone-meniscus-bone (Figure 3.4.7). Decellularised samples appeared to have a more glossy appearance and were less red in colour when compared to native porcine bone-meniscus-bone. Cartilage surfaces were smooth and intact, while the bone appeared white suggesting removal of all marrow. The bone attachments were soft to the touch and seemed to have lost some of their mechanical stiffness when pressed.
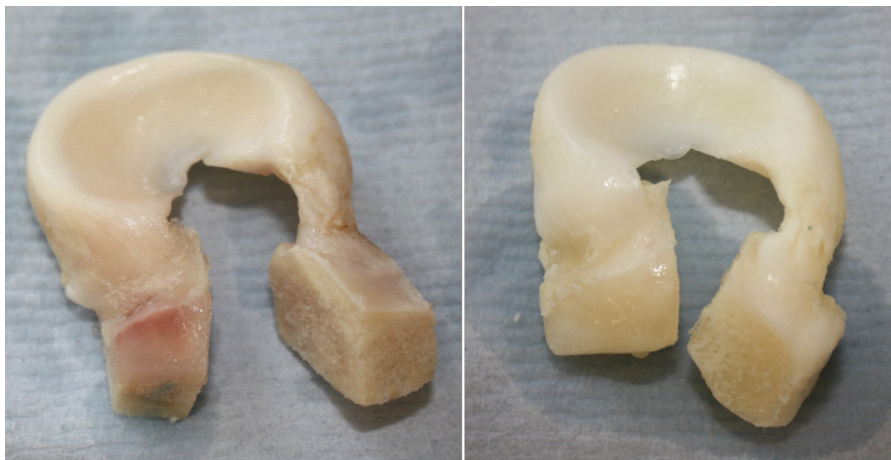


**Figure 3.4.7: Native porcine bone-meniscus-bone (left) and decellularised porcine bone-meniscus-bone (right).**

As seen with the previous methods, H&E staining of menisci revealed retention of major histoarchitecture however the synovial membrane was removed (Figure 3.4.8). Decellularisation appeared to be successful in the meniscus with no nuclear staining present in any region (Figure 3.4.8). Bone attachments were stained using a modified McNeal's tetrachrome stain after embedding in resin, as traditional decalcification may have provided false negative results. McNeal's tetrachrome staining of native bone displayed the distinct layers present within the attachment site: the ligamentous attachment and its insertion point (Figure 3.4.9 A and B), the transition to trabecular bone (Figure 3.4.9 C and D), and the dense enthesis (Figure 3.4.9 E and F). Cells which appeared oval in shape were present between the collagen fibers in the ligamentous attachment with

more spindle shaped cells also found in the associated vasculature. Pockets of fat were also seen throughout the attachment site. Cells in the bone were usually solitary surrounded by mineralised matrix with bone marrow and its associated cells present in the trabecular space. The enthesis was composed of dense mineralised matrix with small pockets of bone marrow and a layer of calcified cartilage towards the tibial surface. The decellularisation protocol was successful in removing whole cells and nuclei from the bone attachment with no nuclear staining present in any of the regions (Figure 3.4.9 B, D and F). Spaces appeared between the collagen fibers of the ligamentous attachment however this was expected given the mechanical manipulation during the process. Otherwise the attachment appeared to be unchanged from the native samples.

Residual DNA was quantitated by extraction using a DNeasy kit and spectrophotometric analysis using a NanoDrop 1000 (Figure 3.4.10). Entire menisci were cut into ~1 mm$^3$ pieces and freeze-dried prior to comminution using a cryomill. This ensured homogenisation and mixing of menisci allowing representative sampling of the whole meniscus. Samples (25 mg for native and 100 mg for decellularised) were then processed as described in Section 2.2.5.3. Native meniscus contained 803.8 $\pm$ 20.0 ng.mg$^{-1}$ whereas decellularised meniscus contained 26.7 $\pm$ 2.4 ng.mg$^{-1}$ (dry weight) which equates to a >96% reduction. The DNA content of porcine bone was slightly higher at 1371.8 $\pm$ 38.5 ng.mg$^{-1}$ (dry weight) with a >91% reduction in DNA observed in decellularised tissue which contained 124.9 $\pm$ 6.0 ng.mg$^{-1}$ (dry weight).
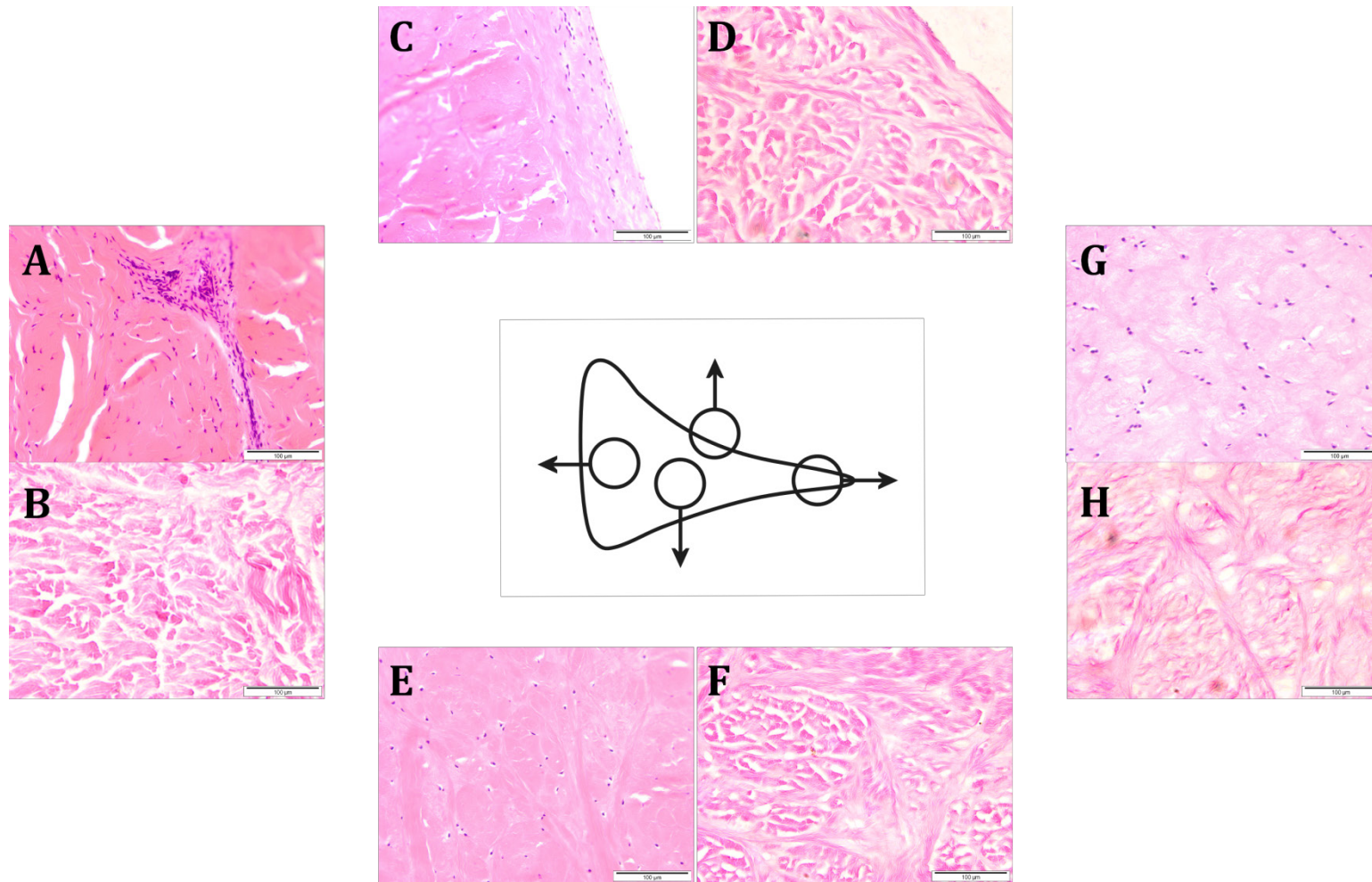
**Figure 3.4.8: Radial Sections of native and decellularised meniscus (bone-meniscus-bone) stained with H&E.** A) Native meniscus red zone B) Decellularised meniscus red zone C) Native meniscus superior surface D) Decellularised meniscus superior surface E) Native meniscus red-white zone F) Decellularised meniscus red-white zone G) Native meniscus white zone H) Decellularised meniscus white zone. Magnification 200x unless stated. Images are representative of the results obtained from n = 3 menisci.
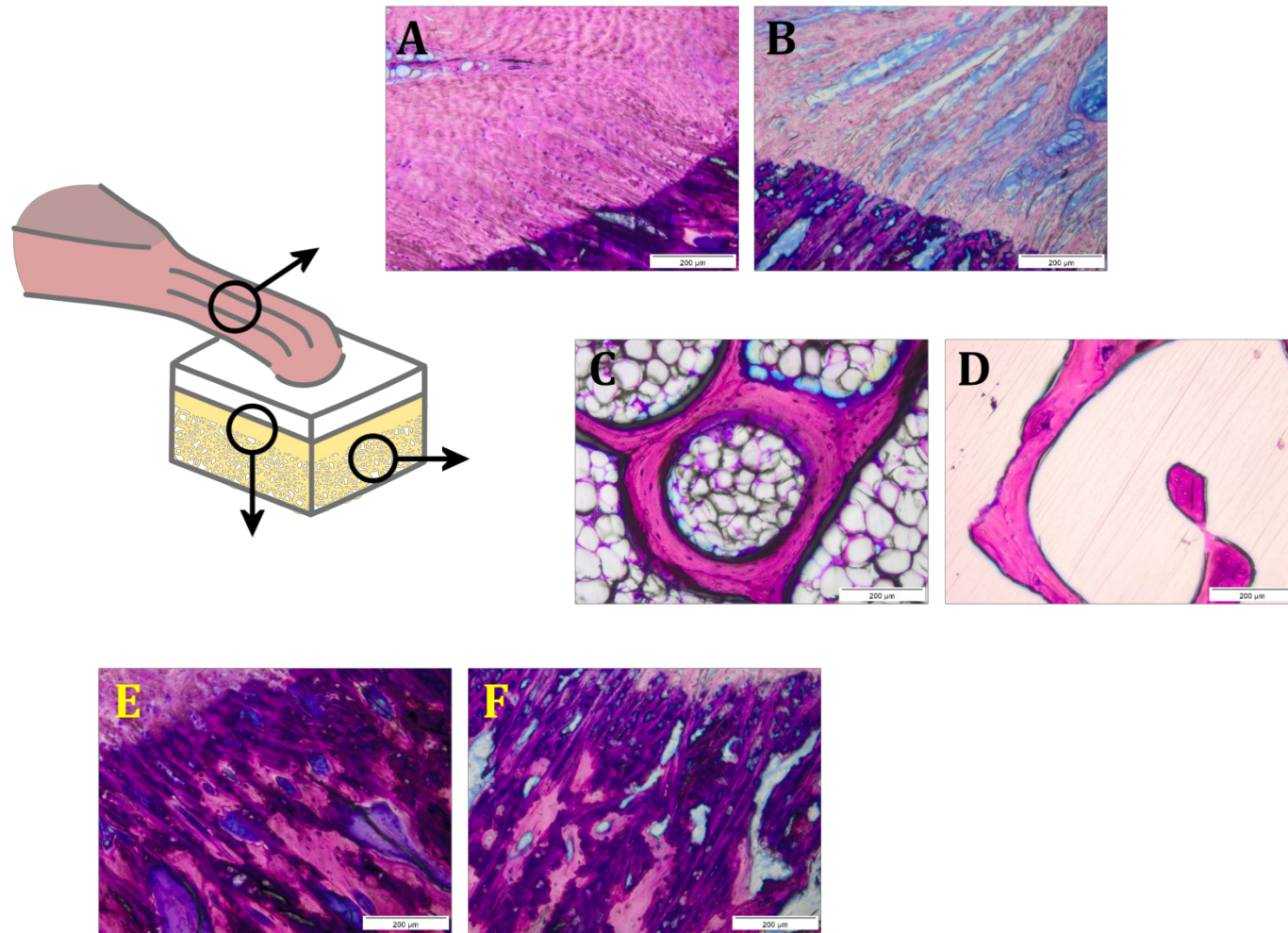
**Figure 3.4.9: Sections of native and decellularised bone block stained with McNeal's Tetrachrome.** A) Native ligament B) Decellularised ligament C) Native trabecular bone D) Decellularised trabecular bone E) Native enthesis F) Decellularised enthesis. Magnification 100x unless stated. Images are representative of the results obtained from n = 3 menisci.
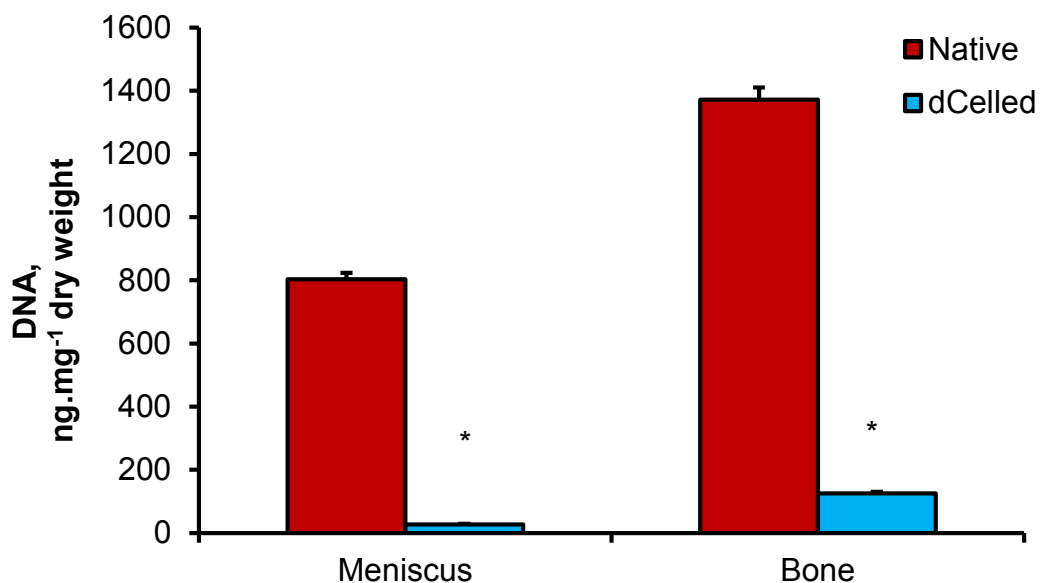
**Figure 3.4.10:** **DNA content of native and decellularised bone-meniscus-bone following extraction and spectrophotometric analysis at 260 nm.** Data presented as mean (n = 3) ± 95% C.I. Statistical analysis performed using student's t-test (* $p<0.05$).

## 3.4.2 **Qualitative analysis of DNA**

PCR was used to determine the presence of functional genes for GAPDH, β-actin and collagen I in native and decellularised bone-meniscus-bone. A representative agarose gel is shown in Figure 3.4.11. Functional genes were amplified in DNA extracted from native porcine bone-meniscus-bone with clear bands for GAPDH, β-actin and collagen I. A clear band localised around 600 base pairs (bp) was seen for DNA extracted from native porcine meniscus and bone and amplified using primers for GAPDH. No band was seen in the corresponding lanes for DNA extracted from decellularised porcine meniscus or bone. DNA from native meniscus and bone amplified using primers for β-actin also displayed clear bands, this time around 300 bp. Again, there was no visible band for decellularised meniscus or bone. The same pattern was repeated for DNA amplified using primers for collagen I, with clear bands present for native samples

and no band for decellularised samples. There was also no band visible for the blank reaction.
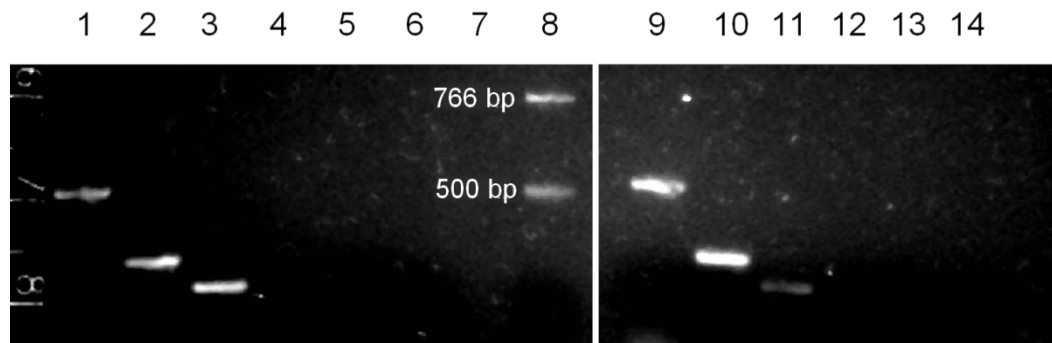


**Figure 3.4.11:** **Gel electrophoresis of genes expanded from native and decellularised porcine bone-meniscus-bone.** 1) Native meniscus GAPDH, 2) Native meniscus β-actin, 3) Native meniscus Collagen I, 4) Decellularised meniscus GAPDH, 5) Decellularised meniscus β-actin, 6) Decellularised meniscus Collagen I, 7) Blank, 8) DNA ladder, 9) Native bone GAPDH, 10) Native bone β-actin, 11) Native bone Collagen I, 12) Decellularised bone GAPDH, 13) Decellularised bone β-actin, 14) Decellularised bone Collagen I.

## 3.5 Discussion

Multiple strategies have been investigated in the search for a suitable meniscal replacement. Both natural and synthetic materials have been evaluated as potential scaffolds to promote the regeneration of meniscal tissue. Other approaches have tried to develop scaffold-free methods for growing replacement meniscal tissue as well as decellularisation of allogeneic or xenogeneic meniscus. The approach evaluated in this study focused on the decellularisation of xenogeneic meniscus and bone attachments to remove immunogenic material in order to create a potential replacement. The bone attachments will be vital to the function of the acellular scaffold following implantation as they provide a relatively simple mechanism for the fixation of the scaffold in the knee joint whilst maintaining the anatomic relationship between the anterior and posterior meniscal horns. It has been shown that grafts' incorporating bone plugs restore contact mechanics close to normal (Alhalki *et al.*, 1999) and termination of the collagen fibres in the bone allow retention of mechanical integrity as hoop stresses can still be generated.

Freeze/thaw cycles were included at the start of the decellularisation process as a means of separating the dense ECM by creating ice crystals, which enhances the diffusion of decellularisation solutions. Repeated freezing and thawing was also useful in lysing cells located deep within the meniscus. The subsequent wash steps in hypotonic buffer were included to further lyse cells. This was followed by incubation in 0.1% (w/v) SDS in hypotonic buffer to solubilise and facilitate removal of cell fragments. The use of SDS has been scrutinized as it is potentially toxic. Higher concentrations of SDS have been reported to cause damage to collagen in studies of the decellularisation of other tissues. However, these studies used 1% (w/v) SDS (Bodnar *et al.*, 1986; Courtman *et al.*, 1994) whereas only 0.1% (w/v) SDS was used here resulting in no signs of damage to the ECM. It has also been postulated that the damage observed in previous studies was not attributable to SDS but to proteases released through cell lysis (Booth *et al.*, 2002). The potential for such damage to occur was

negated in this study by the incorporation of the protease inhibitor aprotinin. It must also be noted that aprotinin is stable at the higher temperatures used during the process, due to its tertiary structure. Wash steps in DPBSa were then included to remove solubilised cell remnants from the previous steps and SDS as this may have inhibited the activity of nucleases in the subsequent step. In order to digest nucleic acids, DNase and RNase were included. This would also reduce sites of calcification associated with the phosphate groups on nucleic acids in the clinical application. Menisci were then washed using hypertonic buffer and DPBSa to wash out any remaining solubilised cellular material followed by disinfection using PAA. The numerous final washes in DPBSa were incorporated to remove all traces of potentially cytotoxic process reagents as well as any cellular remnants.

Initial assessment of the decellularisation method developed by Stapleton *et al*. (2008) (original method, 3.3.1.1) was carried out on meniscus without the bone attachments to gauge the effectiveness of the protocol once EDTA had been removed from decellularisation reagents. Previous studies had revealed softening of bone blocks owing to the inclusion of EDTA in the decellularisation solutions. Haematoxylin and eosin staining of native and decellularised meniscus was performed to assess the level of decellularisation achieved by the original method and method 1, and to compare matrix changes. This revealed an absence of cellular residue in the red, red-white and superficial zones. However, nuclear material, determined by DAPI staining, was visible in the white zone (Figure 3.4.3). The failure of the original method to decellularise meniscus may have been due to intricacies in the protocol not described in the SOP suggesting the process was not robust. Method 1 was employed to assess the impact of EDTA on decellularisation. EDTA was removed from all process reagents and this yielded almost identical results to the original method with nuclear material present in the white zone of decellularised menisci (Figure 3.4.4). This suggested that removing EDTA from process reagents would not have an adverse effect on decellularisation. As neither method was able to achieve complete decellularisation of porcine meniscus, it was

hypothesised that the SDS treatment was insufficient in solubilising and removing cellular material or that residual SDS was inhibiting nuclease activity. Therefore, to achieve complete decellularisation, Method 1 was adapted to include an extra cycle of hypotonic buffer at 4 °C for 24 hours, hypotonic buffer at 37 °C for 24 hours, SDS hypotonic buffer at 45 °C for 24 hours and hypotonic buffer at 45 °C for 24 hours prior to the three washes in wash buffer preceding nuclease treatment was added (method 2, Section 3.3.1.3). This was because there were whole cell nuclei remaining in the tissue suggesting insufficient cell lysis. SDS also acts to aid the removal of cellular detritus. In parallel an adapted protocol incorporating six 12 hour washes in wash buffer to aid removal of SDS from the tissue prior to the nuclease step instead of three 24 hour washes (method 3, Section 3.3.1.4) was also tested. It was hypothesised that residual SDS in the tissue was affecting nuclease activity thereby preventing complete digestion of nuclear material. Therefore it was postulated that extra changes of wash buffer would help reduce residual SDS concentrations and improve nuclease activity. Both protocols proved successful in decellularising porcine meniscus, however as staining revealed cellular remnants in menisci treated using method 2 it was decided that method 3 would be carried forward. Also, the inclusion of further SDS wash steps could damage the ECM and lead to cytotoxicity, whereas method 3 was slightly more economical as wash buffer is less expensive and the length of the decellularisation process remained unchanged.

Decellularisation of bone-meniscus-bone followed the same process as method 3, however, slight alterations were made and steps added to aid decellularisation of the bone blocks. The volume of solutions was increased to match the increased mass, EDTA was removed from all solutions, bone blocks were treated using a water flosser to remove bone marrow and prevent clotted blood in the trabecular space from forming a barrier to penetration and collagen fibers were teased apart at the attachment site to aid diffusion of reagents into the enthesis in both the superior and inferior directions.

The initial level of decellularisation was determined using H&E staining in the meniscus and McNeal's Tetrachrome staining in bone. While histology of the meniscus was fairly straightforward due to available expertise within the group, methods for staining bone without prior decalcification were not available. Decellularised bone was not decalcified as the decalcification process can remove cells from the tissue possibly resulting in a false negative. Hence, it was decided to embed bone in resin as this would preserve the decellularised bone completely allowing for accurate determination of decellularisation. Initially, a method for staining resin embedded bone using H&E was attempted however this resulted in ineffective staining of both cells and ECM. Several adaptations were made and a method incorporating an initial step to remove a layer of resin allowing the staining solutions access to the sample proved successful in staining native porcine bone but not decellularised porcine bone possibly due to interactions between the solvent used and residual decellularisation reagents. Next staining was attempted with Sanderson's Rapid Bone stain however this also was unsuccessful as although bone matrix was stained no cellular staining was seen even on native tissue controls. Finally, a staining protocol using McNeal's Tetrachrome was identified and this revealed complete removal of whole cells from both these regions as well as retention of gross matrix architecture.

To further verify removal of cellular material, DNA was extracted using the DNeasy kit and quantified using spectrophotometry. Again, a method for analysis of bone was not available and so had to be developed as the protocol for soft tissue was not able to successfully extract DNA from bone. Successful extraction was achieved by incorporating SDS and EDTA into the digestion solution to decalcify and solubilise bone resulting in the release of cells surrounded by mineralised matrix and allowing subsequent digestion by proteinase K. Results revealed >96% removal of DNA from meniscus and >90% removal of DNA from bone blocks. Crapo *et al.* (2011) suggested that decellularised matrices should aim to reduce the level of dsDNA to below 50 ng.mg$^{-1}$ of dry weight in order to prevent adverse host reactions. The quantification method used in this study

detected ssDNA and so was more sensitive than those outlined as a standard for decellularised tissues. Even so, the decellularisation protocol reduced the ssDNA content of meniscus to $26.7 \pm 2.4$ ng.mg$^{-1}$ (dry weight) which is well below the quoted standard.

It is crucial to assess the level of DNA removal from decellularised matrices and whether any remaining DNA is functional. PCR was used to determine the presence of functional DNA in decellularised bone-meniscus-bone. DNA was extracted as described in Sections 2.2.6.3 and 2.2.6.4 and amplified for target genes GAPDH, β-actin and collagen I. GAPDH, an enzyme involved in carbohydrate metabolism, and β-actin, a component of the cell cytoskeleton, were selected as they are ubiquitous in cell DNA. Collagen I was selected as it is expressed in abundance by musculoskeletal cells, and so all target genes are reliable markers for residual functional DNA. Results indicated the presence of all target genes in samples extracted from native tissue and an absence in samples obtained from decellularised bone-meniscus-bone. PCR products had a predicted size of 230 bp, 210 bp and 243 bp for GAPDH, β-actin and collagen I, respectively. However, actual PCR product size for GAPDH was ~500 bp and for β-actin was ~300 bp. This may have been due to the presence of both exons and introns in DNA extracted whereas primers were designed from mRNA which only includes exons. The Collagen I PCR product size was as expected.

The results presented in this chapter describe the successful decellularisation of porcine bone-meniscus-bone. Matrix geometry and architecture were preserved and total DNA was reduced to >90% for both soft and hard tissue portions. Further investigations into specific changes to the matrix are detailed in the next chapter.

# Chapter 4.    Characterisation of decellularised porcine bone-meniscus-bone

## 4.1    Introduction

In Chapter 3, a process for the production of an acellular porcine bone-meniscus-bone scaffold was described. It was important to determine how the decellularisation process and reagents affected the ECM of decellularised bone-meniscus-bone as this will impact its *in vivo* efficacy. The impact of various decellularisation reagents have been discussed in the previous chapter.  Histology, immunohistochemistry, and biochemical assays were used to compare native and decellularised bone-meniscus-bone composition, while differential scanning calorimetry and magnetic resonance imaging provided information on structural changes that may have taken place.

### 4.1.1 Meniscal matrix components

Tissues can be separated into two components: the cells, which maintain homeostasis and produce the ECM, which, in turn provides support to the cells and the mechanical function of the tissue.  Meniscal ECM is mainly composed of collagen with proteoglycans, GAGs and elastin making up the remainder.  These constituents form highly organised structures that allow the meniscus to withstand forces transmitted through the knee firstly by the attraction and retention of water by GAGs which creates a Donnan osmotic pressure allowing the fluid phase to bear the initial load before radial displacement of the meniscus leads to the generation of hoop stresses as the collagen fibres act in tension.

#### 4.1.1.1    Collagen

Collagen is used to describe proteins forming a triple helix consisting of polypeptide chains.  Although the different types of collagen display diverse structures they all comprise a right-handed triple helix composed of three α

chains (Kuhn, 1986). The organic matter present in the meniscus is composed of ~80% collagen with fibrillar collagens in abundance. The inner region is hyaline-like and has a high proportion of type II collagen although type I still accounts for 40% of inner region organic matter. The outer region however is composed almost entirely of collagen type I (~99%). The triple helix in collagen I is heterotrimeric and formed from two α1(I) chains and one α2(I) chain, whereas three α1(II) chains comprise the homotrimeric collagen II triple helix (Gelse *et al.*, 2003). Type I collagen provides tensile strength in tendons and, post-calcification, torsional stiffness in bone. Collagen II is predominantly found in hyaline cartilage, however it is also present in the nucleus pulposus of intervertebral discs and corneal epithelium (von der Mark, 1999). Collagen III consists of three α1(III) chains and is usually found associated with collagen I in elastic tissues (von der Mark, 1981). Collagen IV is found on the basement membrane where it provides major structural support and binds other ligands such as laminin to form supramolecular architectures (Poschl *et al.*, 2004). Collagen VI is found in the pericellular matrix and anchors the cell membrane to the ECM (Sardone *et al.*, 2013) where it provides protection from compressive loading. It is also involved in cell-matrix signalling (Fraser *et al.*, 2006) and has been found in bone growth plates where it plays a role in remodelling (Keene *et al.*, 1991).

## 4.1.1.2    Proteoglycans

Proteoglycans are found in meniscal ECM and consist of multiple glycosaminoglycan (GAG) chains covalently bound to a core protein, and so more resemble polysaccharides than proteins. Aggrecan is the major proteoglycan in the meniscus, however perlecan, decorin, biglycan and fibromodulin are also present (Melrose *et al.*, 2005). As described in Chapter (1) proteoglycans are hydrophilic in nature and this restricts the flow of water within the meniscus thereby contributing to the ability of the meniscus to withstand compressive forces, as described by the biphasic theory (Mow *et al.* 1980).

### 4.1.1.3    GAGs

Glycosaminoglycans are linear polysaccharides containing a characteristic repeating disaccharide unit comprised of an amino sugar and uronic acid. Common GAGs are chondroitin sulphate, dermatan sulphate, keratan sulphate and hyaluronic acid.  GAGs, with the exception of hyaluronic acid, are bound to a proteoglycan core protein through serine residues. Hyaluronic acid is, however, able to bind to aggrecan through a link protein forming large aggregating complexes that are highly negatively charged thus able to occupy a larger hydrodynamic space.

### 4.1.2 Bone matrix

The basic building block of bone is the mineralized collagen I fibril.  The mineral component is dahllite, a carbonated apatite, which forms thin plate-shaped crystals.  There are also over 200 non-collagenous proteins present in bone and the most abundant of these is osteocalcin (Hauschka *et al.*, 1989), however these only make up <10% of the total protein content. Water is the other major constituent of bone and plays a major role in bone mechanical properties as dry bone has been shown to have altered mechanical properties to wet bone (Currey, 1990).  Bone can be separated into cortical, or compact, and cancellous, or trabecular, bone.  Long bones, such as the femur, have a cortical shell and a cancellous interior.  The tibia is an example of a long bone and has a layer of hyaline cartilage covering the articulating surfaces.  The medial meniscus is anchored to the superior surface, the tibial plateau, via the meniscal horns allowing it to dissipate load through the generation of circumferential hoop stresses.  Collagen fibres extend into the enthesis of the tibial plateau where they terminate and are secured in place by the mineralised matrix.  The medial meniscus is attached in the same way in both humans and pigs, only to the tibial plateau. However, the lateral meniscus in pigs is attached to the femoral condyle at the posterior horn and the tibial plateau at the anterior horn, whereas in humans it is only attached to the tibial plateau.

## 4.2  Aims and objectives

### 4.2.1 Aims

The aim of the work described in this chapter presented was to characterise decellularised porcine bone-meniscus-bone in comparison to native tissue.

### 4.2.2 Objectives

- To qualitatively compare native and decellularised porcine bone-meniscus-bone composition using immunohistochemistry to investigate the presence of the major collagens..

- To quantitatively determine the total collagen, GAG, and calcium content of native and decellularised porcine bone- meniscus-bone.

- To determine thermal stability of native and decellularised porcine bone-meniscus-bone using differential scanning calorimetry

- To determine the structure of native and decellularised porcine bone-meniscus bone using 9.4T magnetic resonance imaging.

## 4.3   Methods

### 4.3.1 Experimental approach

To complete the studies described in this chapter it was necessary to dissect and decellularise a further 7 bone-meniscus-bone.

- Sections of meniscus obtained for histology as described in Chapter (3) section 3.2.2 were also used for histology in this chapter.

- Four porcine bone-meniscus-bone samples were decellularised using the method described in Chapter (3) Section 3.3.1.5.  Decellularised bone-meniscus-bone was stored on PBS-soaked filter paper at -20 °C prior to use.  These samples were used for quantification of calcium in bone with unused bone blocks (n = 2) used for MRI.

- Three porcine bone-meniscus-bone samples were decellularised using the method described in Chapter (3) Section 3.3.1.5. Decellularised bone-meniscus-bone was stored on PBS-soaked filter paper at -20 °C prior to use.  These samples were used for thermal analysis using differential scanning calorimetry.

### 4.3.2 Quantification of calcium in porcine bone

Samples of native and decellularised porcine bone (~1 g; n = 4) were dried at 95 °C for five days after which they were digested in a microwave using 4 mL nitric acid and 1 mL hydrogen peroxide.  The digest was then diluted 1 in 10 using 18 megohm distilled water in polypropylene tubes. Samples were diluted 1 in 46 using 2% (v/v) nitric acid prior to analysis using ICP-MS.  A commercially available standard solution (Merck) was used to test accuracy of measurements.  Work was carried out at the UK Centre for Tissue Engineering, University of Liverpool.

### 4.3.3 **Thermal analysis**

Native and decellularised bone-meniscus-bone (n = 3) was split into five regions for sampling: white, red-white, horns, enthesis and bone.  Samples of ~10 mg were taken from each region and dehydrated in a graded ethanol series (0%, 20%, 40%, 60%, 80%, 100%, 100%, 100%) by immersion for one hour in each solution.  Ethanol was removed from samples using a vacuum centrifuge for 30 minutes.  Samples were then heated to 200 °C at 10 °C per minute in a differential scanning calorimeter with a blank chamber used as the reference.  Data was generated as temperature (°C) vs heat flow (W/g) and denaturation enthalpy ($\Delta H$) was calculated as the area under the transition peak.

### 4.3.4 **Magnetic Resonance Imaging**

#### 4.3.4.1    Meniscus

Native and decellularised menisci (n = 2) were prepared by slicing in a radial direction to produce slices ~5mm thick.  Samples were placed in a universal (diameter = 25 mm) with tissue paper in the bottom to create a flat surface. MR images of the menisci were obtained using a 9.4T Bruker AVANCE II 400 MHz laboratory NMR system using a 3D-FLASH (3D Fast Low Angle Shot) sequence with a scan duration of 25 hours and 56 minutes.  A total of 100 slices were taken using a matrix size of 512 x 512 pixels with 59 μm spatial resolution in the matrix plane and spatial resolution of 90 μm in the slice direction.  The repetition time (TR) was 38 ms, the echo time (TE) was 4.3 ms, and the flip angle (FA) was 15°.  A total of 48 averages of each slice were taken to produce the final image.

#### 4.3.4.2    Bone

Native and decellularised bone (n = 2) were prepared by removing the meniscus at the horns by sharp dissection.  Whole bone blocks were placed in a universal (diameter = 25 mm) with tissue paper in the bottom to create

a flat surface. MR images of the bone were obtained using a 3D-FLASH sequence with scan duration of 54 hours and 28 minutes. A total of 210 slices were taken using a matrix size of 512 x 512 pixels with 59 μm spatial resolution in the matrix plane and spatial resolution of 90 μm in the slice direction. The repetition time (TR) was 38 ms, the echo time (TE) was 4.3 ms, and the flip angle (FA) was 15°. Again, a total of 48 averages were taken.

## 4.4   Results

### 4.4.1 Histological characterisation

#### 4.4.1.1   Proteoglycans

Sulphated glycosaminoglycans such as chondroitin and dermatan sulphate were stained in histological sections of fresh and decellularised porcine meniscus using Safranin O (Figure 4.4.1).   In the native meniscus this revealed very little staining in the red zone which was mainly associated with blood vessels, with no staining present in the superficial region.   Extensive staining was seen throughout the hyaline-like inner region however no staining was seen in the red-white zone.   Decellularised porcine meniscus tissue exhibited no staining in any region suggesting that decellularisation removed the GAGs from the tissue.

### 4.4.2 Immunohistochemical characterisation

#### 4.4.2.1   Collagen I

Collagen I distribution in native and decellularised porcine meniscus was investigated by immunohistochemical staining (Figure 4.4.2).   Isotype and negative (no antibody) controls did not display any staining (Appendix A). Collagen I was shown to be present throughout the native meniscus with positive staining of cells especially in the superficial and red-white zones. Less positive staining was seen around cells in the white zone.   The level of staining appeared to remain unchanged post-decellularisation. Collagen I staining of the attachment site and bone showed the presence of collagen I throughout the bone and attachment (Figure 4.4.3).   The crimp could be seen on the collagen fibres making up the attachment itself with some staining also present in cells residing between the fibres.   Staining was also present on the mineralised portion of the trabecular bone but not in the cells making up the bone marrow.   Cells residing in the trabecular space within the enthesis however did display collagen I staining as did the
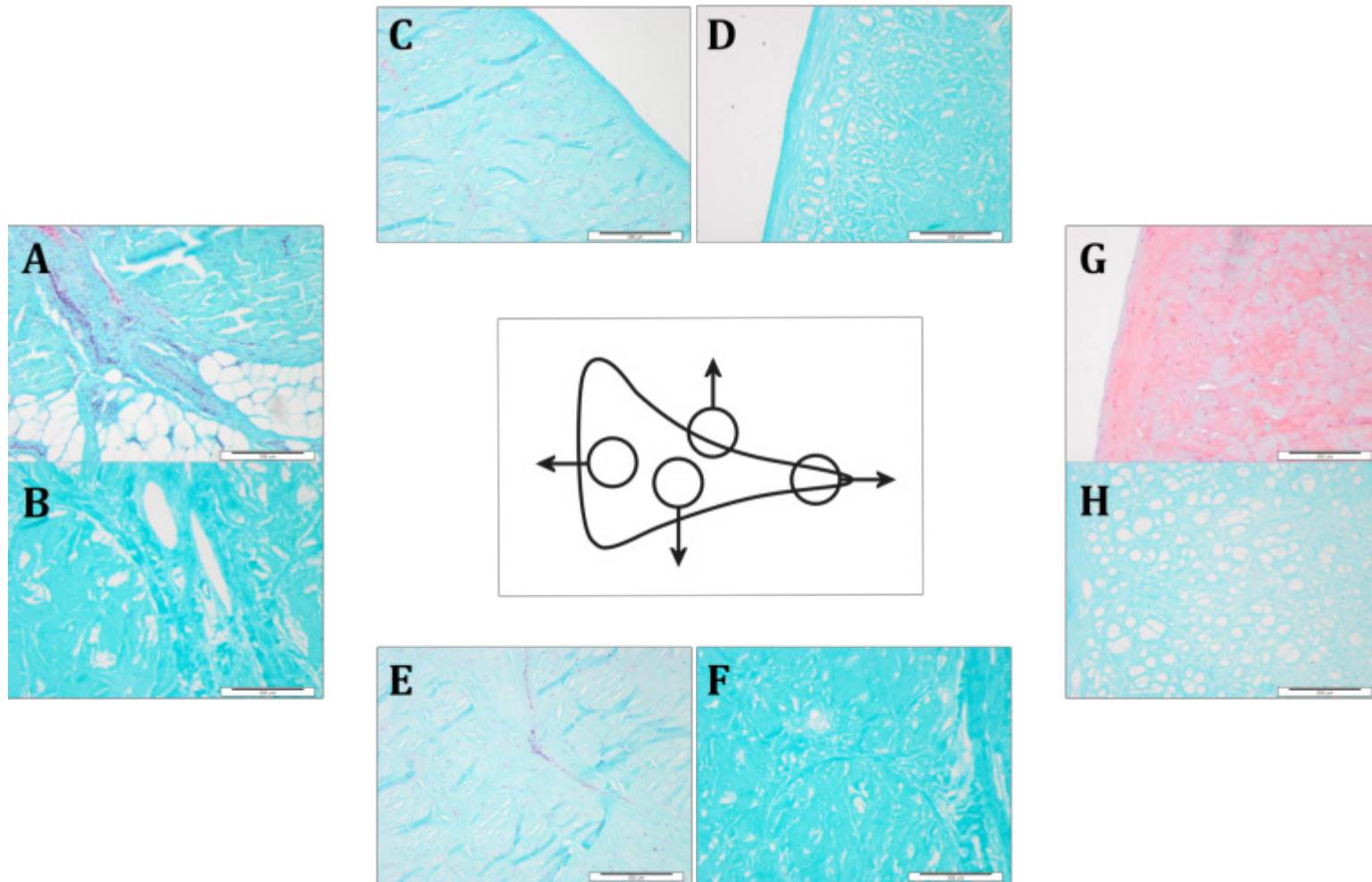
**Figure 4.4.1: Radial sections of native and decellularised meniscus (bone-meniscus-bone) stained with Safranin O.** A) Native meniscus red zone B) Decellularised meniscus red zone C) Native meniscus superior surface D) Decellularised meniscus superior surface E) Native meniscus red-white zone F) Decellularised meniscus red-white zone G) Native meniscus white zone H) Decellularised meniscus white zone. Magnification 100x unless stated. Images are representative of the results obtained from n = 3 menisci.

enthesis. The attachment area of the decellularised meniscus appeared to lose its structure with no crimp visible in the collagen fibres. The mineralised trabeculae and enthesis displayed the same intensity of staining as in the native bone.

### 4.4.2.2    Collagen II

No staining was seen with antibody isotype and negative [no antibody] controls (Appendix A). Collagen II was also present throughout the entire native meniscus and was also seen localised to cells mainly in the white zone but also in the red and red-white zones, however no cellular staining was seen in the superficial layer (Figure 4.4.4). The staining intensity again remained unchanged post-decellularisation of the meniscus however there was more intense staining in the white zone. Collagen II stained slightly less intensely in native attachment than collagen I however there was more intense staining in cells in this region (Figure 4.4.5). Cells in the trabeculae and enthesis also stained positively for collagen II and there was some staining present in the bone marrow. Weak staining was present in the mineralised portions of the trabecular bone and enthesis. The intensity of staining did not appear to change in the decellularised specimens.

### 4.4.2.3    Collagen III

A similar pattern emerged when the tissues were examined immunhistochemically for collagen III (Figure 4.4.6) which was also present throughout the entire meniscus and localised to cells, although to a lesser number of cells than collagen II. There was an absence of staining on the inner tip in decellularised meniscus but no other changes in staining intensity or pattern were observed between native and decellularised menisci. Collagen III staining was present in the native attachment between the collagen fibres and localised to cells, with stronger staining present around the vasculature (Figure 4.4.7). There was weak staining visible in the bone marrow and mineralised matrix within the trabeculae and enthesis. Staining was weak in the decellularised attachment and was
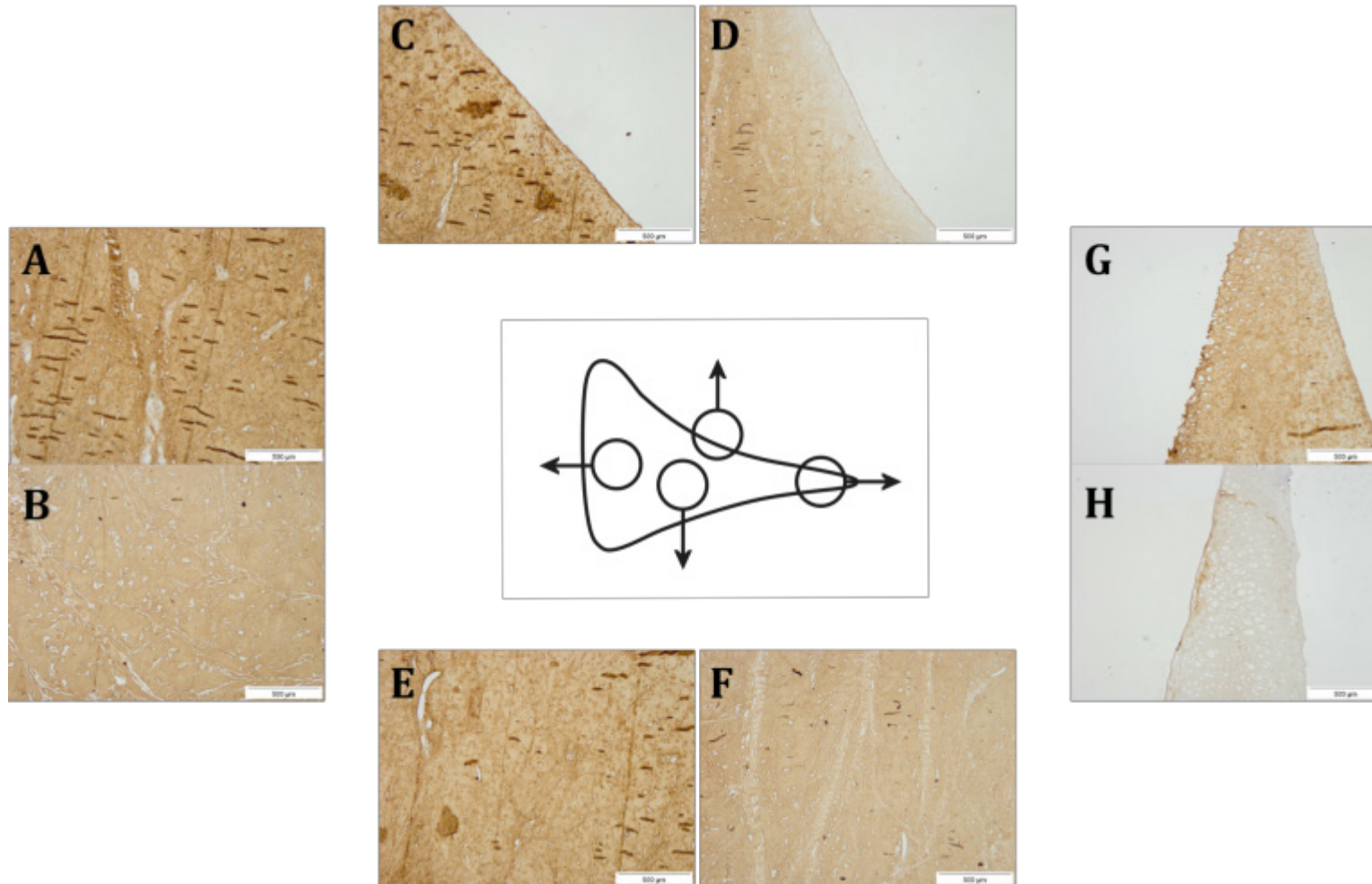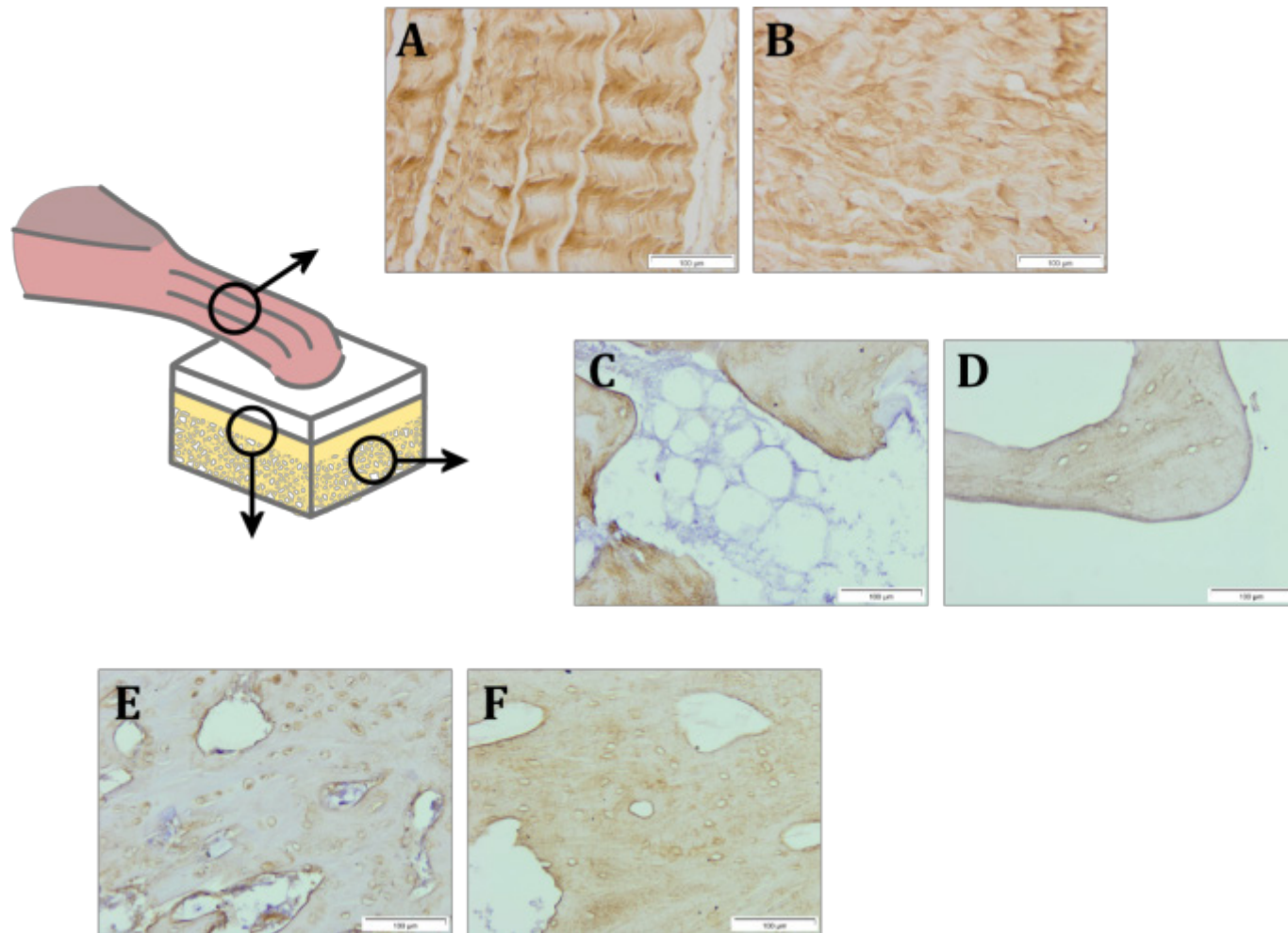
**Figure 4.4.2: Immunohistochemical staining of radial sections of native and decellularised meniscus using antibody against collagen I.** A) Native meniscus red zone B) Decellularised meniscus red zone C) Native meniscus superior surface D) Decellularised meniscus superior surface E) Native meniscus red-white zone F) Decellularised meniscus red-white zone G) Native meniscus white zone H) Decellularised meniscus white zone. Magnification 40x unless stated. Images are representative of the results obtained from n = 3 menisci.

**Figure 4.4.3:  Immunohistochemical staining of anteroposterior sections of native and decellularised bone block using antibody against collagen I.**
A) Native attachment B) Decellularised attachment C) Native trabecular bone D) Decellularised trabecular bone E) Native enthesis F) Decellularised enthesis. Magnification 200x unless stated.  Images are representative of the results obtained from n = 3 bone blocks.
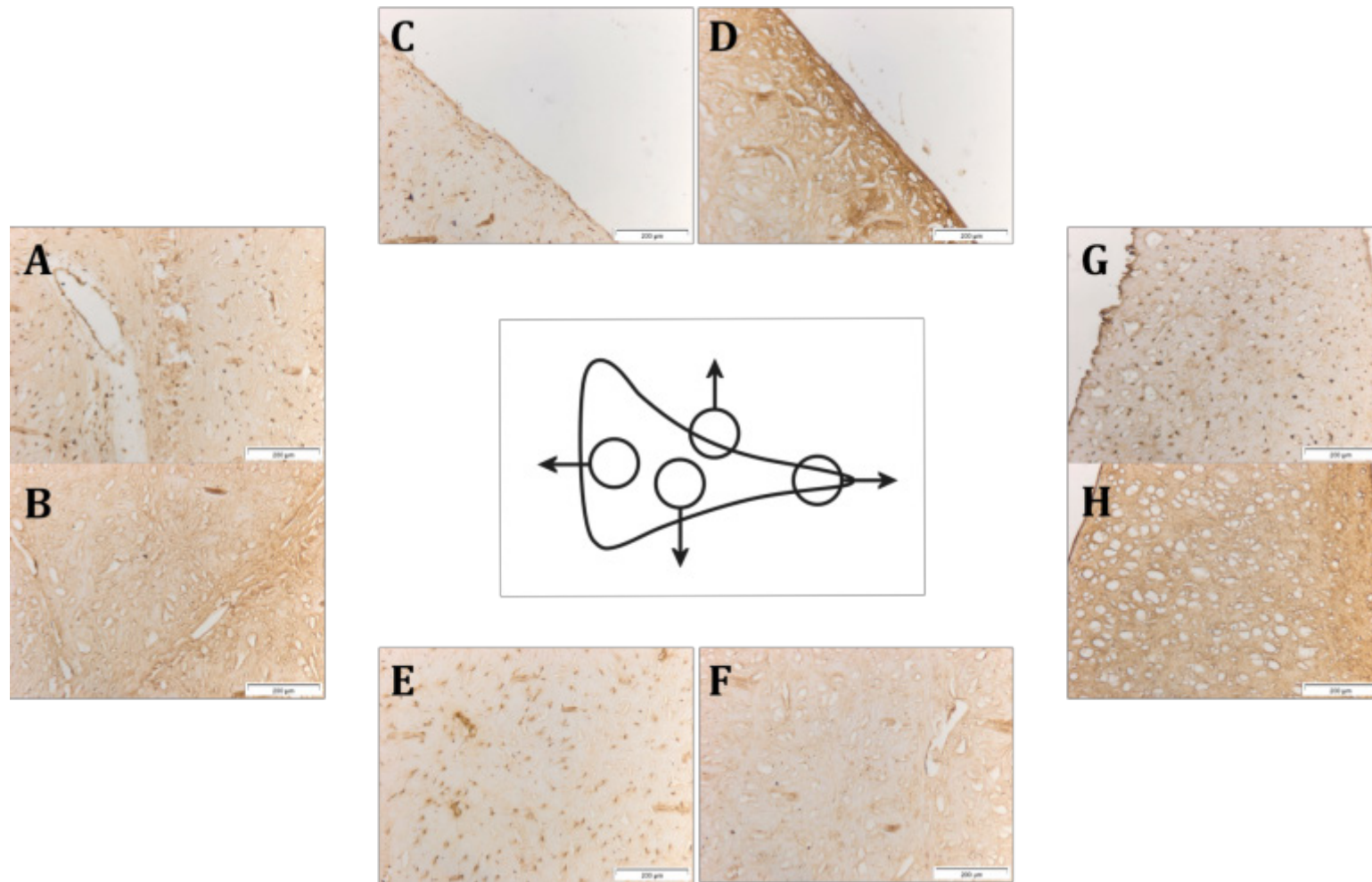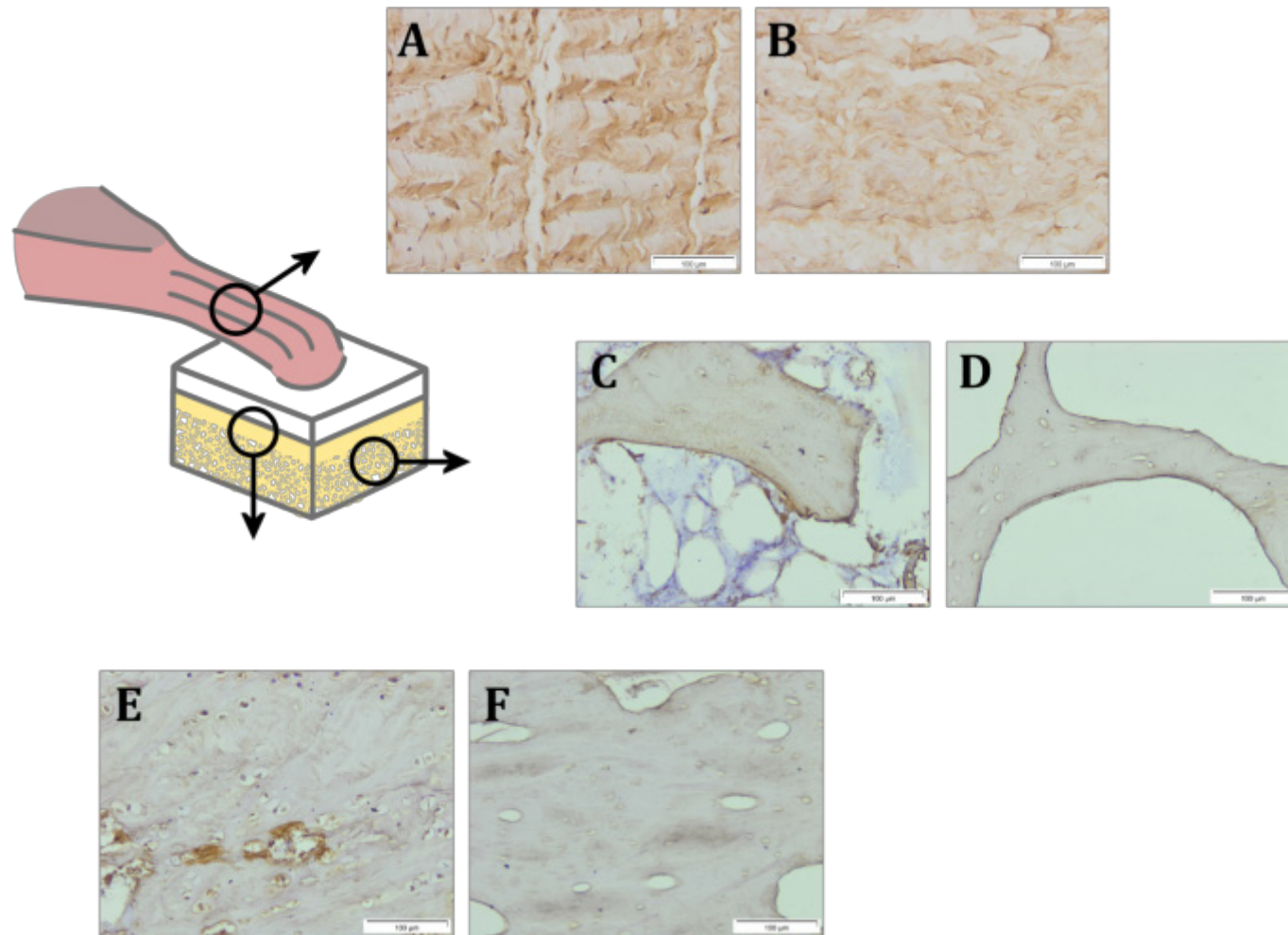
**Figure 4.4.4: Immunohistochemical staining of radial sections of native and decellularised meniscus using antibody against collagen II.** A) Native meniscus red zone B) Decellularised meniscus red zone C) Native meniscus superior surface D) Decellularised meniscus superior surface E) Native meniscus red-white zone F) Decellularised meniscus red-white zone G) Native meniscus white zone H) Decellularised meniscus white zone. Magnification 100x unless stated. Images are representative of the results obtained from n = 3 menisci.

**Figure 4.4.5: Immunohistochemical staining of anteroposterior sections of native and decellularised bone block using antibody against collagen II.**
A) Native attachment B) Decellularised attachment C) Native trabecular bone D) Decellularised trabecular bone E) Native enthesis F) Decellularised enthesis. Magnification 200x unless stated. Images are representative of the results obtained from n = 3 bone blocks.
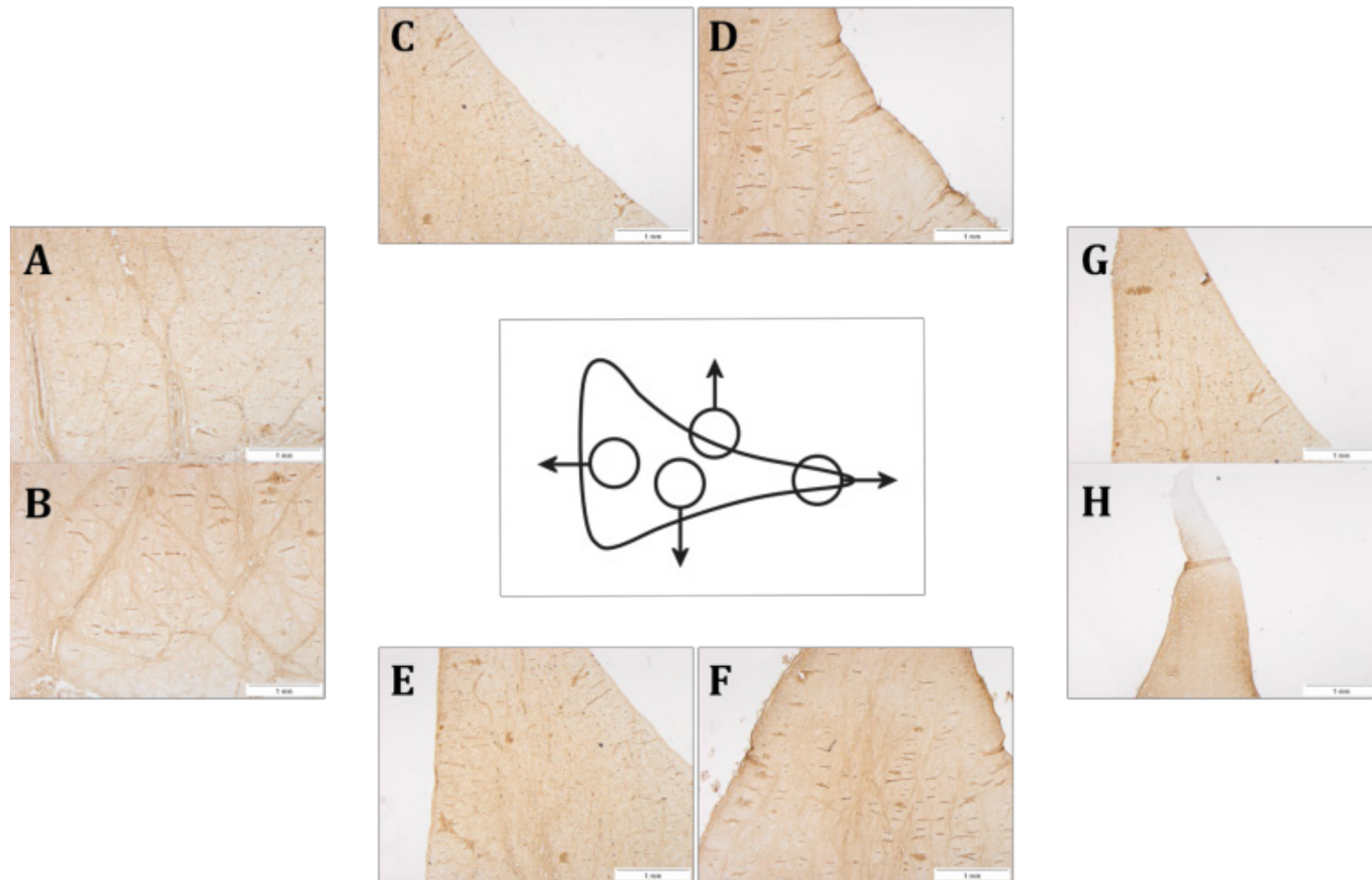
**Figure 4.4.6: Immunohistochemical staining of radial sections of native and decellularised meniscus using antibody against collagen III.** A) Native meniscus red zone B) Decellularised meniscus red zone C) Native meniscus superior surface D) Decellularised meniscus superior surface E) Native meniscus red-white zone F) Decellularised meniscus red-white zone G) Native meniscus white zone H) Decellularised meniscus white zone. Magnification 20x unless stated. Images are representative of the results obtained from n = 3 menisci.
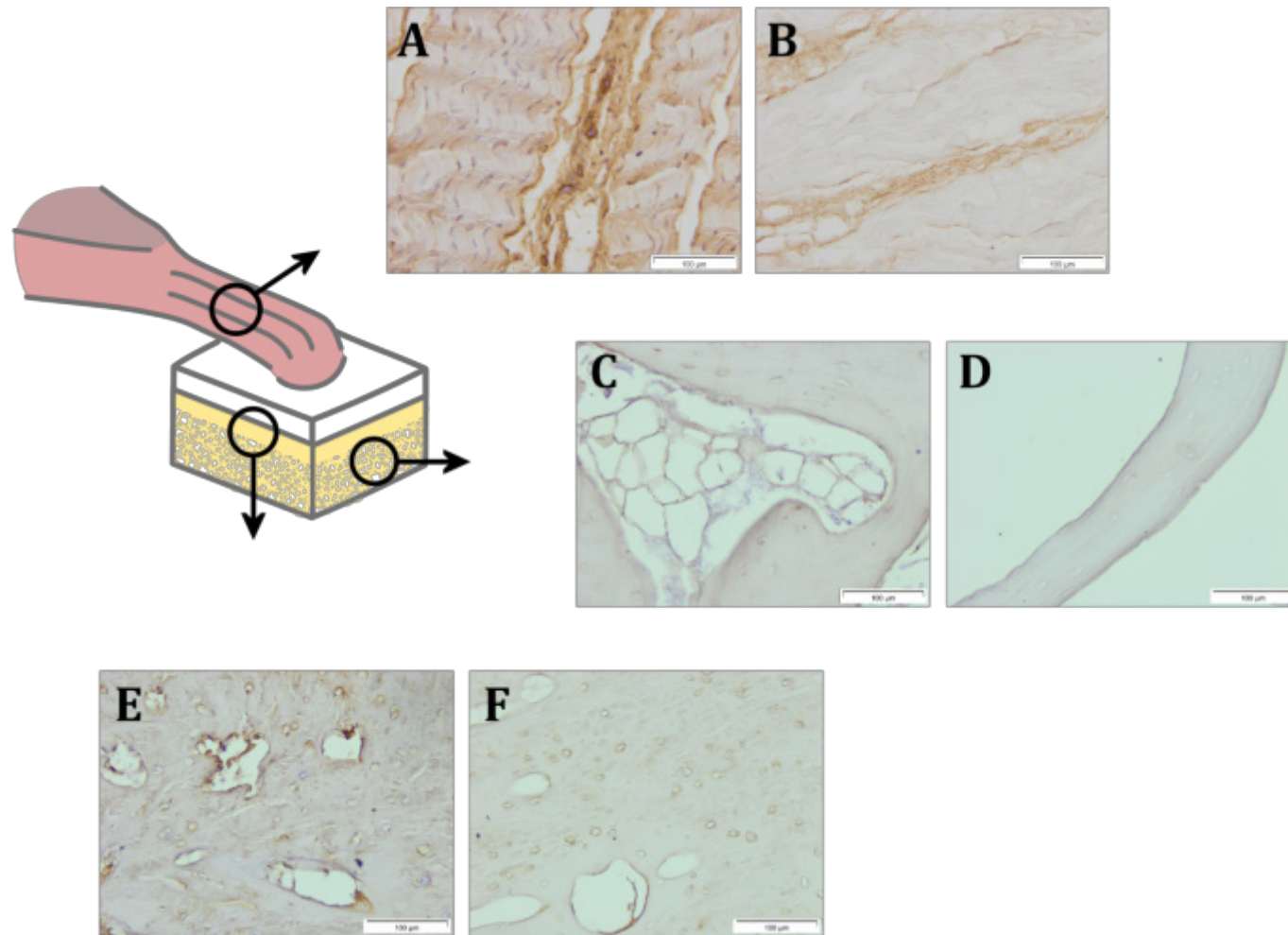
**Figure 4.4.7: Immunohistochemical staining of anteroposterior sections of native and decellularised bone block using antibody against collagen III.** A) Native attachment B) Decellularised attachment C) Native trabecular bone D) Decellularised trabecular bone E) Native enthesis F) Decellularised enthesis. Magnification 200x unless stated. Images are representative of the results obtained from n = 3 bone blocks.

mainly associated with fat remaining in the tissue. Staining was very weak in the trabecular bone however remained unchanged in the enthesis.

### 4.4.2.4    Collagen IV

Native menisci stained for collagen IV (Figure 4.4.8) showed weak staining localised to cells throughout the entire meniscus as well as strong staining associated with the vasculature. This revealed an extensive network of microvasculature in the menisci extending from the outer region well into the inner region with larger vessels present in the outer region reducing in size as they extend in towards the inner region. There was no staining present in any of the regions for decellularised samples. Collagen IV stained predominantly around the vasculature of the attachment with very strong staining along vessel walls, however there was also some staining of cells present between the collagen fibres (Figure 4.4.9). This was also true for the bone with some staining of cells in the bone marrow and further staining of blood vessels in the enthesis. As with the meniscus, once decellularised there was no collagen IV staining visible in any of the regions. No staining was seen with the antibody isotype and negative [no antibody] controls.

### 4.4.2.5    Collagen VI

No staining was seen with antibody isotype and negative [no antibody] controls. Collagen VI staining was evident in the native menisci, again localised to the cell population with more intense staining around the vasculature and synovial membrane. Cells in all regions stained strongly for collagen VI, especially those in the superficial layer. Staining intensity decreased in decellularised menisci with some staining present in the outer, superficial and central regions, and no staining present in the inner region. On gross inspection of decellularised sections there appeared to be a border of weaker staining surrounding the section with intensity increasing towards the centre of the section. The attachment stained positively for collagen VI with strong staining of the cells and within the matrix (Figure 4.4.9). Cells were also stained in the trabecular bone and
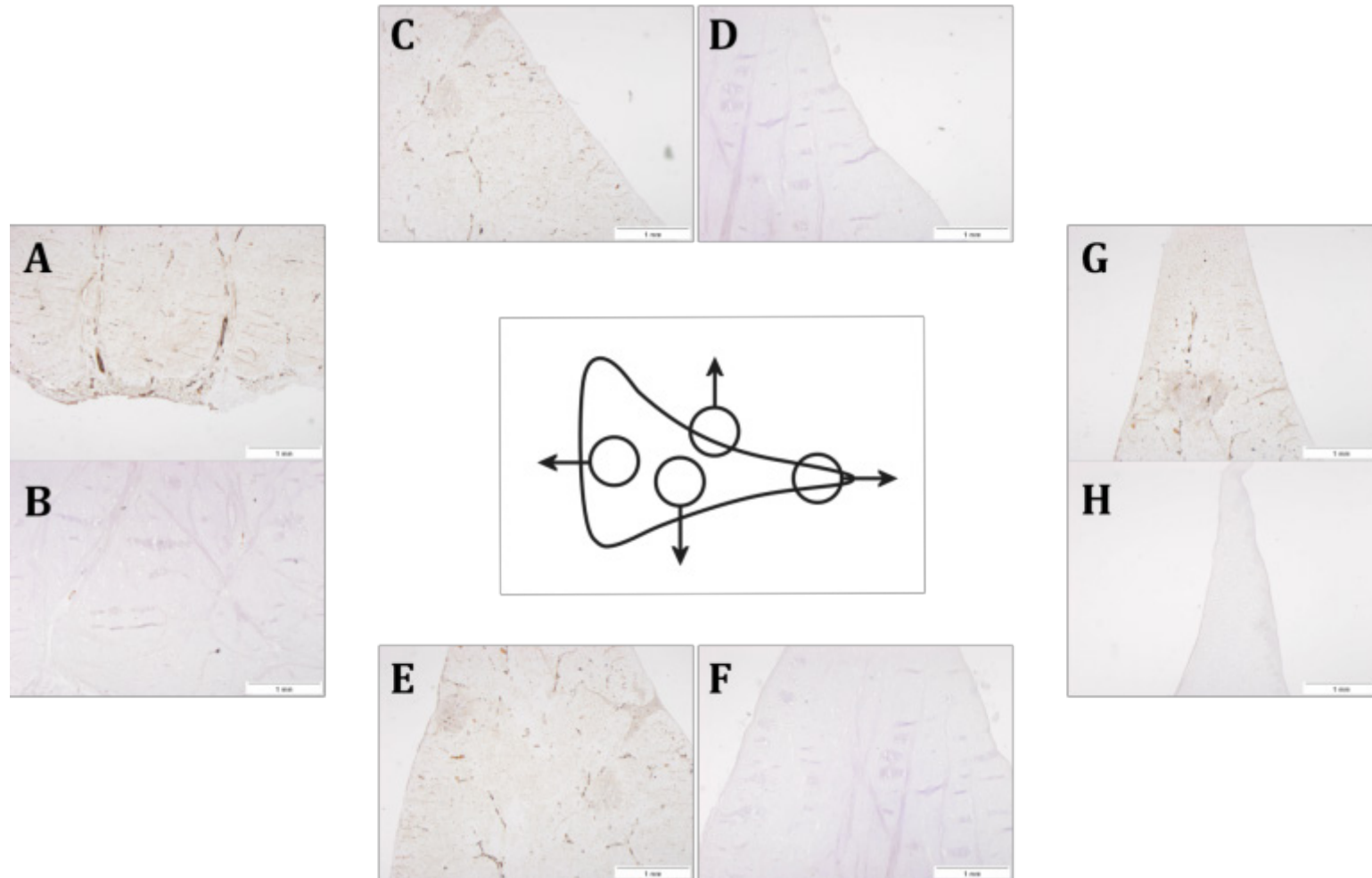
**Figure 4.4.8: Immunohistochemical staining of radial sections of native and decellularised meniscus using antibody against collagen IV.** A) Native meniscus red zone B) Decellularised meniscus red zone C) Native meniscus superior surface D) Decellularised meniscus superior surface E) Native meniscus red-white zone F) Decellularised meniscus red-white zone G) Native meniscus white zone H) Decellularised meniscus white zone. Magnification 20x unless stated. Images are representative of the results obtained from n = 3 menisci.
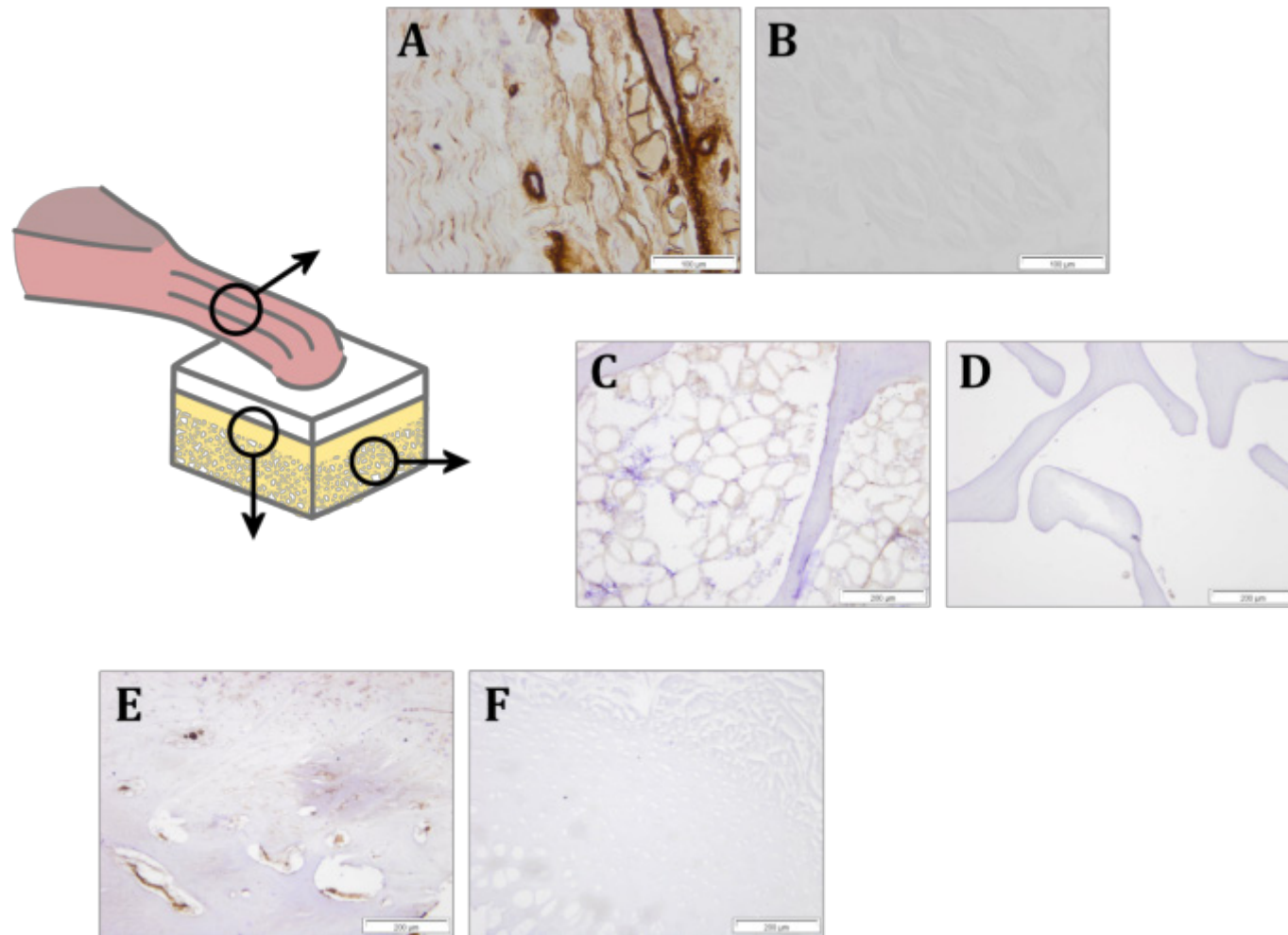
**Figure 4.4.9:  Immunohistochemical staining of anteroposterior sections of native and decellularised bone block using antibody against collagen IV.**  A) Native attachment, magnification 200x B) Decellularised attachment, magnification 200x C) Native trabecular bone D) Decellularised trabecular bone E) Native enthesis F) Decellularised enthesis.  Magnification 100x unless stated.  Images are representative of the results obtained from n = 3 bone blocks.
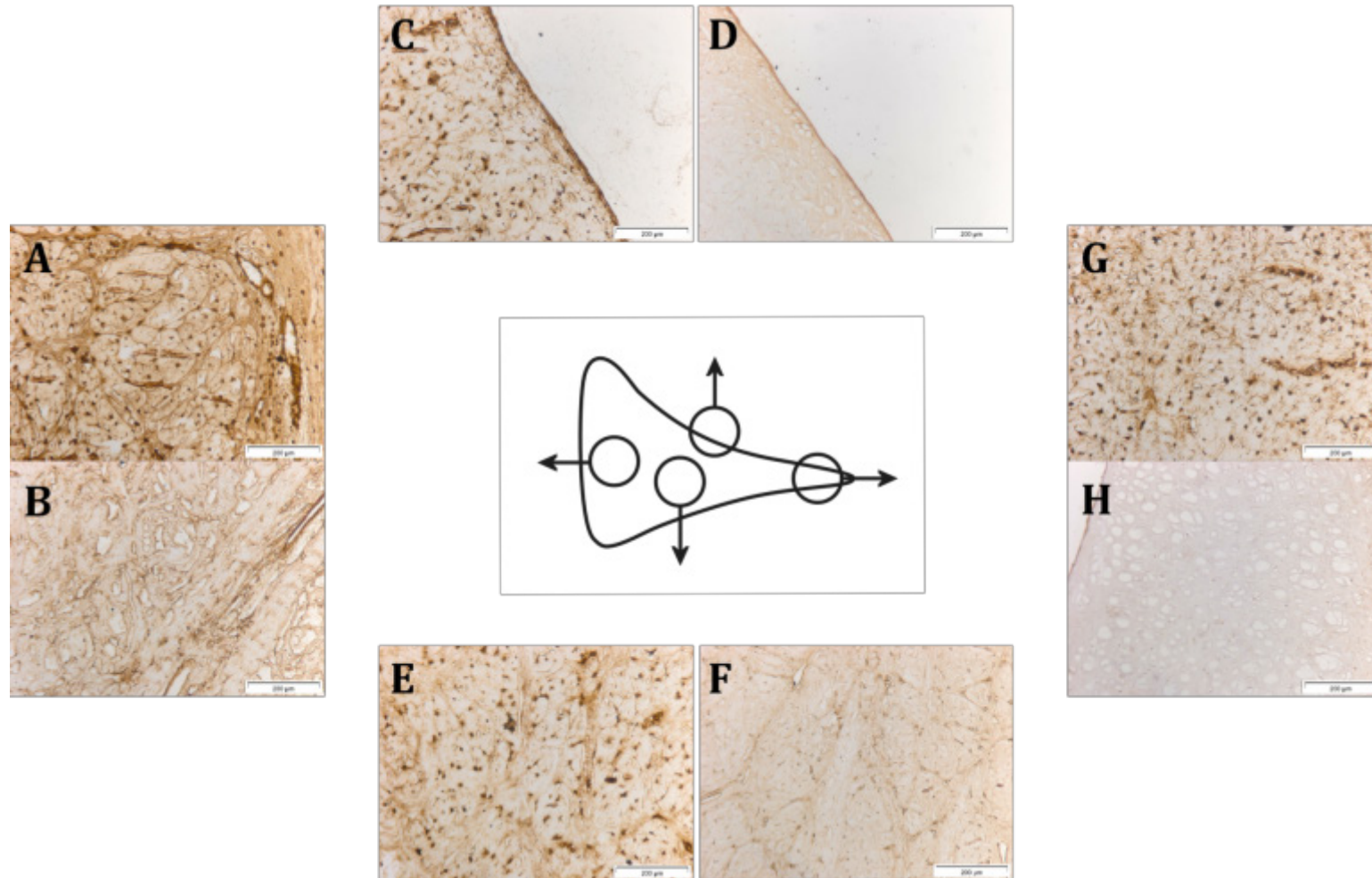
**Figure 4.4.10: Immunohistochemical staining of radial sections of native and decellularised meniscus using antibody against collagen VI.** A) Native meniscus red zone B) Decellularised meniscus red zone C) Native meniscus superior surface D) Decellularised meniscus superior surface E) Native meniscus red-white zone F) Decellularised meniscus red-white zone G) Native meniscus white zone H) Decellularised meniscus white zone. Magnification 100x unless stated. Images are representative of the results obtained from n = 3 menisci.
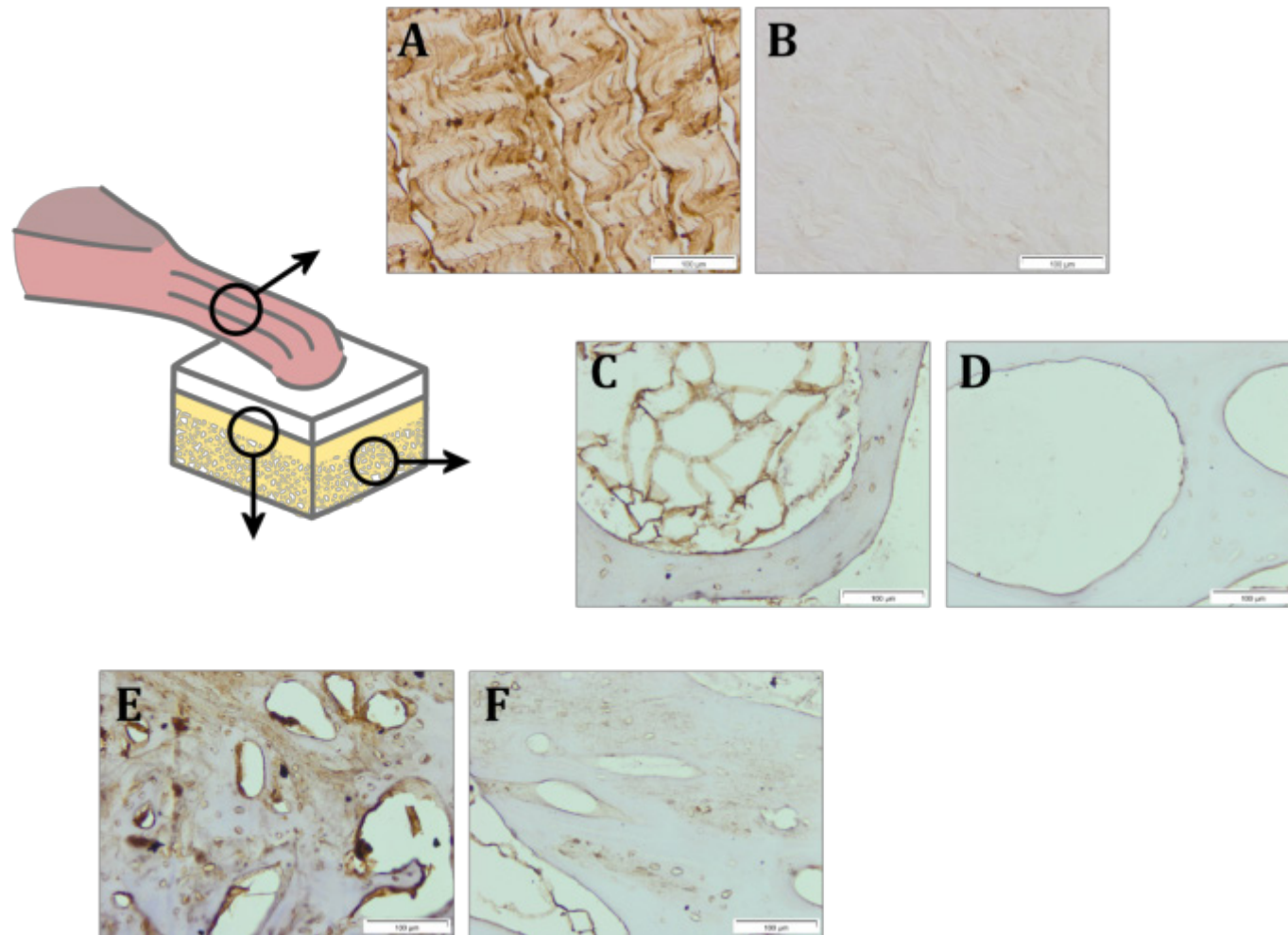
**Figure 4.4.11: Immunohistochemical staining of anteroposterior sections of native and decellularised bone block using antibody against collagen VI.** A) Native attachment B) Decellularised attachment C) Native trabecular bone D) Decellularised trabecular bone E) Native enthesis F) Decellularised enthesis. Magnification 200x unless stated. Images are representative of the results obtained from n = 3 bone blocks.

**Figure 4.4.12: Immunohistochemical staining of anteroposterior sections of native and decellularised bone block using antibody against osteocalcin.**
A) Native attachment B) Decellularised attachment C) Native trabecular bone D) Decellularised trabecular bone E) Native enthesis F) Decellularised enthesis. Magnification 100x unless stated.  Images are representative of the results obtained from n = 3 bone blocks.
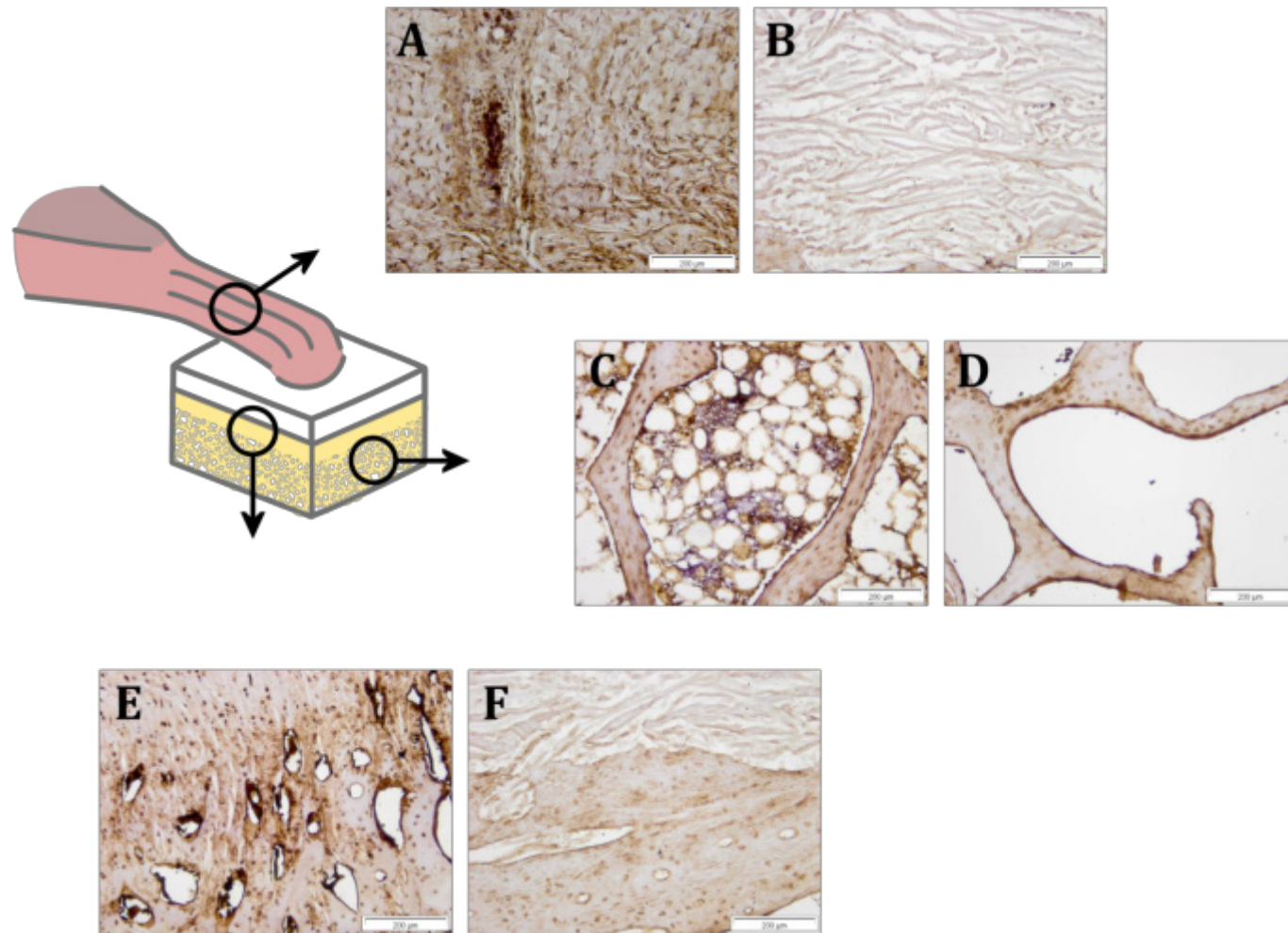
enthesis as well as in the bone marrow however the trabeculae were negative for collagen VI unlike the enthesis where there was some staining. Staining was much weaker in decellularised attachment and this was also seen in the enthesis. There was no staining present in the trabeculae.

### 4.4.2.6    Osteocalcin

No staining was seen with antibody isotype and negative [no antibody] controls. Osteocalcin stained positively in the native meniscal attachment with extensive staining throughout, particularly surrounding the vasculature and cells. This was also seen in the native trabecular bone and enthesis with cells staining very positively for osteocalcin, including in the bone marrow. Staining was less positive in the decellularised attachment however was not affected in the trabecular bone or enthesis where the matrix was stained as intensively as in native specimens.

## 4.4.3 Biochemical characterisation

### 4.4.3.1    Collagen

Collagen content of native and decellularised meniscus and bone was determined using hydroxyproline assay (Figure 4.4.14). Dried soft-tissue samples were acid hydrolysed prior to assay with bone samples decalcified prior to hydrolysis. In order to ensure the accuracy of the data, it was first necessary to determine the time taken for complete hydrolysis of samples. Samples of meniscus were therefore hydrolysed for up to eight hours and the hydroxyproline content determined at two hour intervals. This showed that hydrolysis for 6 hours was sufficient (Figure 4.4.13). This was therefore applied to the samples of meniscus and bone to be tested. Values obtained for hydroxyproline content were converted to collagen content. The collagen content of native meniscus was 802.90 ($\pm$ 52.95, 95% C.I.) mg.g$^{-1}$ dry weight and for decellularised meniscus was 935.35 ($\pm$ 18.03, 95% C.I.) mg.g$^{-1}$ dry weight. The values were not significantly different (student`s t-test; p>0.05). Native bone had a collagen content of 391.42 ($\pm$ 39.51, 95% C.I.) while

decellularised bone contained 501.52 ($\pm$ 100.01, 95% C.I.) mg.g$^{-1}$ dry weight. Again the means were not significantly different (student`s t-test; p>0.05).
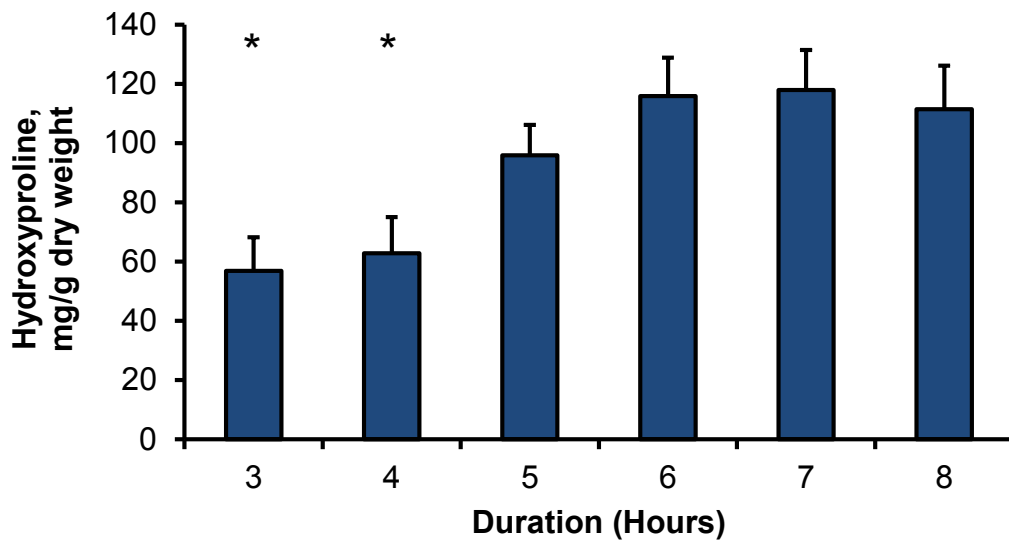


**Figure 4.4.13**: **Hydroxyproline concentrations from investigation of acid hydrolysis duration.** Data presented as mean (n = 3) $\pm$ 95% C.I. Statistical analysis was performed using ANOVA (* p<0.05 compared to all other groups).
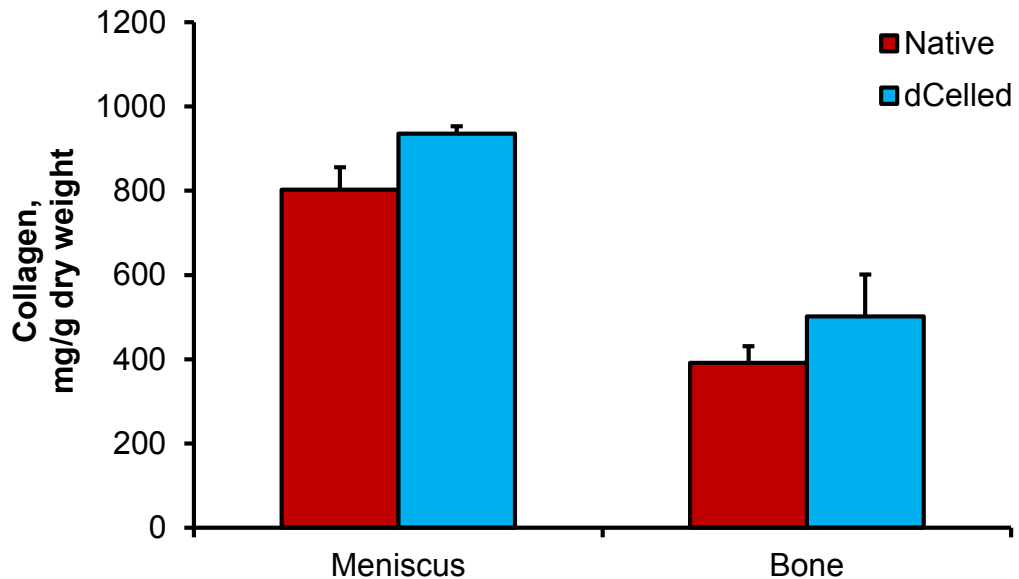


**Figure 4.4.14: Collagen content of native and decellularised bone-meniscus-bone by hydroxyproline assay.** Data presented as mean (n = 3) $\pm$ 95% C.I. Statistical analysis was performed using student's t-tests which revealed no significant difference in the total collagen content of the meniscus or bone before and after decellularisation (p>0.05).

4.4.3.2    GAGs

Glycosaminoglycan content of native and decellularised meniscus was analysed using DMMB assay. Dried soft-tissue samples (n = 3) were digested using papain prior to assay. The time taken for complete digestion of samples was determined through investigation of incubation with papain digestion solution for up to 4 days. DMMB assay was performed every 24 hours and the results showed complete digestion after 72 hours (Figure 4.4.15). Therefore, samples of meniscus were digested for 72 hours prior to DMMB assay. The mean GAG content of native meniscus (Figure 4.4.16) averaged over all regions was 23.49 ($\pm$ 8.63, 95% C.I.) mg.g$^{-1}$ dry weight and for decellularised meniscus was 0.30 ($\pm$ 0.47, 95% C.I.) mg.g$^{-1}$ dry weight. The values were significantly different when analysed by student's t-test (p< 0.05). Regional analysis of GAG content was also undertaken with the meniscus separated into inner, outer and attachment regions. The mean GAG content of native inner meniscus was 64.80 ($\pm$ 1.06, 95% C.I.) mg.g$^{-1}$ dry weight and for decellularised inner meniscus was 3.73 ($\pm$ 14.34, 95% C.I.) mg.g$^{-1}$ dry weight. Again the means were significantly different (student`s t-test; p< 0.05);. The mean GAG content of native outer meniscus was 20.75 ($\pm$ 5.56, 95% C.I.) mg.g$^{-1}$ dry weight and for decellularised outer meniscus was 0.19 ($\pm$ 0.53, 95% C.I.) mg.g$^{-1}$ dry weight. The means were significantly different (student`s t-test; p< 0.05);. The mean GAG content of native attachment was 7.88 ($\pm$ 0.02, 95% C.I.) mg.g$^{-1}$ dry weight and for decellularised attachment was 0.00 ($\pm$ 0.00, 95% C.I.) mg.g$^{-1}$ dry weight.
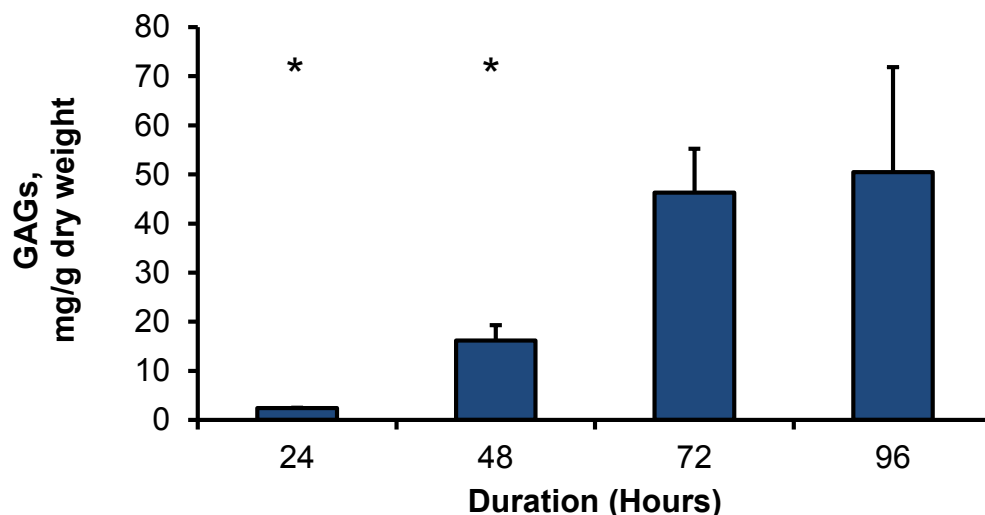
**Figure 4.4.15**: **GAG concentrations from investigation of papain digestion duration.** Data presented as mean (n = 3) $\pm$ 95% C.I. Statistical analysis was performed using ANOVA (* p<0.05 compared to all other groups).



**Figure 4.4.16: GAG content of native and decellularised meniscus by DMMB assay.** Data presented as mean (n = 3) $\pm$ 95% C.I. Statistical analysis performed using student's t-tests which revealed significant differences in the total GAG content between different regions of the meniscus before and after decellurisation (* p<0.05).

## 4.4.3.3  Calcium

Bone samples were dried and dissolved in hydrochloric and nitric acid followed by analysis using inductively-coupled plasma mass spectrometry for quantification of calcium (Figure 4.4.17). Native bone had a calcium concentration of 26.61 ($\pm$ 5.15, 95% C.I.) mg.g$^{-1}$ dry weight compared to

13.015 ($\pm$ 3.37, 95% C.I.) mg.g$^{-1}$ dry weight for decellularised bone.  Means were found to be significantly different when compared by student's t-test (p < 0.05).
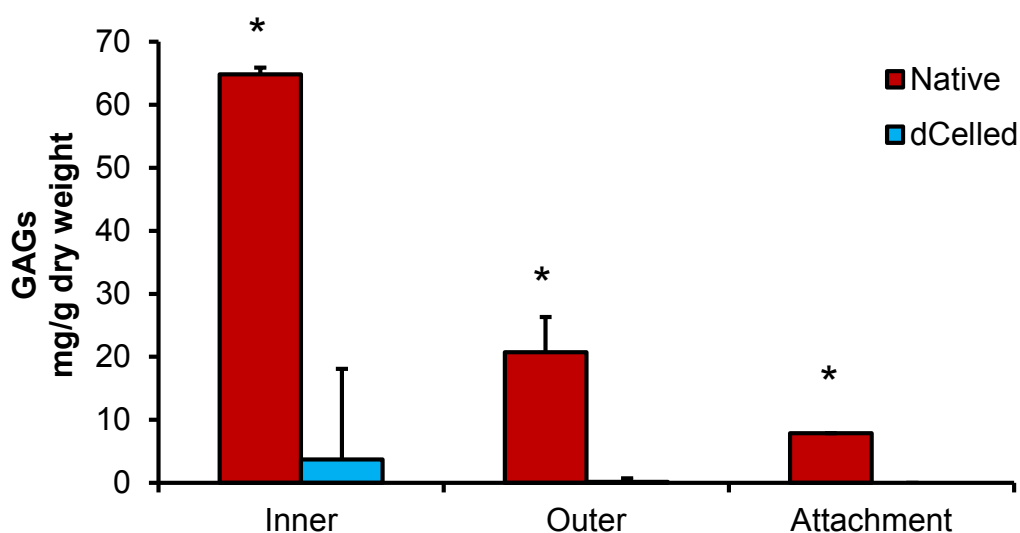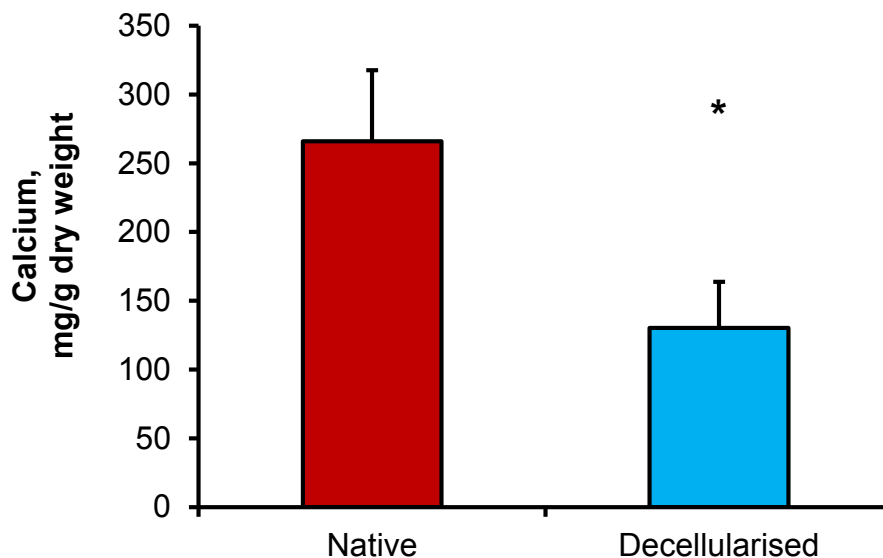


**Figure 4.4.17: Calcium content of native and decellularised bone by ICP-MS.**  Data presented as mean (n = 4) $\pm$ 95% C.I.  Statistical analysis was performed using student's t-test (* p<0.05).

### 4.4.4 Thermal analysis

#### 4.4.4.1   Differential scanning calorimetry

Differential scanning calorimetry was used to compare the thermal stability of native and decellularised bone-meniscus-bone.  Samples were taken from inner, outer, attachment, enthesis, and bone regions from three native and three decellularised bone-meniscus-bone and heated to 200 °C.  Broad peaks were evident on all thermograms corresponding to collagen denaturation.  Results are summarised in Figure 4.4.18 and Figure 4.4.19. Native samples had denaturation temperatures ($T_D$) of 74.43 ($\pm$ 8.03, 95% C.I.), 65.48 ($\pm$ 7.72, 95% C.I.), 76.13 ($\pm$ 17.00, 95% C.I.), 60.52 ($\pm$ 12.10, 95% C.I.), and 51.43 ($\pm$ 4.58, 95% C.I.) °C for inner, outer, attachment, enthesis and bone regions, respectively.   Decellularised samples had

denaturation temperatures of 65.58 (± 13.66, 95% C.I.), 59.87 (± 7.06, 95% C.I.), 53.39 (± 4.23, 95% C.I.), 61.39 (± 6.56, 95% C.I.), and 50.27 (± 1.11, 95% C.I.) °C for inner, outer, attachment, enthesis and bone regions, respectively. There were no significant differences between native and decellularised samples with the exception of the attachment which had a significantly lower denaturation temperature for the decellularised samples compared to native samples (student`s t-test; p < 0.05).


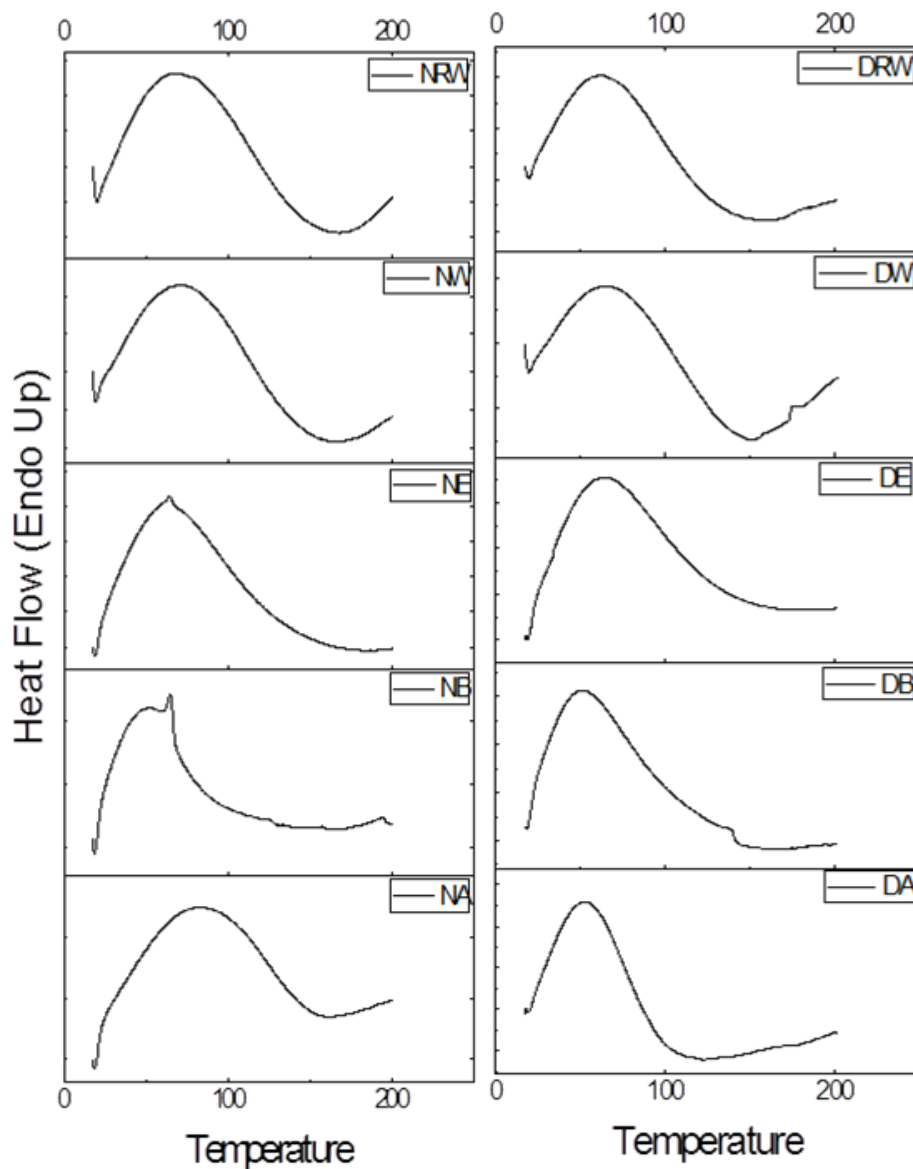
**Figure 4.4.18: DSC thermograms of native and decellularised bone-meniscus-bone.** N = native, D = decellularised, RW = red-white, W = white, B = bone, E = enthesis, and A = attachment. Images are representative of n = 3 samples.
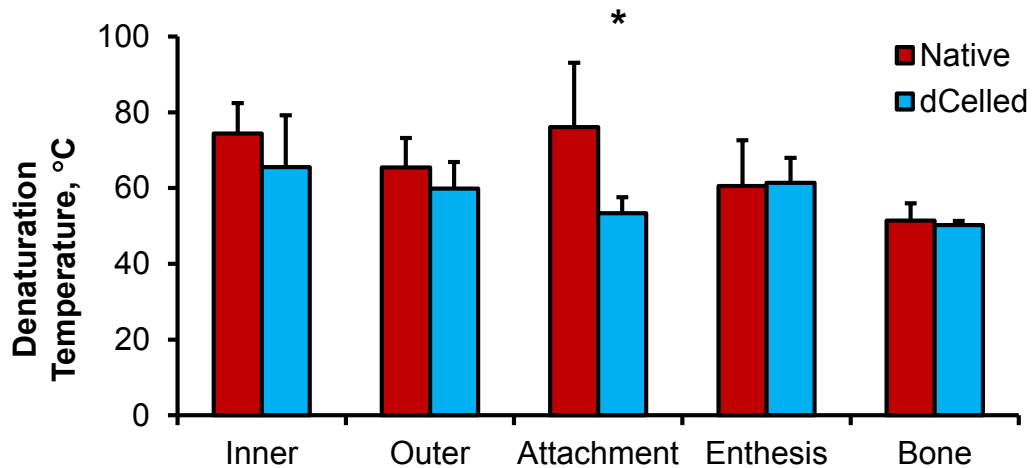
**Figure 4.4.19: Denaturation temperatures of native and decellularised bone-meniscus-bone by DSC.** Data presented as mean (n = 3) ± 95% C.I. Statistical analysis was performed using student's t-test for each region (* p<0.05 when compared to native tissue).

## 4.4.5 **Magnetic Resonance Imaging**

### 4.4.5.1 Meniscus

Magnetic resonance imaging was used to compare the structure of native and decellularised porcine medial meniscus. Menisci (n = 2) were cut radially to produce 5 mm thick slices and imaged by performing a 3D FLASH sequence using a Bruker AVANCE II 400 MHz NMR system. A representative image is displayed in Figure 4.4.20. Imaging of native menisci mainly highlighted structures that appeared to represent the vasculature which extended from the red zone all the way to the white zone. Blood vessels were larger in the red zone and diminished in size and number as they approached the white zone. This correlated with collagen IV staining of native meniscus. The distribution of vasculature through the native porcine meniscus is shown in Figure 4.4.20. Larger vessels are seen emanating from the PMCP and spreading through the body of the meniscus. A smooth outer layer was also visible surrounding the entire meniscus which may have been the synovial membrane. This layer was not seen on the decellularised meniscus instead a rough boundary layer was seen. The

structures, presumed to be blood vessels in native meniscus were not apparent following decellularisation of the meniscus however a clear difference in signal intensity could be seen between the white zone and the rest of the meniscus.
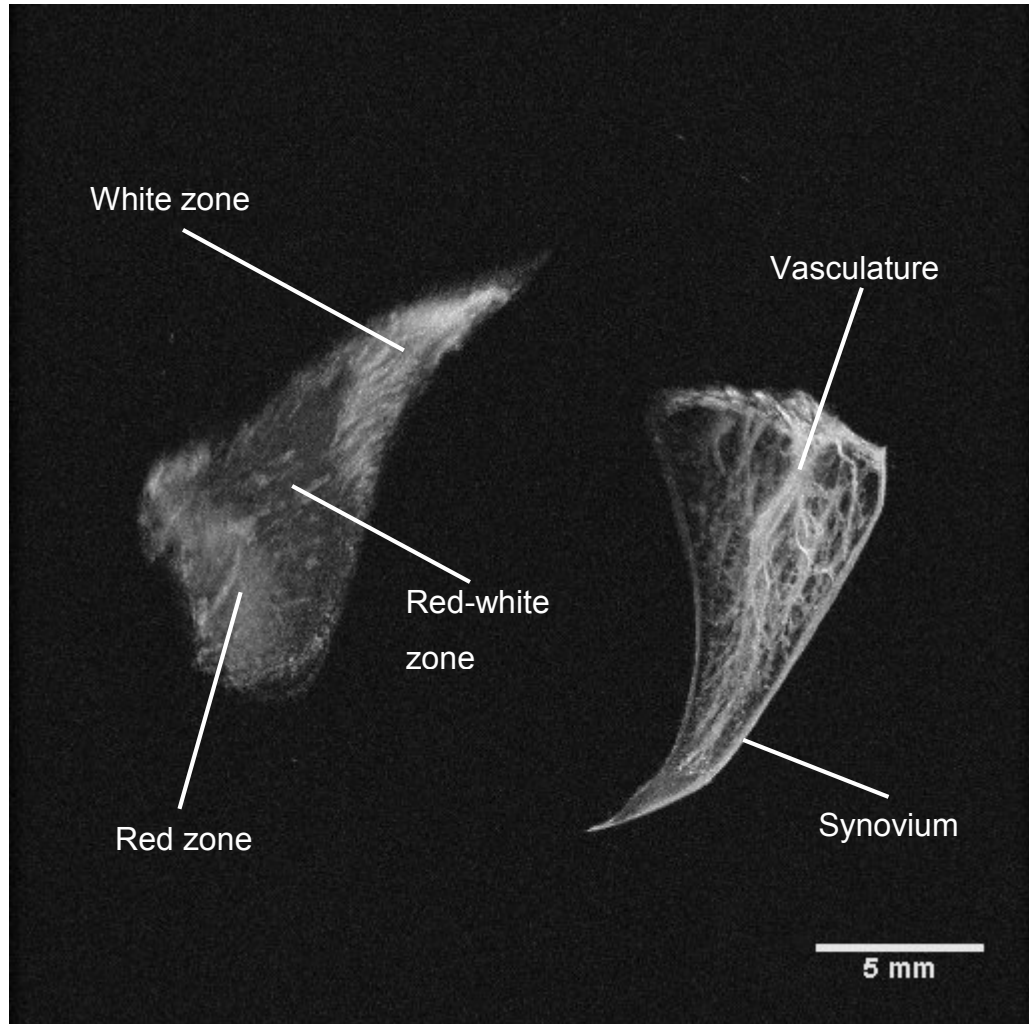


**Figure 4.4.20: 2D image slices extracted from 3D MRI of native (right) and decellularised (left) porcine medial meniscus.** Representative image from n = 2 menisci.

**Figure 4.4.21: Collagen IV staining of native porcine medial meniscus showing distribution of vasculature throughout the immature meniscus.**

## 4.4.5.2  Bone

MR images of bone were obtained using a 3D FLASH sequence on entire bone blocks.  Samples (n = 2) of native and decellularised bone were placed in a universal and scanned for ~56 hours to obtain a 3D representation of the sample.  Images of native porcine bone blocks (Figure 4.4.22) displayed the different regions clearly.  The 3D flash sequence allowed clear distinction of the regions.  Good signal was displayed from cartilage and tendon with collagen structures visible in the meniscal attachments.  The mineralised matrix was displayed through an absence of signal due to the surrounding marrow which is water-rich therefore resulting in a strong signal.  This consisted of the cortical bone, just underneath the cartilage surface of the

tibial plateau and the transition to trabecular bone. The epiphyseal plate could also be seen towards the bottom of the bone block.
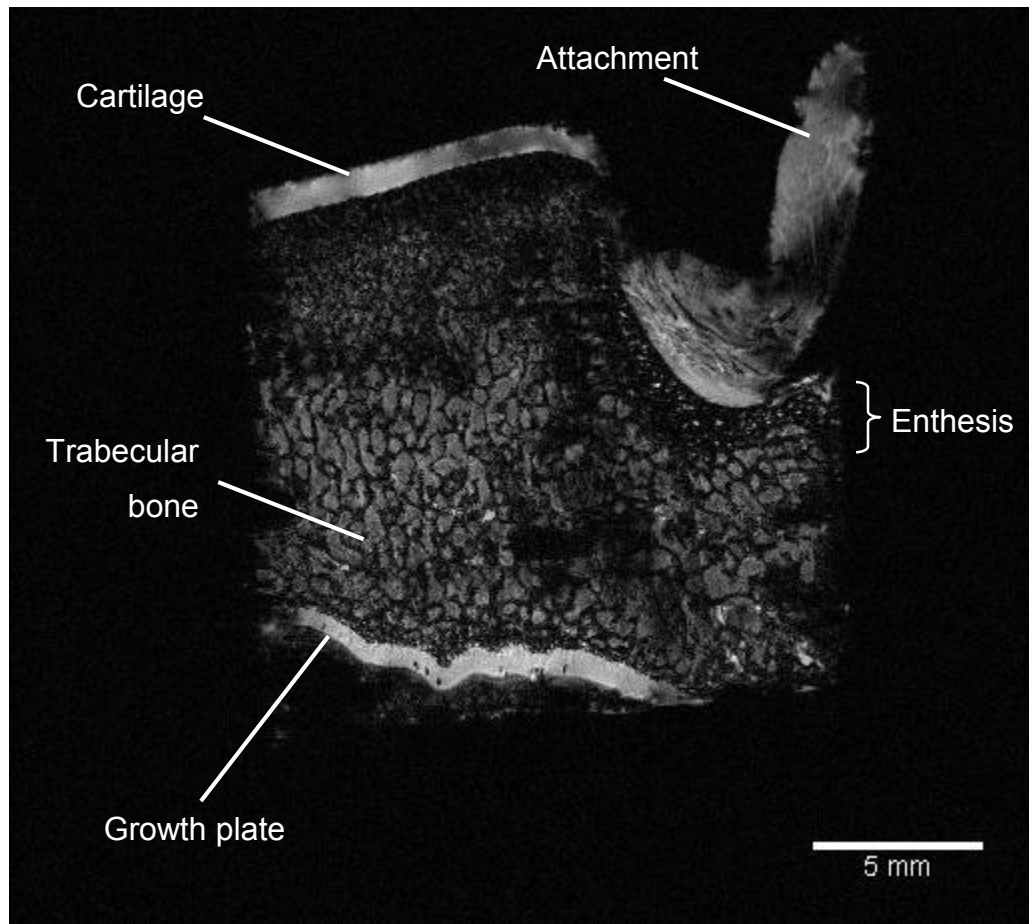


**Figure 4.4.22: MRI of native porcine bone block.** Representative image from n = 2 bone blocks.

Structures were more clearly visible in MR images of decellularised bone blocks due to better contrast between different components (Figure 4.4.23). Again, all regions from the cartilage surface to the epiphyseal plate were displayed. Slight changes in the depth of tibial cartilage were seen with a slightly thicker layer visible on decellularised bone blocks. The attachment also appeared to be looser in structure and swollen when compared to the native attachment.
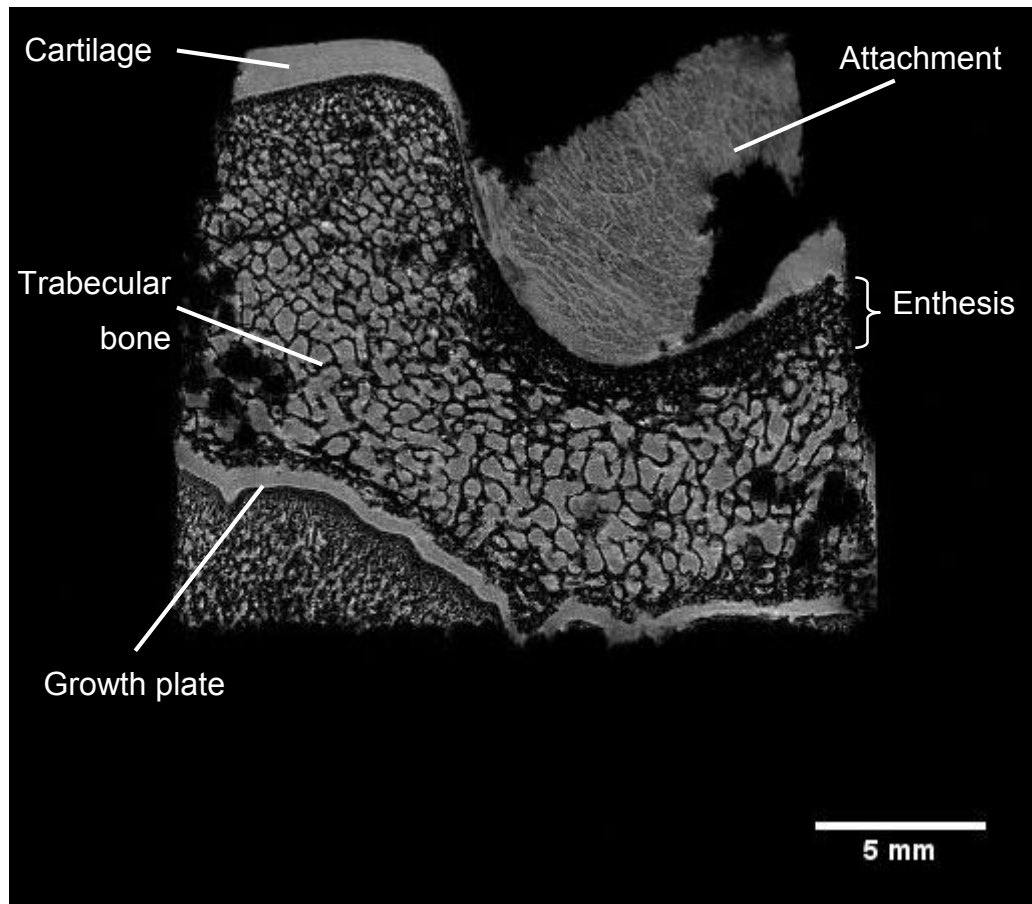
**Figure 4.4.23: MRI of decellularised porcine bone block.** Representative image from n = 2 bone blocks.

## 4.5 Discussion

The work presented in this chapter aimed to determine whether the process developed in Chapter 3 to decellularise the porcine bone-meniscus –bone preserved the extracellular matrix composition and structure. The duration and nature of the protocol required for effective decellularisation suggested that there would be changes to the extracellular matrix. Since the collagen structure within the meniscus is vital to its function it was desirable to retain as much of this as possible. Ionic detergents, such as sodium dodecyl sulfate (SDS), solubilise cell and nucleic membranes and can denature proteins. SDS has been shown to effectively remove cell and nuclear material but can also remove GAGs and growth factors, and damage collagen (Reing *et al.*, 2007; Lumpkins *et al.*, 2008; Stapleton *et al.*, 2008; Deeken *et al.*, 2011). Native and decellularised bone-meniscus-bone samples were evaluated for major matrix constituents both qualitatively and quantitatively.

As mentioned in Chapter 3, H&E staining of meniscus revealed the loss of the synovial membrane post-decellularisation. This is not deemed critical as it has been shown that migrating cells reform the synovial membrane (Arnoczky *et al.*, 1992). H&E staining also highlighted the formation of spaces in the extracellular matrix. This may have been due to the freeze-thaw cycles incorporated in the protocol and/or from the removal of cells and other matrix components. The organised collagen structure was retained allowing the different regions to be clearly distinguished with radial tie-fibers visible throughout the tissue.

Proteoglycans were visualised using safranin O with intense staining present in the inner region of native menisci and very little if any present in the outer. Decellularised samples displayed no safranin O staining suggesting complete removal of proteoglycans by the decellularisation protocol. However, safranin O has been shown to be limited when staining tissue where GAGs have been heavily depleted as antibodies were still able to detect the presence of GAGs (Camplejohn & Allard, 1988). Therefore, DMMB assay was used to verify these results and confirmed that all GAGs

were lost from the outer and attachment regions of decellularised meniscus. However, some GAGs remained in the inner region post-decellularisation, which has a GAG content 3-fold higher than in the outer region and 6-fold higher than in the attachment. This may be because the inner region has higher collagen II content, with higher proportion of hydroxylysine as well as glucosyl and galactosyl residues, which interact with proteoglycans (Mayne, 1989). The loss of GAGs may have an effect on the function of the tissue since GAGs retard fluid flow in the meniscus allowing the fluid phase to bear load before it is transmitted to the solid phase. The effect on the biomechanical properties of the tissue will need to be determined.

Qualitative analysis of the types of collagen present within bone-meniscus-bone and changes to this composition perpetrated by decellularisation was carried out using immunohistochemical staining. Collagen I is the major constituent of meniscal ECM. It forms a complex network of fibril bundles that provide the tensile properties. Intense staining was present throughout the native meniscus, attachment site and bone attachments. This was replicated in decellularised bone-meniscus-bone however collagen I staining intensity was weaker in the inner region and highlighted the loss of collagen structure in the attachment with relaxation of the characteristic crimp. This may have been due to the intentional mechanical disruption of the attachment to enhance diffusion of decellularisation reagents into the enthesis. Collagen II staining assumed a similar pattern to collagen I with staining throughout the meniscus; however intensity was greatest in the inner meniscus and localised to cells both in the bone and meniscus. Collagen III is incorporated into collagen I fibrils during development where it prevents the lateral growth of type I collagen (Birk and Mayne, 1997) and also plays a role in the remodelling response (Sodersten et al., 2013). Uniform staining was present throughout with weak staining visible in the bone, mainly localised to cells. Staining intensity was decreased in the decellularised attachment and bone however as collagen III is deposited within 2-5 days of injury. It is hypothesised that following implantation *in vivo*, migrating host cells would replenish lost collagen III. Collagen IV is found in the pericellular matrix and has been shown to be absent in osteoarthritic

meniscus (Foldager *et al.*, 2014). Collagen IV in native meniscus was seen localized to the vasculature exposing an extensive network extending into the white zone of the meniscus. This was expected as the meniscus is known to be vascularised during development, becoming increasingly avascular with age (Clark and Ogden, 1981). A complete removal of collagen IV was seen in decellularised bone-meniscus-bone. Investigations in the lab have shown that this is caused by peracetic acid (Wilshaw *et al.*, 2014) and so an alternative sterilisation method may have to be developed. However, as the meniscus is largely avascular and studies have shown migration of cells into the meniscus it is not known whether the loss of collagen IV is critical to the *in vivo* function of decellularised bone-meniscus-bone. Type VI collagen is usually found in the pericellular matrix surrounding cells along with fibronectin and GAGs. Collagen VI anchors the cell membrane to the ECM (Sardone *et al.*, 2013) where it provides protection from compressive loading and is involved in cell-matrix signalling (Fraser *et al.*, 2006). Collagen VI has also been found in bone growth plates (Alexopoulos *et al.*, 2009) and plays a role in remodelling (Keene *et al.*, 1991). Immunohistochemical staining of collagen VI in bone-meniscus-bone confirmed its presence in meniscus and tibial bone with strong staining present localized to cells and on the meniscal surface. Some staining was also present in the ECM especially surrounding the vasculature. A decrease in collagen VI staining intensity was seen in decellularised samples with staining intensity increasing towards the centre of the meniscus. This suggested physical removal of collagen VI by hydrostatic pressure as opposed to chemical removal by process reagents. Osteocalcin is the most abundant non-collagenous protein present in bone (Hauschka *et al.*, 1989) and has been shown to be a determinant of bone formation as its absence leads to increased bone formation (Ducy *et al.*, 1996). Immunohistochemistry of native bone blocks using anti-osteocalcin antibodies revealed positive staining localised to cells in all regions including the attachment and marrow, while there was also some staining present on the bone matrix. A similar intensity of staining was seen in decellularised bone suggesting the retention of matrix-associated osteocalcin. Osteocalcin

has been shown to play a role in osteochondrocytic differentiation (Idelevich *et al.*, 2011) and so may influence integration of bone blocks once implanted.

Calcium, in the form of calcium phosphate, is a major component of bone where it provides strength and structure. The strength of bone is dependent on its mass and geometry however it is also dependent on its composition. Therefore, the calcium content of decellularised bone was determined and compared to native bone using inductively coupled plasma mass spectrometry (ICP-MS). ICP-MS allows the determination of elements within an atomic mass range of 7 to 250 by ionising samples with inductively coupled plasma and then quantifying using a mass spectrometer. This analysis was carried out at the U.K. Centre for Tissue Engineering at the University of Liverpool. Results showed a significant reduction in calcium content of decellularised bone (~50%) when compared to native bone. This may adversely impact the mechanical properties *in vivo* with the implanted bone initially unable to withstand compressive forces to the same extent as native bone. Removal of the inorganic mineral may however, prove to be beneficial as studies have shown that demineralised bone matrix, allograft bone that has had the mineral removed, through the exposure of bone morphogenetic proteins displays osteoinductive and osteoconductive properties, thus promoting a healing response (Reddi, 1975; Glowacki and Mulliken, 1985).

Several methods were investigated in the determination of calcium content in porcine bone. Initially a colorimetric assay utilising Arsenazo III was attempted. Arsenazo III is a calcium-sensitive dye that has been used for the determination of calcium in serum (Morgan *et al.*, 1993). This proved to be unsuccessful as estimations of calcium content did not match values obtained from the literature. Atomic absorption spectroscopy (AAS) was then investigated as a method for detection of calcium. AAS utilises a flame to atomise samples which are then excited causing the electrons in the atomised sample to absorb a defined quantity of energy. The wavelength of this absorption is specific to a particular electron transition in a specific element and is then measured using a detector. Total calcium values

obtained using this method were similar to the colorimetric method however the proportional difference between native and decellularised samples was similar to that obtained using ICP-MS. It is unknown why these methods were unable to correctly estimate total calcium content as samples were within the sensitivity limits of each method. It is hypothesised that other elements present within the samples may have interfered with these measurement techniques.

Thermal analysis of decellularised bone-meniscus-bone was undertaken using DSC and compared to that of native tissue. DSC can be used to detect structural changes in samples as they are heated. Samples were dehydrated prior to analysis as hydration of collagen has been shown to influence the denaturation temperature (Miles and Gelashvilli, 1999). Due to the differing compositions between regions present within bone-meniscus-bone five regions were chosen. The white zone is composed of dense hyaline-like cartilage while the red-white, red and meniscal attachments are composed of fibrocartilage. In the bone two distinct regions exist: the dense enthesis and the trabecular bone. DSC revealed no significant differences between denaturation temperatures of native and decellularised samples except for in the attachment where there was a reduction in denaturation temperature. This may be due to the disruption of collagen structures during the decellularisation process as incisions were made in this region to improve access of reagents into the enthesis. Although there was a significant difference between the denaturation temperatures of native and decellularised attachment, the $T_D$ of decellularised attachment was not significantly different to native samples from all other regions suggesting retention of collagen organisation.

Magnetic resonance imaging was utilised to provide a rapid comparison of meniscus and bone block structure. A 3D-FLASH scan was able to reveal detailed images of major meniscal and bone architecture. Interpretation of images proved to be difficult as the MRI was unable to differentiate between the various types of tissue present within bone-meniscus-bone. Hence, morphological analysis was undertaken and compared to histology to

determine structures. MR images of native meniscus displayed a branched network of structures emanating from the PMCP and terminating in the white zone. These structures appeared to resemble those seen with collagen IV staining of native menisci, with large branches appearing from the red zone and terminating in the white zone. Menisci were obtained from skeletally immature pigs (~ 6 months old) and this explains the vascularised meniscus present on the MR images and collagen IV staining. MR signal intensity is dependent on numerous factors but mainly proton density. In collagenous samples, signal intensity is affected by fibre orientation and hydration. Blood vessels contain proportionally more water than ECM due to the presence of blood and high cellularity of the endothelial layer and perivascular cells. It is suggested that the loss of these cells from decellularised menisci and hence equilibration of the water to the surrounding matrix resulted in the loss of these structures from MR images of decellularised menisci. Positive staining in histological images of decellularised menisci also discouraged the notion that these structures may have been radial tie fibres. MRI of bone revealed retention of major architecture however structures were more clearly displayed on decellularised bone samples. This may have been due to improved hydration of decellularised samples with residual PBS post-decellularisation. Images of native bone contained areas of poor signal possibly owing to localised dehydration or interference from marrow. Cartilage present on the tibial surface also appeared rough which may be have been due to degradation and shrinkage over the extended scan time as samples were not fixed.

Characterisation of decellularised meniscus revealed retention of geometry and structure. Major collagens in both meniscus and bone were retained but collagen IV was completely removed. A complete loss of GAGs was also seen with meniscus and bone maintaining thermal stability except for in the attachment region. The impact of these compositional changes on the biomechanical properties and biocompatibility of bone-meniscus-bone are described in the next chapter.

# Chapter 5.    Assessment of the biocompatibility and function of decellularised porcine bone-meniscus-bone

## 5.1    Introduction

The previous chapter described compositional changes to porcine bone-meniscus-bone as a result of the decellularisation process. It was important to investigate whether any changes to the extracellular matrix of the porcine bone-meniscus-bone had any impact on the biomechanical properties and biocompatibility of the tissue which would potentially influence the *in vivo* function of decellularised bone-meniscus-bone. The meniscus plays a critical role in knee joint mechanical stability through the transmission of load, shock absorption and lubrication. Therefore, the ability of decellularised bone-meniscus-bone to provide these functions comparably to native meniscus will be paramount to future clinical translation. Decellularised menisci have been shown to maintain mechanical properties (Maier *et al.*, 2007; Stapleton *et al.*, 2008; Sandmann *et al.*, 2009; Azhim *et al.*, 2013) however other tissues have displayed changes in stiffness post-decellularisation (Liao *et al.*, 2008; Williams *et al.*, 2009).

It was also important to determine whether the decellularised bone-meniscus-bone was biocompatible, in particular as SDS was utilised in the decellularisation protocol, verification of its removal during the wash procedures was important since SDS has been shown to be cytotoxic to cells and prevent cell attachment and infiltration into tissues (Kasimir et al., 2003; Rieder et al., 2004). Pig to primate organ transplantation can result in hyperacute rejection (Galili *et al.*, 1997; McPherson *et al.*, 2000) as lower mammals have the Galactosyl-α(1,3)galactose (α-gal) epitope present on cell membranes. Large titres of anti- α-gal are produced by humans and these cause thrombosis via complement-mediated hyperacute rejection. Incomplete decellularisation can lead to hyperacute rejection (Raeder *et al.,* 2002; Kasimir *et al.,* 2005).

## 5.2   Aims and Objectives

### 5.2.1  Aims

The aim of the work presented in this chapter was to investigate the biocompatibility and material properties of the decellularised porcine bone-meniscus bone.

### 5.2.2  Objectives

- To determine material properties of native and decellularised bone-meniscus-bone using indentation, tensile, and compression tests
- To assess the potential cytotoxicity imparted by decellularised bone-meniscus-bone and by residual soluble components
- To quantify any SDS remaining within decellularised bone-meniscus-bone post-decellularisation

## 5.3  Materials and Methods

### 5.3.1  Experimental approach

To complete the studies described in this chapter it was necessary to dissect and decellularise a further 16 porcine bone-meniscus-bone samples. These were utilised as indicated below. It was also necessary to dissect a further 9 bone-meniscus bone samples for biomechanical testing of fresh tissue. Six of these were used for indentation testing of the meniscus and compression testing of the bone and three for tensile testing.

- Six porcine bone-meniscus bone samples were decellularised using the method described in Chapter (3) Section 3.3.1.5. These were then utilised for indentation testing of the meniscus tissue (n=6) and for compressive testing of the bone blocks (n=6).  Decellularised bone-meniscus-bone was stored on PBS-soaked filter paper at -20 °C prior to testing.

- Three porcine bone-meniscus-bone samples were decellularised using the method described in Chapter (3) Section 3.3.1.5. Decellularised bone-meniscus-bone was stored on PBS-soaked filter paper at -20 °C prior to testing.  These samples were utilised for tensile testing of the meniscus tissue.  Due to the nature of the sampling method, it was not possible to obtain meniscus tissue for both indentation and tensile testing from the same samples.

- Three porcine bone-meniscus-bone samples were prepared aseptically for in vitro cytotoxicity assays. The samples were decellularised as described in Chapter (3) Section 3.3.1.5 with the exception that all steps after PAA sterilisation were undertaken in a Class II safety cabinet using sterile reagents.  Decellularised bone-meniscus-bone was then stored in sterile containers at -20 °C until testing.

- Four porcine bone-meniscus-bone samples were decellularised for quantification of residual SDS. These samples were processed

separately since it was necessary to utilise $^{14}$C radio-labelled SDS in the decellularisation process

## 5.3.2 **Mechanical testing of bone-meniscus-bone**

### 5.3.2.1 Indentation of meniscus

Indentation testing was carried out on a custom designed indentation rig to assess the behaviour of native and decellularised porcine meniscus in unconfined compression. Samples of meniscus (n = 6) 6 mm in diameter and 1.5 mm thickness were obtained from the middle region of menisci using a biopsy punch and loaded using a flat indenter (diameter = 2.5 mm; load = 0.22 N) over the course of an hour. Samples were attached to the base of the sample holder using cyanoacrylate glue to prevent slipping and submerged in PBS at room temperature to maintain hydration. The sample holder was then raised until the indenter tip was <1 mm above the sample and the indenter lowered to contact the sample. An oil-filled dashpot reduced the speed of the indenter shaft and hence the initial impact. Deformation was measured using a linear variable differential transducer (LVDT) and the force measured by a piezo-electric force transformer. Data was collected using Lab View 8 software. The experimental set up is shown in Figure 5.3.1. Displacement values were converted to deformation using the sample height with the deformation at various time points arcsine transformed prior to statistical analysis and back transformed prior to presentation.

The LVDT was calibrated using a series of standard stainless steel step heights placed under the indenter and the measured voltage used to create a standard curve. Linear regression was then performed to obtain the calibration factor (Figure 5.3.2). The force transducer was calibrated by loading known masses incrementally and noting the subsequent voltage readings. Linear regression was performed to convert voltage to Newtons (Figure 5.3.3). Displacement values were converted from LVDT readings

and converted to percentage deformation using the sample height. Percentage deformation was arcsine transformed for statistical analysis.
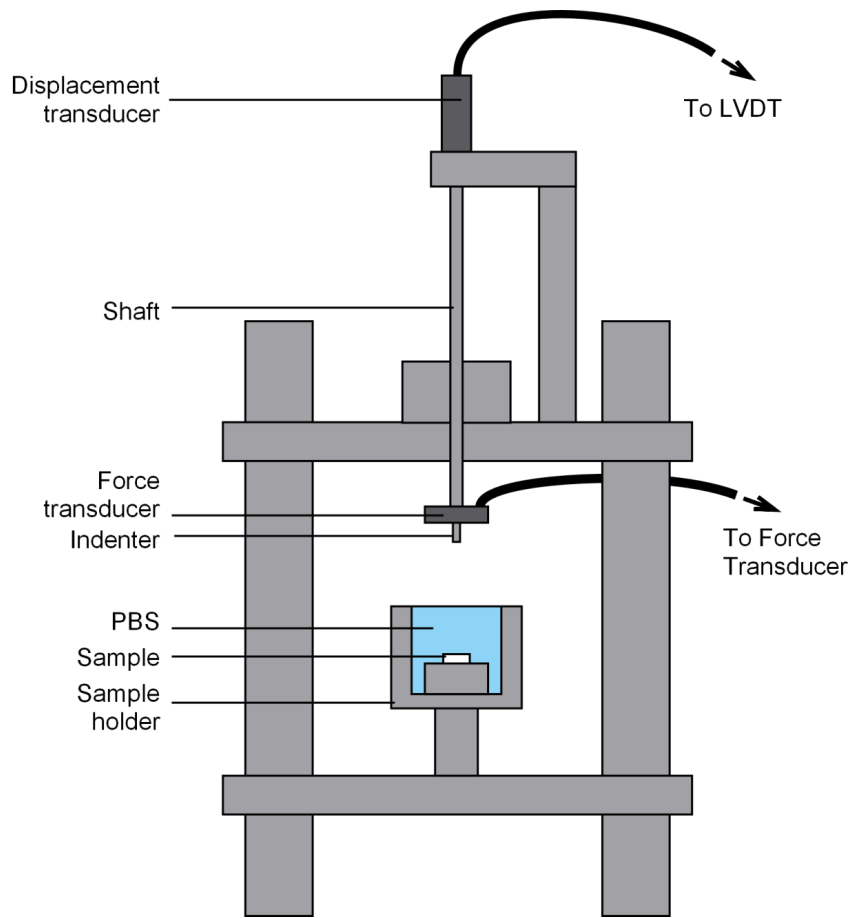


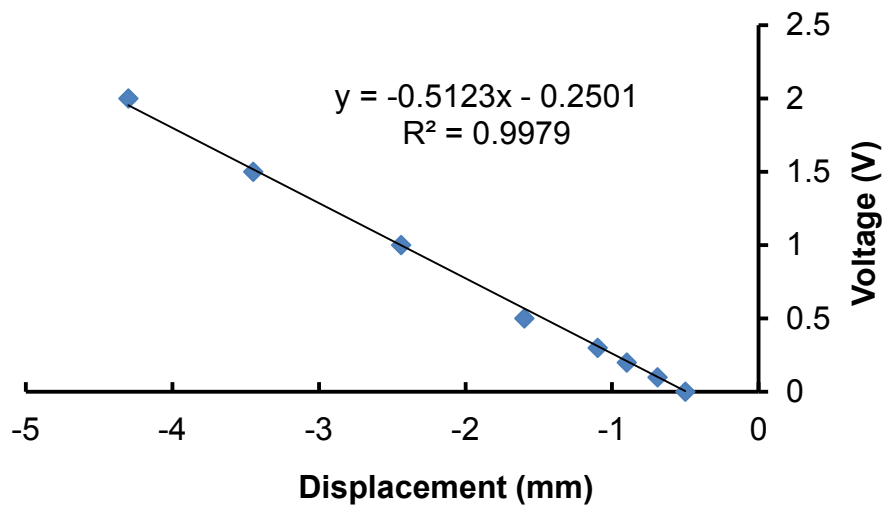**Figure 5.3.1: Indentation apparatus and experimental set up**



**Figure 5.3.2: An example calibration of the LVDT**
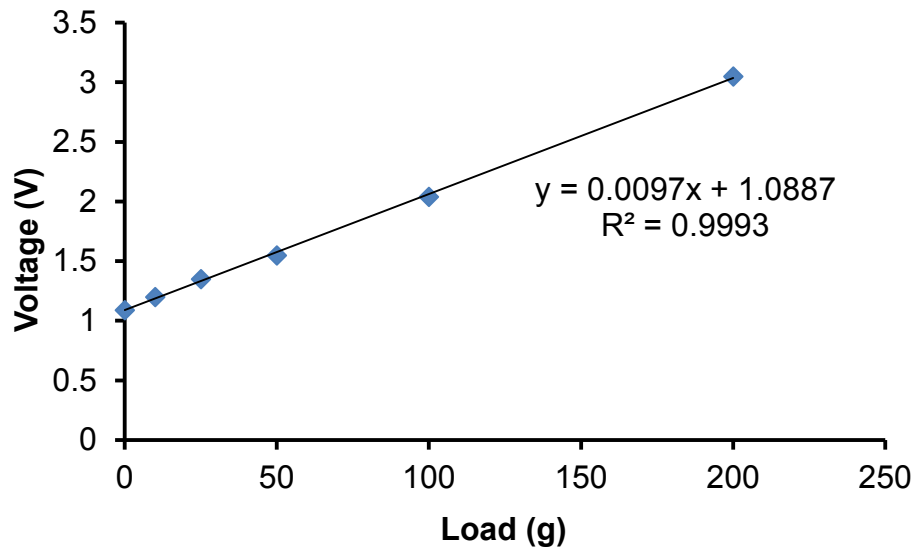
$$y = 0.0097x + 1.0887$$
$$R^2 = 0.9993$$

**Figure 5.3.3: An example calibration of the force transducer**

## 5.3.2.2    Finite element modelling

Deformation curves generated using the method described in Section 5.3.2.1 were used to obtain the aggregate modulus of native and decellularised porcine meniscus using a finite element model. The aggregate modulus is a measure of the stiffness of a material at equilibrium once all fluid has ceased to flow from within it. High values denote stiffer materials, and vice versa. The aggregate modulus can be determined via confined compression employing a porous indenter to allow flow of fluid out of the tissue or via unconfined compression using a non-porous indenter as fluid flow is not restricted. The aggregate modulus of porcine meniscus has been determined using creep indentation apparatus and ranged from 0.13 to 0.27 MPa depending on sample location (Sweigart *et al.*, 2004). The model employed in this study was developed by Mow *et al.* (1989) for derivation of the material properties of cartilage. Assumptions made by the model include that cartilage is an isotropic, homogeneous material and conditions of infinitesimal strain and a frictionless indenter tip were also set.

### 5.3.2.3    Tensile testing of meniscus

Uniaxial tensile testing of native and decellularised porcine meniscus (n = 3) was undertaken to compare their material properties under tension.  Initial testing on meniscus was carried out on straight specimens measuring 3 mm in width to negate the impact of matrix heterogeneity (McDermott *et al.*, 2008a).  This proved unsuccessful as failure occurred at the grips where the sample was weakened due to the force required to tighten the grips in order to prevent the sample from slipping.  Tissue paper was used between the grips and sample to reduce the contact force exerted on the sample by the grip teeth.  This resulted in successful testing of some native samples with failure occurring in the gauge length however consistency could not be achieved.   This   method   was   also   unsuccessful   when   used   with decellularised meniscus with samples slipping or failing at the grips once again.  Hence, it was decided to proceed using dumbbell shaped samples in order to reduce the force required to achieve failure and prevent the sample slipping through wider distribution of pressure at the grip.  Cross-sections of meniscus ~ 1 mm thick were obtained using a specially designed cutter employing two one-sided blades (Figure 5.3.4).  This cross-section was then placed onto a cold block and another cutter used in conjunction with a lever press to obtain dumbbell shaped samples for testing (Figure 5.3.5).  Sample widths were 1 mm with gauge lengths of 5 mm.  Samples were then placed in custom grips (Figure 5.3.6 and Figure 5.3.7) with tissue paper to prevent slipping and alignment of the sample.  A pre-load of 0.02 N was applied to ensure the gauge length was maintained and samples tested to failure on an Instron 3365 at a strain rate of 0.02.  Data were collected using Bluehill 3 software. Raw data was exported from BlueHill 3 software to Microsoft Excel 2007 for analysis and derivation of engineering stress ($\sigma$) and engineering strain ($\varepsilon$) for each run.   The applied force was put into the following calculation to determine stress:

$$\sigma_{eng} = \frac{F}{A}$$

where, F is the applied force and A is the cross-sectional area of the specimen in mm$^2$. A Poisson's ratio of zero was set as changes to the sample cross-sectional area during loading were assumed to be negligible. The measured extension of the sample from the original length was used to calculate the strain:

$$\varepsilon_{eng} = \frac{\Delta L}{L}$$

where, $\Delta L$ is the extension of the specimen in mm, and L is the specimen length (~5 mm) after the application of the pre-load (0.02 N). The material properties that were derived from the stress-strain data were the tensile modulus, the ultimate tensile strength (UTS), and the failure strain. Data presented are averages of n = 3 (± 95% C.I.) specimens and statistical analysis was performed using student's t-test.
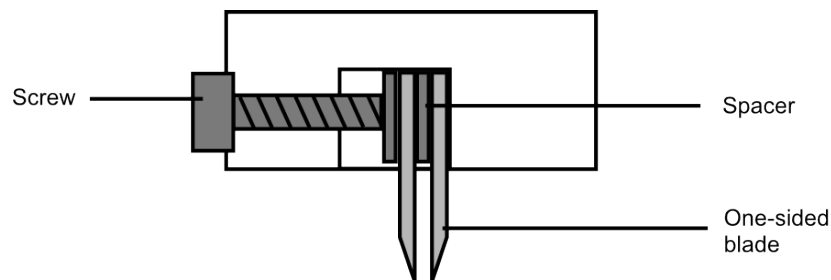


**Figure 5.3.4: Cutting device used to obtain cross-sections of porcine meniscus for tensile testing**
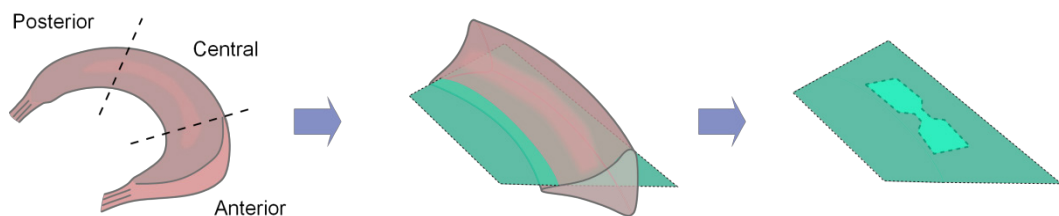


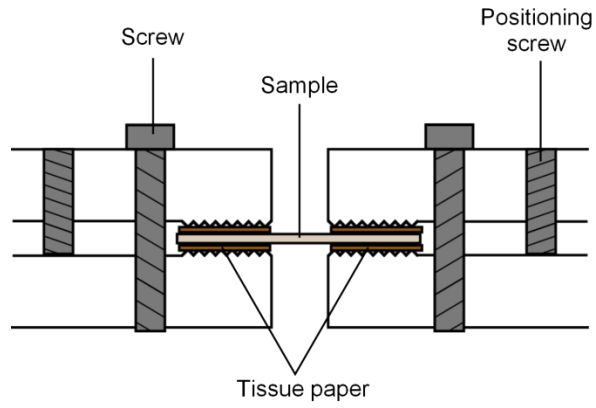**Figure 5.3.5: Method for obtaining dumbbell shaped samples of porcine meniscus for tensile testing**

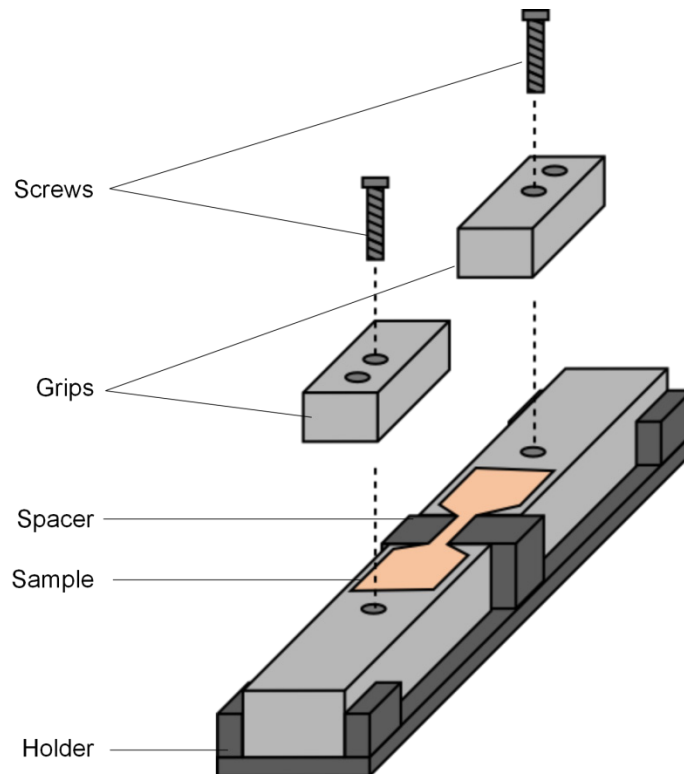**Figure 5.3.6: Cross-section of grips displaying positioning of sample**



**Figure 5.3.7:  Custom grips used for tensile testing of porcine meniscus**

### 5.3.2.4　Compression of bone

Native and decellularised bone was tested to failure under unconfined compression to determine material properties. Cylinders (diameter = ~6.5 mm, height = ~5.5 mm) of bone (n = 6) were obtained from each block using a metal corer and electrical drill (Figure 5.3.8). Cartilage was removed from the bone plugs using a scalpel and bone plugs were then attached to the sample holder (Figure 5.3.9) using cyanoacrylate glue to prevent slipping. Samples were then compressed at a rate of $0.01$ s$^{-1}$ until failure on an Instron 3365. Data were collected using Bluehill 3 software. BlueHill 3 software was used to determine engineering stress ($\sigma$) and strain ($\varepsilon$) for each run as well as ultimate compressive strength and compressive modulus.

The material properties that were derived from the stress-strain data were the ultimate compressive strength (UTS), and the failure strain (). Data presented are averages of n = 6 (± 95% C.I.) specimens and statistical analysis was performed using student's t-test.
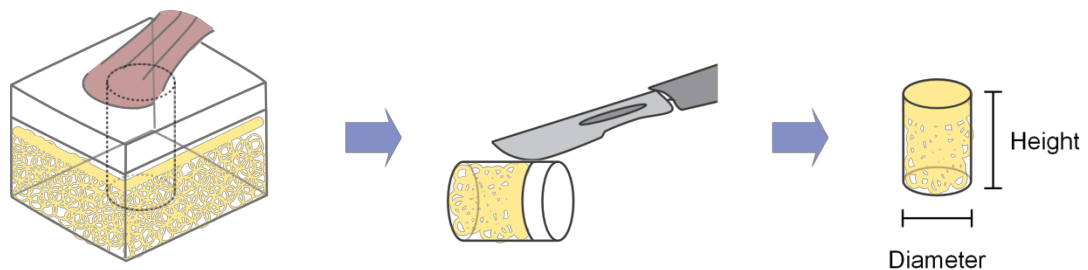


**Figure 5.3.8: Method for obtaining samples for unconfined compression**
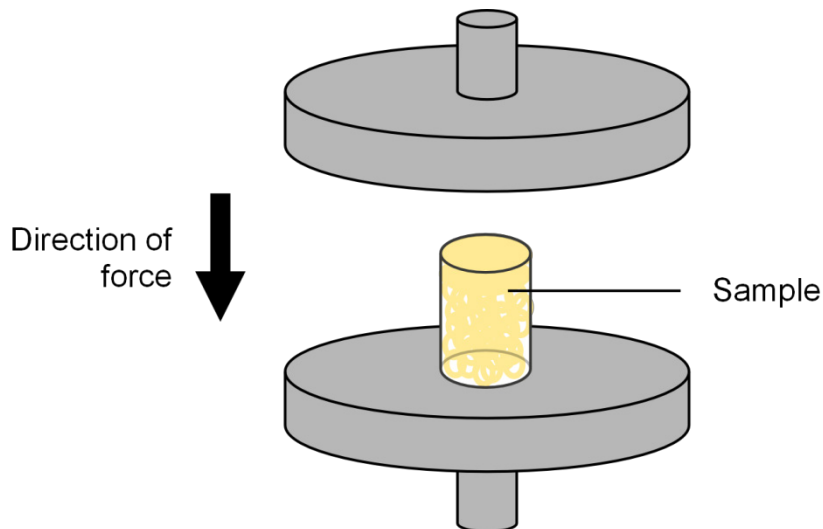
**Figure 5.3.9: Experimental set up for unconfined compression testing of bone**

### 5.3.3 Cytotoxicity assays

#### 5.3.3.1 Contact cytotoxicity assay

Cytotoxicity occurring from decellularised bone-meniscus-bone components was assessed using a contact cytotoxicity assay. Using aseptic technique in a class II safety cabinet, samples (n = 3) of decellularised meniscus and bone from the white, red/red-white, attachment and bone measuring ~5 mm x 5 mm x 1 mm were attached to 6-well tissue culture treated plates using a single steri strip (3M, Minnesota, US). Samples were then washed three times with sterile PBS containing calcium and magnesium and seeded with BHK and 3T3 cells (Section 2.1.3) to achieve confluence after 48 hours. The positive control used in this study was cyanoacrylate glue (n = 3) and the negative controls were either tissue culture plastic alone or a steri strip (n = 3). Following incubation, the culture medium was aspirated and the wells washed with sterile PBS containing calcium and magnesium. Cells were then fixed using 10% (v/v) NBF for 10 minutes and stained using 2 mL of Giemsa solution for 5 minutes. The stain was washed away by repeatedly rinsing using distilled water after which plates were allowed to air dry for 3 hours and visualised under light microscopy.

## 5.3.3.2    Extract cytotoxicity assay

Potentially cytotoxicity from compounds leaching out of decellularised meniscus was investigated using an extract cytotoxicity assay.   Using aseptic technique in a Class II safety cabinet, decellularised bone and meniscus was cut into ~1 mm$^3$ pieces using a scalpel and weighed.  DMEM (3 mL.mg$^{-1}$) was added to bone and meniscus and the samples were incubated at 37 °C for 72 hours with agitation.   Samples were then centrifuged at 500 g for 15 minutes and the supernatant retained for assay. A sterility check was performed by streaking extracts onto agar plates (nutrient, fresh blood and Sabauroud) and incubating nutrient and fresh blood plates at 37 °C and Sabauroud plates at 27 °C in an incubator.  Plates were checked for colonies after 48 hours.  BHK and 3T3 cells were seeded onto 96-well tissue culture treated plates at a concentration deemed suitable to yield confluency after 24 hours.  Once cells had attached (~3 hours) the medium was aspirated and 100 µL cell culture medium containing double strength FBS (DMEM, 20% (v/v) FBS, 200 µg.L$^{-1}$ penicillin, 200 U.mL$^{-1}$ streptomycin, and 2 mM L-Glutamine) was added to each well followed by 100 µL of test extract and plates incubated at 37 °C in an atmosphere of 5% (v/v) $CO_2$ in air for 24 hours.  Controls utilised in this study were 40% (v/v) DMSO in DMEM (positive) and DMEM alone (negative).   Following incubation an ATPLite-M assay was performed to determine cellular adenosine triphosphate content (Section 5.3.3.3).

## 5.3.3.3    ATPLite-M assay

Reagents (Section 2.1.2) were allowed to equilibrate to room temperature prior to use.  The culture medium was aspirated from wells and fresh DMEM (100 µL) and cell lysis solution (50 µL) were added.  The plate was shaken at 700 rpm for two minutes on a plate shaker at room temperature after which the contents of each well were transferred to corresponding wells of a 96-well Optiplate.  Substrate solution (50 µl) was added to each well and the plate shaken for a further five minutes at 700 rpm.  Optiplates were then placed into Top Count, allowed to equilibrate to the dark for 10 minutes prior

to measurement of the luminescence. Data was recorded in counts per second.

### 5.3.4 Detection of α-gal epitope on porcine meniscus

Native and decellularised meniscus (n = 3) were prepared for immunohistochemistry as described in Sections 2.2.3.1, 2.2.4.1-2.2.4.3. Sections of meniscus were then incubated using anti-α-gal antibody, no antibody (negative control) or an isotype control antibody to detect non-specific staining (Section 2.2.7). Once the secondary antibody had been applied and colouration reaction had been terminated, sections were dehydrated and mounted (Section 2.2.4.4) for visualisation using light microscopy.

### 5.3.5 Determination of residual SDS

Decellularised bone-meniscus-bone was tested for residual SDS using $^{14}$C radio-labelled SDS. Reagents containing SDS in the decellularisation protocol were spiked with 5 µCi of $^{14}$C radio-labelled SDS and used during decellularisation of bone-meniscus-bone. During decellularisation, the solutions obtained at the end of each stage of the process were collected and assayed for SDS as described below.

After the decellularisation was complete the bone-mensicus-bone was collected and separated into white, red-white, attachment, and bone regions. Tissue from each region was cut into ~1 mm$^3$ pieces and 40 mg (n = 4) placed into a well of a 96-well Optiplate. To this, 200 µL of micro-scint 20 was added and the plate was read for 20 minutes using Top Count. Samples of decellularisation solution were read in the same way with 40 µL of sample (n = 4) and 160 µL of micro-scint used. A standard curve of 0, 50, 100, 200, 500 and 1000 µg.mL$^{-1}$ of $^{14}$C spiked SDS was produced and linear regression performed to obtain the concentration of SDS in each sample. Values obtained for the tissues were then converted to absolute weights of SDS per weight of tissue.

## 5.4   Results

### 5.4.1  **Mechanical testing**

#### 5.4.1.1    Indentation testing of meniscus

The deformation of meniscus under applied load was assessed using indentation testing.  The deformation of native and decellularised meniscus under load over one hour is shown in Figure 5.4.1.  Native meniscus deformed gradually up to a peak deformation of ~22% after one hour, whereas the initial deformation of decellularised meniscus was more rapid and reached a higher value, ~33%, after one hour.  From these curves it was possible to obtain the aggregate modulus (Figure 5.4.2), a measure of the material's stiffness, using a finite element model developed at the University of Leeds.  Modelling was carried out by Dr. Abdellatif Abdelgaied (iMBE, University of Leeds).  This resulted in an aggregate modulus of 0.123 MPa for native meniscus and 0.100 MPa for decellularised meniscus.  The values obtained were not significantly different ($p > 0.05$).



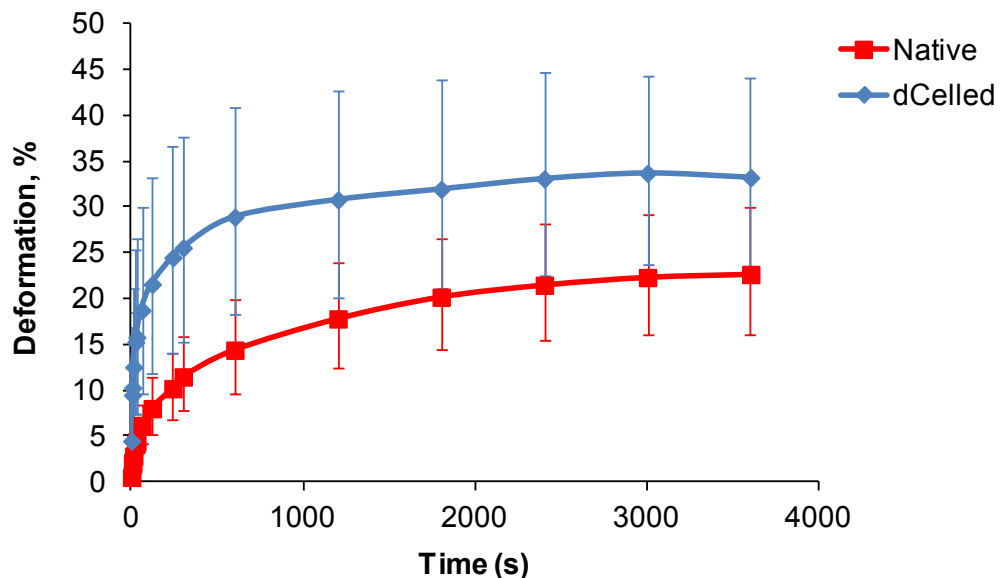**Figure 5.4.1:  Deformation of native and decellularised meniscus over time.**  Data presented as mean (n = 6) ± 95% C.I.   The data was arc sine transformed and analysed using a two-way ANOVA which revealed a significant difference ($p < 0.01$).
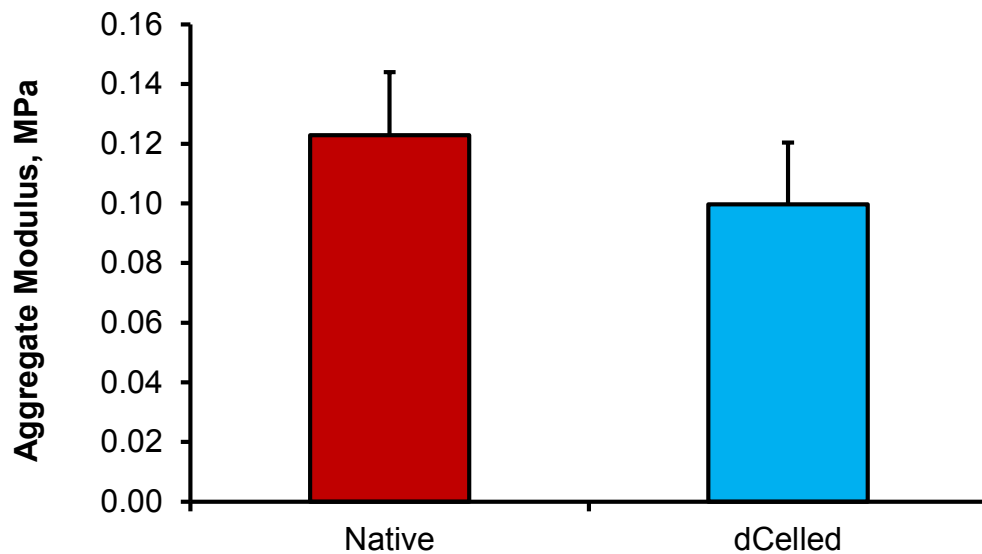
**Figure 5.4.2:** **Aggregate modulus of native and decellularised meniscus obtained using finite element modelling.** The data is presented as the mean (n = 6) ± 95% CI. The data was analysed using students t-test which revealed no significant difference (p = 0.061).

### 5.4.1.2 Tensile testing of meniscus

The material properties of native and decellularised meniscus under tension were investigated using uniaxial tensile testing. Dumbbell-shaped specimens were obtained from the red-white zone and tested to failure. Stress-strain behaviour of native meniscus is shown in Figure 5.4.3 and decellularised meniscus is shown in Figure 5.4.4. There was no significant difference between the tensile modulus, ultimate tensile strength and failure strain of native and decellularised meniscus. There was a decrease in the ultimate tensile strength of decellularised meniscus with an 18% drop from 70.2 MPa to 57.5 MPa however this was not significant (Figure 5.4.5). The tensile modulus was virtually identical between native and decellularised meniscus at 140.6 MPa and 139.6 MPa (Figure 5.4.5). The failure strain of native meniscus was 48% and for decellularised meniscus was 50% (Figure 5.4.6).
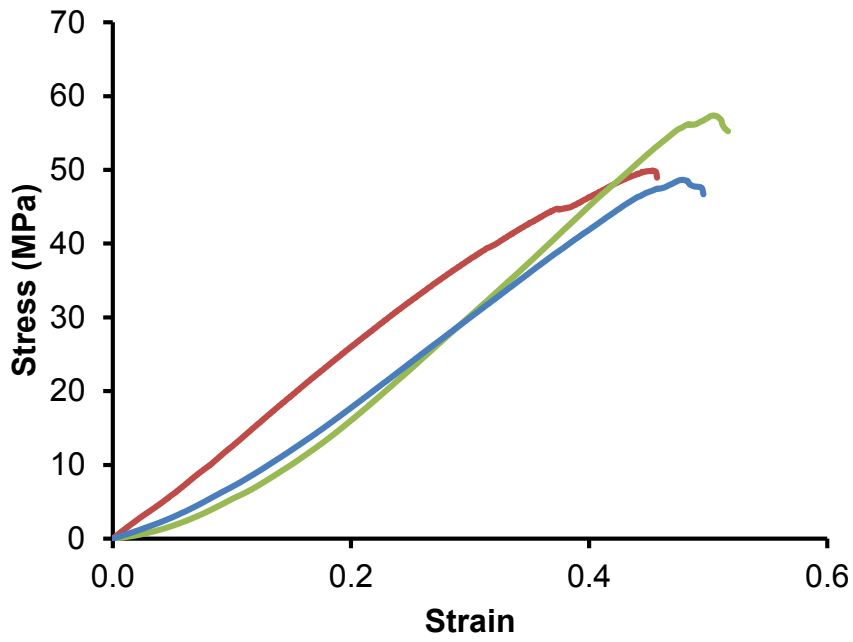
**Figure 5.4.3: Stress-strain behaviour of native meniscus under uniaxial tensile testing.** Each line represents an individual sample tested to failure.
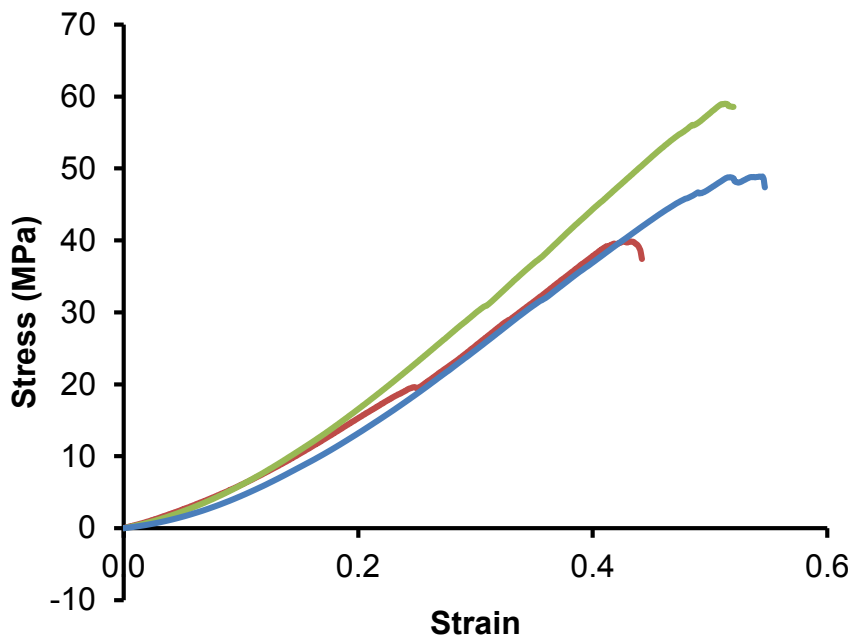


**Figure 5.4.4: Stress-strain behaviour of decellularised meniscus under uniaxial tensile testing.** Each line represents an individual sample tested to failure.
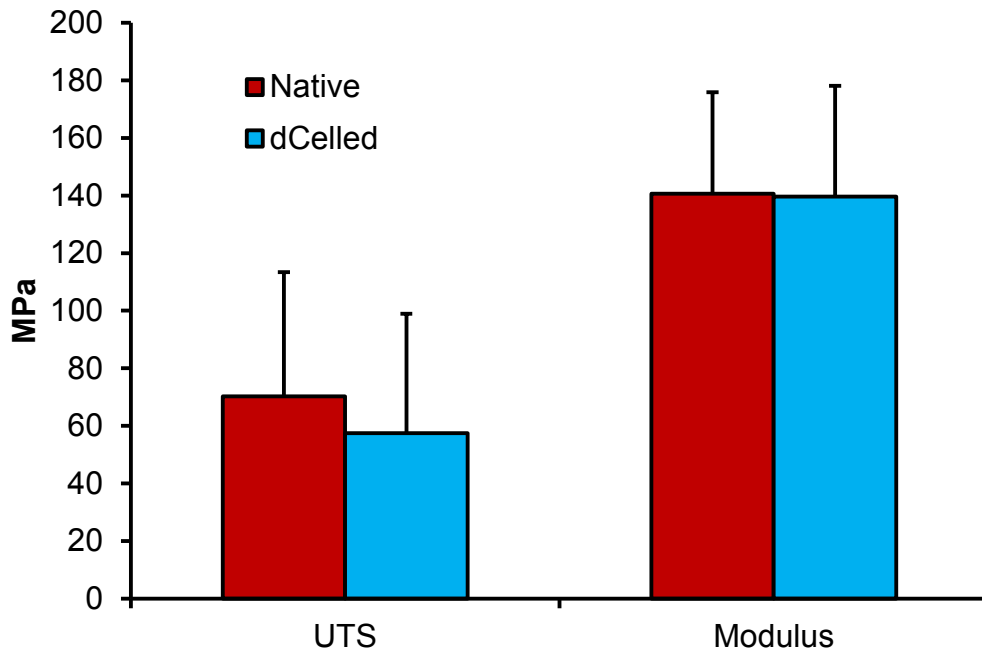
**Figure 5.4.5:** **Ultimate tensile strength (UTS) and tensile modulus of native and decellularised meniscus.** Data presented as mean (n = 3) ± 95% C.I. Statistical analysis performed using student's t-test (p > 0.05) which revealed no significant differences.
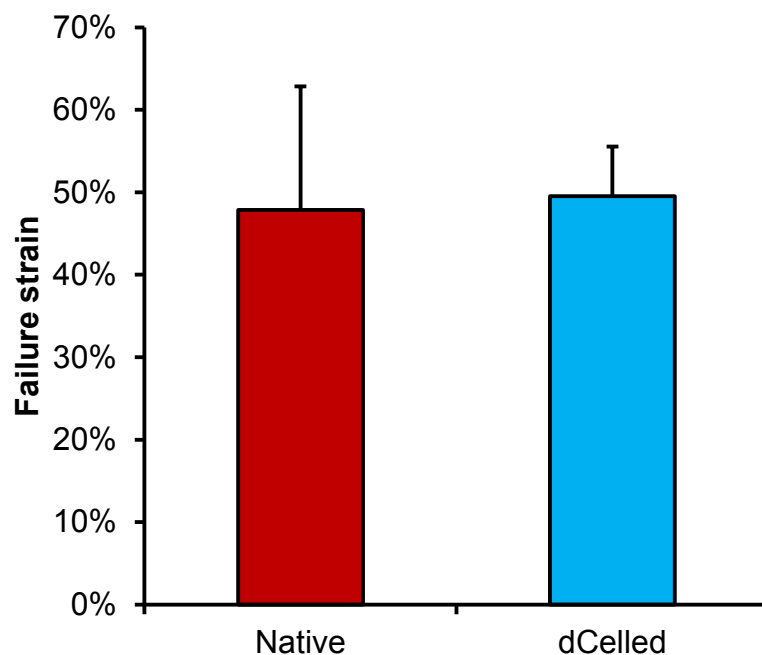


**Figure 5.4.6: Failure strain of native and decellularised meniscus.** Data presented as mean (n = 3) ± 95% C.I. Statistical analysis performed using student's t-test (p = 0.34) which revealed no significant differences.

5.4.1.3    Compression of bone

Native and decellularised bone was tested under unconfined compression to determine compressive strength. The yield point was clearly visible for native bone samples (Figure 5.4.7), however this was not true for decellularised bone where no obvious failure point was seen (Figure 5.4.8). Therefore, an offset of 0.02 was applied parallel to the elastic slope in order to obtain values for compressive load at yield and deformation at yield (Figure 5.4.9) as this value correlated well with the actual yield point for native samples. There was a significant difference between the mean compressive load at yield for native bone (Figure 5.4.10), which was 160.46 N (± 38.23 N, 95% C.I.), and decellularised bone which was 50.66 N (± 27.65 N, 95% C.I.). These values resulted in a mean compressive modulus of 103.0 MPa (± 26.4 MPa, 95% C.I.) for native porcine bone and 12.7 MPa (± 7.5 MPa, 95% C.I.) for decellularised porcine bone (Figure 5.4.11).
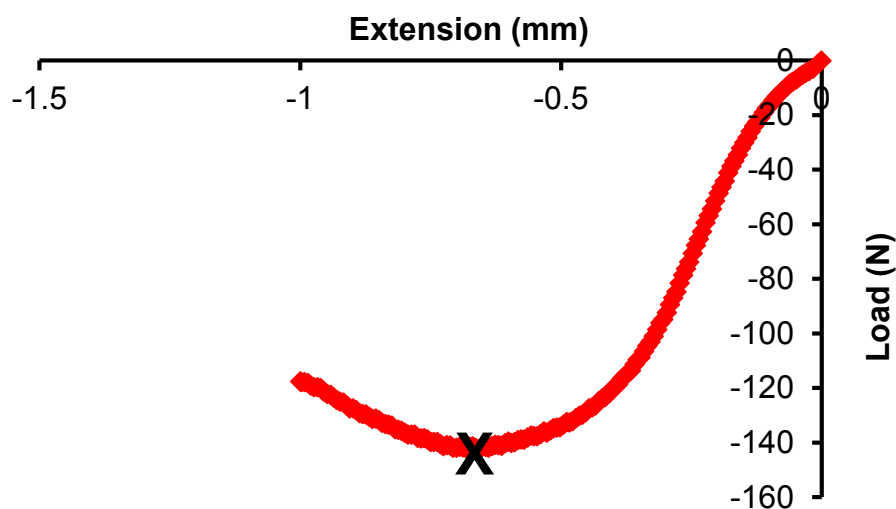


**Figure 5.4.7: Representative load-extension plot showing compression of native porcine bone at a strain rate of 0.01 s$^{-1}$.** Point where gradient is equal to zero signifies yield point (X).
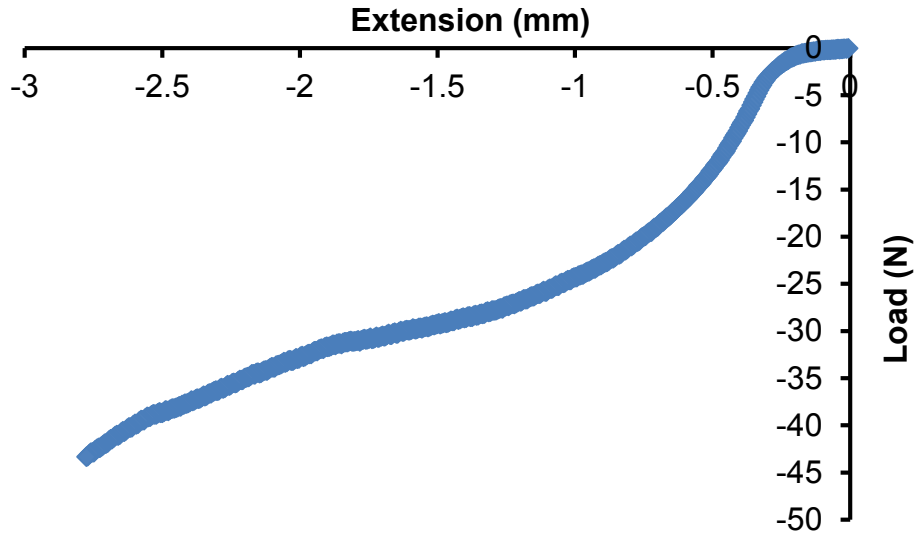
**Figure 5.4.8:** **Representative load-extension plot showing compression of decellularised porcine bone at a strain rate of 0.01 s$^{-1}$.** There is no point where the gradient is zero.
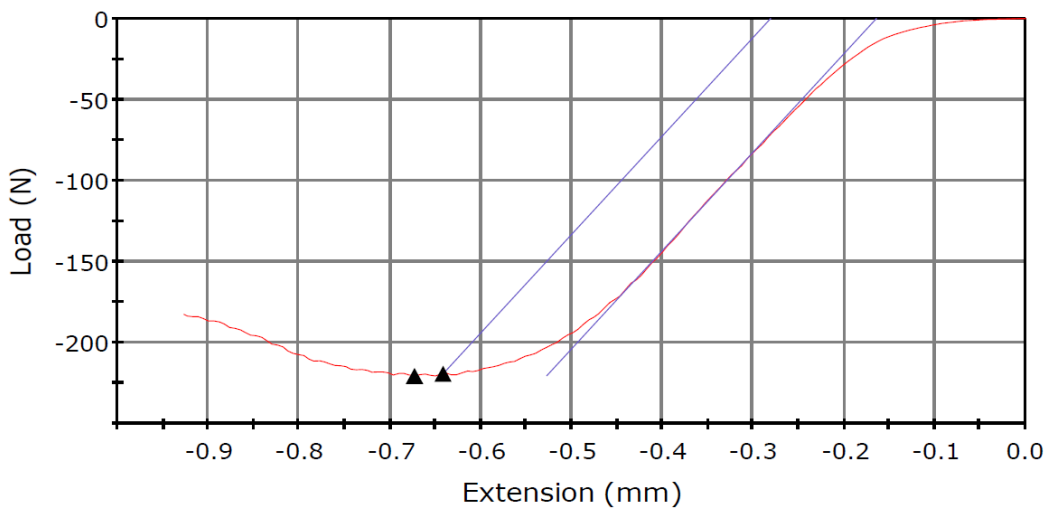


**Figure 5.4.9:** **Load-Extension plot displaying offset method used to obtain compressive load at yield.** The triangle on the left denotes actual yield point and the triangle on the right denotes the estimated yield point using an offset of 0.02% strain.
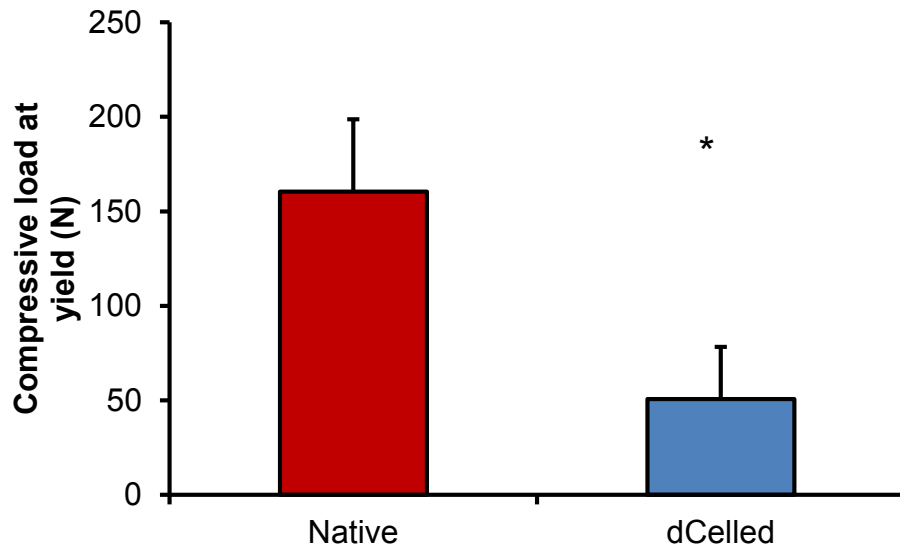
**Figure 5.4.10: Compressive load at yield of native and decellularised bone tested under unconfined compression at a strain rate of 0.01 s$^{-1}$.** Data presented as mean (n = 6) ± 95% C.I. Statistical analysis performed using student's t-test (* $p<0.05$).
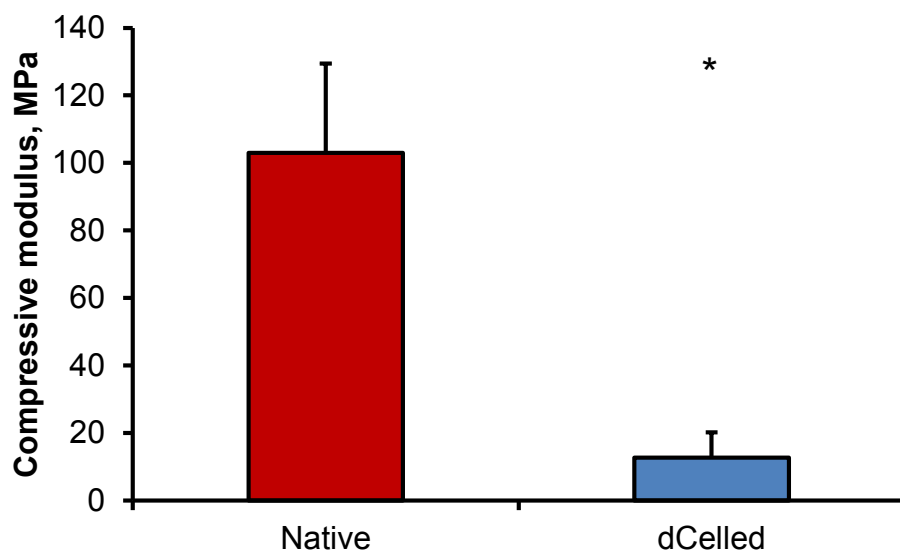


**Figure 5.4.11: Compressive modulus of native and decellularised bone tested under unconfined compression at a strain rate of 0.01 s$^{-1}$.** Data presented as mean (n = 6) ± 95% C.I. Statistical analysis performed using student's t-test (* $p<0.05$).

## 5.4.2 Cytotoxicity assays

### 5.4.2.1 Extract cytotoxicity

Extracts produced from the different regions of decellularised porcine bone-meniscus-bone were used to test the potential cytotoxicity of residual soluble components on 3T3 and BHK cells. The relative ATP content of cells is shown in Figure 5.4.12 and Figure 5.4.13. The positive control samples (cells cultured in DMSO) had significantly lower ATP contents compared to the negative control for both cell types. There was no significant difference observed between the cellular ATP content of cells cultured in extracts from all other regions when compared to their negative control of cells cultured in medium alone ($p > 0.05$).
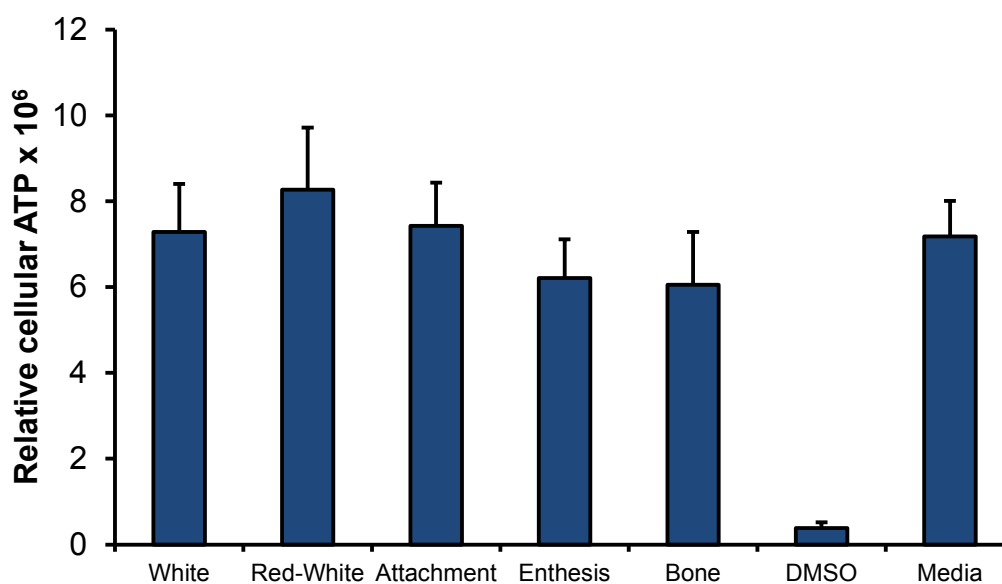


**Figure 5.4.12: Relative cellular ATP content of BHK cells cultured in extracts from different regions of decellularised porcine bone-meniscus-bone.** Data presented as mean ± 95% C.I. (n = 3). Data was analysed using one way ANOVA ($p > 0.05$ when compared to Media only controls).
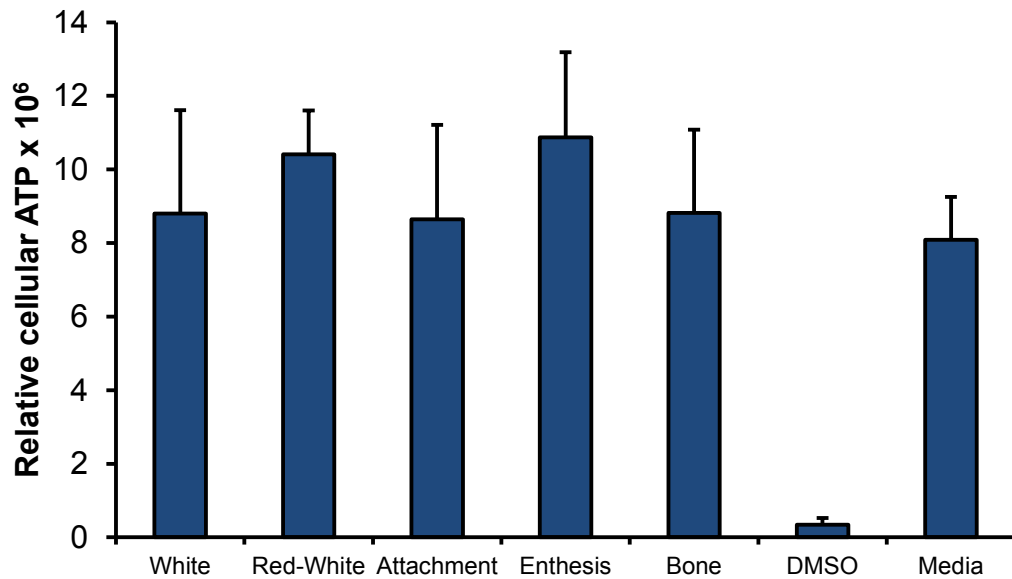
**Figure 5.4.13: Relative cellular ATP content of 3T3 cells cultured in extracts from different regions of decellularised porcine bone-meniscus-bone.** Data presented as mean ± 95% C.I. (n = 3). Data was analysed using one way ANOVA ($p > 0.05$ when compared to Media only controls).

## 5.4.2.2    Contact cytotoxicity

Potential cytotoxicity from insoluble components of decellularised porcine bone-meniscus-bone was assessed by culturing cells directly in contact with samples of decellularised bone-meniscus-bone. Controls (Figure 5.4.14) utilised in this study were tissue culture plastic alone (negative), a steri strip (negative), and cyanoacrylate glue (positive for cytotoxicity). Both BHK and 3T3 cells were seen to grow up to and in contact with steri strips (Figure 5.4.14 A and C), however for cyanoacrylate glue a clear boundary was visible surrounding the glue where cells did not grow (Figure 5.4.14 B and D). Cells grew normally on tissue culture plastic. Images of Giemsa stained 3T3 and BHK cells (Figure 5.4.15) showed that both cell lines grew up to and in contact with samples taken from all regions of decellularised bone-meniscus-bone.
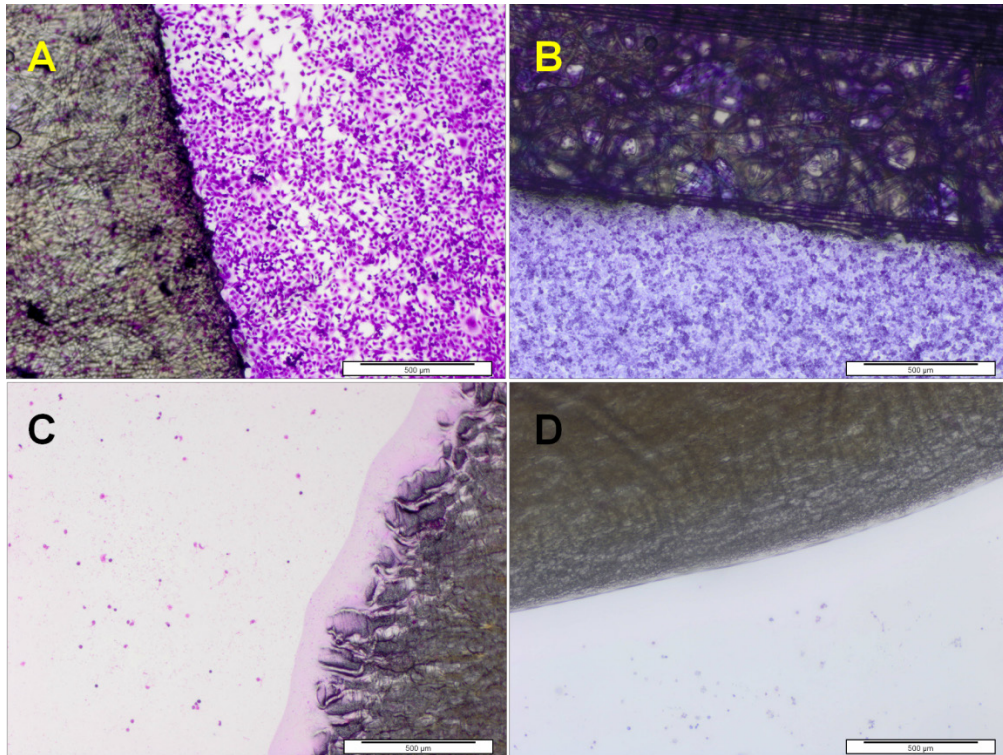
**Figure 5.4.14: Controls used for contact cytotoxicity study stained using Giemsa.** A) 3T3 cells in contact with steri strip, B) BHK cells in contact with steri strip, C) 3T3 cells in contact with cyanoacrylate glue, D) BHK cells in contact with cyanoacrylate glue. Representative images from n = 3, 40x magnification.

## 5.4.3 Detection of α-gal epitope on porcine meniscus

Controls showed no positive staining, verifying specificity of the antibody (Appendix A). Staining of native meniscus revealed positive staining localised to the vasculature, specifically the vascular cells (Figure 5.4.16 A, C, E and G). Positive colouration could be seen in the red, superficial and red-white zone; however no staining was detected in the white zone. Decellularised meniscus displayed no positive staining throughout the entire tissue (Figure 5.4.16 B, D, F and H).
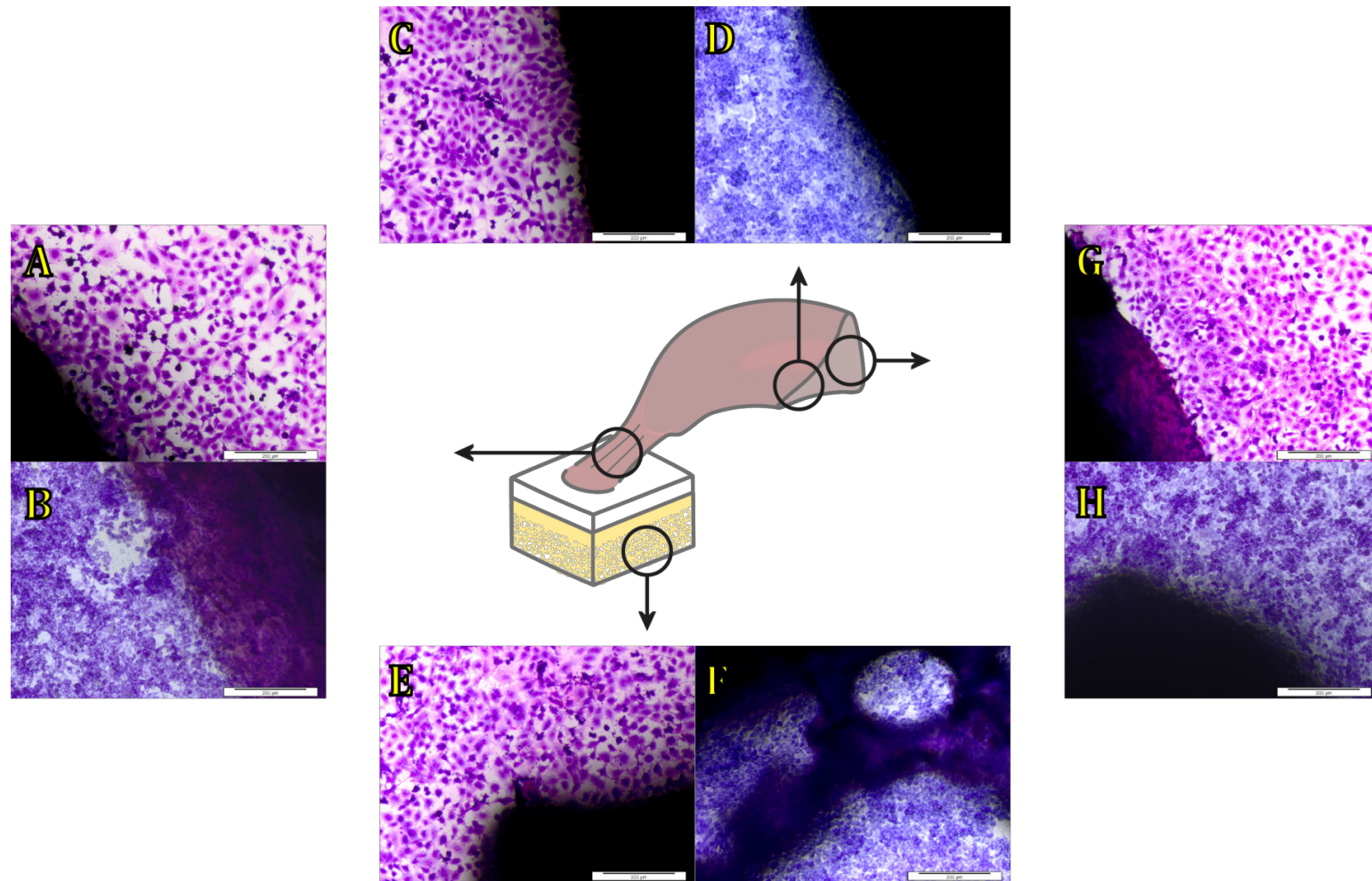
**Figure 5.4.15: Contact cytotoxicity assay using 3T3 and BHK cells stained with Giemsa.** A) 3T3 cells in contact with attachment, B) BHK cells in contact with attachment, C) 3T3 cells in contact with white meniscus, D) BHK cells in contact with white meniscus, E) 3T3 cells in contact with bone, F) BHK cells in contact with bone, G) 3T3 cells in contact with red-white meniscus, H) BHK cells in contact with red-white meniscus. Images representative of n = 3 bone-meniscus-bone. Magnification 100x unless stated.
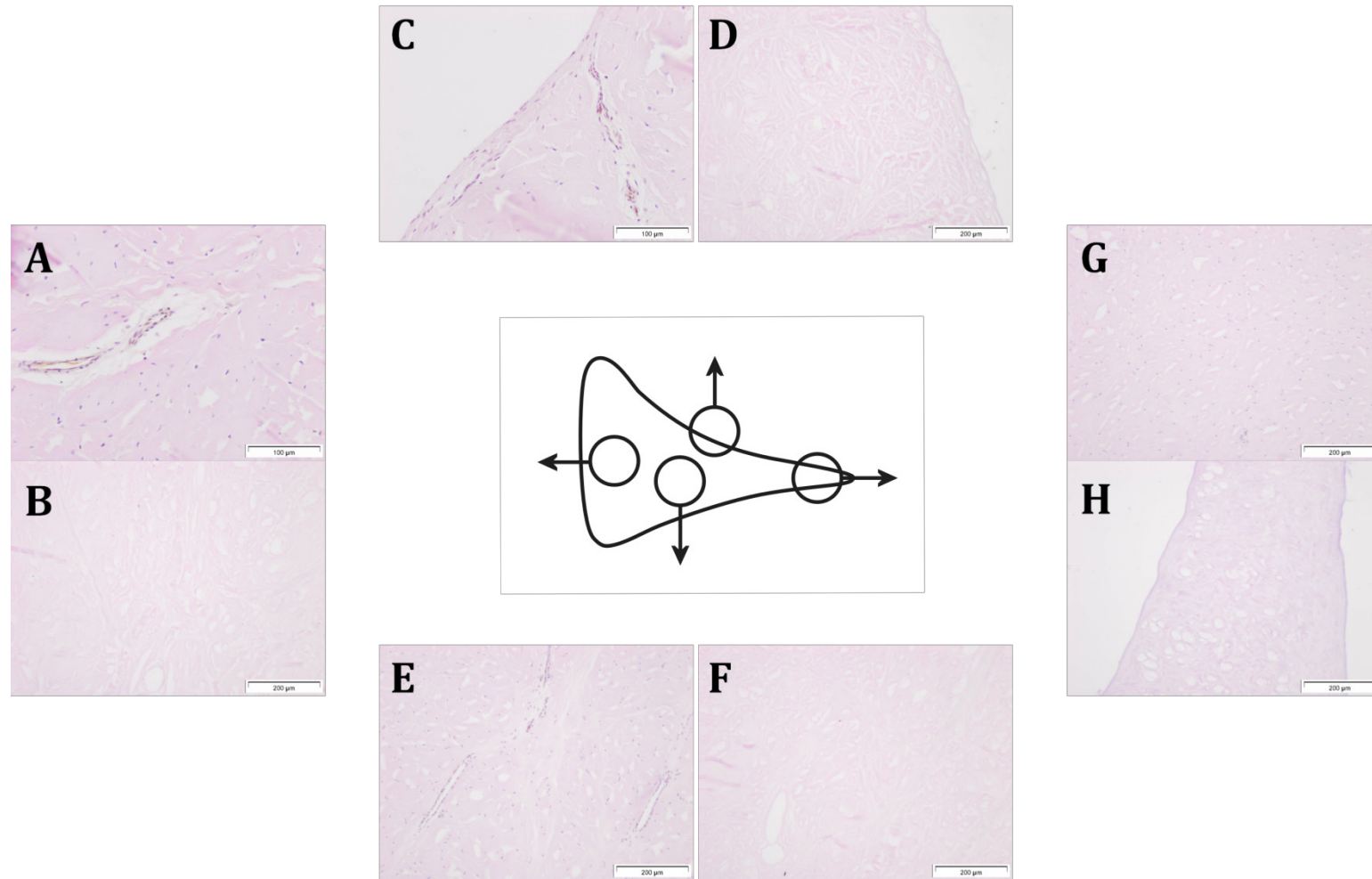
**Figure 5.4.16: Immunohistochemical staining of radial sections of native and decellularised meniscus using antibody against α-gal.** A) Native meniscus red zone B) Decellularised meniscus red zone C) Native meniscus superior surface D) Decellularised meniscus superior surface E) Native meniscus red-white zone F) Decellularised meniscus red-white zone G) Native meniscus white zone H) Decellularised meniscus white zone. Magnification 100x unless stated. Images are representative of the results obtained from n = 3 menisci.

### 5.4.4 Determination of residual SDS in decellularisation solutions and decellularised tissues

The residual SDS content of decellularised bone-meniscus-bone was assessed using $^{14}$C radio-labelled SDS. There was a linear relationship between the concentrations of $^{14}$C radio-labelled SDS used as standards and the counts per minute (Figure 5.4.17), as well as between the absolute SDS weights and the counts per minute (Figure 5.4.18). Determination of SDS in decellularisation process reagents (Figure 5.4.19) showed the highest concentration of SDS was present in the final SDS wash which was 975 µg.mL$^{-1}$ (0.0975% w/v). Since the initial concentration of SDS in this solution was 0.1% w/v, this suggested that some SDS had remained within the bone-meniscus-bone. The SDS concentrations in subsequent solutions from the process showed a gradual decrease as decellularisation progressed, with the final PBS step displaying no SDS content, or possibly falling under the detection limit of the assay. Residual SDS content of decellularised porcine bone-meniscus-bone (Figure 5.4.20) was very low with the attachment and bone displaying slightly higher concentrations of 0.34 µg.mg$^{-1}$ and 0.32 µg.mg$^{-1}$, respectively, compared to 0.23 and 0.21 µg.mg$^{-1}$ for white and red-white meniscus, respectively.
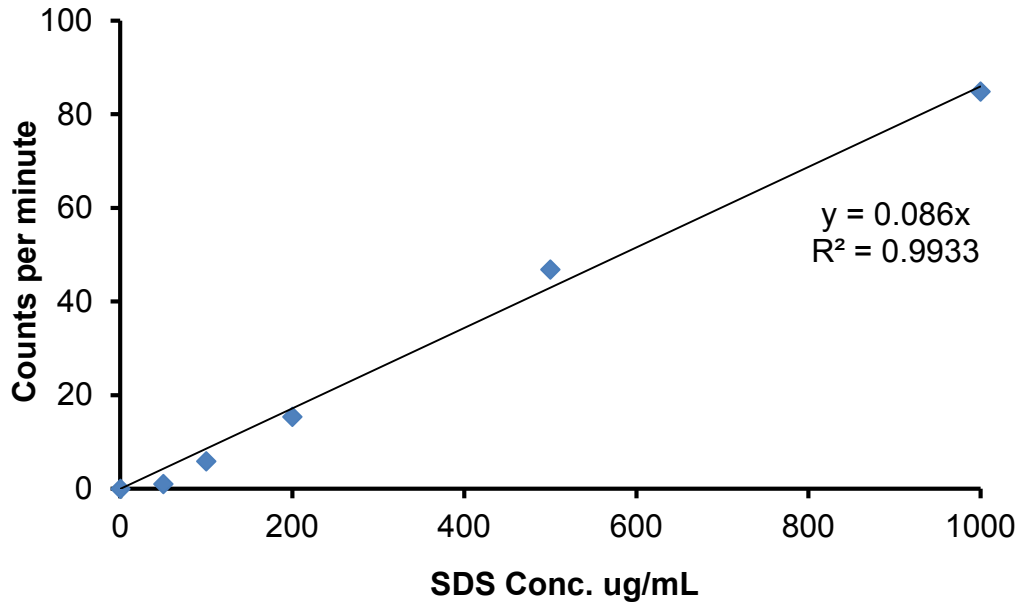
**Figure 5.4.17:  Relationship between SDS concentration and counts per minute readings on Top Count**
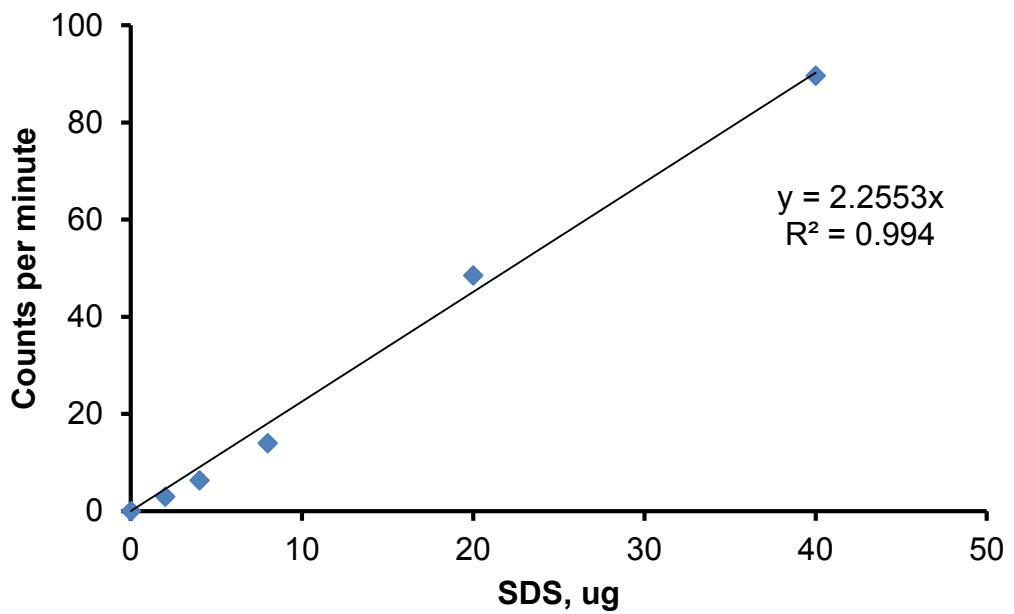


**Figure 5.4.18:  Relationship between absolute weight of SDS and counts per minute readings on Top Count**
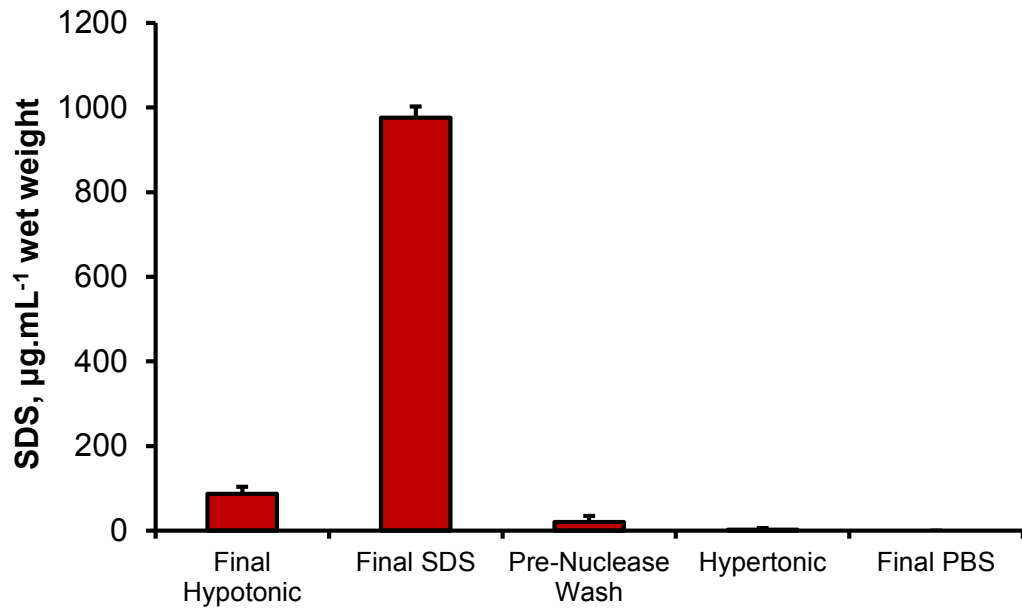
**Figure 5.4.19: SDS concentration of reagents after use during decellularisation of porcine bone-meniscus-bone.** Data presented as mean (n = 4) ± 95% C.I.
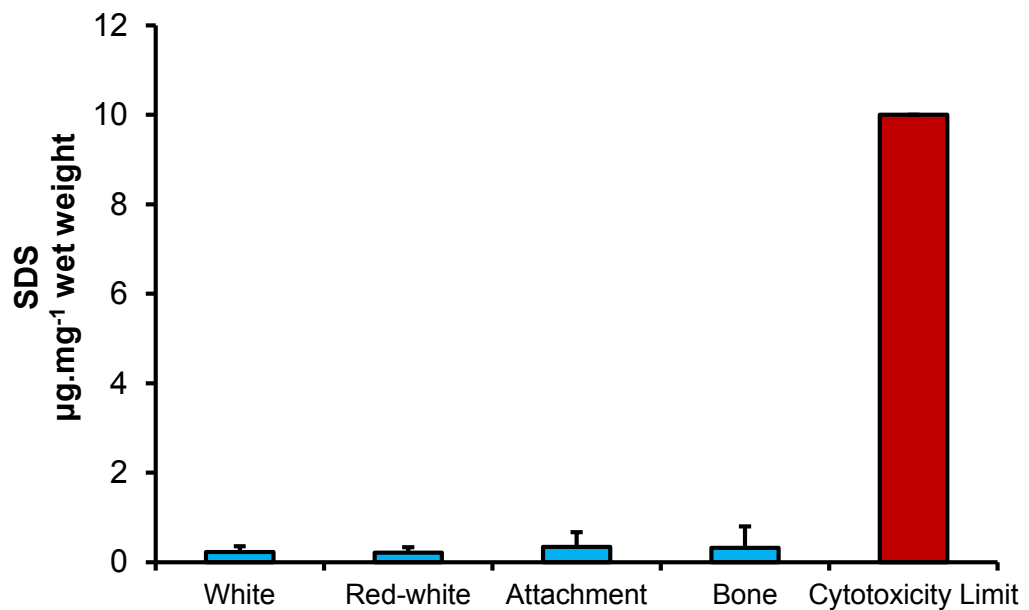


**Figure 5.4.20: Residual SDS content of decellularised porcine bone-meniscus-bone.** Data presented as mean (n = 4) ± 95% C.I. Value for cytotoxicity limit obtained from Gratzer *et al.*, 2006.

## 5.5    Discussion

Having characterised the changes in the porcine bone-meniscus-bone after decellularisation it was necessary to determine the biomechanical properties of the decellularised tissues compared to native tissues and to determine the biocompatibility of the processed tissue.

The primary function of the meniscus is mechanical and so indentation and tensile testing of the meniscus and compressive testing of the bone were undertaken to determine material properties.  Indentation showed an increase in the percentage deformation, and hence a decrease in the stiffness, of decellularised meniscus compared to native meniscus however this was not significant ($p > 0.05$).  This change may be attributable to the loss of GAGs from the tissue as the GAGs play a critical role in the biphasic behaviour of meniscus.

Anchoring of the meniscus at the horns converts vertical compressive forces into circumferential tensile forces as the meniscus is radial displaced.  This results in the dissipation of load through the generation of hoop stresses. The orientation of collagen fibres in the red-white and red zones provides this tensile strength.  Tensile testing of native and decellularised meniscus revealed no significant differences in the tensile modulus, ultimate tensile strength and failure strain.  Stress-strain behaviour was characteristic of collagenous tissue with a low modulus elastin phase and a high modulus collagen phase.  Values obtained for the young's modulus and ultimate tensile strength were comparable to those obtained in the literature for native human meniscus (Fithian *et al.*, 1990; Lechner *et al.*, 2000) however literature on porcine meniscus is limited.  Maintenance of the tensile properties of decellularised meniscus suggests that the decellularisation protocol does not damage meniscal ECM, and specifically collagen I which is responsible for the tensile strength.

Compressive testing of native and decellularised bone revealed a decrease of compressive strength in decellularised bone.  An ultimate compressive strength of ~160 MPa was determined for native bone and ~50 MPa for

decellularised bone. Values obtained for the ultimate compressive strength of native bone corresponded well with other studies where testing of human and bovine compact bone was performed at 0.01 s$^{-1}$ strain (McElhaney and Byars, 1965; Crowninshield and Pope, 1974; Carter and Hayes, 1976). The reduction in compressive strength of decellularised bone may hinder the fixation of bone to the tibia in patients and so should be further investigated. The Poisson's ratio was assumed to be zero for this study and so all stress values calculated did not consider the potential barrelling of samples under compression. It should also be noted that *in vivo* decellularised bone will be confined and so the material properties may be different to those established in this study using unconfined compression.

Rejection is an issue when transplanting tissue from xenogeneic sources to humans. This usually occurs in the form of hyperacute rejection brought on by an immune response to α-gal (Galili *et al.*, 1997). The α-gal epitope is present on cell membrane glycolipids and glycoproteins of lower mammals but not in humans, apes or Old World monkeys. Humans naturally produce large titres of antibody against α-gal and so it was important to ensure the removal of the α-gal epitope from decellularised bone-meniscus-bone. Immunohistochemical staining revealed the absence of α-gal from decellularised meniscus. It is postulated that the mechanism of removal of collagen IV (Section 4.4.2.4) is also responsible for the removal of α-gal as α-gal has been shown to be localised to the basement membrane (McKenzie *et al.*, 1994). This occurs during the PAA sterilisation step (Section 3.3.1.5) as shown by Wilshaw *et al.* (2014). Only staining of the meniscus was possible as issues with procurement of the antibody meant detection of α-gal in bone could not be attempted. However, given the loss of collagen IV seen in decellularised bone (Figure 4.4.9) it is hypothesised that α-gal will also be removed from decellularised bone.

Qualitative contact cytotoxicity assays were undertaken using 3T3 and BHK cells to assess potential cytotoxic effects from decellularised bone-meniscus-bone. Results indicated no cytotoxic effects from any region including both deep and superficial areas, with cells growing up to and in

contact with decellularised bone-meniscus-bone and appearing to maintain normal morphology. Extract cytotoxicity assays were also undertaken to investigate possible cytotoxic effects from soluble components of decellularised bone-meniscus-bone. The mean ATP content of cells was measured by ATPLite-M assay, revealing no significant differences between cells cultured using extracts and the negative control (cell culture medium). Another source of potential cytotoxicity is SDS remaining from decellularisation with studies showing that removal of SDS is essential for recellularisation of decellularised matrices (Kim *et al.*, 2002; Rieder *et al.*, 2004). SDS was quantified in decellularised bone-meniscus-bone and wash solutions using $^{14}$C radio-labelled SDS. Results revealed a small quantity of SDS was still present within decellularised bone-meniscus-bone. Gratzer *et al.* (2006) showed that the lower cytotoxicity threshold for residual SDS in tissue is 10 µg per mg of tissue, whereas the mean SDS content of decellularised bone-meniscus-bone was 0.28 µg per mg of tissue. Results from extract and contact cytotoxicity assays consolidated this finding by demonstrating a lack of cytotoxicity.

In conclusion, decellularised bone-meniscus-bone was shown to be non-cytotoxic to BHK and 3T3 cells with only a small quantity of SDS remaining within the matrix and complete removal of the immunogenic α-gal epitope. Mechanical testing revealed retention of meniscal material properties under tension however significant differences were seen for both decellularised meniscus and bone under compression.

# Chapter 6.    Discussion

## 6.1   Discussion

The aim of this study was to use xenogeneic tissue to develop an immunologically inert meniscal replacement with a view to future clinical translation incorporating bone blocks to aid fixation.   Porcine bone-meniscus-bone was decellularised using physical, chemical and enzymatic methods.   Histology revealed the complete removal of porcine cellular material and analysis of DNA demonstrated >90% reduction in total DNA as well as an absence of functional DNA.  Investigations also revealed retention of matrix architecture and constituents however there was a loss of GAGs, a ~50% reduction in calcium content of bone as well as depletion of collagen IV.  Biomechanical testing demonstrated significantly different behaviour of the decellularised meniscus compared to the native tissue under indentation however finite element modelling showed that decellularised meniscus was not significantly stiffer than native meniscus.  Decellularised meniscus was not significantly different to native meniscus under tensile testing however compressive properties of decellularised bone were diminished. Biocompatibility was assessed using cytotoxicity assays which demonstrated a lack of cytotoxicity.

A real clinical need exists for a meniscal replacement owing to the current and ever increasing incidence of meniscal injury and lack of long term treatment options.  Approximately 1.5 million procedures related to the meniscus are performed each year and many of these are secondary surgeries burdening health service providers and patients.  Meniscal injury can be incurred through sport, accounting for the majority of injury in younger people, or other non-sporting activities, usually occurring later in life (Drosos and Pozo, 2004).   Injury usually reveals itself through various symptoms including pain and swelling (Choi and Victoroff, 2006), which impair quality of life.  The meniscus is largely avascular and so a limited healing response is activated resulting in the formation of mechanically inferior repair tissue (Roeddecker *et al.,* 1994).   Prognosis is best with injury to the red zone

(Brindle *et al.*, 2001) however repair may not be possible depending on the type of injury, location of the injury and other factors associated with the patient and in some cases will not heal (Adams *et al.*, 2005) and in these cases resection of the meniscus is chosen to alleviate symptoms. Resection of the meniscus in this way preserves the load distribution characteristics of the meniscus (Messner and Gao, 1998) however degeneration still proceeds and is proportional to the amount of tissue removed (Andersson-Molina *et al.*, 2002). Therefore, various tissue engineering strategies have been investigated for the repair or replacement of the meniscus. These include both natural and synthetic biomaterials in conjunction with cells and growth factors to restore mechanical function and promote regeneration of the meniscus. The different types of biomaterial offer various advantages and disadvantages, with synthetic materials offering reproducible production and customisation but lack natural signalling cues and can impart a foreign body response, whereas natural materials are less toxic however batch to batch variability is greater. Success has been limited with these approaches as the meniscus is a highly complex structure composed of multiple components and cell types which are critical to its function and challenging to replicate using current techniques. Therefore the approach used in this study was to use readily available xenogeneic tissue, already comprising the highly complex matrix and natural cell signalling cues, and remove all potentially immunogenic components leaving an immunologically inert natural scaffold capable of restoring mechanical function and regeneration.

Decellularisation of tissues should leave a nontoxic, acellular scaffold capable of supporting cell repopulation and inducing a regenerative response whilst maintaining the biomechanical properties required of the replacement. Decellularised matrices have been used clinically in the form of porcine small intestinal submucosa (Surgisis, Cook Biotech Inc), heart valves and dermis (Tissue Regenix plc) with further decellularised tissues undergoing development (Ingram *et al.*, 2007; Partington *et al.*, 2013). Porcine tissue is readily available from abattoirs and porcine meniscus is anatomically similar to human meniscus. Issues with differences in geometry can be overcome by size matching of replacement tissue using

magnetic resonance imaging (MRI) techniques already employed in the clinic. Studies have shown how effective size matching of meniscal replacements can improve outcomes (Verdonk *et al.*, 2006). The medial meniscus is smaller (McDermott *et al.*, 2004) and less mobile (Vedi *et al.*, 1999) than the lateral meniscus resulting in an increase in the incidence of injury (Boyd and Myers, 2003). The medial meniscal attachments can be more easily accessed than the lateral meniscal attachments and so surgical fixation is less problematic. Bone blocks provide a simple yet effective method of fixation with bone to bone healing showing superior mechanical properties after 24 weeks when compared to bone to soft tissue fixation (Leung *et al.*, 2002). It has also been suggested that suture fixation of soft tissue allows the meniscus to extrude altering the load distribution profile as the meniscal horns are not anchored as well as when bone plugs used (Alhalki *et al.*, 1999). Various protocols are in development to produce decellularised meniscus however to date there are none that incorporate a bone element for fixation.

Strategies have shifted from devitalized grafts (Arnoczky *et al.*, 1992; Peretti *et al.*, 2004; Yamasaki *et al.*, 2008) to decellularised grafts (Maier *et al.*, 2007; Stapleton *et al.*, 2008; Sandmann *et al.*, 2009; Stabile *et al.*, 2010). This shift may have occurred due to the unfavourable results produced using devitalised meniscus with degeneration similar to meniscectomised knees reported. Decellularisation of meniscus has been undertaken using tissue from various sources including murine, ovine, porcine and human. Various protocols have been developed usually incorporating a detergent wash or enzymatic digestion. Trypsin has been used to decellularise meniscus resulting in removal of xenogeneic cells and generation of a biocompatible scaffold however trypsin treatment resulted in loss of GAGs and extensive damage to the matrix (Maier *et al.*, 2007). Stabile *et al.* (2010) had more success using a lower concentration of trypsin (0.05% compared to 0.25%) on ovine meniscus resulting in the generation of a biocompatible scaffold with retention of material properties, however only a ~55% reduction in total DNA was achieved. SDS has been used widely to decellularise tissues with concentrations ranging from 0.1-1% (w/v) used to decellularise meniscus

(Stapleton *et al.*, 2008; Sandmann *et al.*, 2009). Higher concentrations of SDS have been shown to damage ECM proteins (Bodnar *et al.*, 1986; Courtman *et al.*, 1994), although it has also been suggested that damage to ECM is caused by endogenous proteases released as cells are lysed and not SDS (Booth *et al.*, 2002).

Work leading to the current study was completed by Stapleton *et al.* (2008) in which porcine menisci were successfully decellularised using a protocol utilising physical, chemical and enzymatic methods. The protocol was based on the process developed by Booth *et al.* (2002) to decellularise porcine heart valves. Menisci were prepared by creating spaces in the extracellular matrix using freeze-thaw cycles. Hypotonic solutions were used in conjunction with SDS to cause cell lysis and solubilise cellular material with protease inhibitors included to prevent damage to the matrix from endogenous proteases (Booth *et al.*, 2002). Subsequently released nucleic acids were digested using nucleases to prevent potential sites of calcification associated with phosphate groups (Schoen and Levy, 2005) and a hypertonic buffer wash step was added to aid removal of hydrophobic proteins. The method developed by Stapleton *et al.* (2008) for decellularising porcine menisci was able to produce a biocompatible acellular scaffold retaining biochemical, structural and biomechanical properties of the native tissue. Whole porcine medial menisci were subjected to three dry freeze-thaw cycles followed by three freeze-thaw cycles in hypotonic buffer. Menisci were then treated using hypotonic buffer at 4 °C for 24 hours, hypotonic buffer at 37 °C for 24 hours, followed by two incubations in 0.1% (w/v) SDS at 45 °C for 24 hours each with all steps containing aprotinin and EDTA as protease inhibitors. This cycle was repeated twice more before washing in PBS containing aprotinin three times for 12 hours each. After washing, menisci were treated thrice using nuclease solution containing DNase and RNase for three hours each at 37 °C. A hypertonic wash was then employed prior to another PBS wash at room temperature for 24 hours. This was followed by a sterilisation step in 0.1% (v/v) peracetic acid for three hours and final washing in PBS five times at 45 °C, 37 °C and 4 °C for 24 hours each. This protocol resulted in a decellularised scaffold which retained

biochemical, structural and biomechanical properties when compared to native menisci and was biocompatible.

Initial investigations by Stapleton *et al.* (2008) into decellularisation of bone-meniscus-bone resulted in decalcification of bone blocks owing to the inclusion of EDTA in wash solutions and incomplete decellularisation of the enthesis region of the bone blocks. Therefore, for the current study EDTA was removed from all decellularisation solutions. Other changes that were required to aid decellularisation were physical manipulation of the attachment site to improve diffusion of reagents into the enthesis, increases in sample processing volumes owing to the increased size and weight of bone-meniscus-bone compared to meniscus alone, processing at only 4 °C or 42 °C to reduce the potential of bio burden build up, removal of bone marrow from bone blocks to prevent clotting which could prevent decellularisation solutions from penetrating the bone, and increased wash buffer changes prior to the nuclease step to prevent inactivation of nucleases by SDS. To the authors knowledge the current study represents the first known example of successful decellularisation of tissue with both soft and hard components. Given the dense nature of the meniscus it is conceivable that the current process would successfully decellularise similar tissue from a variety of sources to produce bone-tendon and bone-ligament grafts.

Decellularisation of porcine bone-meniscus-bone resulted in complete removal of whole cells and nuclei as evidenced by histology and analysis of residual DNA. Initial assessment of decellularisation in bone was not attempted using traditional histological tissue preparation techniques as decalcification prior to paraffin embedding may result in decellularisation as mineralised matrix is removed. Therefore resin embedding was chosen as the desired method for histological analysis of bone as this preserves the tissue in its absolute state eradicating the possibility of a false negative. As histological techniques may not be suitable or lack the sensitivity to detect all residual DNA, DNA from decellularised bone-meniscus-bone was extracted using a DNeasy kit and quantified by spectrophotometry as well as assessed for functional genes using PCR and gel electrophoresis. All

techniques employed revealed an absence of functional DNA or whole DNA fragments. It has been suggested that decellularised matrices should contain no more than 50 ng.mg$^{-1}$ of dsDNA (Crapo *et al.,* 2011) as phosphate groups present on DNA can result in calcification (Schoen and Levy, 2005). Decellularised meniscus contained 26.7 ng.mg$^{-1}$ of total DNA whereas decellularised bone contained 124.9 ng.mg$^{-1}$ of total DNA. As these values represent total DNA which includes both double stranded and single stranded DNA the actual content of dsDNA will be much lower. Even though the total DNA content of bone was above the definition, calcification within the bone would not be detrimental, whereas calcification in the soft tissue could affect mechanical function. It has been suggested that DNA fragment length is related to the host response to decellularised grafts (Keane *et al.,* 2012). Larger fragments (>500 bp) have been associated with an inflammatory response whereas smaller fragments (<500 bp) correlated with a remodelling response. It should be noted, however, that this effect may be attributable to different degrees of decellularisation as alternative sources of antigenicity were not determined. Gel electrophoresis of DNA extracted from decellularised bone-meniscus-bone and amplified using PCR for three genes ubiquitous in this type of tissue failed to reveal the presence of large fragments of DNA. This may have been because there was not enough total DNA of that size to be visible as the concentration of DNA extracted from native and decellularised tissue was different. To counteract this and prevent extracted DNA samples falling below the detection limit of the spectrophotometer increased amounts of decellularised tissue were digested compared to native tissue for DNA extraction. Decellularised bone-meniscus-bone was also absent of functional DNA suggesting digestion of nuclear material by nucleases during the process. This along with solubilisation and removal of cells should prevent the transfer of latent viral DNA to the host, although insertion of porcine endogenous retroviral DNA has been shown to be inefficient at best and otherwise non-existent in *in vitro studies* (Bisset *et al.,* 2007).

The general structure and geometry of native and decellularised bone meniscus bone was assessed using 9.4T MRI. Non-destructive imaging of

tissues in three dimensions whilst preserving the native form is valuable as the impact of tribological testing can be investigated. Images obtained allowed clear distinction between the different regions and tissue types present within porcine bone and meniscus. The 3D FLASH sequence used allowed visualisation of the internal structures of bone and meniscus in any plane. The main differences seen between native and decellularised meniscus were the loss of the synovium and vasculature in decellularised meniscus, and changes to the structure of the attachment site in bone. These changes correlated well with histological and immunohistochemical studies. Loss of the synovium is not seen as critical as it is hypothesised that cells infiltrating from the synovium will regenerate a new synovium (Rodeo *et al.*, 2000). Porcine bone-meniscus-bone was obtained from young pigs (~6 months) in which the meniscus is not fully developed and remains largely vascularised with vessels extending into the white zone. Loss of the vasculature may prove beneficial as the channels that remain span the entire meniscus and may improve access for infiltrating cells into the deep portions of the meniscus, thereby accelerating the remodelling response.

The extracellular matrix (ECM) was characterised using histology, immunohistochemistry and biochemical assays. The collagen structure is responsible for the function of the meniscus with circumferential fibres dissipating compressive load through the generation of hoop stresses. Histology and biochemical assays showed retention collagen and maintenance of structure whilst immunohistochemistry revealed changes to the composition of meniscal ECM. Collagen I, II and III were unchanged in decellularised meniscus however collagen IV was completely removed and some collagen VI was removed. This may be because collagen I, II and II are structural collagens which form organised fibres and so are more resistant to washing out. Studies in our laboratory have demonstrated how the removal of collagen IV is a chemical process (Wilshaw et al., 2014 - publication in progress) whereas removal of collagen VI appeared to be a more physical process with a boundary visible towards the periphery of the meniscus inside which collagen VI staining remained comparable to native

meniscus. GAGs contribute to the biphasic nature of the meniscus by retarding the flow of water molecules leaving the matrix on application of load, thereby creating the Donnan osmotic pressure which bears the initial portion of the load, and attracting water back into the matrix once the meniscus is unloaded. Histology suggested a complete loss of GAGs from the meniscus and this was verified by DMMB assay. This may have been due to the immaturity of the tissue as well as the effect of SDS on ECM constituents (Reing *et al.*, 2007; Lumpkins *et al.*, 2008; Stapleton *et al.*, 2008; Deeken *et al.*, 2011). Compositional changes to the bone post-decellularisation followed a similar pattern to the meniscus. Major collagens I, II and III were all unchanged with complete loss of collagen IV once more and a decrease in collagen VI staining intensity. Osteocalcin, the most abundant non-collagenous protein in bone, was also stained for as a bone-specific target. Staining of osteocalcin was mainly localised to cells and so with the removal of cells the level of staining decreased however staining intensity in the bone matrix remained unchanged. The calcium content of bone was determined using inductively coupled plasma mass spectrometry (ICPMS). Calcium content was ~50% lower in decellularised bone when compared to native bone. Studies have shown that removal of the mineralised matrix exposes bone morphogenetic proteins which promote a healing response (Reddi, 1975; Glowacki and Mulliken, 1985) and so this may not necessarily be detrimental to clinical success.

Mechanical testing of meniscus and bone was undertaken to determine the impact of changes in matrix composition on material properties. Indentation and tensile testing were performed on meniscus and compressive testing was performed on bone. DMMB assay on the different regions of meniscus revealed the highest concentration of GAGs in the white zone however owing to the size of the meniscus repeatable sampling for indentation tests could only be carried out in the red zone. Ideally testing should be performed on the whole meniscus in order to fully understand the mechanisms by which the meniscus functions mechanically. Indentation testing revealed a significant difference between the deformation profiles of native and decellularised meniscus. This can be attributed to the loss of GAGs from the

tissue. Finite element modelling of meniscus was undertaken to determine the material properties of meniscus. A low load was used (0.22 N) to prevent deformation exceeding 50% as the model does not permit such high deformations due to mesh alterations near the corner of the plane ended indenter. Modelling did not reveal a significant difference between the aggregate modulus of native and decellularised meniscus however this may be because the model used was developed for cartilage and given sampling of meniscus occurred in the fibrocartilaginous zone and not the hyaline-like white zone alterations may be required to ensure the model is suitable for determining meniscal material properties. Also, peak deformations were relatively high (~30%) and it is recommended that low deformations (5-10%) are used with the model.

Tensile testing of meniscus was undertaken to investigate the effect of decellularisation on the tensile properties of meniscus. Compressive forces are converted to circumferential hoop stresses by the radial displacement of the meniscus as it is anchored at the horns. No significant differences were found for the ultimate tensile strength, failure strain or Young's modulus of native and decellularised meniscus. Studies on human menisci in the literature where similar sample dimensions were used obtained values ranging from 83 to 129 MPa for the Young's modulus (Tissakht and Ahmed, 1995; Lechner *et al.*, 2000) which is comparable to the value obtained in this study. However, further investigations should be undertaken using a standard testing method and sample geometry in order to obtain a true comparison between decellularised porcine meniscus and native human meniscus. Retention of the complex collagen structure is advantageous over artificially produced replacements as randomly organised natural and/or synthetic polymers are unable to confer the requisite mechanical strength of native meniscus.

The reduction in the calcium content of decellularised bone alluded to a decrease in mechanical strength of the bone. Unconfined compression of bone revealed significant differences for the compressive load at yield and the compressive modulus between native and decellularised bone. As the

graft will be confined once implanted the material properties under compression may be different. Fixation of the bone blocks is crucial to the success of the decellularised graft. Fixation needs to be secure in order to anchor the meniscus in place and prevent excessive displacement of the meniscus as this can lead to extrusion and altered load distribution within the knee (Costa *et al.*, 2004; Lerer *et al.*, 2004). Future studies should investigate the effect the reduction in mechanical strength of decellularised bone blocks has on integration and meniscal load transmission using clinically relevant fixation techniques.

Depletion of GAGs will no doubt impact the response of the meniscus under loading *in vivo*, however the success of the bone-meniscus-bone implant will depend on the extent of these effects. As already discussed in this section, a significant difference was seen in the response of decellularised meniscus under compressive load and this can be attributed to the loss of GAGs. Collagen gels with bound GAGs and cultured with fibroblasts were shown to have reduced biomechanical properties when compared to gels without cells (Saddiq *et al.*, 2005). This may be due to the remodelling response initiated by the fibroblasts as they populate and proliferate in the collagen matrix, degrading the matrix prior to rebuilding it. Once decellularised bone-meniscus-bone is implanted into the knee, cells infiltrating the meniscus and bone will begin to remodel the construct as they respond to tensile and compressive forces exerted on them. The success of decellularised bone-meniscus-bone as a meniscal replacement will depend on its ability to direct this remodelling response to prevent resorption while providing mechanical function. Mechanical testing of aortic valve cusps with GAGs depleted displayed altered viscoelastic properties however stiffness of the tissue was not changed (Borghi *et al.*, 2013). Tensile properties of the meniscus have not been affected by decellularisation therefore the decellularised construct should provide mechanical function within the patient knee. CMI, comprised of an unorganised collagen I matrix, has been extensively used as a meniscal replacement with varying degrees of success, suggesting a replacement with the varied composition and complex matrix organisation

present within native meniscus should provide improved mechanical properties.

Bone forms through three basic processes: synthesis of extracellular matrix, mineralisation, and remodelling. Healing in long bones, such as the tibia, occurs through endochondral ossification where bone growth occurs from an underlying cartilage model. Removal of calcium through decellularisation retains the extracellular matrix and some mineral content potentially allowing more rapid mineralisation and remodelling as extensive resorption does not need to occur. Retention of bone structures may also allow infiltration of cells from the marrow through Haversian canals facilitating the healing response. Bone is constantly being remodelled to prevent accumulation of microdamage (Turner, 1998). Loss of mechanical strength due to the loss of calcium should not be detrimental to the success of decellularised bone-meniscus-bone as compressive loading of the tibia at the attachment site is minimal with the meniscus bearing the majority of the load (Walker and Erkman, 1975). A point of concern may be the ability to properly fix decellularised bone blocks into the tibia without forces generated during activity causing bone blocks to be damaged and dislodge. A study conducted in the group on porcine bone decellularised using the method described in Section 3.3.1.5 was implanted into murine tibia and fixed in place using sutures and allowed to heal. Bone displayed good integration to the native tissue with no adverse reactions noted (data not published). This displays bio- and immune-compatibility of decellularised bone, which contained higher residual DNA content than meniscus, in a non-homologous animal model, providing a good basis for predicting that porcine meniscus produced in the same method will also prove biocompatible. An appropriate rehabilitation programme can also be employed to minimise potential damage to the knee and meniscus to allow repopulation and replenishment of GAGs by patient cells and healing and integration of bone to the tibia.

It is clear that *in vivo* investigations are required in order to fully elucidate the effect of GAG and calcium depletion from decellularised bone-meniscus-bone as well as inform the remodelling response initiated by the

decellularised graft. Tensile properties have been maintained suggesting strategies can be applied to reduce the impact of increased deformation of decellularised meniscus under load. These could be in the form of a physiotherapy and rehabilitation regime where loading on the knee is reduced to minimise excessive stress on the meniscus, or introduction of a cell population prior to implantation to accelerate cell infiltration and population of the graft thereby promoting the replenishment of the meniscus with GAGs and initiating the remodelling response. Any cells used in this way should be autologous and minimally manipulated to maintain process simplicity and reduce the regulatory burden.

Biocompatibility of the decellularised porcine bone-meniscus-bone has to be determined prior to clinical use. The current study focussed on the removal of the immunogenic α-gal epitope and removal of SDS as well as *in vitro* biocompatibility assays using BHK and 3T3 cells to assess soluble and contact cytotoxicity. Immunohistochemical evaluation revealed an absence of α-gal in decellularised meniscus however studies on bone could not be completed due to issues in procuring the antibody. It is postulated that α-gal is removed chemically along with collagen IV by PAA (Wilshaw *et al.*, 2014 – manuscript under review) and, as it is located on cells, during washing out of cell fragments by SDS. As mentioned previously, SDS is known to damage proteins and has been shown to be cytotoxic at increased concentrations (Zorn-Kruppa *et al.*, 2004). Residual SDS was quantified using $^{14}$C radio-labelled SDS resulting in a mean SDS content of 0.28 µg.mg$^{-1}$ in decellularised bone-meniscus-bone. This was well below the cytotoxicity threshold defined by Gratzer *et al.* (2006) of 10 µg.mg$^{-1}$ suggesting bone-meniscus-bone would not be cytotoxic to cells. Contact and extract cytotoxicity assays corroborated this finding as BHK and 3T3 cells grew normally up to and in contact with decellularised bone-meniscus-bone with no evidence of cytotoxicity.

It is paramount that decellularised bone-meniscus-bone is sterilised prior to implantation to prevent the transmission of viruses and other infectious agents. Exposure to porcine endogenous retrovirus (PERV) is unavoidable

as these viruses are a permanent part of the mammalian genome (Blusch *et al.*, 2002) however transmission rate is low and replication of endogenous retroviruses does not usually occur (Patience *et al.*, 1997). As mentioned earlier, decellularisation renders all nuclear material replication incompetent and so retroviral transmission should not occur. The current protocol used 0.1% (v/v) PAA as a terminal sterilisation step. No sign of contamination was seen during cytotoxicity assays suggesting PAA is an effective method of sterilisation. PAA has been used extensively to disinfect biomaterials and has been shown to inactivate viruses, spores and mycoplasma (Sprossig *et al.*, 1976; Pruss *et al.*, 1999) while also leaving biologically active growth factors behind (Hodde *et al.*, 2007). However, PAA sterilisation has been shown to inhibit remodelling of ACL allografts (Scheffler *et al.*, 2008) although other studies have shown PAA does not affect repopulation of decellularised matrices (Bolland *et al.*, 2007). Alternative methods of sterilisation should be investigated to circumvent this as well as studies assessing recellularisation of decellularised bone-meniscus-bone sterilised using the current method. Gamma irradiation and ethylene oxide treatment are two options that are available. Gamma irradiation has been shown to weaken cortical bone whereas ethylene oxide does not (Zhou *et al.*, 2011).

The current study has described a process for obtaining acellular, biocompatible porcine bone-meniscus-bone which retains the geometry and collagen organisation of native meniscus and displays excellent potential as a meniscal replacement. Future studies should focus on *in vivo* performance and optimisation of surgical techniques for fixation. Consideration should also be given to large-scale manufacture of decellularised bone-meniscus-bone using scale-up rather than scale-out methodologies and optimisation of tissue harvest procedures.

## 6.2 Future work

Further in vitro testing needs to be undertaken in order to ascertain the potential utility of decellularised bone-meniscus-bone. The tensile testing

described in Section 5.3.2.3 should be completed by bringing the number of native and decellularised samples tested to 6 each. This will allow accurate determination of the tensile performance of decellularised bone. The α-gal content of decellularised bone-meniscus-bone should also be quantified using an ELISA, as even though immunohistochemical staining revealed an absence in decellularised tissue a quantitative method provides a more comprehensive method of determination.

The ability of decellularised bone-meniscus-bone to support a cell population also needs to be evaluated. This can be done by seeding the decellularised construct using mesenchymal stem cells. It will be interesting to see the response of these cells to mechanical stimulation, tension and/or compression, in bioreactors currently available in the group (TenCell II and ComCell). Constructs should be cultured for 28 days prior to removal and assessment of infiltration and cell phenotype using histology and immunocytochemistry. If longer term culture is possible then possible conditioning of decellularised meniscus should be investigated using mechanical testing methods described in Section 5.3.2.

To complete the product development cycle and market decellularised bone-meniscus-bone as a class III medical device a set of further investigations need to take place. This should begin with characterisation of human meniscus and comparison of structure, composition and biomechanical properties in order to compare to decellularised meniscus and reveal areas for development. Evaluation of alternative sterilisation techniques, such as ethylene oxide, should then be undertaken in order to prevent detrimental changes to the matrix owing to PAA sterilisation. Safety and fixation techniques can then be assessed in a large animal study, e.g. sheep, and should take approximately one month to complete. Size matching of grafts can be investigated using MRI techniques with histology and immunohistochemistry used to assess the host response. Once these have been determined a longer term study investigating the integration of the decellularised graft to the knee joint should be carried out with explants also analysed for the type of immune response elicited. Longer term studies for

clinical efficacy, i.e. biomechanical function and regeneration, can then occur which will conclude the initial phase of development. The secondary phase should focus on development of a suitable bioprocess that adheres to GMP in order to obtain a market authorisation for decellularised bone-meniscus-bone. Design of experiments (DoE) should be used to fully understand the decellularisation process and obtain critical process parameters. Once this process is finalised, bone-meniscus-bone produced using this optimised protocol will have to be investigated in a large animal study to demonstrate safety and also where comparisons to the previous study can be made. This should then be followed by a first-in-man study comprising 20-30 patients to assess the safety of the GMP product, successful completion of which will enable CE marking of the product in Europe and FDA approval in the US.

## 6.3   Conclusion

In conclusion, this study represents the first time decellularisation has been successfully achieved in grafts comprising both bone and a soft tissue component. No cell nuclei were visible on inspection and total DNA was reduced by >90% in the decellularised graft. Further investigation into the impact of compositional changes on potential clinical utility need to be undertaken prior to progression of developmental activities.

# Chapter 7.  Bibliography

Adams, M. E., Billingham, M. E. J. & Muir, H. 1983. The glycosaminoglycans involved in menisci in experimental and natural osteoarthritis. Arthritis and Rheumatism, 26, 69-76.

Adams, S. B., Randolph, M. A. & Gill, T. J. 2005. Tissue engineering for meniscus repair. J Knee Surg, 18, 25-30.

Alexopoulos, L. G., Youn, I., Bonaldo, P. & Guilak, F. 2009. Developmental and osteoarthritic changes in col6a1-knockout mice biomechanics of type VI collagen in the cartilage pericellular matrix. Arthritis and Rheumatism, 60, 771-779.

Alhalki, M. M., Howell, S. M. & Hull, M. L. 1999. How three methods for fixing a medial meniscal autograft affect tibial contact mechanics. Am J Sports Med, 27, 320-8.

Allen, C. R., Wong, E. K., Livesay, G. A., Sakane, M., Fu, F. H. & Woo, S. L. Y. 2000. Importance of the medial meniscus in the anterior cruciate ligament-deficient knee. Journal of Orthopaedic Research, 18, 109-115.

Allen, P. R., Denham, R. A. & Swan, A. V. 1984. Late degenerative changes after meniscectomy - factors affecting the knee after operation. Journal of Bone and Joint Surgery-British Volume, 66, 666-671.

Andersson-Molina, H., Karlsson, H. & Rockborn, P. 2002. Arthroscopic partial and total meniscectomy: A long-term follow-up study with matched controls. Arthroscopy-the Journal of Arthroscopic and Related Surgery, 18, 183-189.

Angele, P., Johnstone, B., Kujat, R., Zellner, J., Nerlich, M., Goldberg, V. & Yoo, J. 2008. Stem cell based tissue engineering for meniscus repair. Journal of Biomedical Materials Research Part A, 85A, 445-455.

Arnoczky, S. P., Dicarlo, E. F., Obrien, S. J. & Warren, R. F. 1992. Cellular repopulation of deep-frozen meniscal allografts - an experimental study in the dog. Arthroscopy, 8, 428-436.

Arnoczky, S. P., Dodds, J. A. & Wickiewics, T. L. 1996. Basic science of the knee, Philadelphia, Lippincott-Raven Publishers.

Arnoczky, S. P. & Warren, R. F. 1982. Microvasculature of the human meniscus. American Journal of Sports Medicine, 10, 90-95.

Arnoczky, S. P. & Warren, R. F. 1983. The microvasculature of the meniscus and its response to injury - an experimental study in the dog. American Journal of Sports Medicine, 11, 131-141.

Arnoczky, S. P., Warren, R. F. & Spivak, J. M. 1988. Meniscal repair using an exogenous fibrin clot - an experimental study in dogs. Journal of Bone and Joint Surgery-American Volume, 70A, 1209-1216.

Aspden, R. M., Yarker, Y. E. & Hukins, D. W. L. 1985. Collagen orientations in the meniscus of the knee joint. Journal of Anatomy, 140, 371-380.

Athanasiou, K. A. & Sanchez-Adams, J. 2009. Engineering the knee meniscus, Morgan & Claypool.

Aufderheide, A. C. & Athanasiou, K. A. 2005. Comparison of scaffolds and culture conditions for tissue engineering of the knee meniscus. Tissue Engineering, 11, 1095-1104.

Aufderheide, A. C. & Athanasiou, K. A. 2007. Assessment of a bovine co-culture, scaffold-free method for growing meniscus-shaped constructs. Tissue Engineering, 13, 2195-2205.

Azhim, A., Ono, T., Fukui, Y., Morimoto, Y., Furukawa, K. & Ushida, T. 2013. Preparation of decellularised meniscal scaffolds using sonication treatment for tissue engineering. Conf Proc IEEE Eng Med Biol Soc, 2013, 6953-6.

Badylak, S. F., Tullius, R., Kokini, K., Shelbourne, K. D., Klootwyk, T., Voytik, S. L., Kraine, M. R. & Simmons, C. 1995. The use of xenogeneic small-intestinal submucosa as a biomaterial for achilles tendon repair in a dog model. Journal of Biomedical Materials Research, 29, 977-985.

Baker, B. M., Nathan, A. S., Huffman, G. R. & Mauck, R. L. 2009. Tissue engineering with meniscus cells derived from surgical debris. Osteoarthritis and Cartilage, 17, 336-345.

Balint, E., Gatt, C. J., Jr. & Dunn, M. G. 2012. Design and mechanical evaluation of a novel fibre-reinforced scaffold for meniscus replacement. Journal of Biomedical Materials Research Part A, 100A, 195-202.

Bamac, B., Ozdemir, S., Sarisoy, H. T., Colak, T., Ozbek, A. & Akansel, G. 2006. Evaluation of medial and lateral meniscus thicknesses in early osteoarthritis of the knee with magnetic resonance imaging. Saudi Medical Journal, 27, 854-857.

Baratz, M. E., Fu, F. H. & Mengato, R. 1986. Meniscal tears - the effect of meniscectomy and of repair on the intrarticular contact areas and stresses in the human knee - a preliminary report. American Journal of Sports Medicine, 14, 270-275.

Beaupre, A., Choukroun, R., Guidouin, R., Garneau, R., Gerardin, H. & Cardou, A. 1986. Knee menisci - correlation between microstructure and biomechanics. Clinical Orthopaedics and Related Research, 72-75.

Beaver, R. J., Mahomed, M., Backstein, D., Davis, A., Zukor, D. J. & Gross, A. E. 1992. Fresh osteochondral allografts for post-traumatic defects in the knee - a survivorship analysis. Journal of Bone and Joint Surgery-British Volume, 74, 105-110.

Berg, E. E. & Deholl, D. 1999. The lateral elbow ligaments - a correlative radiographic study. American Journal of Sports Medicine, 27, 796-800.

Berjon, J. J., Munuera, L. & Calvo, M. 1991. Degenerative lesions in the articular-cartilage after meniscectomy - preliminary experimental study in dogs. Journal of Trauma-Injury Infection and Critical Care, 31, 342-350.

Berthiaume, M. J., Raynauld, J. P., Martel-Pelletier, J., Labonte, F., Beaudoin, G., Bloch, D. A., Choquette, D., Haraoui, B., Altman, R. D., Hochberg, M., Meyer, J. M., Cline, G. A. & Pelletier, J. P. 2005. Meniscal tear and extrusion are strongly associated with progression of symptomatic knee osteoarthritis as assessed by quantitative magnetic resonance imaging. Annals of the Rheumatic Diseases, 64, 556-563.

Birk, D. E. & Mayne, R. 1997. Localization of collagen types i, iii and v during tendon development. Changes in collagen types i and iii are correlated with changes in fibril diameter. European Journal of Cell Biology, 72, 352-361.

Bisset, L. R., Boni, J., Lutz, H. & Schupbach, J. 2007. Lack of evidence for PERV expression after apoptosis-mediated horizontal gene transfer between porcine and human cells. Xenotransplantation, 14, 13-24.

Bjelle, A. 1981. Cartilage matrix in hereditary pyrophosphate arthropathy. Journal of Rheumatology, 8, 959-964.

Blusch, J. H., Seelmeir, S. & Von Der Helm, K. 2002. Molecular and enzymatic characterization of the porcine endogenous retrovirus protease. J Virol, 76, 7913-7.

Bodnar, E., Olsen, E. G. J., Florio, R. & Dobrin, J. 1986. Damage of porcine aortic-valve tissue caused by the surfactant sodium dodecyl sulfate. Thoracic and Cardiovascular Surgeon, 34, 82-85.

Bolland, F., Korossis, S., Wilshaw, S.-P., Ingham, E., Fisher, J., Kearney, J. N. & Southgate, J. 2007. Development and characterisation of a full-

thickness acellular porcine bladder matrix for tissue engineering. Biomaterials, 28, 1061-1070.

Booth, C., Korossis, S. A., Wilcox, H. E., Watterson, K. G., Kearney, J. N., Fisher, J. & Ingham, E. 2002. Tissue engineering of cardiac valve prostheses i: Development and histological characterization of an acellular porcine scaffold. Journal of Heart Valve Disease, 11, 457-462.

Borghi, A., New, S. E. P., Chester, A. H., Taylor, P. M. & Yacoub, M. H. 2013. Time-dependent mechanical properties of aortic valve cusps: Effect of glycosaminoglycan depletion. Acta Biomaterialia, 9, 4645-4652.

Boyd, K. T. & Myers, P. T. 2003. Meniscus preservation; rationale, repair techniques and results. Knee, 10, 1-11.

Bradley, M. P., Fadale, P. D., Hulstyn, M. J., Muirhead, W. R. & Lifrak, J. T. 2007. Porcine small intestine submucosa for repair of goat meniscal defects. Orthopedics, 30, 650-656.

Brindle, T., Nyland, J. & Johnson, D. 2001. The meniscus: Review of basic principles with application to surgery and rehabilitation. The Journal of Athletic Training, 36, 160-169.

Brophy, R. H., Gill, C. S., Lyman, S., Barnes, R. P., Rodeo, S. A. & Warren, R. F. 2009. Effect of anterior cruciate ligament reconstruction and meniscectomy on length of career in national football league athletes a case control study. American Journal of Sports Medicine, 37, 2102-2107.

Brown, B. N., Freund, J. M., Han, L., Rubin, J. P., Reing, J. E., Jeffries, E. M., Wolf, M. T., Tottey, S., Barnes, C. A., Ratner, B. D. & Badylak, S. F. 2011. Comparison of three methods for the derivation of a biologic scaffold composed of adipose tissue extracellular matrix. Tissue Engineering Part C-Methods, 17, 411-421.

Brown, B. N., Valentin, J. E., Stewart-Akers, A. M., Mccabe, G. P. & Badylak, S. F. 2009. Macrophage phenotype and remodelling outcomes in

response to biologic scaffolds with and without a cellular component. Biomaterials, 30, 1482-1491.

Bruns, J., Kahrs, J., Kampen, J., Behrens, P. & Plitz, W. 1998. Autologous perichondral tissue for meniscal replacement. Journal of Bone and Joint Surgery-British Volume, 80B, 918-923.

Bulgheroni, P., Murena, L., Ratti, C., Bulgheroni, E., Ronga, M. & Cherubino, P. 2010. Follow-up of collagen meniscus implant patients: Clinical, radiological, and magnetic resonance imaging results at 5 years. Knee, 17, 224-229.

Bullough, P. G., Munuera, L., Murphy, J. & Weinstein, A. M. 1970. The strength of the menisci of the knee as it relates to their fine structure. J Bone Joint Surg Br, 52, 564-7.

Buma, P., Van Tienen, T. & Veth, R. P. 2007. The collagen meniscus implant. Expert Review of Medical Devices, 4, 507-516.

Burks, R. T., Metcalf, M. H. & Metcalf, R. W. 1997. Fifteen-year follow-up of arthroscopic partial meniscectomy. Arthroscopy-the Journal of Arthroscopic and Related Surgery, 13, 673-679.

Bursac, P., Arnoczky, S. & York, A. 2009. Dynamic compressive behaviour of human meniscus correlates with its extra-cellular matrix composition. Biorheology, 46, 227-237.

Cameron, J. C. & Saha, S. 1997. Meniscal allograft transplantation for unicompartmental arthritis of the knee. Clinical Orthopaedics and Related Research, 164-171.

Camplejohn, K. L. & Allard, S. A. 1988. Limitations of safranin-o staining in proteoglycan-depleted cartilage demonstrated with monoclonal-antibodies. Histochemistry, 89, 185-188.

Cao, M., Stefanovic-Racic, M., Georgescu, H. I., Miller, L. A. & Evans, C. H. 1998. Generation of nitric oxide by lapine meniscal cells and its effect

on matrix metabolism: Stimulation of collagen production by arginine. Journal of Orthopaedic Research, 16, 104-111.

Carter, D. R. & Hayes, W. C. 1976. Fatigue life of compact bone .1. Effects of stress amplitude, temperature and density. Journal of Biomechanics, 9, 27-&.

Carter, T. R. 1999. Meniscal allograft transplantation. Sports Medicine and Arthroscopy Review, 7, 51-62.

Cebotari, S., Tudorache, I., Jaekel, T., Hilfiker, A., Dorfman, S., Ternes, W., Haverich, A. & Lichtenberg, A. 2010. Detergent decellularisation of heart valves for tissue engineering: Toxicological effects of residual detergents on human endothelial cells. Artificial Organs, 34, 206-209.

Cheung, H. S. 1987. Distribution of type I, type II, type III, and type V in the pepsin solubilized collagens in bovine menisci. Connective Tissue Research, 16, 343-356.

Chia, H. N. & Hull, M. L. 2008. Compressive moduli of the human medial meniscus in the axial and radial directions at equilibrium and at a physiological strain rate. Journal of Orthopaedic Research, 26, 951-956.

Chiari, C., Koller, U., Dorotka, R., Eder, C., Plasenzotti, R., Lang, S., Ambrosio, L., Tognana, E., Kon, E., Salter, D. & Nehrer, S. 2006. A tissue engineering approach to meniscus regeneration in a sheep model. Osteoarthritis and Cartilage, 14, 1056-1065.

Choi, N. H. & Victoroff, B. N. 2006. Anterior horn tears of the lateral meniscus in soccer players. Arthroscopy-the Journal of Arthroscopic and Related Surgery, 22, 484-488.

Clark, C. R. & Ogden, J. A. 1981. Prenatal and postnatal development of human knee joint menisci. Iowa Orthopaedic Journal, 1, 20-27.

Cook, J. L. & Fox, D. B. 2007. A novel bioabsorbable conduit augments healing of avascular meniscal tears in a dog model. American Journal of Sports Medicine, 35, 1877-1887.

Cook, J. L., Fox, D. B., Malaviya, P., Tomlinson, J. L., Kuroki, K., Cook, C. R. & Kladakis, S. 2006. Long-term outcome for large meniscal defects treated with small intestinal submucosa in a dog model. American Journal of Sports Medicine, 34, 32-42.

Cook, J. L., Tomlinson, J. L., Arnoczky, S. P., Fox, D. B., Cook, C. R. & Kreeger, J. M. 2001. Kinetic study of the replacement of porcine small intestinal submucosa grafts and the regeneration of meniscal-like tissue in large avascular meniscal defects in dogs. Tissue Engineering, 7, 321-334.

Costa, C. R., Morrison, W. B. & Carrino, J. A. 2004. Medial meniscus extrusion on knee MRI: Is extent associated with severity of degeneration or type of tear? American Journal of Roentgenology, 183, 17-23.

Courtman, D. W., Pereira, C. A., Kashef, V., Mccomb, D., Lee, J. M. & Wilson, G. J. 1994. Development of a pericardial acellular matrix biomaterial - biochemical and mechanical effects of cell extraction. Journal of Biomedical Materials Research, 28, 655-666.

Cox, B. & Emili, A. 2006. Tissue subcellular fractionation and protein extraction for use in mass-spectrometry-based proteomics. Nature Protocols, 1, 1872-1878.

Cox, J. S., Nye, C. E., Schaefer, W. W. & Woodstein, I. J. 1975. Degenerative effects of partial and total resection of medial meniscus in dogs. Clinical Orthopaedics and Related Research, 178-183.

Crapo, P. M., Gilbert, T. W. & Badylak, S. F. 2011. An overview of tissue and whole organ decellularisation processes. Biomaterials, 32, 3233-3243.

Crownins.Rd & Pope, M. H. 1974. Response of compact bone in tension at various strain rates. Annals of Biomedical Engineering, 2, 217-225.

Currey, J. D. & Brear, K. 1990. Hardness, young modulus and yield stress in mammalian mineralized tissues. Journal of Materials Science-Materials in Medicine, 1, 14-20.

Dandy, D. J. 1990. The arthroscopic anatomy of symptomatic meniscal lesions. Journal of Bone and Joint Surgery-British Volume, 72, 628-633.

De Holl, P. D., Burt, D. M., Zhu, C. F., Agrawal, C. M. & Athanasiou, K. A. 1999. Creep indentation biomechanics of medial bovine meniscus. Transactions of the Orthopaedic Research Society, 1048.

Deboer, H. H. & Koudstaal, J. 1994. Failed meniscus transplantation - a report of 3 cases. Clinical Orthopaedics and Related Research, 155-162.

Deeken, C. R., White, A. K., Bachman, S. L., Ramshaw, B. J., Cleveland, D. S., Loy, T. S. & Grant, S. A. 2011. Method of preparing a decellularised porcine tendon using tributyl phosphate. Journal of Biomedical Materials Research Part B-Applied Biomaterials, 96B, 199-206.

Degroot, J. H., Zijlstra, F. M., Kuipers, H. W., Pennings, A. J., Klompmaker, J., Veth, R. P. H. & Jansen, H. W. B. 1997. Meniscal tissue regeneration in porous 50/50 copoly(l-lactide/epsilon-caprolactone) implants. Biomaterials, 18, 613-622.

Dehaven, K. E. 1999. Meniscus repair. American Journal of Sports Medicine, 27, 242-250.

Djurasovic, M., Aldridge, J. W., Grumbles, R., Rosenwasser, M. P., Howell, D. & Ratcliffe, A. 1998. Knee joint immobilization decreases aggrecan gene expression in the meniscus. American Journal of Sports Medicine, 26, 460-466.

Dong, X., Wei, X., Yi, W., Gu, C., Kang, X., Liu, Y., Li, Q. & Yi, D. 2009. Rgd-modified acellular bovine pericardium as a bioprosthetic scaffold for tissue engineering. Journal of Materials Science-Materials in Medicine, 20, 2327-2336.

Drosos, G. I. & Pozo, J. L. 2004. The causes and mechanisms of meniscal injuries in the sporting and non-sporting environment in an unselected population. Knee, 11, 143-149.

Ducy, P., Boyce, B. F., Story, B., Dunstan, C. & Karsenty, G. 1996. Increased bone formation in osteocalcin-deficient mice without bone resorption defect. Journal of Bone and Mineral Research, 11, 43-43.

Engler, A. J., Sen, S., Sweeney, H. L. & Discher, D. E. 2006. Matrix elasticity directs stem cell lineage specification. Cell, 126, 677-689.

Fabbriciani, C., Lucania, L., Milano, G., Schiavone Panni, A. & Evangelisti, M. 1997. Meniscal allografts: Cryopreservation vs deep-frozen technique. An experimental study in goats. Knee Surg Sports Traumatol Arthrosc, 5, 124-34.

Fairbank, T. J. 1948. Knee joint changes after meniscectomy. Journal of Bone and Joint Surgery-British Volume, 30, 664-670.

Farng, E. & Sherman, O. 2004. Meniscal repair devices: A clinical and biomechanical literature review. Arthroscopy-the Journal of Arthroscopic and Related Surgery, 20, 273-286.

Favenesi, J. A., Shaffer, J. C. & Mow, V. C. 1983. Biphasic mechanical properties of knee meniscus. Orthopaedic Transactions, 7, 264-265.

Fink, C., Fermor, B., Weinberg, J. B., Pisetsky, D. S., Misukonis, M. A. & Guilak, F. 2001. The effect of dynamic mechanical compression on nitric oxide production in the meniscus. Osteoarthritis and Cartilage, 9, 481-487.

Fithian, D. C. M. D., Kelly, M. a. M. D. & Mow, V. C. P. D. 1990. Material properties and structure-function relationships in the menisci. Clinical Orthopaedics & Related Research March, 252, 19-31.

Foldager, C. B., Toh, W. S., Gomoll, A. H., Olsen, B. R. & Spector, M. 2014. Distribution of basement membrane molecules, laminin and collagen type IV, in normal and degenerated cartilage tissues. Cartilage, 5, 123-132.

Fox, D. B., Warnock, J. J., Stoker, A. M., Luther, J. K. & Cockrell, M. 2010. Effects of growth factors on equine synovial fibroblasts seeded on synthetic scaffolds for avascular meniscal tissue engineering. Research in Veterinary Science, 88, 326-332.

Fox, J. M., Rintz, K. G. & Ferkel, R. D. 1993. Trephination of incomplete meniscal tears. Arthroscopy, 9, 451-455.

Fraser, S. A., Crawford, A., Frazer, A., Dickinson, S., Hollander, A. P., Brook, I. M. & Hatton, P. V. 2006. Localization of type VI collagen in tissue-engineered cartilage on polymer scaffolds. Tissue Engineering, 12, 569-577.

Freymann, U., Endres, M., Neumann, K., Scholman, H. J., Morawietz, L. & Kaps, C. 2012. Expanded human meniscus-derived cells in 3-d polymer-hyaluronan scaffolds for meniscus repair. Acta Biomaterialia, 8, 677-685.

Freytes, D. O., Stoner, R. M. & Badylak, S. F. 2008. Uniaxial and biaxial properties of terminally sterilized porcine urinary bladder matrix scaffolds. Journal of Biomedical Materials Research Part B: Applied Biomaterials, 84B, 408-414.

Fukubayashi, T. & Kurosawa, H. 1980. The contact area and pressure distribution pattern of the knee - a study of normal and osteoarthritic knee joints. Acta Orthopaedica Scandinavica, 51, 871-879.

Funamoto, S., Nam, K., Kimura, T., Murakoshi, A., Hashimoto, Y., Niwaya, K., Kitamura, S., Fujisato, T. & Kishida, A. 2010. The use of high-hydrostatic pressure treatment to decellularise blood vessels. Biomaterials, 31, 3590-3595.

Gabrion, A., Aimedieu, P., Laya, Z., Havet, E., Mertl, P., Grebe, R. & Laude, M. 2005. Relationship between ultrastructure and biomechanical properties of the knee meniscus. Surgical and Radiologic Anatomy, 27, 507-510.

Galili, U., Latemple, D. C., Walgenbach, A. W. & Stone, K. R. 1997. Porcine and bovine cartilage transplants in cynomolgus monkey .2. Changes in anti-gal response during chronic rejection. Transplantation, 63, 646-651.

Galley, N. K., Gleghorn, J. P., Rodeo, S., Warren, R. F., Maher, S. A. & Bonassar, L. J. 2011. Frictional properties of the meniscus improve after scaffold-augmented repair of partial meniscectomy: A pilot study. Clinical Orthopaedics and Related Research, 469, 2817-2823.

Garrett, J. C. 1993. Meniscal transplantation: A review of 43 cases with 2- to 7-year follow-up. Sports Medicine and Arthroscopy Review, 1, 164-167.

Garrett, J. C. & Stevensen, R. N. 1991. Meniscal transplantation in the human knee: A preliminary report. Arthroscopy: The Journal of Arthroscopic & Related Surgery, 7, 57-62.

Gelse, K., Poschl, E. & Aigner, T. 2003. Collagens - structure, function, and biosynthesis. Advanced Drug Delivery Reviews, 55, 1531-1546.

Gershuni, D. H., Skyhar, M. J., Danzig, L. A., Camp, J., Hargens, A. R. & Akeson, W. H. 1989. Experimental models to promote healing of tears in the avascular segment of canine knee menisci. Journal of Bone and Joint Surgery-American Volume, 71A, 1363-1370.

Ghadially, F. N., Lalonde, J. M. A. & Wedge, J. H. 1983. Ultrastructure of normal and torn menisci of the human knee joint. Journal of Anatomy, 136, 773-791.

Ghadially, F. N., Thomas, I., Yong, N. & Lalonde, J. M. A. 1978. Ultrastructure of rabbit semi-lunar cartilages. Journal of Anatomy, 125, 499-517.

Ghadially, F. N., Wedge, J. H. & Lalonde, J. M. A. 1986. Experimental methods of repairing injured menisci. Journal of Bone and Joint Surgery-British Volume, 68, 106-110.

Gilbert, T. W., Stewart-Akers, A. M., Simmons-Byrd, A. & Badylak, S. F. 2007. Degradation and remodelling of small intestinal submucosa in canine achilles tendon repair. Journal of Bone and Joint Surgery-American Volume, 89A, 621-630.

Glowacki, J. & Mulliken, J. B. 1985. Demineralized bone implants. Clin Plast Surg, 12, 233-41.

Goble, E. M., Kohn, D., Verdonk, R. & Kane, S. M. 1999. Meniscal substitutes - human experience. Scandinavian Journal of Medicine & Science in Sports, 9, 146-157.

Goertzen, D. J., Budney, D. R. & Cinats, J. G. 1997. Methodology and apparatus to determine material properties of the knee joint meniscus. Medical Engineering & Physics, 19, 412-419.

Golshayan, D., Buhler, L., Lechler, R. I. & Pascual, M. 2007. From current immunosuppressive strategies to clinical tolerance of allografts. Transplant International, 20, 12-24.

Gorschewsky, O., Puetz, A., Riechert, K., Klakow, A. & Becker, R. 2005. Quantitative analysis of biochemical characteristics of bone-patellar tendon-bone allografts. Bio-Medical Materials and Engineering, 15, 403-411.

Gratzer, P. F., Harrison, R. D. & Woods, T. 2006. Matrix alteration and not residual sodium dodecyl sulphate cytotoxicity affects the cellular repopulation of a decellularised matrix. Tissue Engineering, 12, 2975-2983.

Grauss, R. W., Hazekamp, M. G., Oppenhuizen, F., Van Munsteren, C. J., Gittenberger-De Groot, A. C. & Deruiter, M. C. 2005. Histological evaluation of decellularised porcine aortic valves: Matrix changes due to different decellularisation methods. European Journal of Cardio-Thoracic Surgery, 27, 566-571.

Greis, P. E., Bardana, D. D., Holmstrom, M. C. & Burks, R. T. 2002. Meniscal injury: I. Basic science and evaluation. J Am Acad Orthop Surg, 10, 168-76.

Gruber, H. E., Mauerhan, D., Chow, Y., Ingram, J. A., Norton, H. J., Hanley, E. N. & Sun, Y. 2008. Three-dimensional culture of human meniscal cells: Extracellular matrix and proteoglycan production. Bmc Biotechnology, 8.

Gu, Y., Zhu, W., Hao, Y., Lu, L., Chen, Y. & Wang, Y. 2012. Repair of meniscal defect using an induced myoblast-loaded polyglycolic acid mesh in a canine model. Experimental and Therapeutic Medicine, 3, 293-298.

Gulati, A. K. 1988. Evaluation of acellular and cellular nerve grafts in repair of rat peripheral nerve. Journal of Neurosurgery, 68, 117-123.

Guo, S. Z., Ren, X. J., Wu, B. & Jiang, T. 2010. Preparation of the acellular scaffold of the spinal cord and the study of biocompatibility. Spinal Cord, 48, 576-581.

Gupte, C. M., Smith, A., Mcdermott, I. D., Bull, A. M. J., Thomas, R. D. & Amis, A. A. 2002. Meniscofemoral ligaments revisited - anatomical study, age correlation and clinical implications. Journal of Bone and Joint Surgery-British Volume, 84B, 846-851.

Hammer, C. 2003. Xenotransplantation: The good, the bad, and the ugly or how far are we to clinical application? Transplantation Proceedings, 35, 1256-1257.

Hannink, G., Van Tienen, T. G., Schouten, A. J. & Buma, P. 2011. Changes in articular cartilage after meniscectomy and meniscus replacement using a biodegradable porous polymer implant. Knee Surgery Sports Traumatology Arthroscopy, 19, 441-451.

Hasan, J., Fisher, J. & Ingham, E. 2014. Current strategies in meniscal regeneration. Journal of Biomedical Materials Research Part B: Applied Biomaterials, 102, 619-634.

Hauschka, P. V. & Wians, F. H. 1989. Osteocalcin-hydroxyapatite interaction in the extracellular organic matrix of bone. Anatomical Record, 224, 180-188.

Hellio Le Graverand, M. P., Ou, Y., Schield-Yee, T., Barclay, L., Hart, D., Natsume, T. & Rattner, J. B. 2001. The cells of the rabbit meniscus: Their arrangement, interrelationship, morphological variations and cytoarchitecture. J Anat, 198, 525-35.

Herwig, J., Egner, E. & Buddecke, E. 1984. Chemical changes of human knee joint menisci in various stages of degeneration. Annals of the Rheumatic Diseases, 43, 635-640.

Hidaka, C., Ibarra, C., Hannafin, J. A., Torzilli, P. A., Quitoriano, M., Jen, S. S., Warren, R. F. & Crystal, R. G. 2002. Formation of vascularized meniscal tissue by combining gene therapy with tissue engineering. Tissue Engineering, 8, 93-105.

Hoben, G. M., Hu, J. C., James, R. A. & Athanasiou, K. A. 2007. Self-assembly of fibrochondrocytes and chondrocytes for tissue engineering of the knee meniscus. Tissue Engineering, 13, 939-946.

Hodde, J., Janis, A., Ernst, D., Zopf, D., Sherman, D. & Johnson, C. 2007. Effects of sterilization on an extracellular matrix scaffold: Part i.

Composition and matrix architecture. Journal of Materials Science-Materials in Medicine, 18, 537-543.

Hopker, W. W., Angres, G., Klingel, K., Komitowski, D. & Schuchardt, E. 1986. Changes of the elastin compartment in the human meniscus. Virchows Archiv a-Pathological Anatomy and Histopathology, 408, 575-592.

Horie, M., Sekiya, I., Muneta, T., Ichinose, S., Matsumoto, K., Saito, H., Murakami, T. & Kobayashi, E. 2009. Intra-articular injected synovial stem cells differentiate into meniscal cells directly and promote meniscal regeneration without mobilization to distant organs in rat massive meniscal defect. Stem Cells, 27, 878-887.

Hoshino, A. & Wallace, W. A. 1987. Impact-absorbing properties of the human knee. Journal of Bone and Joint Surgery-British Volume, 69, 807-811.

Hough, A. J. & Webber, R. J. 1990. Pathology of the meniscus. Clinical Orthopaedics and Related Research, 32-40.

Hudson, T. W., Liu, S. Y. & Schmidt, C. E. 2004. Engineering an improved acellular nerve graft via optimized chemical processing. Tissue Eng, 10, 1346-58.

Idelevich, A., Rais, Y. & Monsonego-Ornan, E. 2011. Bone gla protein increases hif-1 alpha-dependent glucose metabolism and induces cartilage and vascular calcification. Arteriosclerosis Thrombosis and Vascular Biology, 31, E55-U70.

Ingram, J. H., Korossis, S., Howling, G., Fisher, J. & Ingham, E. 2007. The use of ultrasonication to aid recellularisation of acellular natural tissue scaffolds for use in anterior cruciate ligament reconstruction. Tissue Engineering, 13, 1561-1572.

Ionescu, L. C., Lee, G. C., Huang, K. L. & Mauck, R. L. 2012. Growth factor supplementation improves native and engineered meniscus repair in vitro. Acta Biomaterialia, 8, 3687-3694.

Ishida, K., Kuroda, R., Miwa, M., Tabata, Y., Hokugo, A., Kawamoto, T., Sasaki, K., Doita, M. & Kurosaka, M. 2007. The regenerative effects of platelet-rich plasma on meniscal cells in vitro and its in vivo application with biodegradable gelatin hydrogel. Tissue Engineering, 13, 1103-1112.

Isoda, K. & Saito, S. 1998. In vitro and in vivo fibrochondrocyte growth behaviour in fibrin gel: An immunohistochemical study in the rabbit. Am J Knee Surg, 11, 209-16.

Jackson, D. W., Mcdevitt, C. A., Simon, T. M., Arnoczky, S. P., Atwell, E. A. & Silvino, N. J. 1992. Meniscal transplantation using fresh and cryopreserved allografts - an experimental study in goats. American Journal of Sports Medicine, 20, 644-656.

Jackson, D. W., Whelan, J. & Simon, T. M. 1993. Cell survival after transplantation of fresh meniscal allografts - DNA probe analysis in a goat model. American Journal of Sports Medicine, 21, 540-550.

Jackson, J. P. 1968. Degenerative changes in knee after meniscectomy. British Medical Journal, 2, 525-&.

Jay, G. D., Torres, J. R., Rhee, D. K., Helminen, H. J., Hytinnen, M. M., Cha, C. J., Elsaid, K., Kim, K. S., Cui, Y. J. & Warman, M. L. 2007. Association between friction and wear in diarthrodial joints lacking lubricin. Arthritis and Rheumatism, 56, 3662-3669.

Johnson, L. L. & Feagin, J. A. 2000. Autogenous tendon graft substitution for absent knee joint meniscus: A pilot study. Arthroscopy-the Journal of Arthroscopic and Related Surgery, 16, 191-196.

Joshi, M. D., Suh, J. K., Marui, T. & Woo, S. L. Y. 1995. Interspecies variation of compressive biomechanical properties of the meniscus. Journal of Biomedical Materials Research, 29, 823-828.

Kambic, H. E. & Mcdevitt, C. A. 2005. Spatial organization of types I and II collagen in the canine meniscus. Journal of Orthopaedic Research, 23, 142-149.

Kang, S.-W., Son, S.-M., Lee, J.-S., Lee, E.-S., Lee, K.-Y., Park, S.-G., Park, J.-H. & Kim, B.-S. 2006. Regeneration of whole meniscus using meniscal cells and polymer scaffolds in a rabbit total meniscectomy model. J Biomed Mater Res A, 78, 659-71.

Kasimir, M. T., Rieder, E., Seebacher, G., Wolner, E., Weigel, G. & Simon, P. 2005. Presence and elimination of the xenoantigen gal (alpha 1, 3) gal in tissue-engineered heart valves. Tissue Engineering, 11, 1274-1280.

Keane, T. J., Londono, R., Turner, N. J. & Badylak, S. F. 2012. Consequences of ineffective decellularisation of biologic scaffolds on the host response. Biomaterials, 33, 1771-81.

Keene, D. R., Sakai, L. Y. & Burgeson, R. E. 1991. Human bone contains type-iii collagen, type-VI collagen, and fibrillin - type-iii collagen is present on specific fibres that may mediate attachment of tendons, ligaments, and periosteum to calcified bone cortex. Journal of Histochemistry & Cytochemistry, 39, 59-69.

Kempson, G. 1980. The mechanical properties of articular cartilage, New York, Academic Press, Inc.

Kim, J.-M., Lee, B.-S., Kim, K.-H., Kim, K.-A. & Bin, S.-I. 2012. Results of meniscus allograft transplantation using bone fixation 110 cases with objective evaluation. American Journal of Sports Medicine, 40, 1027-1034.

Kim, W. G., Park, J. K. & Lee, W. Y. 2002. Tissue-engineered heart valve leaflets: An effective method of obtaining acellularized valve xenografts. International Journal of Artificial Organs, 25, 791-797.

Klebe, R. J. 1974. Isolation of a collagen-dependent cell attachment factor. Nature, 250, 248-251.

Klompmaker, J., Jansen, H. W. B., Veth, R. P. H., Nielsen, H. K. L., Degroot, J. H., Pennings, A. J. & Kuijer, R. 1992. Meniscal repair by fibrocartilage - an experimental study in the dog. Journal of Orthopaedic Research, 10, 359-370.

Klompmaker, J., Veth, R. P. H., Jansen, H. W. B., Nielsen, H. K. L., Degroot, J. H. & Pennings, A. J. 1996. Meniscal replacement using a porous polymer prosthesis: A preliminary study in the dog. Biomaterials, 17, 1169-1175.

Kobayashi, Y., Yasuda, K., Kondo, E., Katsura, T., Tanabe, Y., Kimura, M. & Tohyama, H. 2010. Implantation of autogenous meniscal fragments wrapped with a fascia sheath enhances fibrocartilage regeneration in vivo in a large harvest site defect. The American Journal of Sports Medicine, 38, 740-748.

Kohn, D. 1993. Autograft meniscus replacement: Experimental and clinical results. Knee Surgery, Sprots Traumatology, Arthroscopy, 1, 123-125.

Kohn, D., Wirth, C. J., Reiss, G., Plitz, W., Maschek, H., Erhardt, W. & Wulker, N. 1992. Medial meniscus replacement by a tendon autograft - experiments in sheep. Journal of Bone and Joint Surgery-British Volume, 74, 910-912.

Kon, E., Filardo, G., Tschon, M., Fini, M., Giavaresi, G., Reggiani, L. M., Chiari, C., Nehrer, S., Martin, I., Salter, D. M., Ambrosio, L. & Marcacci, M. 2012. Tissue engineering for total meniscal substitution: Animal study in sheep model-results at 12 months. Tissue Engineering Part A, 18, 1573-1582.

Kopf, S., Birkenfeld, F., Becker, R., Petersen, W., Starke, C., Wruck, C. J., Tohidnezhad, M., Varoga, D. & Pufe, T. 2010. Local treatment of meniscal lesions with vascular endothelial growth factor. Journal of Bone and Joint Surgery-American Volume, 92A, 2682-2691.

Krause, W. R., Pope, M. H., Johnson, R. J. & Wilder, D. G. 1976. Mechanical changes in knee after meniscectomy. Journal of Bone and Joint Surgery-American Volume, 58, 599-604.

Kuhn, J. E. & Wojtys, E. M. 1996. Allograft meniscus transplantation. Clinics in Sports Medicine, 15, 537-+.

Kurosawa, H., Fukubayashi, T. & Nakajima, H. 1980. Load-bearing mode of the knee-joint - physical behaviour of the knee-joint with or without menisci. Clinical Orthopaedics and Related Research, 283-290.

Lange, A. K., Singh, M. a. F., Smith, R. M., Foroughi, N., Baker, M. K., Shnier, R. & Vanwanseele, B. 2007. Degenerative meniscus tears and mobility impairment in women with knee osteoarthritis. Osteoarthritis and Cartilage, 15, 701-708.

Langer, F., Gross, A. E., West, M. & Urovitz, E. P. 1978. Immunogenicity of all allograft knee-joint transplants. Clinical Orthopaedics and Related Research, 155-162.

Lechner, K., Hull, M. L. & Howell, S. M. 2000. Is the circumferential tensile modulus within a human medial meniscus affected by the test sample location and cross-sectional area? Journal of Orthopaedic Research, 18, 945-951.

Lee, S. Y., Niikura, T. & Reddi, A. H. 2008. Superficial zone protein (lubricin) in the different tissue compartments of the knee joint: Modulation by transforming growth factor beta 1 and interleukin-1 beta. Tissue Engineering Part A, 14, 1799-1808.

Lerer, D. B., Umans, H. R., Hu, M. X. & Jones, M. H. 2004. The role of meniscal root pathology and radial meniscal tear in medial meniscal extrusion. Skeletal Radiology, 33, 569-574.

Leung, K. S., Qin, L., Fu, L. K. & Chan, C. W. 2002. A comparative study of bone to bone repair and bone to tendon healing in patella-patellar tendon complex in rabbits. Clin Biomech (Bristol, Avon), 17, 594-602.

Levy, I. M., Torzilli, P. A. & Warren, R. F. 1982. The effect of medial meniscectomy on the anterior-posterior motion of the knee. Journal of Bone and Joint Surgery-American Volume, 64, 883-888.

Lewis, P. B., Williams, J. M., Hallab, N., Virdi, A., Yanke, A. & Cole, B. J. 2008. Multiple freeze-thaw cycled meniscal allograft tissue: A biomechanical, biochemical, and histologic analysis. Journal of Orthopaedic Research, 26, 49-55.

Liao, J., Joyce, E. M. & Sacks, M. S. 2008. Effects of decellularization on the mechanical and structural properties of the porcine aortic valve leaflet. Biomaterials, 29, 1065-1074.

Lohmander, L. S., Englund, P. M., Dahl, L. L. & Roos, E. M. 2007. The long-term consequence of anterior cruciate ligament and meniscus injuries - osteoarthritis. American Journal of Sports Medicine, 35, 1756-1769.

Lumpkins, S. B., Pierre, N. & Mcfetridge, P. S. 2008. A mechanical evaluation of three decellularisation methods in the design of a xenogeneic scaffold for tissue engineering the temporomandibular joint disc. Acta Biomaterialia, 4, 808-816.

Maier, D., Braeun, K., Steinhauser, E., Ueblacker, P., Oberst, M., Kreuz, P. C., Roos, N., Martinek, V. & Imhoff, A. B. 2007. In vitro analysis of an allogenic scaffold for tissue-engineered meniscus replacement. Journal of Orthopaedic Research, 25, 1598-1608.

Mandal, B. B., Park, S.-H., Gil, E. S. & Kaplan, D. L. 2011. Multilayered silk scaffolds for meniscus tissue engineering. Biomaterials, 32, 639-651.

Marsano, A., Vunjak-Novakovic, G. & Martin, I. 2006. Towards tissue engineering of meniscus substitutes: Selection of cell source and culture environment. Conf Proc IEEE Eng Med Biol Soc, 1, 3656-8.

Martin, U., Kiessig, V., Blusch, J. H., Haverich, A., Von Der Helm, K., Herden, T. & Steinhoff, G. 1998. Expression of pig endogenous retrovirus by primary porcine endothelial cells and infection of human cells. Lancet, 352, 692-694.

Masouros, S. D., Mcdermott, I. D., Amis, A. A. & Bull, A. M. J. 2008. Biomechanics of the meniscus-meniscal ligament construct of the knee. Knee Surgery Sports Traumatology Arthroscopy, 16, 1121-1132.

Mayne, R. 1989. Cartilage collagens - what is their function, and are they involved in articular disease. Arthritis and Rheumatism, 32, 241-246.

Mccann, L., Ingham, E., Jin, Z. & Fisher, J. 2009. Influence of the meniscus on friction and degradation of cartilage in the natural knee joint. Osteoarthritis and Cartilage, 17, 995-1000.

Mcdermott, I. D. & Amis, A. A. 2006. The consequences of meniscectomy. Journal of Bone and Joint Surgery-British Volume, 88B, 1549-1556.

Mcdermott, I. D., Lie, D. T. T., Edwards, A., Bull, A. M. J. & Amis, A. A. 2008b. The effects of lateral meniscal allograft transplantation techniques on tibio-femoral contact pressures. Knee Surgery Sports Traumatology Arthroscopy, 16, 553-560.

Mcdermott, I. D., Masouros, S. D. & Amis, A. A. 2008a. Biomechanics of the menisci of the knee. Current Orthopaedics, 22, 193-201.

Mcdermott, I. D., Sharifi, F., Bull, A. M. J., Gupte, C. M., Thomas, R. W. & Amis, A. A. 2004. An anatomical study of meniscal allograft sizing. Knee Surgery Sports Traumatology Arthroscopy, 12, 130-135.

Mcdevitt, C. A. & Webber, R. J. 1990. The ultrastructure and biochemistry of meniscal cartilage. Clinical Orthopaedics and Related Research, 8-18.

Mcelhaney, J. & Byars, E. F. 1965. Dynamic response of biological materials, New York, American Society of Mechanical Engineers.

Mcginity, J. B., Geuss, L. F. & Marvin, R. A. 1977. Partial or total meniscectomy - comparative analysis. Journal of Bone and Joint Surgery-American Volume, 59, 763-766.

Mckenzie, I. F., Xing, P. X., Vaughan, H. A., Prenzoska, J., Dabkowski, P. L. & Sandrin, M. S. 1994. Distribution of the major xenoantigen (gal (alpha 1-3)gal) for pig to human xenografts. Transplant immunology, 2, 81-6.

Mcpherson, T. B., Liang, H., Record, R. D. & Badylak, S. F. 2000. Ga1 alpha(1,3) ga1 epitope in porcine small intestinal submucosa. Tissue Engineering, 6, 233-239.

Melrose, J., Smith, S., Cake, M., Read, R. & Whitelock, J. 2005. Comparative spatial and temporal localisation of perlecan, aggrecan and type I, II and IV collagen in the ovine meniscus: An ageing study. Histochemistry and Cell Biology, 124, 225-235.

Messner, K. & Gao, J. Z. 1998. The menisci of the knee joint. Anatomical and functional characteristics, and a rationale for clinical treatment. Journal of Anatomy, 193, 161-178.

Milachowski, K. A., Weismeier, K. & Wirth, C. J. 1989. Homologous meniscus transplantation - experimental and clinical results. International Orthopaedics, 13, 1-11.

Miles, C. A. & Ghelashvili, M. 1999. Polymer-in-a-box mechanism for the thermal stabilization of collagen molecules in fibres. Biophys J, 76, 3243-52.

Mizuno, K., Muneta, T., Morito, T., Ichinose, S., Koga, H., Nimura, A., Mochizuki, T. & Sekiya, I. 2008. Exogenous synovial stem cells adhere to defect of meniscus and differentiate into cartilage cells. Journal of medical and dental sciences, 55, 101-11.

Moglo, K. E. & Shirazi-Adl, A. 2003. Biomechanics of passive knee joint in drawer: Load transmission in intact and ACL-deficient joints. Knee, 10, 265-276.

Moon, M. S. & Chung, I. S. 1988. Degenerative changes after meniscectomy and meniscal regeneration. International Orthopaedics, 12, 17-19.

Morgan, B. R., Artiss, J. D. & Zak, B. 1993. Calcium determination in serum with stable alkaline arsenazo-III and triglyceride clearing. Clinical Chemistry, 39, 1608-1612.

Mow, V. C., Gibbs, M. C., Lai, W. M., Zhu, W. B. & Athanasiou, K. A. 1989. Biphasic indentation of articular-cartilage .2. A numerical algorithm and an experimental-study. Journal of Biomechanics, 22, 853-861.

Mow, V. C., Kuei, S. C., Lai, W. M. & Armstrong, C. G. 1980. Biphasic creep and stress-relaxation of articular-cartilage in compression - theory and experiments. Journal of Biomechanical Engineering-Transactions of the Asme, 102, 73-84.

Mueller, S. M., Schneider, T. O., Shortkroff, S., Breinan, H. A. & Spector, M. 1999a. Alpha-smooth muscle actin and contractile behaviour of bovine meniscus cells seeded in type I and type II collagen-GAG matrices. Journal of Biomedical Materials Research, 45, 157-166.

Mueller, S. M., Shortkroff, S., Schneider, T. O., Breinan, H. A., Yannas, I. V. & Spector, M. 1999b. Meniscus cells seeded in type I and type II collagen-GAG matrices in vitro. Biomaterials, 20, 701-709.

Nagata, S., Hanayama, R. & Kawane, K. 2010. Autoimmunity and the clearance of dead cells. Cell, 140, 619-630.

Nemzek, J. A., Arnoczky, S. P. & Swenson, C. L. 1994. Retroviral transmission by the transplantation of connective tissue allografts - an experimental study. Journal of Bone and Joint Surgery-American Volume, 76A, 1036-1041.

Noble, J. & Hamblen, D. L. 1975. Pathology of degenerate meniscus lesion. Journal of Bone and Joint Surgery-British Volume, 57, 180-186.

Noyes, F. R., Paulos, L., Mooar, L. A. & Signer, B. 1980. Knee sprains and acute knee hemarthrosis - mis-diagnosis of the anterior cruciate ligament tears. Physical Therapy, 60, 1596-1601.

Ochi, M., Ikuta, Y., Ishida, O. & Akiyama, M. 1993. Cellular and humoral immune responses after fresh meniscal allografts in mice - a preliminary report. Archives of Orthopaedic and Trauma Surgery, 112, 163-166.

Paletta, G. A., Manning, T., Snell, E., Parker, R. & Bergfeld, J. 1997. The effect of allograft meniscal replacement on intraarticular contact area and pressures in the human knee - a biomechanical study. American Journal of Sports Medicine, 25, 692-698.

Pangborn, C. A. & Athanasiou, K. A. 2005a. Effects of growth factors on meniscal fibrochondrocytes. Tissue Engineering, 11, 1141-1148.

Pangborn, C. A. & Athanasiou, K. A. 2005b. Growth factors and fibrochondrocytes in scaffolds. Journal of Orthopaedic Research, 23, 1184-1190.

Partington, L., Mordan, N. J., Mason, C., Knowles, J. C., Kim, H. W., Lowdell, M. W., Birchall, M. A. & Wall, I. B. 2013. Biochemical changes caused by decellularisation may compromise mechanical integrity of tracheal scaffolds. Acta Biomaterialia, 9, 5251-5261.

Patience, C., Takeuchi, Y. & Weiss, R. A. 1997. Infection of human cells by an endogenous retrovirus of pigs. Nature Medicine, 3, 282-286.

Paul, J. P. 1976. Approaches to design - force actions transmitted by joints in human body. Proceedings of the Royal Society of London Series B-Biological Sciences, 192, 163-172.

Peña, E., Calvo, B., Martínez, M. A. & Doblaré, M. 2006. A three-dimensional finite element analysis of the combined behaviour of ligaments and menisci in the healthy human knee joint. Journal of Biomechanics, 39, 1686-1701.

Peretti, G. M., Gill, T. J., Xu, J. W., Randolph, M. A., Morse, K. R. & Zaleske, D. J. 2004. Cell-based therapy for meniscal repair - a large animal study. American Journal of Sports Medicine, 32, 146-158.

Perey, O. 1962. Follow-up results of meniscectomy with regard to the working capacity. Acta Orthop Scand, 32, 457-60.

Peters, G. & Wirth, C. J. 2003. The current state of meniscal allograft transplantation and replacement. Knee, 10, 19-31.

Petersen, T. H., Calle, E. A., Zhao, L., Lee, E. J., Gui, L., Raredon, M. B., Gavrilov, K., Yi, T., Zhuang, Z. W., Breuer, C., Herzog, E. & Niklason, L. E. 2010. Tissue-engineered lungs for in vivo implantation. Science, 329, 538-541.

Petersen, W. & Tillmann, B. 1998. Collagenous fibril texture of the human knee joint menisci. Anatomy and Embryology, 197, 317-324.

Phillips, M., Maor, E. & Rubinsky, B. 2010. Nonthermal irreversible electroporation for tissue decellularisation. Journal of Biomechanical Engineering-Transactions of the Asme, 132.

Poschl, E., Schlotzer-Schrehardt, U., Brachvogel, B., Saito, K., Ninomiya, Y. & Mayer, U. 2004. Collagen IV is essential for basement membrane stability but dispensable for initiation of its assembly during early development. Development, 131, 1619-1628.

Proctor, C. S., Schmidt, M. B., Whipple, R. R., Kelly, M. A. & Mow, V. C. 1989. Material properties of the normal medial bovine meniscus. Journal of Orthopaedic Research, 7, 771-782.

Prokopis, P. M. & Schepsis, A. A. 1999. Allograft use in ACL reconstruction. Knee, 6, 75-85.

Pruss, A., Kao, M., Kiesewetter, H., Von Versen, R. & Pauli, G. 1999. Virus safety of avital bone tissue transplants: Evaluation of sterilization steps of spongiosa cuboids using a peracetic acid-methanol mixture. Biologicals, 27, 195-201.

Puetzer, J. L., Ballyns, J. J. & Bonassar, L. J. 2012. The effect of the duration of mechanical stimulation and post-stimulation culture on the structure and properties of dynamically compressed tissue-engineered menisci. Tissue Engineering Part A, 18, 1365-1375.

Pufe, T., Petersen, W. J., Miosge, N., Goldring, M. B., Mentlein, R., Varoga, D. J. & Tillmann, B. N. 2004. Endostatin/collagen XVIII - an inhibitor of angiogenesis - is expressed in cartilage and fibrocartilage. Matrix Biology, 23, 267-276.

Raeder, R. H., Badylak, S. F., Sheehan, C., Kallakury, B. & Metzger, D. W. 2002. Natural anti-galactose alpha 1,3 galactose antibodies delay, but do not prevent the acceptance of extracellular matrix xenografts. Transplant Immunology, 10, 15-24.

Rath, E. & Richmond, J. C. 2000. The menisci: Basic science and advances in treatment. British Journal of Sports Medicine, 34, 252-257.

Rath, E., Richmond, J. C., Yassir, W., Albright, J. D. & Gundogan, F. 2001. Meniscal allograft transplantation - two- to eight-year results. American Journal of Sports Medicine, 29, 410-414.

Reckers, L. J., Fagundes, D. J. & Cohen, M. 2009. The ineffectiveness of fibrin glue and cyanoacrylate on fixation of meniscus transplants in rabbits. Knee, 16, 290-294.

Record, R. D., Hillegonds, D., Simmons, C., Tullius, R., Rickey, F. A., Elmore, D. & Badylak, S. F. 2001. In vivo degradation of c-14-labeled

small intestinal submucosa (sis) when used for urinary bladder repair. Biomaterials, 22, 2653-2659.

Reddi, A. H. 1975. Collagenous bone matrix and gene expression in fibroblasts.

Reguzzoni, M., Manelli, A., Ronga, M., Raspanti, M. & Grassi, F. A. 2005. Histology and ultrastructure of a tissue-engineered collagen meniscus before and after implantation. Journal of Biomedical Materials Research Part B-Applied Biomaterials, 74B, 808-816.

Reing, J. E., Brown, B. N., Daly, K. A., Freund, J. M., Gilbert, T. W., Hsiong, S. X., Huber, A., Kullas, K. E., Tottey, S., Wolf, M. T. & Badylak, S. F. 2010. The effects of processing methods upon mechanical and biologic properties of porcine dermal extracellular matrix scaffolds. Biomaterials, 31, 8626-8633.

Renstrom, P. & Johnson, R. J. 1990. Anatomy and biomechanics of the menisci. Clinics in Sports Medicine, 9, 523-538.

Rieder, E., Kasimir, M. T., Silberhumer, G., Seebacher, G., Wolner, E., Simon, P. & Weigel, G. 2004. Decellularisation protocols of porcine heart valves differ importantly in efficiency of cell removal and susceptibility of the matrix to recellularisation with human vascular cells. Journal of Thoracic and Cardiovascular Surgery, 127, 399-405.

Rodeo, S. A., Seneviratne, A., Suzuki, K., Felker, K., Wickiewicz, T. L. & Warren, R. F. 2000. Histological analysis of human meniscal allografts - a preliminary report. Journal of Bone and Joint Surgery-American Volume, 82A, 1071-1082.

Rodkey, W. G., Dehaven, K. E., Montgomery, W. H., Iii, Baker, C. L., Jr., Beck, C. L., Jr., Hormel, S. E., Steadman, J. R., Cole, B. J. & Briggs, K. K. 2008. Comparison of the collagen meniscus implant with partial meniscectomy - a prospective randomized trial. Journal of Bone and Joint Surgery-American Volume, 90A, 1413-1426.

Rodkey, W. G., Steadman, J. R. & Ho, C. P. 1999. Role of MR imaging in sports medicine research. Basic science and clinical research studies. Magn Reson Imaging Clin N Am, 7, 191-203.

Roeddecker, K., Muennich, U. & Nagelschmidt, M. 1994. Meniscal healing - a biomechanical study. Journal of Surgical Research, 56, 20-27.

Saddiq, Z. A., Barbenel, J. C. & Grant, M. H. 2009. The mechanical strength of collagen gels containing glycosaminoglycans and populated with fibroblasts. J Biomed Mater Res A, 89, 697-706.

Sandmann, G. H., Eichhorn, S., Vogt, S., Adamczyk, C., Aryee, S., Hoberg, M., Milz, S., Imhoff, A. B. & Tischer, T. 2009. Generation and characterization of a human acellular meniscus scaffold for tissue engineering. J Biomed Mater Res A, 91, 567-74.

Sardone, F., Traina, F., Tagliavini, F., Pellegrini, C., Merlini, L., Squarzoni, S., Santi, S., Neri, S., Faldini, C., Maraldi, N. & Sabatelli, P. 2014. Effect of mechanical strain on the collagen VI pericellular matrix in anterior cruciate ligament fibroblasts. J Cell Physiol, 229, 878-86.

Scheffler, S. U., Gonnermann, J., Kamp, J., Przybilla, D. & Pruss, A. 2008. Remodelling of ACL allografts is inhibited by peracetic acid sterilization. Clinical Orthopaedics and Related Research, 466, 1810-1818.

Schlossberg, S., Umans, H., Flusser, G., Difelice, G. S. & Lerer, D. B. 2007. Bucket handle tears of the medial meniscus: Meniscal intrusion rather than meniscal extrusion. Skeletal Radiology, 36, 29-34.

Schmidt, T. A., Gastelum, N. S., Nguyen, Q. T., Schumacher, B. L. & Sah, R. L. 2007. Boundary lubrication of articular cartilage - role of synovial fluid constituents. Arthritis and Rheumatism, 56, 882-891.

Schoen, F. J. & Levy, R. J. 2005. Calcification of tissue heart valve substitutes: Progress toward understanding and prevention. Annals of Thoracic Surgery, 79, 1072-1080.

Schumacher, B. L., Schmidt, T. A., Voegtline, M. S., Chen, A. C. & Sah, R. L. 2005. Proteoglycan 4 (prg4) synthesis and immunolocalisation in bovine meniscus. Journal of Orthopaedic Research, 23, 562-568.

Scott, P. G., Nakano, T. & Dodd, C. M. 1997. Isolation and characterization of small proteoglycans from different zones of the porcine knee meniscus. Biochimica Et Biophysica Acta-General Subjects, 1336, 254-262.

Seddon, A. M., Curnow, P. & Booth, P. J. 2004. Membrane proteins, lipids and detergents: Not just a soap opera. Biochimica Et Biophysica Acta-Biomembranes, 1666, 105-117.

Sekiya, J. K. & Ellingson, C. I. 2006. Meniscal allograft transplantation. Journal of the American Academy of Orthopaedic Surgeons, 14, 164-174.

Setton, L. A., Guilak, F., Hsu, E. W. & Vail, T. P. 1999. Biomechanical factors in tissue engineered meniscal repair. Clinical Orthopaedics and Related Research, S254-S272.

Shaffer, B., Kennedy, S., Klimkiewicz, J. & Yao, L. 2000. Preoperative sizing of meniscal allografts in meniscus transplantation. American Journal of Sports Medicine, 28, 524-533.

Shelbourne, K. D. & Dickens, J. F. 2006. Digital radiographic evaluation of medial joint space narrowing after partial meniscectomy of bucket-handle medial meniscus tears in anterior cruciate ligament-intact knees. The American Journal of Sports Medicine, 34, 1648-1655.

Shelton, W. R. 2007. Meniscus allograft transplantation. Operative Techniques in Sports Medicine, 15, 81-85.

Shirakura, K., Niijima, M., Kobuna, Y. & Kizuki, S. 1997. Free synovium promotes meniscal healing - synovium, muscle and synthetic mesh compared in dogs. Acta Orthopaedica Scandinavica, 68, 51-54.

Shoemaker, S. C. & Markolf, K. L. 1985. Effects of joint load on the stiffness and laxity of ligament-deficient knees - an in vitro study of the anterior cruciate and medial collateral ligaments. Journal of Bone and Joint Surgery-American Volume, 67A, 136-146.

Shrive, N. 1974. Weight-bearing role of menisci of knee. Journal of Bone and Joint Surgery-British Volume, B 56, 381-381.

Skaggs, D. L., Warden, W. H. & Mow, V. C. 1994. Radial tie fibres influence the tensile properties of bovine medial meniscus. Journal of Orthopaedic Research, 12, 176-185.

Smillie, I. S. 1968. Current pattern of pathology of meniscus tears. Proceedings of the Royal Society of Medicine-London, 61, 44-&.

Sodersten, F., Hultenby, K., Heinegard, D., Johnston, C. & Ekman, S. 2013. Immunolocalization of collagens (I and III) and cartilage oligomeric matrix protein in the normal and injured equine superficial digital flexor tendon. Connective Tissue Research, 54, 62-69.

Song, Y., Greve, J. M., Carter, D. R. & Giori, N. J. 2008. Meniscectomy alters the dynamic deformational behaviour and cumulative strain of tibial articular cartilage in knee joints subjected to cyclic loads. Osteoarthritis and Cartilage, 16, 1545-1554.

Spilker, R. L., Donzelli, P. S. & Mow, V. C. 1992. A transversely isotropic biphasic finite element model of the meniscus. Journal of Biomechanics, 25, 1027-1045.

Sprossig, M., Wutzler, P., Schweizer, H. & Mucke, H. 1976. Serum sterilization in cold by peracetic-acid. Journal of Hygiene Epidemiology Microbiology and Immunology, 20, 157-163.

Stabile, K. J., Odom, D., Smith, T. L., Northam, C., Whitlock, P. W., Smith, B. P., Van Dyke, M. E. & Ferguson, C. M. 2010. An acellular, allograft-derived meniscus scaffold in an ovine model. Arthroscopy-the Journal of Arthroscopic and Related Surgery, 26, 936-948.

Stapleton, T. W., Ingram, J., Katta, J., Knight, R., Korossis, S., Fisher, J. & Ingham, E. 2008. Development and characterization of an acellular porcine medial meniscus for use in tissue engineering. Tissue Engineering Part A, 14, 505-518.

Steadman, J. R. & Rodkey, W. G. 2005. Tissue-engineered collagen meniscus implants: 5-to 6-year feasibility study results. Arthroscopy-the Journal of Arthroscopic and Related Surgery, 21, 515-525.

Stollsteimer, G. T., Shelton, W. R., Dukes, A. & Bomboy, A. L. 2000. Meniscal allograft transplantation: A 1- to 5-year follow-up of 22 patients. Arthroscopy, 16, 343-347.

Stone, K. R., Rodkey, W. G., Mckinney, L. A. & Steadman, J. R. 1995. Autogenous replacement of the meniscus cartilage - analysis of results and mechanisms of failure. Arthroscopy, 11, 395-400.

Stone, K. R., Steadman, J. R., Rodkey, W. G. & Li, S. T. 1997. Regeneration of meniscal cartilage with use of a collagen scaffold - analysis of preliminary data. Journal of Bone and Joint Surgery-American Volume, 79A, 1770-1777.

Sugita, T., Kawamata, T., Ohnuma, M., Yoshizumi, Y. & Sato, K. 2001. Radial displacement of the medial meniscus in varus osteoarthritis of the knee. Clinical Orthopaedics and Related Research, 171-177.

Sun, Y. L., Berger, E. J., Zhao, C. F., An, K. N., Amadio, P. C. & Jay, G. 2006. Mapping lubricin in canine musculoskeletal tissues. Connective Tissue Research, 47, 215-221.

Sweigart, M. A. & Athanasiou, K. A. 2001. Toward tissue engineering of the knee meniscus. Tissue Engineering, 7, 111-129.

Sweigart, M. A., Zhu, C. F., Burt, D. M., Deholl, P. D., Agrawal, C. M., Clanton, T. O. & Athanasiou, K. A. 2004. Intraspecies and interspecies comparison of the compressive properties of the medial meniscus. Annals of Biomedical Engineering, 32, 1569-1579.

Szomor, Z. L., Martin, T. E., Bonar, F. & Murrell, G. a. C. 2000. The protective effects of meniscal transplantation on cartilage - an experimental study in sheep. Journal of Bone and Joint Surgery-American Volume, 82A, 80-88.

Tan, G.-K., Dinnes, D. L. M., Butler, L. N. & Cooper-White, J. J. 2010. Interactions between meniscal cells and a self-assembled biomimetic surface composed of hyaluronic acid, chitosan and meniscal extracellular matrix molecules. Biomaterials, 31, 6104-18.

Tanaka, T., Fujii, K. & Kumagae, Y. 1999. Comparison of biochemical characteristics of cultured fibrochondrocytes isolated from the inner and outer regions of human meniscus. Knee Surgery Sports Traumatology Arthroscopy, 7, 75-80.

Teeple, E., Elsaid, K. A., Fleming, B. C., Jay, G. D., Aslani, K., Crisco, J. J. & Mechrefe, A. P. 2008. Coefficients of friction, lubricin, and cartilage damage in the anterior cruciate ligament-deficient guinea pig knee. Journal of Orthopaedic Research, 26, 231-237.

Testa Pezzin, A. P., Cardoso, T. P., Do Carmo Alberto Rincon, M., De Carvalho Zavaglia, C. A. & De Rezende Duek, E. A. 2003. Bioreabsorbable polymer scaffold as temporary meniscal prosthesis. Artif Organs, 27, 428-31.

Tham, S. C., Tsou, I. Y. Y. & Chee, T. S. G. 2008. Knee and ankle ligaments: Magnetic resonance imaging findings of normal anatomy and at injury. Annals Academy of Medicine Singapore, 37, 324-329.

Tienen, T. G., Heijkants, R., De Groot, J. H., Pennings, A. J., Schouten, A. J., Veth, R. P. H. & Buma, P. 2006. Replacement of the knee meniscus by a porous polymer implant - a study in dogs. American Journal of Sports Medicine, 34, 64-71.

Tissakht, M. & Ahmed, A. M. 1995. Tensile stress-strain characteristics of the human meniscal material. Journal of Biomechanics, 28, 411-422.

Tomford, W. W. 1995. Transmission of disease through transplantation of musculoskeletal allografts. Journal of Bone and Joint Surgery-American Volume, 77A, 1742-1754.

Upton, M. L., Chen, J., Guilak, F. & Setton, L. A. 2003. Differential effects of static and dynamic compression on meniscal cell gene expression. Journal of Orthopaedic Research, 21, 963-969.

Upton, M. L., Chen, J. & Setton, L. A. 2006a. Region-specific constitutive gene expression in the adult porcine meniscus. Journal of Orthopaedic Research, 24, 1562-1570.

Upton, M. L., Guilak, F., Laursen, T. A. & Setton, L. A. 2006b. Finite element modelling predictions of region-specific cell-matrix mechanics in the meniscus. Biomechanics and Modelling in Mechanobiology, 5, 140-149.

Upton, M. L., Hennerbichler, A., Fermor, B., Guilak, F., Weinberg, J. B. & Setton, L. A. 2006c. Biaxial strain effects on cells from the inner and outer regions of the meniscus. Connective Tissue Research, 47, 207-214.

Uysal, M., Akpinar, S., Bolat, F., Cekin, N., Cinar, M. & Cesur, N. 2008. Apoptosis in the traumatic and degenerative tears of human meniscus. Knee Surgery Sports Traumatology Arthroscopy, 16, 666-669.

Valiyaveettil, M., Mort, J. S. & Mcdevitt, C. A. 2005. The concentration, gene expression, and spatial distribution of aggrecan in canine articular cartilage, meniscus, and anterior and posterior cruciate ligaments: A new molecular distinction between hyaline cartilage and fibrocartilage in the knee joint. Connective Tissue Research, 46, 83-91.

Van Arkel, E. R. A. & De Boer, H. H. 1995. Human meniscal transplantation - preliminary results at 2 to 5-year follow-up. Journal of Bone and Joint Surgery-British Volume, 77B, 589-595.

Van Der Rest, M. & Garrone, R. 1991. Collagen family of proteins. Faseb Journal, 5, 2814-2823.

Vandermeer, R. D. & Cunningham, F. K. 1989. Arthroscopic treatment of the discoid lateral meniscus: Results of long-term follow-up. Arthroscopy, 5, 101-109.

Vangsness, C. T., Garcia, I. A., Mills, C. R., Kainer, M. A., Roberts, M. R. & Moore, T. M. 2003. Allograft transplantation in the knee: Tissue regulation, procurement, processing, and sterilization. American Journal of Sports Medicine, 31, 474-481.

Vedi, V., Williams, A., Tennant, S. J., Spouse, E., Hunt, D. M. & Gedroyc, W. M. W. 1999. Meniscal movement - an in-vivo study using dynamic MRI. Journal of Bone and Joint Surgery-British Volume, 81B, 37-41.

Verdonk, P. C., Verstraete, K. L., Almqvist, K. F., De Cuyper, K., Veys, E. M., Verbruggen, G. & Verdonk, R. 2006. Meniscal allograft transplantation: Long-term clinical results with radiological and magnetic resonance imaging correlations. Knee Surg Sports Traumatol Arthrosc, 14, 694-706.

Verdonk, P. C. M., Demurie, A., Almqvist, F., Veys, E. M., Verbruggen, G. & Verdonk, R. 2005b. Transplantation of viable meniscal allograft - survivorship analysis and clinical outcome of one hundred cases. Journal of Bone and Joint Surgery-American Volume, 87A, 715-724.

Verdonk, P. C. M., Forsyth, R. G., Wang, J., Almqvist, K. F., Verdonk, R., Veys, E. M. & Verbruggen, G. 2005a. Characterisation of human knee meniscus cell phenotype. Osteoarthritis and Cartilage, 13, 548-560.

Verdonk, R. 1997. Alternative treatments for meniscal injuries. Journal of Bone and Joint Surgery-British Volume, 79B, 866-873.

Verdonk, R., Verdonk, P., Huysse, W., Forsyth, R. & Heinrichs, E.-L. 2011. Tissue ingrowth after implantation of a novel, biodegradable

polyurethane scaffold for treatment of partial meniscal lesions. American Journal of Sports Medicine, 39, 774-782.

Veth, R. P. H., Denheeten, G. J., Jansen, H. W. B. & Nielsen, H. K. L. 1983. An experimental study of reconstructive procedures in lesions of the meniscus - use of synovial flaps and carbon-fibre implants for artificially made lesions in the meniscus of the rabbit. Clinical Orthopaedics and Related Research, 250-254.

Veth, R. P. H., Jansen, H. W. B., Leenslag, J. W., Pennings, A. J., Hartel, R. M. & Nielsen, H. K. L. 1986. Experimental meniscal lesions reconstructed with a carbon fibre-polyurethane-poly(l-lactide) graft. Clinical Orthopaedics and Related Research, 286-293.

Voloshin, A. S. & Wosk, J. 1983. Shock absorption of meniscectomised and painful knees - a comparative in vivo study. Journal of Biomedical Engineering, 5, 157-161.

Von Der Mark, K., Schober, S. & Goodman, S. L. 1999. Integrins in cell migration. Methods in molecular biology (Clifton, N.J.), 129, 219-30.

Vondermark, K. 1981. Localization of collagen types in tissues. International Review of Connective Tissue Research, 9, 265-324.

Walker, P. S. & Erkman, M. J. 1975. Role of menisci in force transmission across knee. Clinical Orthopaedics and Related Research, 184-192.

Walker, P. S. & Hajek, J. V. 1972. Load-bearing area in knee joint. Journal of Biomechanics, 15, 581-&.

Washington, E. R., Root, L. & Liener, U. C. 1995. Discoid lateral meniscus in children - long-term follow-up after excision. Journal of Bone and Joint Surgery-American Volume, 77, 1357-1361.

Webber, R. J., Harris, M. G. & Hough, A. J. 1985. Cell culture of rabbit meniscal fibrochondrocytes: Proliferative and synthetic response to

growth factors and ascorbate. Journal of Orthopaedic Research, 3, 36-42.

Weinand, C., Xu, J. W., Peretti, G. M., Bonassar, L. J. & Gill, T. J. 2009. Conditions affecting cell seeding onto three-dimensional scaffolds for cellular-based biodegradable implants. Journal of Biomedical Materials Research Part B-Applied Biomaterials, 91B, 80-87.

Welch, J. A., Montgomery, R. D., Lenz, S. D., Plouhar, P. & Shelton, W. R. 2002. Evaluation of small-intestinal submucosa implants for repair of meniscal defects in dogs. American Journal of Veterinary Research, 63, 427-431.

Welsing, R. T. C., Van Tienen, T. G., Ramrattan, N., Heijkants, R., Schouten, A. J., Veth, R. F. H. & Buma, P. 2008. Effect on tissue differentiation and articular cartilage degradation of a polymer meniscus implant - a 2-year follow-up study in dogs. American Journal of Sports Medicine, 36, 1978-1989.

Whipple, R., Wirth, C. R. & Mow, V. C. Mechanical properties of the meniscus. In: SPILKER, R. L., ed. ASME Advances in Bioengineering, 1984 New York. 32-33.

Williams, C., Liao, J., Joyce, E. M., Wang, B., Leach, J. B., Sacks, M. S. & Wong, J. Y. 2009. Altered structural and mechanical properties in decellularised rabbit carotid arteries. Acta Biomaterialia, 5, 993-1005.

Wilshaw, S.-P., Berry, H., Rooney, P., Kearney, J. N., Homer-Vanniasinkam, S., Fisher, J. & Ingham, E. 2014. Development and characterisation of acellular xenogeneic biological scaffolds for vascular bypass Tissue Engineering - Part C.

Wood, D. J., Minns, R. J. & Strover, A. 1990. Replacement of the rabbit medial meniscus with a polyester carbon-fibre bioprosthesis. Biomaterials, 11, 13-16.

Woods, T. & Gratzer, P. F. 2005. Effectiveness of three extraction techniques in the development of a decellularised bone-anterior cruciate ligament-bone graft. Biomaterials, 26, 7339-7349.

Xu, C. C., Chan, R. W. & Tirunagari, N. 2007. A biodegradable, acellular xenogeneic scaffold for regeneration of the vocal fold lamina propria. Tissue Engineering, 13, 551-566.

Yahia, L. H., Drouin, G. & Zukor, D. 1993. The irradiation effect on the initial mechanical properties of meniscal grafts. Bio-Medical Materials and Engineering, 3, 211-221.

Yamasaki, T., Deie, M., Shinomiya, R., Yasunaga, Y., Yanada, S. & Ochi, M. 2008. Transplantation of meniscus regenerated by tissue engineering with a scaffold derived from a rat meniscus and mesenchymal stromal cells derived from rat bone marrow. Artificial Organs, 32, 519-524.

Yang, M., Chen, C.-Z., Wang, X.-N., Zhu, Y.-B. & Gu, Y. J. 2009. Favourable effects of the detergent and enzyme extraction method for preparing decellularised bovine pericardium scaffold for tissue engineered heart valves. Journal of Biomedical Materials Research Part B-Applied Biomaterials, 91B, 354-361.

Zaffagnini, S., Muccioli, G. M. M., Lopomo, N., Bruni, D., Giordano, G., Ravazzolo, G., Molinari, M. & Marcacci, M. 2011. Prospective long-term outcomes of the medial collagen meniscus implant versus partial medial meniscectomy a minimum 10-year follow-up study. American Journal of Sports Medicine, 39, 977-985.

Zellner, J., Mueller, M., Berner, A., Dienstknecht, T., Kujat, R., Nerlich, M., Hennemann, B., Koller, M., Prantl, L., Angele, M. & Angele, P. 2010. Role of mesenchymal stem cells in tissue engineering of meniscus. Journal of Biomedical Materials Research Part A, 94A(4), 1150-1161.

Zhang, H., Leng, P. & Zhang, J. 2009. Enhanced meniscal repair by overexpression of higf-1 in a full-thickness model. Clin Orthop Relat Res, 467, 3165-74.

Zhang, Z., Tu, K., Xu, Y., Zhang, W., Liu, Z. & Ou, S. 1988. Treatment of longitudinal injuries in avascular area of meniscus in dogs by trephination. Arthroscopy, 4, 151-159.

Zhang, Z. N. & Arnold, J. A. 1996. Trephination and suturing of avascular meniscal tears: A clinical study of the trephination procedure. Arthroscopy, 12, 726-731.

Zhang, Z. N., Arnold, J. A., Williams, T. & Mccann, B. 1995. Repairs by trephination and suturing of longitudinal injuries in the avascular area of the meniscus in goats. American Journal of Sports Medicine, 23, 35-41.

Zhou, Z., Qin, T., Yang, J., Shen, B., Kang, P. & Pei, F. 2011. Mechanical strength of cortical allografts with gamma radiation versus ethylene oxide sterilization. Acta Orthopaedica Belgica, 77, 670-675.

Zhu, W. B., Chern, K. Y. & Mow, V. C. 1994. Anisotropic viscoelastic shear properties of bovine meniscus. Clinical Orthopaedics and Related Research, 34-45.

Zorn-Kruppa, M., Tykhonova, S., Belge, G., Diehl, H. A. & Engelke, M. 2004. Comparison of human corneal cell cultures in cytotoxicity testing. Altex, 21, 129-34.

# Appendix A – Supplementary Material

## Antibody controls

Representative images of negative controls (isotype and antibody omission) used in Chapter 4, Section 4.4.2 and Chapter 5, Section 5.4.3 are shown here. All anti-collagen antibodies were IgG's, anti-osteocalcin antibody was IgG2a and anti-α-gal was IgM.
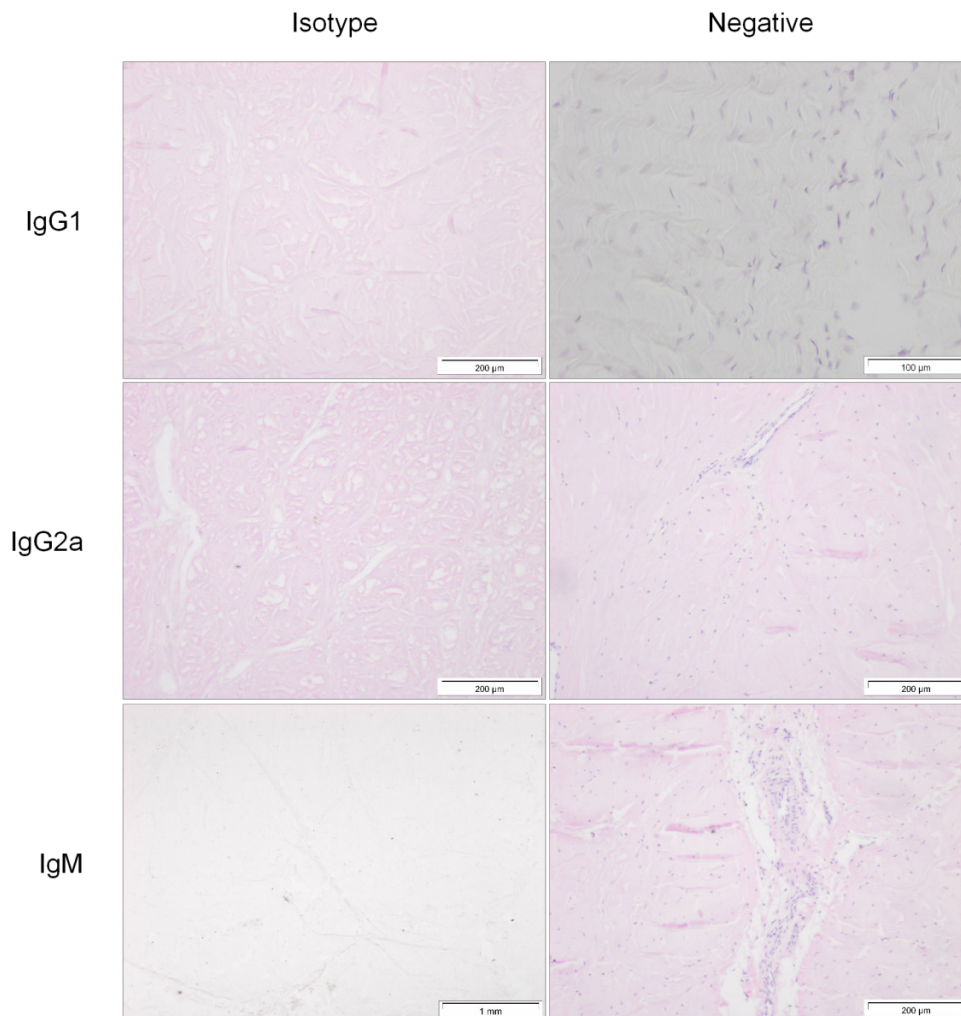


**Figure A1: Representative images from n = 3 menisci/bone of negative controls used for immunohistochemistry.** All controls were negative for staining.

## Animation of 3D FLASH MRI sequence

A CD is included with this study and contains an animation of MRI images showing the entire stack of images captured during scanning native and decellularised bone-meniscus-bone.

# Appendix B – Publications

- Hasan, J., Fisher, J., and Ingham, E. (2014).  Current strategies in meniscal regeneration.  *Journal of Biomedical Materials Research Part B: Applied Biomaterials,* 102(3), 619-634.

- Hasan, J., Jones, G. L., Stanley, M. J., Fisher, J., Ingham, E. (2012) Development of a tissue engineered meniscal replacement.  *Journal of Tissue Engineering and Regenerative Medicine*, 6, 47-47. (Published abstract)

- Hasan, J., Jones, G., Fermor, H.L., Fisher, J., Ingham, E. Priority date 4th September 2013. Filed UK Patent – Composite connective tissue and bone implants. No. GB1215725.1.

# Appendix C – Presentations

- Hasan, J., Jones, G. L., Stanley, M. J., Fisher, J., Ingham, E. (2012) Development of a tissue engineered meniscal replacement. Regener8, Gateshead, UK.

- Hasan, J., Jones, G. L., Stanley, M. J., Fisher, J., Ingham, E. (2012) Development of a tissue engineered meniscal replacement. TERMIS, Vienna, Austria.